

**FACTORS INFLUENCING THE EFFICIENCY
OF PHOTOINITIATION IN RADIATION
CURABLE INK FORMULATIONS**

Statement

The experimental work in this thesis has been carried out by the author in the Coates Lorilleux Research laboratories between January 1992 and October 1996. This work has not, and is not currently being presented for any other degree.

January 1997

ACKNOWLEDGMENTS

I would like to sincerely thank Dr. Colin Armstrong for both suggesting and funding this submission, and to my supervisors Professor R Stephen Davidson, Dr. Graham Battersby and Dr. Andrew Boon for their help and guidance during the course of this work.

For their help in setting up the RT-FTIR I am grateful to Dr. Mike Simpson and Arran Bibby; both formally of Mattson Instruments, and to David Easterby and Tim Reed of the Coates Lorilleux Research analytical laboratory. Thanks also to John Humphrey of the Coates Lorilleux Research analytical laboratory for his help in setting up and interpreting data from the GC-CI-MS.

Special acknowledgments are also due to Carol Orpwood for typing the first two chapters and Lesley Taylor for setting me up with voice activated software to 'type' the remainder myself. Thanks also to Yoshihiro Murayama for his miracle touch with a set of accupuncture needles.

Last, but by no means least, a special thank you to my wife Patricia for keeping me sane and focussed through the last two years.

PUBLISHED PAPERS

Some of the work contained in this thesis has previously been published:

C Armstrong, S Herlihy; *The use of photoinitiators in the inks and coatings industry*, Proceedings of the Paint Research Association conference "Aspects of Photoinitiation", Egham England, 1 (1993).

S L Herlihy, G C Battersby; *UV inner filter effects and photoinitiation efficiency*, Proceedings of the conference "RADTECH", Florida, USA, 156 (1994)

ABSTRACT

In an effort to be able to use photoinitiators to their maximum potential, the sequence of events that occurs in an ink formulation during the UV curing process has been studied and information presented to allow more effective formulation. Emphasis has been placed on highlighting the variables that have the greatest impact both on photoinitiator efficiency and on the suitability of individual photoinitiators and synergists for use in particular applications. These variables were found to be photoinitiator thermal stability, UV light utilisation, reaction mechanisms and cure reactivity.

A wide range of photoinitiators and synergists were investigated using thermogravimetric analysis (TGA) and thermogravimetric analysis-mass spectroscopy (TGA-MS) to define both their thermal stability and whether under heating they thermally decompose or merely evaporate.

Differential photocalorimetry (DPC) was used to determine which wavelengths from a typical medium pressure mercury curing lamp are the most important for providing cure, with both theoretical and practical methods being used to define the extent to which these wavelengths penetrate into pigmented and non-pigmented coatings. A procedure was devised and validated for this purpose.

The reaction mechanism and photodecomposition products of a range of photoinitiators were investigated using gas chromatography-mass spectroscopy (GC-MS) and radical trapping experiments. The reaction mechanisms are discussed in terms of available literature knowledge. Evidence is also presented suggesting that, with only particular exceptions, cleavage photoinitiators can also react by a hydrogen abstraction mechanism in the presence of an amine synergist.

A real time infrared spectrometer (RTIR) was set up and a method validated for following the UV curing reaction through changes in the acrylate double bond concentration. The advantages and disadvantages of this instrument are discussed in terms of other similar instruments reported in the literature, and the technique subsequently used to measure the reaction rates of a wide range of photoinitiators. Other factors such as photoinitiator concentration, amine synergist type / level and formulation viscosity were also investigated to determine their influence on the cure process.

CONTENTS

	<u>Page number</u>
<u>CHAPTER 1 GENERAL INTRODUCTION</u>	1
1.1 Introduction	2
1.2 Photoinitiated free radical curing of acrylates	5
1.2.1 The formation of excited states	5
1.2.2 The efficiency of photoinitiation	9
1.2.3 Energy transfer reactions	10
1.2.4 The reactivity of excited states	10
1.2.5 The polymerisation process	11
1.3 The light absorption process	14
1.4 Photoinitiator systems	15
1.4.1 Type I photoinitiators	15
1.4.2 Type II photoinitiators	17
1.4.3 Polymeric/polymerisable photoinitiators	19
1.4.4 Amine synergists	20
1.4.5 Oxygen inhibition	22
1.5 UV sources	24
1.5.1 Low pressure mercury vapour lamps	24
1.5.2 Medium pressure mercury vapour lamps	24
1.5.3 High pressure mercury vapour lamps	26
1.5.4 Electrodeless lamps	27
1.5.5 Doped lamps	28
1.5.6 Excimer lamps	30
1.5.7 Focussing of lamp emissions and heat management	30
1.5.8 Hazards associated with UV light sources	32
1.6 Formulating UV curable coatings	32
1.6.1 Pigment	32
1.6.2 Oligomers	35
1.6.3 Monomers	36
1.6.4 The measurement of cure	36
1.7 References	38
<u>CHAPTER 2 DEFINING THE NEED FOR A BROAD STUDY INTO THE FACTORS THAT AFFECT THE EFFICIENCY OF PHOTINITIATION</u>	44
2.1 Introduction	45
2.2 Selection of photoinitiators	45

2.3	The need for a broad study into the factors that affect photoinitiator efficiency	46
2.4	Outline of the project	48
2.5	References	50
<u>CHAPTER 3 PHOTINIATOR PHYSICAL PROPERTIES</u>		51
3.1	INTRODUCTION	52
3.2	RESULTS AND DISCUSSION	55
3.2.1	Volatility and thermal stability of photoinitiators and synergists	55
3.2.1.1	Benzoin type photoinitiators	59
3.2.1.2	Hydroxyalkylphenone type photoinitiators	60
3.2.1.3	Acylphosphine oxide type photoinitiators	61
3.2.1.4	α -Aminoalkylphenone type photoinitiators	64
3.2.1.5	Miscellaneous Type I photoinitiators	66
3.2.1.6	Xanthone and thioxanthone type photoinitiators	67
3.2.1.7	Benzophenone type photoinitiators	69
3.2.1.8	Quinone type photoinitiators	70
3.2.1.9	Aromatic 1,2-diketone type photoinitiators	71
3.2.1.10	Miscellaneous Type II photoinitiators	71
3.2.1.11	Aliphatic amine synergists	72
3.2.1.12	Aromatic amine synergists	73
3.2.2	The solubility of photoinitiators in an oligomer / monomer blend	74
3.3	CONCLUSIONS	77
3.4	EXPERIMENTAL	78
3.4.1	Volatility and thermal stability of photoinitiators and synergists	78
3.4.2	Solubility of photoinitiators in an oligomer / monomer blend	78
3.5	REFERENCES	79
<u>CHAPTER 4 UV LIGHT UTILISATION</u>		80
4.1	INTRODUCTION	81
4.1.1	Competitive light absorption	81
4.1.2	Extent of UV light absorption	82
4.1.3	Wavelength of light absorption	83
4.1.4	Sensitization	84
4.2	RESULTS AND DISCUSSION	88
4.2.1	UV light absorption	88
4.2.1.1	Most effective curing wavelengths of photoinitiators	88
4.2.1.2	UV light absorption by pigments	99
4.2.1.3	UV light absorption by amine synergists	108

4.2.2	UV light utilisation through a film	110
4.2.2.1	Extrapolation of the Beer-Lambert law to thin films	110
4.2.2.2	Validation of the modified Beer-Lambert law	112
4.2.2.3	UV transmission spectra of printed ink films	116
4.2.2.4	The occurrence and consequences of screening	120
4.2.3	Sensitization	126
4.2.3.1	Energy transfer reactions	126
4.2.3.2	Electron / proton transfer reactions	129
4.3	CONCLUSIONS	130
4.4	EXPERIMENTAL	131
4.4.1	UV / vis absorption spectra	131
4.4.2	Determining the most effective curing wavelengths for photoinitiators by DPC	131
4.4.3	The effect of competitive light absorption by amine synergists	132
4.4.4	The occurrence and consequences of screening	132
4.4.5	Sensitization	133
4.5	REFERENCES	134

CHAPTER 5 PHOTINIATOR REACTION MECHANISMS AND PHOTO-DECOMPOSITION PRODUCTS

		137
5.1	INTRODUCTION	138
5.1.1	Radical trapping techniques	140
5.1.2	Identification of photolysis products	142
5.2	RESULTS AND DISCUSSION	144
5.2.1	Photolysis in the absence of amine synergist	144
5.2.1.1	Benzoin type photoinitiators	144
5.2.1.2	Hydroxyalkylphenone type photoinitiators	151
5.2.1.3	Benzil ketal type photoinitiators	156
5.2.1.4	Acylphosphine oxide type photoinitiators	159
5.2.1.5	α -Aminoalkylphenone type photoinitiators	164
5.2.1.6	Thioxanthone type photoinitiators	172
5.2.1.7	Benzophenone type photoinitiators	172
5.2.1.8	Quinone type photoinitiators	175
5.2.1.9	Aromatic 1,2 diketone type photoinitiators	176
5.2.1.10	Phenyl glyoxylates	177
5.2.1.11	Amine synergists	178
5.2.2	Photolysis in the presence of amine synergist	178
5.2.2.1	Type II photoinitiators	178
5.2.2.2	Type I photoinitiators	184

5.2.3	Radical trapping experiments	186
5.3	CONCLUSIONS	191
5.4	EXPERIMENTAL	192
5.4.1	Photolysis byproducts in the absence of amine synergist	192
5.4.2	Photolysis byproducts in the presence of amine synergist	192
5.4.3	Radical trapping experiments	193
5.5	REFERENCES	194

CHAPTER 6 FACTORS AFFECTING THE POLYMERISATION REACTION 198

6.1	INTRODUCTION	199
6.1.1	Measuring curing efficiencies of photoinitiators and synergists	200
6.1.2	Factors that affect the polymerisation reaction	202
6.2	RESULTS AND DISCUSSION	204
6.2.1	Developing an RT-FTIR system and procedure	204
6.2.1.1	System configuration and data acquisition	204
6.2.1.2	Sampling procedure	205
6.2.1.3	Data handling	206
6.2.2	Curing effectiveness of photoinitiators by RT-FTIR	212
6.2.3	Curing effectiveness of amine synergists	224
6.2.4	The effect of viscosity on oxygen inhibition in the polymerisation process	228
6.2.5	The effect of photoinitiator concentration on cure efficiency	233
6.2.6	The influence of the amine synergist concentration on cure efficiency	236
6.2.7	The influence of photoinitiator to amine synergist ratio on cure efficiency	239
6.3	CONCLUSIONS	241
6.4	EXPERIMENTAL	242
6.4.1	Curing effectiveness of photoinitiators by RT-FTIR	242
6.4.2	Molecular modelling of benzophenone derivatives	242
6.4.3	Curing effectiveness of amine synergists by DPC	242
6.4.4	The effect of oxygen inhibition	242
6.4.5	The effect of photoinitiator concentration on cure efficiency	243
6.4.6	The influence of amine synergist concentration on cure efficiency	244
6.4.7	The influence of photoinitiator to amine synergist ratio on cure efficiency	244
6.5	REFERENCES	245

CHAPTER 7 GENERAL CONCLUSIONS 248

APPENDIX 1 GENERAL EXPERIMENTAL

CHAPTER 1

General introduction

1.1 Introduction

The term radiation curing has been recently described as the polymerisation of a chemical system initiated by incident radiation¹. This definition is clearly quite broad and allows for the inclusion of a number of reaction chemistries and radiation types. In the preparation of surface coatings the most successfully commercialized reaction chemistries have been¹⁻³:

i) Maleic/fumaric unsaturated polyesters in styrene.

First commercialized in the 1960's, this was the first of the radiation curable free radical technologies. It is now considered to be slow curing, and as such only finds significant use in the wood coatings industry where cure speed is not critical. This type of formulation is being replaced by more reactive acrylic systems.

ii) Acrylate

With the exception of the wood coatings market, acrylate containing systems are by far the most important in the surface coatings industry, giving a highly crosslinked network by a free radical polymerisation reaction. Methacrylate materials are significantly less reactive than acrylates but find some use as property modifiers.

iii) Thiol-ene

The polymerisation of polythiols with multifunctional alkenes proceeds by a step growth addition mechanism that is propagated by a free radical chain transfer process. Although used in the preparation of adhesives and photopolymer printing plates, this technology finds little use in the production of inks and decorative coatings, possibly due to the highly odorous nature of the raw materials.

iv) Cationic

Cationic systems generally contain cycloaliphatic epoxides which cure when the photoinitiators used generate Lewis acids that initiate a ring opening chain reaction. Vinyl ether substituted materials can also be polymerised by a cationic mechanism. Despite a number of advantages such as no oxygen inhibition and good adhesion due to their low shrinkage, these materials have only a relatively small share of the radiation curing market. Cationic technology is often held up as a replacement for acrylates, but its disadvantages of moisture and temperature sensitivity make it a valid alternative in certain application areas only.

Other notable radiation curing technologies are the photocycloaddition reactions of polyvinyl cinnamate derivatives³ and vinyl ether maleate copolymerisations⁴, the latter of which is currently receiving considerable interest.

A wide range of electromagnetic radiation wavelengths have also been used to initiate polymerisation reactions in the chemical systems described. Long wavelength radiation such as microwave and infra-red are not sufficiently energetic to initiate polymerisation, but their use has been described as a heating source used to evaporate solvents from applied coatings^{1,5}. The more energetic visible and particularly ultraviolet (UV) wavelengths are capable of initiating polymerisation directly, although they do so at a very slow rate, so photoinitiators are used which efficiently convert the light energy into chemically reactive species and greatly accelerate the process⁶. Short wavelength radiation such as X-rays and γ rays will also initiate polymerisation directly, but are seldom used other than in research applications because of the heavy lead shielding and stringent safety requirements. Non-ionising radiation such as an electron beam is also sufficiently energetic to initiate a polymerisation reaction directly, but its greater ease of use compared to X-rays and γ rays means that it has found more widespread use¹.

Of the type of radiation and chemical systems outlined, the most important sector in the inks and coatings business is the free radical polymerisation of acrylates using photoinitiators that absorb light in the UV and short wavelength visible regions. The dominance of this technology in the radiation curing market is such that it is given the general description of UV curing. Although an important and a rapidly growing field, a perspective should be kept since UV curing accounts for only a minor share of the total inks and coatings business, the dominant technology still being solvent-based oleoresinous materials, often referred to as 'conventional inks'.

The advantages of UV curing over solvent-based systems have been well documented^{1-3,5-13}, the most important of these, in relation to the inks and coatings market, being:

- UV-curable coatings contain no volatile solvents and therefore conform to current and impending emission levels legislation.
- Temperature-sensitive substrates can be used.
- UV lamp installations require less space than thermal ovens.
- UV has the capability for inter-station drying (curing between the application of each colour), improving print quality over normal 'wet trapping' techniques.
- Lower power consumption than solvent-based technology.
- Immediate product processing without the need for airing.
- Less clean-up time, as the inks do not dry on standing.
- Better resistance properties due to their crosslinked nature.

Of course, there are also disadvantages to UV curing, but many of these, such as the irritancy of some acrylate monomers, slow cure and poor rheology have been greatly improved upon in recent years as new materials have become available. One of the key issues affecting the industry at the moment is whether UV printed material can be effectively recycled. Some reports suggest that this is more

difficult with UV inks and, in particular, UV varnishes due to their crosslinked nature¹⁴⁻¹⁶, but other sources report that this is in fact an advantage because, once de-inked, the larger particle size of the residues means that they can be more effectively separated from the paper pulp, leading to a whiter pulp colour¹⁷.

Patents on UV curing existed prior to the 1970s, but it was not until then that the materials necessary for commercialisation became available¹⁶. As with all new technology, there was an initial reluctance to accept it, but the oil crisis of the early 1970s allowed it to gain the all-important first foothold because of its advantage of lower power consumption. From that time, although there was a large price premium to pay, the aesthetic and practical advantages such as higher gloss and better resistance properties attracted further business as customers realised that these could be used effectively to sell more of their products. As the total market continued to grow, the prices fell due to economies of scale, and UV curing became viable in other product areas⁷.

Market growth and product diversity came not just through economies of scale but also through raw material availability. Early markets were based largely on high gloss, clear coatings such as those for floor tiles, record sleeves, books and high value magazine covers^{1,18}, but, with the availability of some new photoinitiators that absorb strongly enough at long wavelengths to effectively compete with pigments for the available light, the curing of pigmented inks became possible. UV curing is now used in products as diverse as inks for plastic bottles, cardboard, paper, metal drinks cans and printed circuit boards, with coatings being used in silicone release papers, pressure sensitive adhesives and fibre optic cables^{1,10,11,13,19}. Within Europe, the United Kingdom has been the area of most rapid market growth for UV inks and coatings over the past few years²⁰, but although some figures are available for the size of both European and worldwide markets^{1,21}, these are difficult to generalise about, since they vary significantly from country to country.

Although retro-fitting an existing solvent-based technology printing press to run UV curing inks is expensive, the benefits of UV curing are such that this is still a common occurrence. When new printing presses are being built, it is reported to be cheaper to set these up to run UV inks rather than solvent-based inks because of the large capital cost of the thermal ovens; indeed, some press manufacturers install a UV curing capability as standard^{7,15}. A similar situation exists in the rapidly expanding markets of China and the former Soviet Union, where investment in new equipment is being made²², much of it either for, or with the capability of, UV curing. These trends are set to continue, particularly because of the ever increasing atmospheric pollution legislation which so drastically affects the conventional inks and coatings.

Within this project, work has concentrated exclusively on the UV initiated free radical polymerisation of acrylate based inks and coatings.

1.2 Photoinitiated free radical curing of acrylates

Formulations containing acrylate functional materials will, upon irradiation in the wavelength region of the acrylate bond absorption at 205 nm, undergo a free radical polymerisation reaction to yield a crosslinked three-dimensional network²³. This reaction is very slow, but can be greatly accelerated by the addition to the formulation of a photoinitiator which efficiently converts light energy into sufficient free radicals to start a more rapid polymerisation reaction.

Almost all photoinitiator molecules used in UV curing are based around the carbonyl chromophore, typically attached to a phenyl ring in order to shift the useful electronic transition bands into the UV region 250–390 nm through increased conjugation^{24–26}. Frequently, these phenyl rings are substituted further, or form part of a cyclic structure to modify both the absorbance and the physical properties of the material.

As long as the UV spectral absorption bands of the photoinitiator molecule overlap the emission bands of the UV source, some light energy will be absorbed and converted into excited states (photophysical processes) and, ultimately, free radicals (photochemical processes)^{27,28}.

1.2.1 The formation of excited states

When a molecule is irradiated, the photophysical processes occurring are most easily expressed in terms of the molecule's molecular orbitals (MO). The combination of two electron containing atomic orbitals in a chemical bond gives rise to two MOs, one of which has a lower energy than the original atomic orbitals (bonding MO) and the other a higher energy (antibonding MO; denoted by *). To minimise the energy of the bond, both electrons occupy the lower energy bonding orbital and form a pair with opposite spins^{5,6,24,27}, as shown in Figure 1.0.

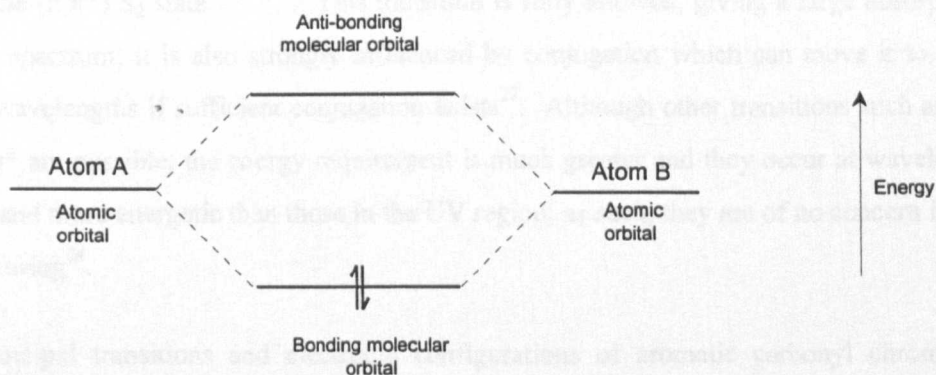


Figure 1.0 *The combination of atomic orbitals to form a chemical bond*

Atomic orbitals can combine to give two types of chemical bonds: σ (sigma) or π (pi). Overlap of S and some types of P atomic orbitals gives rise to a σ bond, containing σ and σ^* MOs, but where a σ bond already exists, parallel P atomic orbitals can laterally overlap to give a π bond, containing π and π^* MOs. The π orbitals on adjacent atoms in the molecule can also overlap further to give a

delocalised system where the electrons are able to move freely across the extent of the delocalisation^{24,27}; this is also termed conjugation.

Heteroatoms, particularly nitrogen, oxygen and sulphur, contain lone pairs of electrons known as 'n' electrons. These do not participate in bonding, being localised around the atomic nuclei, but are still important to the photophysical processes that occur upon UV irradiation. These 'n' electrons normally occupy an energy level between the π and π^* MOs, but have no equivalent antibonding orbital^{5,6,24,27}.

Prior to the generation of initiating radicals, the formation of an excited state occurs, when, as a result of the absorption of light, an electron is promoted from a bonding or non-bonding orbital to an antibonding orbital. An excited state will by definition have two unpaired electrons, but as a consequence of selection rules governing the possible transitions, these will still have opposite spins and are termed singlet states, denoted by S_1 (first excited singlet state), S_2 (second excited singlet state), etc. Spin inversion to give an equivalent triplet state $T_1, T_2 \dots$ where both electrons have the same spin direction is possible, but only through a post excitation process known as Inter System Crossing (ISC) because the probability of spin inversion taking place at the same time as the much more rapid absorption process is very low, as defined by the Franck-Condon principle^{26,27,29-31}. Since the non-bonding orbitals of the carbonyl bond are the highest energy occupied orbitals, the promotion of an electron from here to the π^* orbital involves the least energy and is termed a ($n-\pi^*$) transition, giving rise to the (n,π^*) S_1 state^{6,24,26,31}. However, because the two orbitals involved occupy different regions of space, the ($n-\pi^*$) transition is symmetry forbidden by selection rules and is reflected by its weak absorption band in the UV spectrum^{24,27,32}. The promotion of an electron from the π bonding orbital to the π^* antibonding orbital, a ($\pi-\pi^*$) transition, generally involves more energy and gives rise to the (π,π^*) S_2 state^{6,24,26,31}. This transition is fully allowed, giving a large absorption peak in the UV spectrum; it is also strongly influenced by conjugation which can move it to significantly longer wavelengths if sufficient conjugation exists²⁷. Although other transitions such as $\sigma-\pi^*$, $n-\sigma^*$ and $\pi-\sigma^*$ are possible, the energy requirement is much greater and they occur at wavelengths much shorter and more energetic than those in the UV region; as such, they are of no concern in the subject of UV curing²⁴.

The principal transitions and electronic configurations of aromatic carbonyl chromophores are summarised in Figure 1.1.

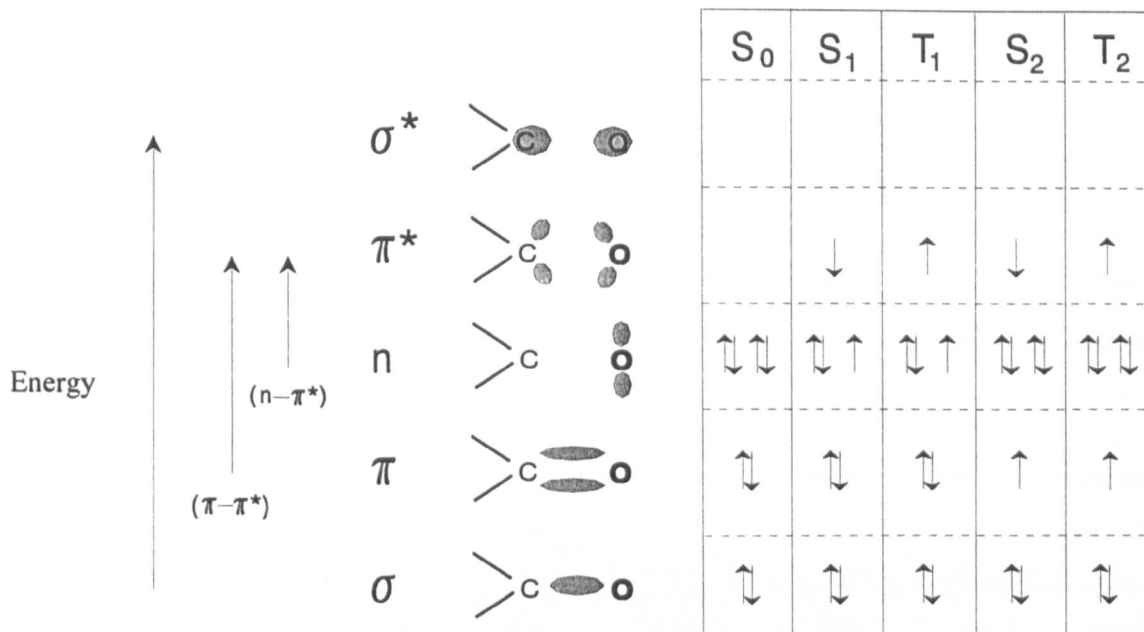


Figure 1.1 *Electronic configuration of excited carbonyl groups*

The Stark-Einstein law states that, in order to effect an electronic transition, the energy of the photon should correspond exactly to the difference between the energies of the ground state E_0 and the excited state E_1 ^{3,27,30}. This situation would result in a line spectrum, because the energy of the photon would correspond to an exact wavelength according to the equation:

$$E = E_1 - E_0 = h\nu = h\frac{c}{\lambda} = hc\bar{\nu} \quad (1)$$

where h is Planck's constant ($6.626 \times 10^{-34} \text{ J s}^{-1}$), ν is the frequency (sec^{-1}), λ is the wavelength of light (nm), c is the velocity of light ($3 \times 10^8 \text{ m s}^{-1}$), $\bar{\nu}$ is the wave number (cm^{-1}) and E_0 and E_1 are the energies of the ground state and excited state respectively^{3,5,24,26}.

UV absorbance spectra are actually band-like in nature because, as well as the electronic energy (E_{elec}), molecules have additional vibrational and rotational energy (E_{vib} and E_{rot} respectively) that contributes to the overall energy (E_{total})^{3,27,29,30,32}.

$$E_{\text{total}} = E_{\text{elec}} + E_{\text{vib}} + E_{\text{rot}} \quad (2)$$

where; $E_{\text{elec}} > E_{\text{vib}} \gg E_{\text{rot}}$

Some vibrational bands are often seen in vapour phase spectra as fine structure on the electronic bands, but frequent collisions with solvent molecules mean that this is rarely the case with solution spectra²⁹.

It can be said that the Stark-Einstein law is being obeyed as long as the total excited state energy E_1 minus the total ground state energy E_0 is equal to the energy of the photon^{3,29-31}.

$$E = h\nu = (E_{\text{elec}} + E_{\text{vib}} + E_{\text{rot}})_1 - (E_{\text{elec}} + E_{\text{vib}} + E_{\text{rot}})_0 \quad (3)$$

The absorption of a photon can therefore take place across a wavelength (energy) range, with energy in excess of the minimum required for effecting the electronic transition being vibrational and rotational energy. The minimum energy required for the transition can be identified as the longest wavelength evident in an absorption peak³¹.

Excess vibrational and rotational energy is quickly dissipated through a non-radiative process called internal conversion (IC) to the lowest excited singlet state S_1 ^{3,29-31}. Once this state has been achieved, there are a number of competing radiative and non-radiative pathways available to the excited state. These are: internal conversion (IC) to the ground state S_0 , fluorescence (F) to S_0 and inter-system crossing (ISC) to the first excited triplet state T_1 ^{3,26,29,32}. ISC is the most important of these, since it involves spin inversion of the unpaired electron in the π^* orbital to give the T_1 state from where most photochemical reactions occur. This process is favourable because T_1 generally has a lower energy than S_1 due to the repulsive nature of the spin-spin interaction between electrons of the same spin. The magnitude of this difference varies with the amount of orbital overlap, such that filled orbitals in the (n,π^*) state occupy different regions of space and consequently have a small energy difference, whereas those in (π,π^*) states occupy similar regions so the energy difference is larger^{27,29,31}. This, along with the fact that the (n,π^*) transition is also forbidden in the reverse direction, means that the lifetimes of the (n,π^*) lowest excited singlet states are generally longer than those of the equivalent (π,π^*) state. ISC is therefore more likely for (n,π^*) than for (π,π^*) lowest excited states.

The deactivation pathways for the T_1 state are principally IC, and phosphorescence to the ground state S_0 , with ISC' (reverse ISC back to the S_1 state) not being favourable because, as well as requiring a certain amount of vibrational energy just to achieve an energy state greater than or equal to S_1 , the process is forbidden in the reverse direction as well as the forward direction^{26,27}. These factors, along with the relatively long time taken for the phosphorescence process, provide the T_1 state with a long lifetime relative to that of the S_1 state and are the principal reason for its high reactivity.

Only rarely is a T_2 state or higher formed as a result of ISC immediately following an electronic transition. This is a consequence of the second and third excited singlet states, S_2 and S_3 respectively, undergoing a rapid internal conversion process to yield the lowest excited singlet state S_1 before ISC to the corresponding T_2 and T_3 states can occur^{3,29-31}.

The photophysical processes described are often displayed in the form of a Jablonski diagram, as shown in Figure 1.2, where radiative processes (F, P) are represented by straight arrows and non-radiative processes (IC, ISC, ISC') are represented by wavy arrows.

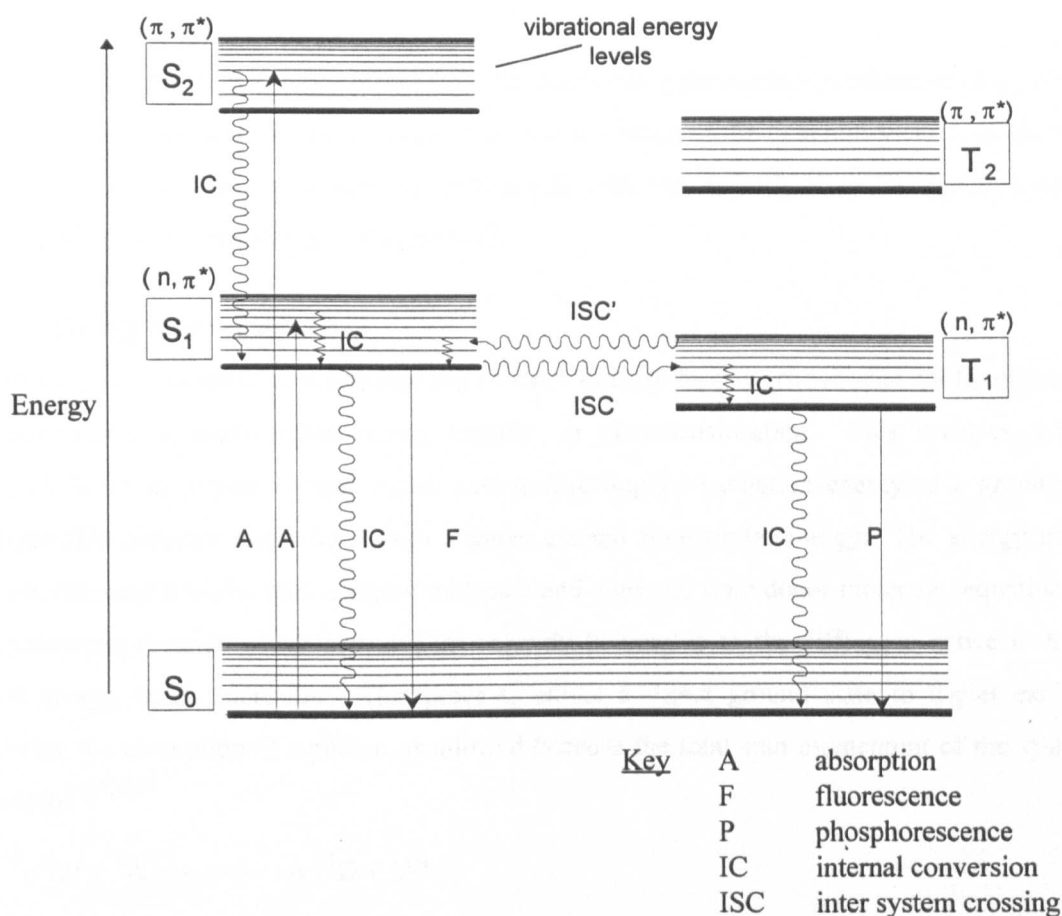


Figure 1.2 A Jablonski diagram

1.2.2 The efficiency of photoinitiation

The efficiency of photophysical and photochemical pathways is often measured in terms of a quantum yield, which defines the amount of a reaction product P formed in a process A following the absorption of a known amount of light^{5,29}. This is shown by the general equation:

$$\text{Quantum yield for a process A} = \Phi_A = \frac{\text{number of molecules P formed}}{\text{number of photons absorbed}} \quad (4)$$

Quantum yields, denoted by Φ , can be defined for any individual aspect of the photoinitiation process, such as the quantum yield of intersystem crossing Φ_{isc} , fluorescence $\Phi_{\text{fluorescence}}$, or for more general processes such as initiation $\Phi_{\text{initiation}}$ and polymerisation $\Phi_{\text{polymerisation}}$.

A quantum yield value of 1 would imply that 1 molecule of product is formed for every photon absorbed. When the value falls to less than unity, the process is not efficient and other deactivation pathways such as oxygen quenching or cage recombination are becoming important. Values of greater than 1 imply that a chain reaction is taking place, with each absorbed photon producing more

than one molecule of reaction product. Exceptions to this general situation do exist, such as the quantum yield for initiation using a cleavage photoinitiator which, if the process is efficient, has a value of 2, since the cleavage of each photoinitiator molecule leads to the formation of two primary radicals.

Quantum yield measurements are often useful for determining the reaction mechanism of a particular process and determining the rate limiting steps, but the value of the quantum yield depends on the method of measurement, often varying considerably with factors such as concentration, excitation wavelength, reaction medium and temperature⁵.

1.2.3 Energy transfer reactions

In certain cases it is possible to generate triplet states directly from a ground state configuration by a process known as triplet-triplet energy transfer, or photosensitisation. This involves a donor molecule D in its lowest excited triplet state transferring its excitation energy to a ground state configuration acceptor molecule A with a lower excited state triplet energy. The energy transfer process produces a triplet state acceptor molecule and a ground state donor molecule (equation 5) in an exothermic reaction which becomes increasingly favourable as the difference between the two triplet energy levels increases. This process, unlike a direct ground state to triplet excitation following the absorption of a photon, is allowed because the total spin momentum of the system is conserved^{3,27,30,33}.



One of the principal advantages of an energy transfer reaction is that it is capable of producing excited state acceptor molecules which may not otherwise be attainable, either because the intersystem crossing from S_1 to T_1 states is not efficient, or because the acceptor molecule does not absorb light at the irradiation wavelength(s)³. A good example of a triplet-triplet energy transfer reaction in UV curing is that observed between the commercial photoinitiator 2-methyl-1-[4-(methylthio)phenyl]-2-morpholino-propan-1-one (Irgacure 907) and a number of thioxanthone derivatives³⁴⁻³⁷. This finds widespread commercial use in the form of a combination of Irgacure 907 and isopropyl thioxanthone (Quantacure ITX).

Intramolecular energy transfer processes have also been reported for 4-phenyl benzophenone³⁸, which contains two independently absorbing but conjugated chromophores. Energy transfer is thought to occur between the two triplet states of these chromophores.

1.2.4 The reactivity of excited states

Photoinitiator molecules in excited states show very different properties to those in the ground state since the promotion of an electron into the previously empty π^* orbital changes the shape and electron density distribution of the chromophore. In the ground state, the carbonyl group has an sp^2

hybridised carbon atom and the group is planar, but in the singlet and triplet excited states the half-filled π^* orbital caused the carbon to be much more like an sp^3 hybrid, changing the shape to pyramidal and lengthening the C-O bond³⁰.

Reactivity and lifetime of excited states for carbonyl groups are also influenced by the origin of the promoted electron. The loss of an electron from the non-bonding orbital on the oxygen makes the oxygen atom electron-deficient and the carbon atom electron-rich. The carbonyl group then shows a marked nucleophilic behaviour and has properties similar to an alkoxy radical, such as the tendency to undergo hydrogen abstraction reactions. This is not observed in the case of a promotion from the π orbital, since the excitation is distributed over the entire delocalised system³³.

In addition to the electron density distribution of the different excited states influencing their reactivity, the difference in energy level spacing is also important. Where the energy level spacing between S_1 and T_1 is small, such as in the (n,π^*) lowest excited states, inter-system crossing to yield the reactive triplet state T_1 is favoured. Benzophenone has been reported to be a good example of this, where its lowest excited singlet state with an (n,π^*) character undergoes ISC to the lowest excited triplet state with almost 100% efficiency^{27,39,40}.

The exact nature of photoinitiator excited states is often determined by transient absorption spectroscopy following laser flash photolysis^{41,42}. This technique provides information on triplet lifetime and thereby the nature of the lowest excited triplet state, since $(\pi-\pi^*)$ triplet states generally have shorter lifetimes than $(n-\pi^*)$ ones. The identity of the excited state is particularly important with photoinitiators that work via a bimolecular reaction, since their mechanism of reaction will be strongly dependent on this.

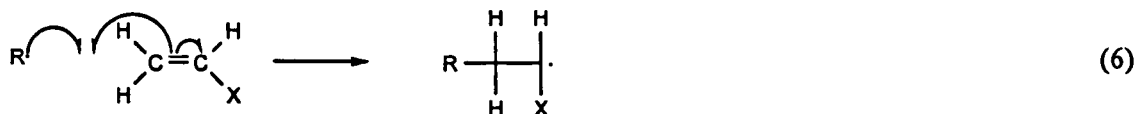
1.2.5 The polymerisation process

Photoinitiated free radical polymerisation almost exclusively involves the addition polymerisation reaction of olefinic double bonds such as in the acrylate functional group. This reaction proceeds rapidly to give a highly crosslinked, three-dimensional network that is characteristic of radiation-cured materials. The photoinitiator's involvement in the overall cure process is to generate sufficient radical centres to allow the reaction to proceed freely and overcome the effects of oxygen which strongly inhibits it. The polymerisation process can be divided into three distinct stages: initiation, propagation and termination^{3,5,27,44}.

i) Initiation

The initiation process involves the addition of the photoinitiator-derived free radical to an acrylate double bond in order to generate the first monomer radical. Even at this stage, the identity of the photoinitiator used is important, since the reactivity of radicals towards the double bond is not always the same, with the methyl radical generated from benzil dimethyl ketal (Irgacure 651) reported to be

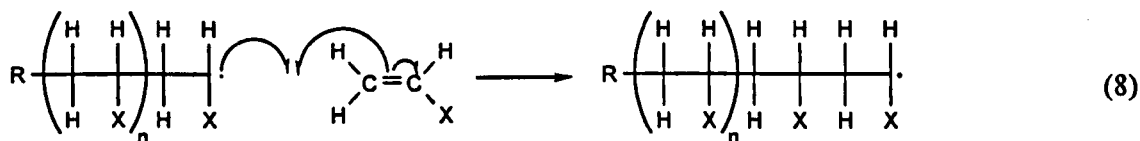
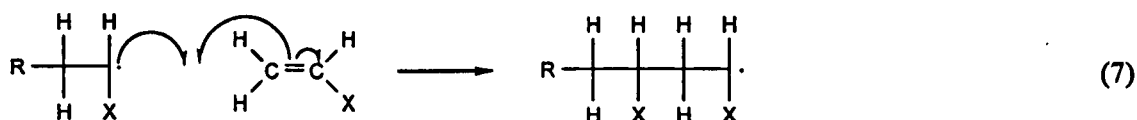
highly reactive⁴³, whereas the ketyl radical produced by benzophenone is known to be relatively unreactive⁵. The reaction between the photoinitiator-derived radical R• and the acrylate monomer involves one electron from the carbon double bond forming a carbon to carbon sigma bond with the unpaired electron of the free radical. The remaining electron in the carbon double bond then moves to the adjacent carbon atom to give the relatively more stable secondary radical, with some additional stabilization afforded by the adjacent carboxyl functionality.



Once these monomer initiating radicals have been formed, the photoinitiator plays no further part in aiding the polymerisation process, the rate and extent of reaction being determined by factors such as the number of functional groups present, and the presence of chain transfer agents and oxygen.

ii) Propagation

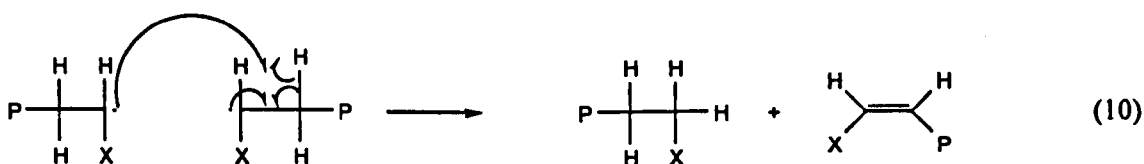
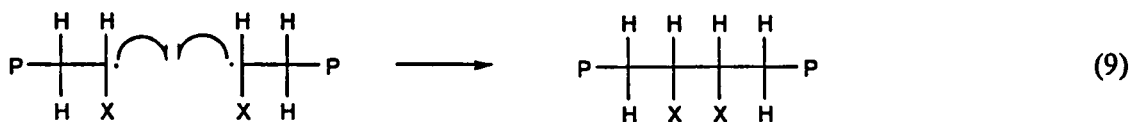
Once the initiating monomer radical has been formed, other double bonds add to this in the same way in a chain reaction that produces a growing polymer backbone with an unpaired electron at the growing end.



If there were no competing reactions, propagation would continue until either all the monomer units had been consumed or until the mobility of the growing polymer was sufficiently low that no growing polymer chains come into close contact with an unreacted monomer group.

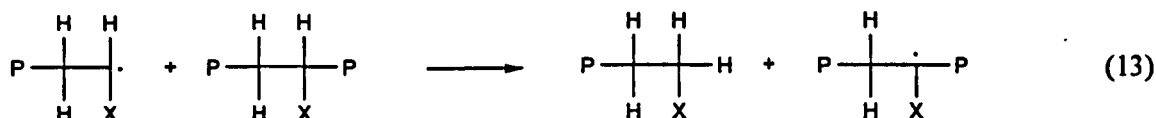
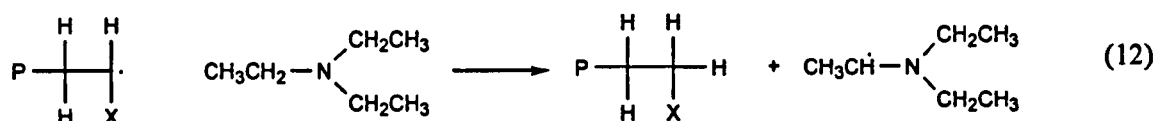
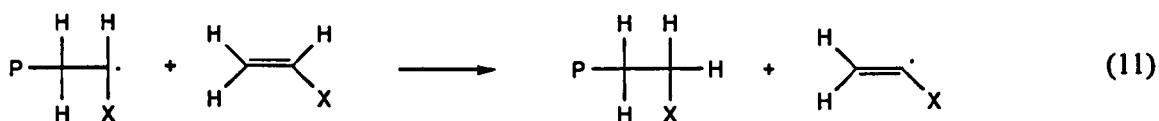
iii) Termination

Termination competes with the propagation reaction to stop the polymerisation process when two radicals interact, halting the growth of both polymer chains. This can occur by either a combination reaction (9) or a disproportionation reaction (10), where a hydrogen abstraction from one species to the other occurs.



Chain transfer reactions

Chain transfer competes with the propagation reaction and involves abstraction of a hydrogen atom by the growing chain from another species, typically unreacted monomer (11), amine synergist (12) or part of an existing polymer chain (13). The process results in the termination of the growing polymer chain and the formation of a new initiating radical capable of continuing the polymerisation reaction. With the exception of when the new radical formed by the chain transfer process is of a lower reactivity than the growing polymer chain, the overall rate of reaction and amount of monomer consumed are not significantly affected by chain transfer, although the properties of a coating may change as a result of a lowering of the molecular weight.



Rate of polymerisation

The rate of polymerisation R_p in a UV curing reaction is given under ideal conditions as^{3,27,44-48}

$$R_p = K_p \cdot \left(\frac{R_i}{K_t} \right)^{\frac{1}{2}} \cdot [M] \quad (14)$$

K_p = propagation rate constant ($\text{dm}^3 \text{mol}^{-1} \text{s}^{-1}$), $[M]$ = concentration of acrylate bonds (mol dm^{-3}), K_t is the termination rate constant ($\text{dm}^3 \text{mol}^{-1} \text{s}^{-1}$), R_i = rate of initiation.

Where R_i , the rate of initiation, is given by

$$R_i = \Phi_i \cdot I_0 (1-10^{-A}) \quad (15)$$

Φ_i = quantum yield for production of radical pairs by the photoinitiator, I_0 = incident light intensity, A = light absorbed by the photoinitiator at the incident wavelength.

The use of the equation (14) is limited in practice because of factors such as the requirement for monochromatic light, the attenuation of light through the film and the inhibiting effect of oxygen.

1.3 The light absorption process

The Grotthus-Draper law states that only light that is absorbed is capable of initiating a photochemical process^{26,27}, therefore in the study of UV curing reactions it is necessary to define in which spectral regions and to what extent light absorption occurs. The probability of absorption of a photon by a molecule and its variation with wavelength is reflected in the absorbance spectrum of that molecule, with each electronic transition showing as a band, the position and intensity of which is directly linked to the molecule's structure³¹. A typical photoinitiator for use in UV curing has only two transitions of sufficiently low energy to occur in the UV region, ($n-\pi^*$) and ($\pi-\pi^*$). Generally, the fully allowed ($\pi-\pi^*$) transition is of higher energy and occurs at wavelengths of around 250 nm as a large peak, whereas the forbidden ($n-\pi^*$) transition is of lower energy and shows as a weak peak at longer wavelengths^{24,27,32}.

The absorption of light by a molecule is governed by the Beer-Lambert law, which states that the intensity I of an incident beam I_0 decreases exponentially with increasing path length d (cm) and concentration c (mol dm^{-3}) as it passes through a sample^{24,26,27,29-31}.

$$I = I_0 \cdot 10^{-\varepsilon \cdot c \cdot d} \quad (16)$$

ε is the molar extinction coefficient ($\text{mol dm}^{-3}\text{cm}^{-1}$) which is independent of concentration and path length and defines the probability of light absorption at any wavelength. Large values of ε correspond to a high probability of absorption.

The Beer-Lambert law can also be used to describe the absorbance A or optical density OD and the percentage transmission I_T of light at any wavelength, as shown in equations (17) and (18).

$$A = OD = \varepsilon \cdot c \cdot d \quad (17)$$

$$A = \log_{10} \left(\frac{I_0}{I_T} \right) \quad (18)$$

The absorption of light is a cumulative process, so the total absorbance in a multi-component system can be obtained using equation (19), which is a slight modification of equation (17)^{27,49}.

$$A = d \left(\varepsilon_1 c_1 + \varepsilon_2 c_2 + \dots + \varepsilon_n c_n \right) \quad (19)$$

This is an important consideration when dealing with surface coatings, since rarely do they contain only one UV absorbing component. In order to achieve the desired final properties, formulations normally contain a number of different photoinitiators, synergists and pigments, most of which absorb light in the UV region⁵⁰. Therefore, the light available to an individual photoinitiator is dependent on the identity and concentration of other components and cannot be studied effectively without a consideration of these factors.

The Beer-Lambert law and its relationship with coated films has been explored further with varying levels of complexity by a number of workers in an attempt to calculate the available light for a photoinitiator at a given wavelength, photoinitiator concentration and film thickness in both pigmented⁵¹ and non-pigmented films^{23,52,53}. However, it is more usual to empirically compare spectra in an attempt to optimise curing performance of a coating by making sure that the photoinitiators absorb light where other components do not. The most significant competitive UV light absorption comes from pigments, whose UV absorption bands are not particularly strong but are made to be significant by virtue of the large amounts used in ink formulations. With these materials, the regions of weaker UV light absorption have been termed the "pigment window" and are where it is desirable to have strong absorption bands in the photoinitiator spectrum. A number of these empirical comparisons have been reported⁵⁴⁻⁵⁸, but their scope is mostly limited to only a few pigments and photoinitiators, the exception to this being the widely referenced article by Hencken⁵⁹, which contains the UV spectra of 23 pigments as aqueous dispersions.

1.4 Photoinitiator systems

Once the area of UV curing had established itself in the marketplace during the 1970s, the previously available photoinitiators used in early formulations were complemented and largely superseded by purpose-designed materials. These helped to give greater cure speeds, increased stability and allowed the curing of pigmented coatings. In addition, new market areas appeared such as cationic and water-based UV curing, all of which required new photoinitiators to be developed. Thriving research programmes now exist in both industry and academia into new photoinitiators for the rapidly growing UV curing market, with the type and reaction mechanism of the available photoinitiators having been comprehensively reviewed in a number of articles^{3,49,60-65}.

Photoinitiators are most often classified according to their reaction mechanisms or the type of active species evolved. In the UV curing of inks and coatings, most photoinitiators generate free radicals by either a cleavage reaction or a bimolecular reaction with an amine synergist; these are generally termed Type I and Type II reactions respectively, and should not be confused with the Norrish Type I and Norrish Type II processes⁶⁰. The exception to this general situation is the use of cationic photoinitiators, which generate weak Lewis acids that typically react with cycloaliphatic epoxides and vinyl ethers to give a cure reaction. The subject of cationic polymerisation has been extensively reviewed, but is beyond the scope of this work^{64,66-68}.

1.4.1 Type I photoinitiators

Where photoinitiators contain a bond with a dissociation energy lower than the excitation energy of the molecule, absorption of UV light leads to direct fragmentation to give two radical species. In the majority of photoinitiators, the cleavage occurs at the bond adjacent to the carbonyl group, in which case they are termed Norrish Type I, or simply α cleavage photoinitiators. Photoinitiators that cleave

at the β position are less common, although this has been reported for α -chlorinated acetophenones⁶⁹ and some sulphonyl ketones⁷⁰.

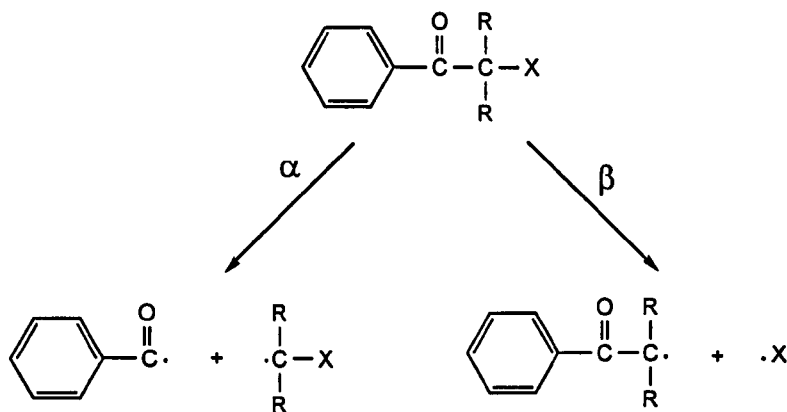
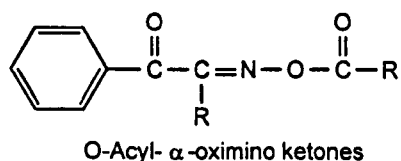
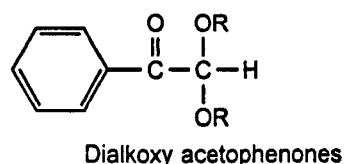
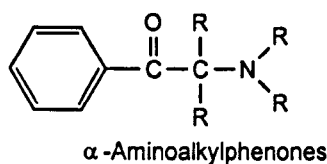
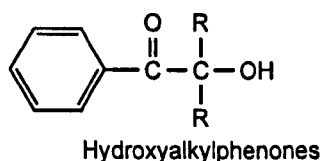
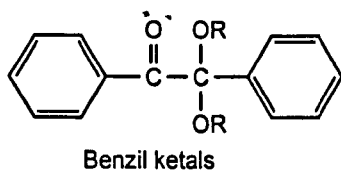
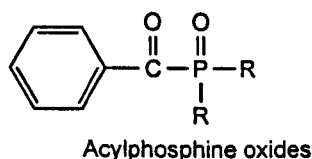
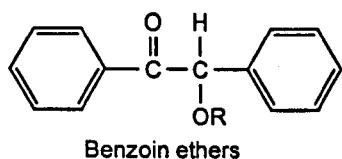


Figure 1.3 α and β cleavage reactions of a typical photoinitiator

The most widely used cleavage photoinitiators in UV curing can be divided into a number of distinct structural types:

- i) Benzoin ethers
- ii) Acylphosphine oxides
- iii) Benzil ketals
- iv) Hydroxyalkylphenones
- v) α -Aminoalkylphenones
- vi) Dialkoxy acetophenones
- vii) O-Acyl- α -oximinoketones



R = H, alkyl or substituted alkyl
Phenyl rings may be substituted

Figure 1.4 Basic structural types of commercial Type I photoinitiators

A number of other Type I photoinitiator structural types have been reported which, at the time of writing, are not commercially available. These include S-benzoyl O-ethyl xanthates⁷¹, α -thiocyanatoketones^{72,73}, dihydroxy and dibromo derivatives of dibenzoyl methanes^{74,75}, S-phenyl thiobenzoates⁷⁶, benzophenone peresters⁷⁷ and α -hydroxymethylbenzoin sulfonic ester derivatives^{78,79}.

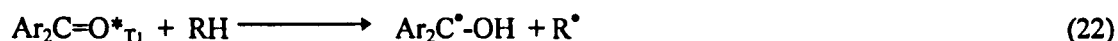
1.4.2 Type II photoinitiators

The term Type II describes photoinitiators which have excitation energies lower than any of the molecule's bond energies. These photoinitiators produce free radicals via a bimolecular reaction with a coinitiator, both of which are required to be present for the reaction to be efficient. The coinitiator, more commonly termed a synergist, acts as a source of hydrogens for the photoinitiator and, in the field of UV curing of inks and coatings, is almost always a tertiary amine.

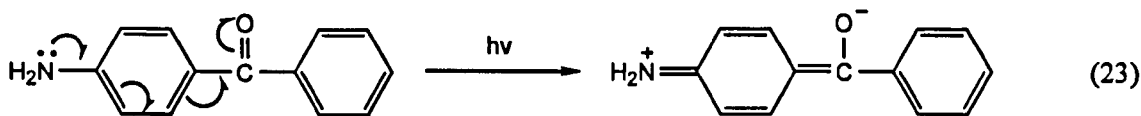
It is widely accepted that there are two mechanisms by which this bimolecular reaction can occur; (a) hydrogen abstraction, and (b) electron transfer followed by proton transfer within an excited state complex^{3,24,29}. The existence of the latter has been shown by the observation of the radical anion using flash photolysis^{42,80} but, since both reactions give the same ketyl and alkylamino radical products, it is difficult to say to what extent each reaction occurs, although it is generally believed that the electron/proton transfer mechanism is dominant.

Hydrogen abstraction

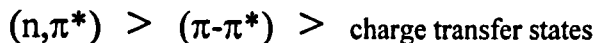
In the presence of a hydrogen donor RH, excited state carbonyls will abstract a hydrogen atom to give a ketyl radical and a radical derived from the donor molecule. This process is most easily illustrated using benzophenone.



As previously mentioned, the reactivity of an excited state is dependent on its nature. For the hydrogen abstraction process, the highest reactivity is observed for an (n,π^*) lowest excited state which has an electron deficient oxygen atom and an electron rich carbon, with the (π,π^*) lowest excited state showing a lower reactivity because the oxygen atom has a higher electron density^{29,81}. In situations where a powerful electron donating group is present on the aromatic ring, such as 4-aminobenzophenone, the lowest lying triplet state displays a charge transfer character (23) and the hydrogen abstraction from a donor molecule is very unfavourable due to the resultant high electron density on the oxygen²⁹.



The hydrogen abstraction ability of excited states can therefore be said to be:



Other factors which affect the efficiency of this process include the excited state energy and the R-H bond strength of the donor molecule. Suitable hydrogen donor molecules include alcohols, ethers and amines.

Electron/proton transfer

Compounds with low ionisation potentials, such as amines, can be used to reduce carbonyl excited states, undergoing electron transfer followed by either proton transfer to the carbonyl within an excited state complex known as an Exciplex, or back electron transfer regenerating the starting materials. The products of this reaction are the ketyl radical and an alkylamino radical, as shown in Figure 1.5 using benzophenone as an example⁸²⁻⁸⁵.

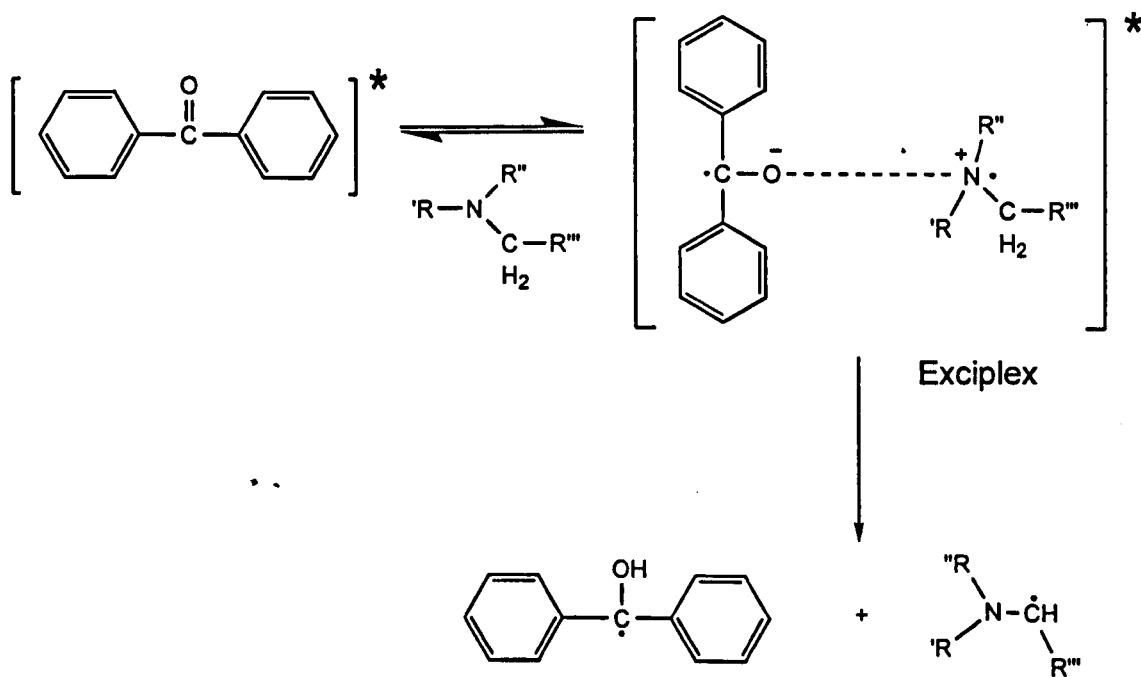


Figure 1.5 *The electron and proton transfer reaction mechanism for Type II photoinitiators with amine synergists*

The most widely used Type II photoinitiators can be classified according to their structural types:

- i) Benzophenones
- ii) Thioxanthenes
- iii) Anthraquinones
- iv) Aromatic 1,2 diketones
- v) Phenyl glyoxylates

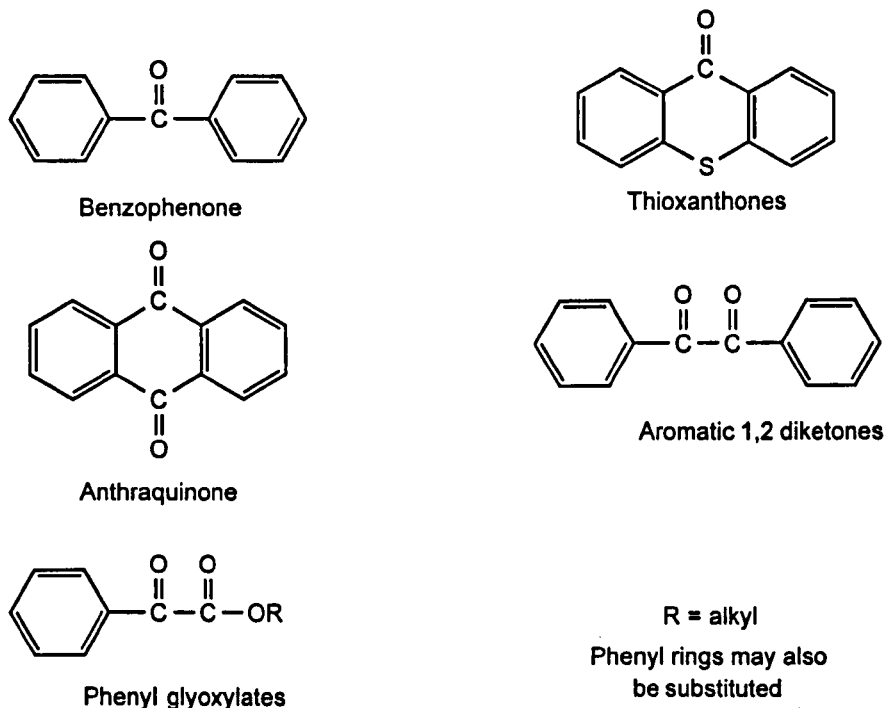


Figure 1.6 Basic structural types of commercial Type II photoinitiators

Other Type II photoinitiators not available commercially, but known to be effective, are ketocoumarins^{86,87}, acridines^{88,89} and α -sulphonyl ketones⁹⁰.

1.4.3 Polymeric/polymerisable photoinitiators

One of the principal problems with UV curing compared to electron beam (EB) curing is that of extractable material. Many inks and coatings are used in areas such as food packaging where unreacted photoinitiators, synergists and their reaction products can migrate, causing taint and odour problems for the manufacturer. It was this type of problem that encouraged the development of polymeric and polymerisable photoinitiators.

The two types of material are distinct in that polymeric photoinitiators generally have pendant groups on a polymer backbone which resemble common photoinitiator molecules, whereas polymerisable photoinitiators are acrylate functional photoinitiator molecules⁹¹. This distinction is shown in Figure 1.7 for three materials which are either commercially available or, in the case of ZLI3331, have been an experimental material produced by a major photoinitiator manufacturer⁹¹.

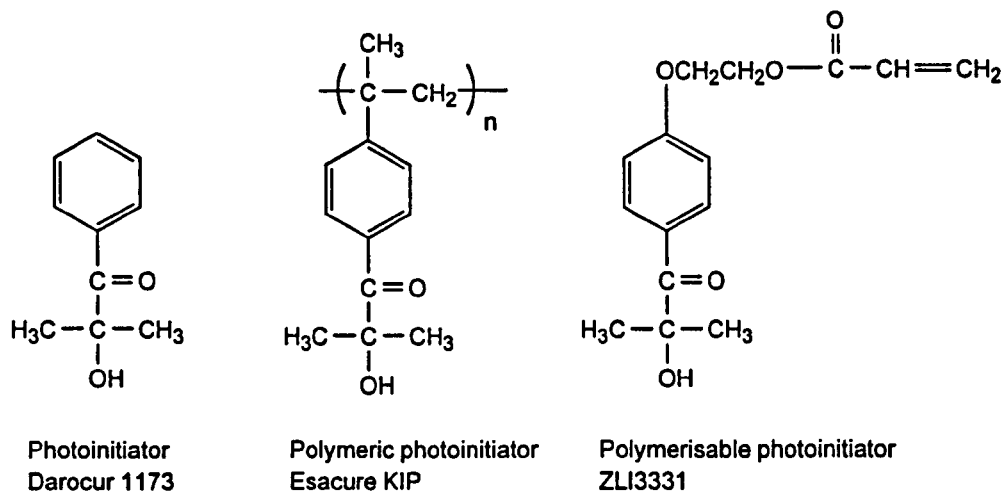


Figure 1.7 *Structural characteristics of polymeric and polymerisable photoinitiators*

The major benefits of polymeric photoinitiators are claimed to be:

- i) Lower amounts of extractable material
- ii) Potentially higher reactivity than their monomeric counterparts due to energy migration along the polymer chain, also known as the antennae effect⁹²
- iii) Synergistic effects when different functional groups are attached to the same polymer backbone⁹³

Polymerisable photoinitiators have also been shown to give lower levels of extractable material than conventional photoinitiators as a result of incorporation into the crosslinked network during cure⁹¹.

Whilst a wide range of both Type I and Type II polymeric and polymerisable photoinitiators have been studied⁹⁴⁻⁹⁶, their relatively high synthesis costs, together with sometimes difficult handling characteristics, mean that they are often not cost effective. To date, only the polymeric α -hydroxy ketone, Esacure KIP, has achieved any significant commercial success.

1.4.4 Amine synergists

As previously outlined, the use of tertiary amine synergists is known to be important for the effective generation of free radicals when using Type II photoinitiators, with the alkylamino radicals being most reactive towards acrylate double bonds. Although there has been some work investigating the structure/activity relationships of aliphatic^{54,97} and aromatic amines⁹⁸⁻¹⁰¹, the author was unable to identify any study involving a comparison of a wide range of amine structural types.

When investigating the effect of different amines on the efficiency of a cure reaction, there are two major factors to consider; the efficiency of the electron and proton transfer process and the reactivity of the resultant alkylamino radicals toward acrylate double bonds. These factors have been reported to be dependent on the ionisation potential of the amine and the nature of the adjacent substituents respectively¹⁰².

There are four basic types of amine synergist used in the UV curing of inks and coatings:

i) Aliphatic amines

These are simple molecules such as triethylamine, triethanolamine and N-methyl diethanolamine. They find most use in screen inks and some coater and dry offset varnishes, but are not used in lithographic applications, as they are water-soluble and will dissolve readily in a fountain solution.

ii) Aromatic amines

The strong odour and high toxicity of aromatic amines such as N,N'-dimethyl aniline mean that almost all the aromatic amines used are esters of 4-dimethylaminobenzoic acid, with the most popular ones being the ethyl and 2-ethyl hexyl derivatives. These types of material are insoluble in water and are the most common synergists used in inks and coatings for lithographic printing processes.

iii) Amino acrylates

These are products of a Michael addition reaction between a secondary amine, normally diethylamine, and an excess of an acrylate monomer, the excess being controlled to give the desired balance of amine groups and acrylate groups in the product. These materials will polymerise into the film and, therefore, extract and migrate less than other amines. Their low cost results in their extensive use in overprint varnishes, but their potential solubility in water and tendency to affect rheology means that they are rarely used in lithographic inks.

iv) Amine functional photoinitiators

4,4'-Bis(dimethylamino)benzophenone, commonly known as Michlers ketone, is the best example of this type of material. Although known not to be a particularly efficient photoinitiator when used on its own, when used in conjunction with benzophenone the combination is very effective⁵⁹. Michlers ketone is no longer used for toxicity reasons, but 4,4'-Bis(diethylamino)benzophenone is still used in some applications, despite some concerns over its safety. Similar materials have been described¹⁰³⁻¹⁰⁵ and the effect of varying the amine group has been investigated, but none are available commercially.

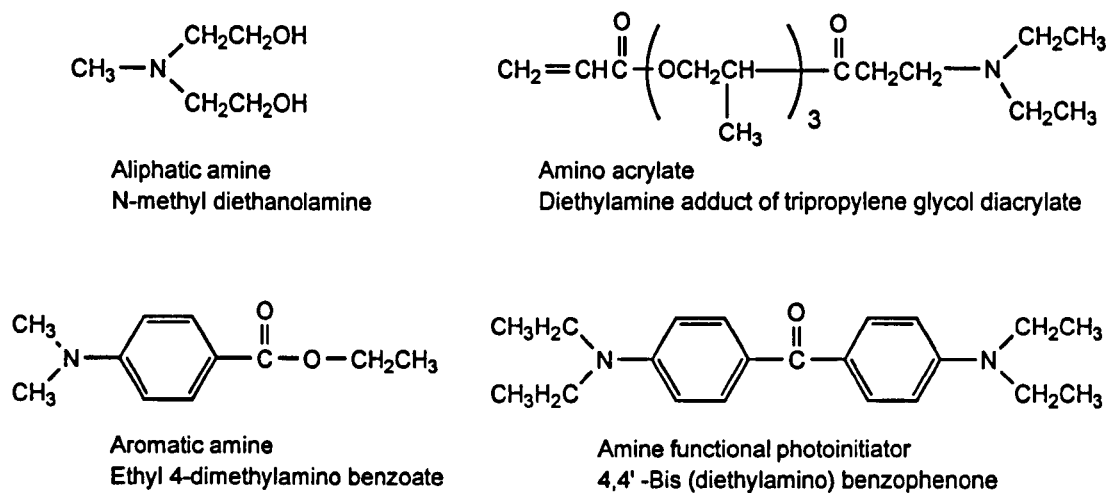


Figure 1.8 *Examples of the types of commonly-used amine synergist*

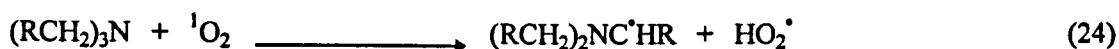
1.4.5 Oxygen inhibition

Virtually all UV curing applications are carried out in a static air environment, often with dissolved oxygen also present in the coating. The effect of molecular oxygen is one of the most serious limitations for UV curing, since it severely inhibits the cure process, leading to a polymerisation induction period, slower polymerisation rates and a lower overall extent of acrylate bond reaction¹⁰⁶. This inhibitory effect increases in severity with decreasing film thickness, since the oxygen can diffuse into a greater part of the film's thickness. However, even in very thick films this results in a tacky surface due to uncured material. These symptoms are a result of two different inhibitory effects of atmospheric oxygen; quenching of excited states and scavenging of free radicals.

Quenching of excited states

Molecular oxygen exists in a triplet ground state configuration which has the ability to quench photoinitiator excited states. This interaction produces the ground state photoinitiator and the excited singlet state oxygen, which quickly reverts to the triplet ground state in a radiationless process. This effect is of little importance with Type I photoinitiators since the singlet and triplet state lifetimes are very short, but the much longer triplet lifetimes for Type II photoinitiators means that they are very susceptible to oxygen quenching in hydrogen abstraction reactions, but not in electron and proton transfer reactions where the radicals are generated within an exciplex⁶⁰.

The unstable singlet oxygen produced when molecular oxygen quenches a photoinitiator excited state has also been claimed^{107,108} to be physically quenched by, and to chemically react with, tertiary amines to yield an alkylamino radical. The relative importance of this process is not known.



Radical scavenging

Since molecular oxygen in its triplet ground state is essentially a diradical, it undergoes reactions with available radicals to produce the significantly less reactive peroxy radicals. These scavenged radicals can be based on an initiator, monomer, aminoalkyl or growing polymer chain. Although the peroxy radical is capable of abstracting a hydrogen from a donor to give a hydroperoxide and a new initiating radical, the process is very slow in comparison with the uninhibited polymerisation reaction, so the high rate of propagation cannot be maintained¹⁰⁶.

The use of amine synergists effectively reduces the effects of oxygen scavenging in a chain reaction, as shown in Figure 1.9 where a peroxy radical, formed when an alkylamino radical reacts with oxygen, rapidly abstracts a hydrogen from another amine synergist molecule to give the hydroperoxide and another highly reactive alkylamino radical^{100,109,110}.

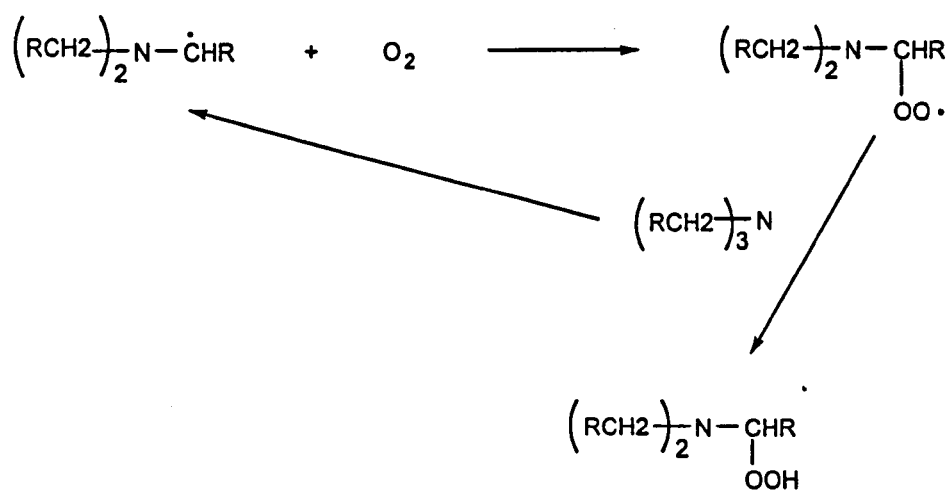


Figure 1.9 *The use of amine synergists to reduce the effects of oxygen scavenging*

The extent of oxygen inhibition can be reduced in a number of ways which fall into two categories:

i) *Physical barrier methods*

By preventing oxygen reaching the surface, inhibition will be restricted to the oxygen dissolved in the coating. This is achieved by the use of an inert nitrogen blanket, either to eliminate or to reduce the level of oxygen, but can also be achieved by use of a polyethylene film or paraffin wax layer¹¹¹. More recently, a photoinitiator has been described which, upon cleavage, allows a lithium alkyl sulphonate to migrate to the surface and act as a barrier⁷⁹.

ii) *Increasing the active radical concentration*

Use of this approach will overwhelm rather than eliminate the effects of oxygen and can be achieved by the use of higher light intensities, higher photoinitiator concentrations, more reactive photoinitiators and the use of oxygen scavengers such as tertiary amines.

1.5 UV sources

A photoinitiator will only become excited and generate the necessary free radicals required for the photopolymerisation of unsaturated groups if it absorbs light of an appropriate wavelength. In the study of photocuring reactions, it is therefore necessary to consider both the absorption spectrum of the photoinitiator and the emission spectrum of the curing lamp used, in order to ensure that the necessary wavelengths are available.

Almost all lamps used in UV curing processes contain mercury to generate the UV radiation. Mercury is particularly suited to this application because of its high volatility in comparison with other metals, allowing significant pressures of mercury vapour to be attained at temperatures of only a few hundred degrees.

The radiation emitted by a mercury vapour lamp is a consequence of electronic transitions occurring in the vapour phase as excited mercury atoms revert back to their ground state configuration. The nature of these electronic transitions has been extensively studied^{5,27,32,112-114}, with all the spectral lines capable of being described, although, for the medium and high pressure mercury lamps, most involve a second excitation from the relatively long-lived $\text{Hg}(^3\text{P}_1)$ state. Decay from these higher states gives rise to a more complex spectrum with emissions throughout the UV, visible and IR regions.

1.5.1 Low pressure mercury vapour lamps

These operate at pressures of 10^{-3} mm Hg and are most often used in germicidal applications such as water sterilisation, but find little use in UV curing since they are relatively low power and essentially monochromatic at 253.7 nm. The small amount of 185 nm light produced (~5%) is absorbed by the tube walls unless highly transmitting quartz is used for the tube manufacture²⁷.

1.5.2 Medium pressure mercury vapour lamps

This type of lamp dominates the UV curing industry, having become an accepted standard over the last 20 years. A typical medium pressure mercury vapour lamp consists of a sealed quartz tube with an electrode at each end containing an exact amount of mercury and a low pressure of a starter gas, typically argon. The starter gas is used to aid the lamp ignition process since, when cold, the lamp contains very few vapour phase mercury atoms. As well as a small amount of direct excitation, the few stray electrons present are accelerated by the applied voltage to energies sufficient to ionise the argon. Recombination of ions and electrons then gives rise to excited argon atoms which, upon collision with mercury atoms, undergo an energy transfer phenomenon called the Penning effect^{27,32}. This is demonstrated in Scheme 1.

Scheme 1

These reactions generate heat which vaporises more of the mercury; a self-accelerating process that, after a few minutes, leads to a state where all the mercury has evaporated and a stable arc exists between the two electrodes. At this point, the surface temperature of the lamp is 600-800°C and the mercury vapour pressure is approximately 1 atmosphere. The high mercury vapour pressure compared to that of the argon starter gas during normal operation means that, once the arc is established, the argon has almost no effect, such that the reactions occurring involve only mercury, as shown in Scheme 2. Also, only a small fraction of electrons have sufficient energy either to excite an argon atom or ionise a mercury atom from the ground state; therefore most ionisations take place in more than one stage.

Scheme 2

Although it is the decay of excited mercury atoms to their ground state that results in the emission of light, the generation of mercury ions is also important, since they act as current carriers between the two electrodes.

The two emission lines at 185 nm and 253.7 nm, which dominate the spectrum of the low pressure mercury vapour lamp, are virtually non-existent in the medium pressure lamp spectrum because of self-absorption of these wavelengths by other mercury atoms nearer the tube walls. Although predominantly still a line spectrum, the emission spectrum of the medium pressure mercury lamp shows some line broadening due to temperature and pressure effects with lines that extend throughout the UV, visible and infra-red regions. A representation of this spectrum is shown in Figure 1.10. This spectrum is characteristic in terms of the major emission lines, but spectra vary slightly owing to differences in mercury pressure and lamp dimensions.

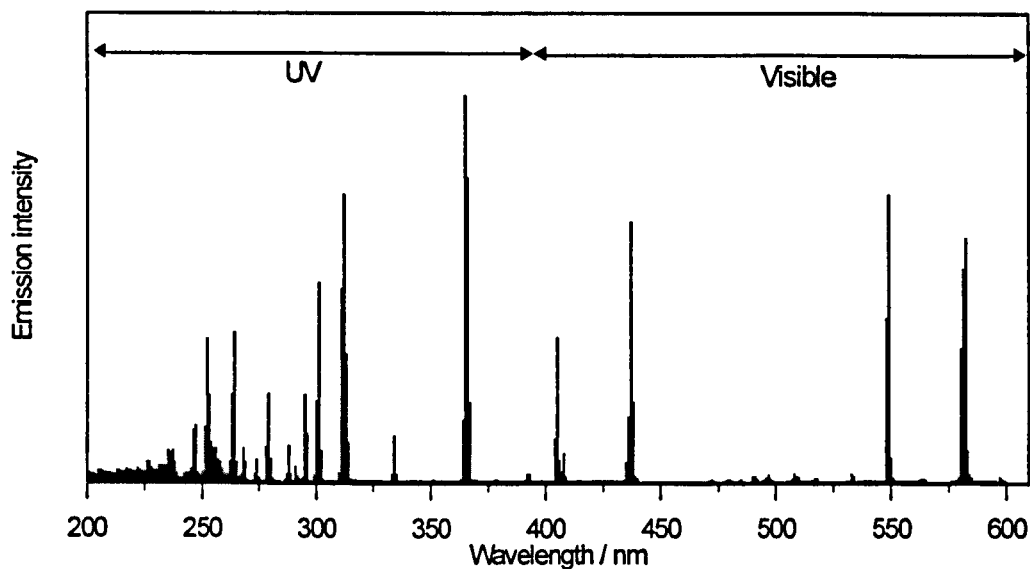


Figure 1.10 Representation of the emission spectrum of a typical medium pressure mercury vapour lamp

The broad hump at wavelengths below 245 nm is still unassigned, but is thought to be due to an ion-electron recombination^{27,113}, which is in the form of a continuum because the kinetic energy of the participants in the collision and of the neutral atom produced could vary continuously. This process is shown in (32).



A typical medium pressure mercury vapour lamp can last in excess of 1000 hours, but lamp failures are rare. The requirement to change a lamp, generally set at approximately 1000 hours^{18,113,115}, is difficult to judge since it is characterised by a slow decline in intensity, particularly at short wavelengths, as the electrodes degrade and contaminate the quartz envelope.

The electrodes consist of a thoriated tungsten rod wrapped in tungsten wire and connected to the electrode leads by molybdenum foil seals. These foil seals are prone to problems, as they must be kept below 300°C to prevent oxidation, while the rest of the lamp operates at 600-800°C; they are one of the few sources of lamp failure¹¹². Electrode deterioration generally results from the sputtering that occurs during the first few seconds of lamp operation¹¹⁶. Although the argon starter gas does help to reduce the extent of this problem, it is the principal reason for lamp ageing; consequently, a lamp's lifetime will be considerably shorter if it is frequently turned on and off.

1.5.3 High pressure mercury vapour lamps

Also called mercury arc capillary lamps, these run at pressures of several hundred atmospheres, containing a mixture of mercury and xenon. They are used in photolithography, but are not generally used in UV curing of coatings and inks because of their short lifetimes of 50-70 hours^{112,117} and their requirement for forced air cooling due to very high operating temperatures.

Although they are ten times as intense as medium pressure lamps²⁷, their emission spectrum is continuous with a light superimposition of line emissions. This is partly due to temperature and pressure effects giving line broadening and partly due to the formation of excited dimers with ground state mercury atoms³², as shown in Scheme 3.

Scheme 3



1.5.4 Electrodeless lamps

The Fusion Systems Corporation (FSC) in the USA supplies a patented medium pressure mercury vapour lamp which has a similar emission spectrum to the conventional electrode-containing lamp²⁷, shown in Figure 1.10, but uses different technology to achieve it. The lamps have no electrodes, consisting of a sealed quartz tube containing mercury and a starter gas. The excitation power source is, instead of an electrical arc, a 2450MHz microwave field around the lamp created by two matched 1500W magnetrons. The ignition is triggered by a small low pressure lamp which irradiates the mercury droplets with 253.7 nm radiation, causing the emission of photoelectrons. These then accelerate in the microwave field, causing a rapid increase in the number of current carriers and the evaporation of mercury as the lamp warms up. The whole ignition process is very fast, taking approximately 10 seconds, or 2-3 seconds if the magnetrons are kept in their standby mode.

There is a number of advantages and disadvantages associated with this design relative to conventional electrode-containing lamps^{18,27,115}. These are summarised below, but it is the balance of these factors which determines which choice is more desirable for a given process. In the printing ink industry, the electrode-containing lamps are still dominant by far.

Advantages of electrodeless lamps

- 1 Simple, easy to install, modular system.
- 2 Longer lifetimes (~3000 hours compared with ~1000 hours for electrode-containing lamps).
- 3 Fast warm up times (2-3 seconds compared to several minutes).
- 4 No requirement for lamp to cool for 10 minutes before re-strike.
- 5 Smaller and lighter tubes result in a lower heat capacity, so when the lamps are switched off there is virtually no residual infra-red from the lamp and therefore no requirement for a shutter system.
- 6 Smaller tube diameter allows increased intensity through better focusing.
- 7 Doping materials can be easily used to alter the emission spectrum. These materials are difficult to use in conventional lamps because they attack the electrodes.
- 8 The discharge occupies the whole length of the tube, so an array is possible.

Disadvantages of electrodeless lamps

- 1 They are only available in 24cm length tubes; longer lengths would require a series of 4 or more matched magnetrons which would make them much more expensive.
- 2 The relatively expensive magnetrons require replacement every 5000 hours.
- 3 High power input required due to low efficiency microwave generation process.
- 4 The modular arrangement requires a lot of space.

1.5.5 Doped lamps

Doped lamps contain both mercury and a small amount of another metal which modifies the emission spectrum to some degree. The lower volatility of these additive metals is such that they are generally added as the metallic iodide which volatilises and dissociates at the high plasma temperatures during operation to give the parent metal and iodine²⁷. The lower ionisation and excitation energy of the typical dope metal means that, even at the low additive level, it can dominate the emission spectrum of the lamp.

The most successful use of doped lamps has been with the FSC electrodeless lamps, where a number of different doped lamps are available, the UV emission spectra of which are shown in Figure 1.11 (a-d). Analysis of the extra emission lines produced²⁷ identified the doping metals as tin in the A type lamp, iron in the D type, lead in the M type and gallium in the V type. Although these doped lamps have been available for some time and are claimed to offer a number of advantages in terms of cure speed¹¹⁸⁻¹²⁰ and depth of cure, they have not been well used in the inks and coatings market.

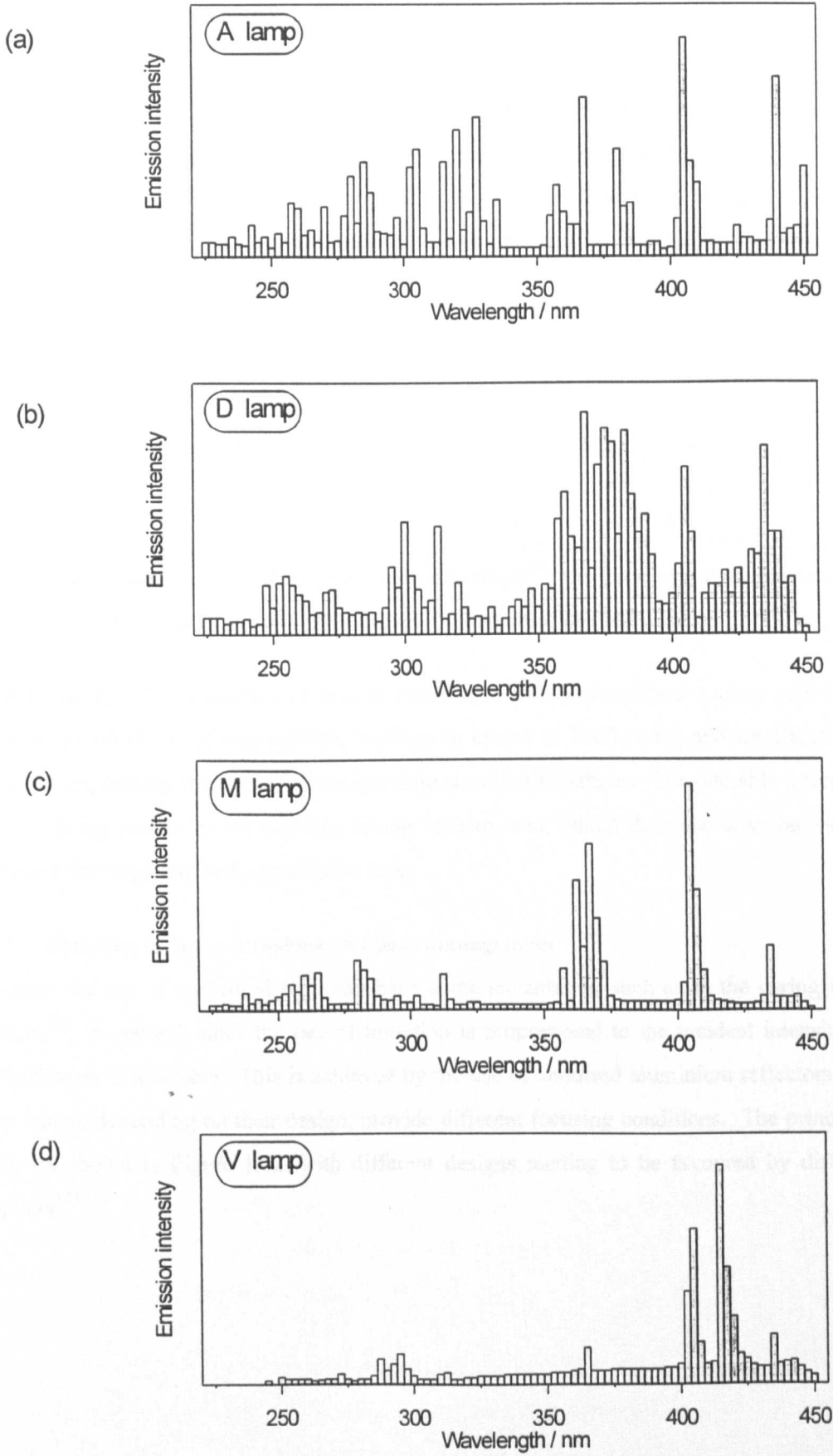


Figure 1.11 *UV emission spectra of doped lamps*

1.5.6 Excimer lamps

Excimer lamps, originally developed by ABB Infocom Ltd, Switzerland^{121,122}, have recently been commercialised by Heraeus Noblelight GmbH, Germany¹²³. In contrast to the polychromatic emission spectra of conventional medium-pressure mercury curing lamps, these have largely monochromatic emissions, the wavelength of which is dependent on the gas used in the bulb. Their operating principle is based on the excitation of molecules within a gas mixture to form excited dimers (excimers), which then revert back to the ground state giving out light of a characteristic wavelength, as shown in scheme 4.

Scheme 4



Although many excimer emissions have been described¹²³, the currently available lamps include Xenon (172 nm), Krypton chloride (222 nm) and Xenon chloride (308 nm).

Excimer lamps offer a number of unique advantages over conventional curing lamps, the most important of which are instant ignition, lifetimes in excess of 1000 hours, and significantly reduced IR emissions, making them ideal for temperature sensitive substrates. Considerable interest in these lamps is being shown by the radiation curing industry and, whilst their use is so far very limited, continued developments will attract more users.

1.5.7 Focusing of lamp emissions and heat management

Although the use of unfocused light can have some advantages, such as in the curing of irregular surfaces¹¹⁵, in general, since the rate of initiation is proportional to the incident intensity, a highly focused beam is desirable. This is achieved by the use of anodised aluminium reflectors behind the lamp which, depending on their design, provide different focusing conditions. The principal design types are shown in Figure 1.12, with different designs tending to be favoured by different lamp suppliers¹²⁴.

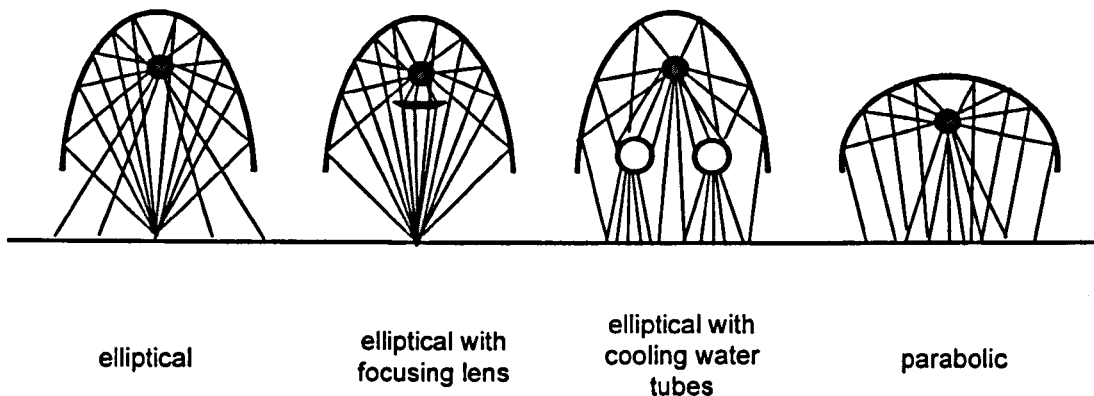


Figure 1.12 *Types of reflector used with UV curing lamps*

The problem associated with focusing of UV radiation is one of heat; approximately 60% of the energy output from a UV lamp is in the form of infra-red radiation, so if the UV radiation is focused, so is the heat. In the event of a sudden stoppage this large heat output can cause problems such as the ignition of the substrate. For this reason, many commercial lamp systems are fitted with shutters, sometimes in the form of revolving reflectors that move between the lamp and the substrate in the event of a line stoppage.

Heat is of potential benefit to the UV curing process, since it will reduce the viscosity of the formulation and thereby increase the mobility of the acrylate groups during polymerisation. However, the amount of heat generated is far in excess of the amount required for this benefit and, if unregulated, would lead to a number of potentially serious problems such as the evaporation of volatile components in the formulation, evaporation of water from paper based substrates affecting their mechanical properties, and shrinkage or deformation of plastic substrates^{113,125}.

A number of methods of heat removal have been developed by lamp suppliers, a combination of which is generally used in most situations^{115,124-126}:

- i) chilled heat sink behind the substrate;
- ii) chilled print drum;
- iii) chilled reflectors;
- iv) dichroic reflectors (reflect most of the UV, but allow IR to pass through);
- v) water filters between the lamps and the substrate;
- vi) positive or negative air purge.

Situations where the lamps are over-cooled can also be problematic since a stable arc cannot exist at reduced temperatures. Consequently lamps cutting out is a common occurrence.

The energy output of UV curing lamps has increased greatly since the first commercial press was installed in 1972¹²⁶. Early lamps were rated at 80 W/cm, but this has now increased to a standard of 120 W/cm or 160 W/cm. The increase in power is very beneficial to the cure rate, with one 160

W/cm lamp being as powerful in terms of curing ability as two 120 W/cm lamps^{119,120}. However, the large amount of additional heat and the shorter lifetimes of these high power lamps have prevented the development and use of even higher power versions^{18,120}.

1.5.8 Hazards associated with UV light sources

There are two principal hazards to the operator associated with the use of UV curing equipment: stray UV radiation and ozone production. The damaging effects of UV radiation on the eyes and skin are well understood²⁷; consequently, legislation exists for the design of these systems such that not even reflected radiation escapes from the equipment. The effect of ozone is much more serious because of its highly oxidising nature. It is produced by the action of short wavelength UV radiation (< 240 nm) on oxygen, and is particularly problematic during the initial startup of medium pressure lamps where, before they reach normal operating temperatures and pressures, they behave like low pressure lamps, emitting radiation at 185 nm^{18,27,113}. During normal operation, self-absorption of 185 nm light and the temperature-dependent shift in the transmission cut-off of the quartz envelope towards longer wavelengths, reduce the ozone production²⁷, but good extraction is still required to prevent over-exposure.

Ozone-free lamps have been described²⁷ which use additives in the quartz to prevent the emission of light below 240 nm. Whilst these are safer, they have also been found to be considerably less effective in curing terms because much of the important radiation below 300 nm is reduced^{18,57}.

1.6 Formulating UV curable coatings

Although almost all UV curable inks and coatings use similar raw materials, they are extremely diverse in their exact composition owing to the number of different printing processes and applications for which they are formulated. With the exception of varnishes which do not contain pigment, all UV curable formulations contain the following materials⁵⁰.

Pigment	5-25%
Oligomer	20-60%
Monomer	10-50%
Photoinitiator	3-8%
Synergist	2-10%
Additives	1-10%

1.6.1 Pigment

Inks appear coloured to an observer by virtue of their interaction with incident light in the visible region of the electromagnetic spectrum (390-780 nm). The incident light is scattered by, penetrates into and is reflected off an ink film by the pigment particles such that the perceived colour is determined by what wavelengths of visible light remain in what reaches the observer^{127,128}. Pigment

is therefore the single most important component in an ink formulation, since, at the most basic level, all the other components serve to keep the pigment in place on the substrate.

In 1905, Munsell introduced the concept of colour space¹²⁹, a system that could define all colours in three dimensional space. The three axes used to define the colour are most often called hue, lightness and chroma. Hue represents the shade of colour, for which there are ten major divisions based on blue, purple, red, yellow, green and one subdivision between each. These are arranged into a Munsell hue circle where each of these ten major divisions is subdivided into ten more, such that, as shown in Figure 1.13, a yellow shade may be described as a 3Y and a greenish yellow shade as a 9GY.

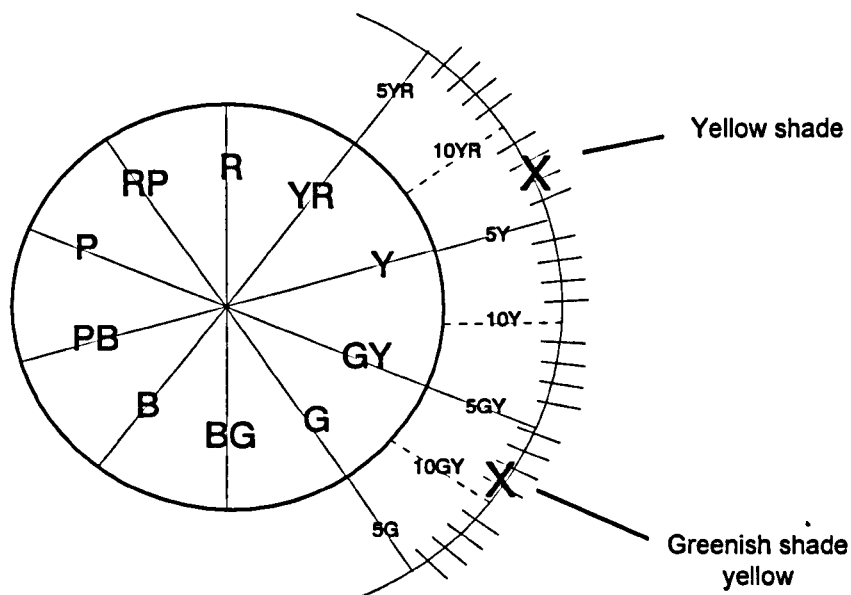


Figure 1.13 *A Munsell hue circle*

The Munsell hue circle, often called a colour wheel, is also used to describe the chroma, additionally known as the intensity, strength or saturation of a colour. This is indicated by the distance away from the centre of the wheel, with greater distances representing stronger colours.

The perceived colours black and white cannot strictly be termed colours because they do not possess a hue. However, they can be described in terms of their degree of lightness, where black has a lightness of 0% and white has a lightness of 100%. This third axis of colour space runs vertically through the centre of the colour wheel.

When considered together, the hue lightness and chroma give rise to the three dimensional concept of colour space, shown graphically in Figure 1.14. Using this system, a colour may be described as a 10Y8/7, which means it is a yellow shade with a hue of 10, lightness of 8 and chroma of 7. The CIELab (Commission Internationale de l'Eclairage - International Commission on Illumination) colour matching system is based on this approach, describing colour numerically; standardised by controlling all the factors which affect the perceived colour such as particle size, film thickness and

the type of light source. Colour matching is largely based on the use of reference standards such as those held by all printing ink manufacturers, as well as a number of national and international sets like the Pantone™ system, but computer aided colour matching is proving to be ever more reliable.

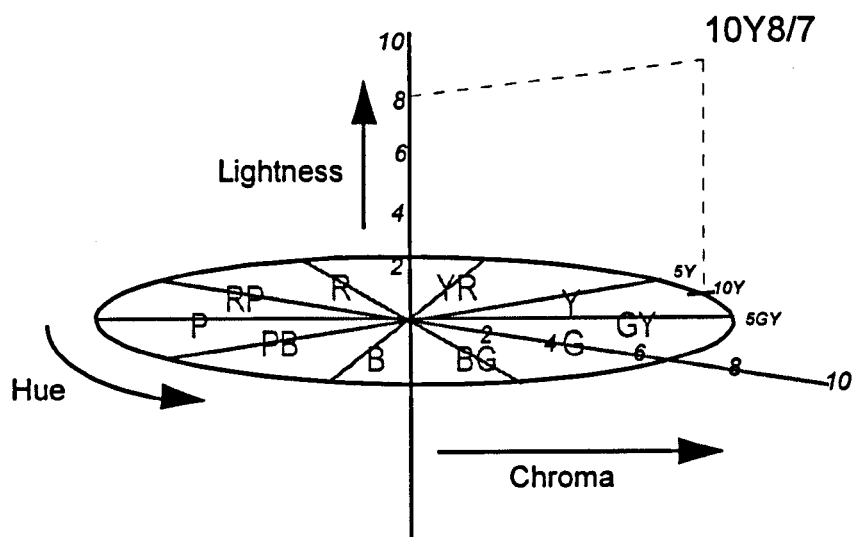


Figure 1.14 Graphical representation of a colour in colour space

As well as being able to describe a colour using the concept of colour space, the pigments themselves can be described using their Colour Index (CI) classification and number. The Colour Index system was introduced in 1924 by the British Society of Dyers and Colourists and classifies pigments according to their chemical structure using a Colour Index name such as Pigment Red 8 or Pigment Yellow 13 and a serial number. A variety of other trivial names are also frequently associated with a particular pigment, but these are not part of the CI classification system.

In addition to its shade, a formulator would choose an appropriate pigment based on a number of other factors, including ease of dispersion, flow properties of the ink, light-fastness and price. A pigment is chosen for the best balance of these properties, but often requires toning with other pigments to achieve the desired shade.

As well as absorbing light in the visible region of the electromagnetic spectrum, pigments also absorb UV light, competing for incident light with the photoinitiator. However, despite the relatively weak pigment chromophores in the UV region, by virtue of the large quantities of pigment used their effect is quite significant and is discussed in greater detail in Chapter 4.

In general, printers use a four colour 'process' set of inks consisting of yellow, magenta, cyan and black to achieve the desired image by printing them as a series of dots, which when viewed from a distance resemble a particular shade; rather like the picture construction on a television. However, large areas of a particular shade are often generated using a specific ink, termed a 'spot' colour, which is manufactured either using a blend scheme system or as a special formulation. Spot colours

are often used in cases where, for example, a specific corporate colour is required that may be difficult to control adequately using four colour process printing. Since each spot colour requires a dedicated print station, a particular printing job would rarely involve more than two spot colours in addition to the four process colours.

1.6.2 Oligomers

The oligomer, also known as the prepolymer, is used to disperse the pigment and provides much of the structural and cure characteristics of the formulated coating. With the exception of unsaturated polyesters, which are used almost exclusively for the wood coatings industry, there are three types of oligomer that find significant use in UV curing; epoxies, urethanes and polyesters; although within each category there is a large number of structural variants. It is rare to find one oligomer that will work in all situations, so several different oligomers are often required in a formulation to give the correct balance of properties^{6,50,130}.

i) *Epoxy acrylates*

These are prepared by the reaction of an epoxy group with acrylic acid, the most common example being the reaction product of bisphenol A diglycidyl ether with acrylic acid. Epoxy acrylates are fast-curing, but have high viscosities and relatively poor pigment wetting ability, although this is often addressed by esterifying some of the residual hydroxyl groups with long chain fatty acids. Their low cost means that they are generally the main oligomer used in ink formulations.

iii) *Urethane acrylates*

Urethane acrylates are prepared by reacting isocyanate groups with an alcohol functionality, typically hydroxy ethyl acrylate. Although generally noted for their toughness, the wide range of isocyanates available, together with the use of polyols, polyesters and polyethers as flexibilising groups, means that a very diverse set of structural properties can be achieved using urethane technology. The relatively high cost of the raw materials, particularly the aliphatic isocyanates such as hexamethylene diisocyanate (HMDI) precludes a more widespread use.

iii) *Polyester acrylates*

Polyester acrylates are made by the condensation reaction of acrylic acid with the hydroxyl groups on a polyether backbone, or by the reaction of the polyester acid group with a hydroxy acrylate. Although their specific properties can vary quite considerably, polyesters show generally good pigment wetting ability but poor resistance properties, particularly to alkalis. Their generally low viscosities, low cost and good compatibility with other oligomers means they are used extensively.

1.6.3 Monomers

The original use of monomers or multifunctional acrylates (MFAs) was as a viscosity reducer for the highly viscous oligomers used in radiation curing, enabling the inks and coatings to be printed by the

same process as the inherently lower viscosity conventional systems. The earliest monomers used for this purpose were typically 2-ethylhexyl acrylate and butyl acrylate, but these were soon replaced by acrylates of polyols such as pentaerythritol, trimethylolpropane, tripropylene glycol, hexanediol and neopentyl glycol¹³⁰. These highly functional diluents proved to be very reactive and led to their additional use specifically as "reactive diluents", improving cure speed and, through the formation of a more highly crosslinked network, resistance properties.

The high irritancy of many of the monomers listed above has led to their declining use and was the main reason for early health concerns associated with UV curing. Indeed, although many are still used widely throughout Europe and the rest of the world, all but tripropylene glycol diacrylate (TPGDA) have been the subject of a voluntary ban in the UK by the Society of British Printing Ink Manufacturers (SBPIM). Use of these materials has been largely replaced by lower irritancy alkoxyated polyol acrylates such as ethoxyated trimethylolpropane triacrylate (TMPTOEA) and propoxyated glycerol triacrylate (GPTA) which retain good cure speed and have improved flexibility over earlier materials.

Use of monomers with functionalities greater than 3 is much less common because of the greater brittleness associated with coatings containing them, but di-trimethylol propane tetraacrylate (Di-TMPTA) and di-pentaerythritol pentaacrylate (Di-PETA) are the most commonly used examples. Use of monofunctional monomers is also rare in printing inks because of the greater risk of unreacted extractable material and their generally higher odour. However, their very high flexibility means that monofunctional acrylates, such as dodecyl acrylate find some use in thicker coatings such as screen inks where this property is of greater importance.

1.6.4 The measurement of cure

The curing process occurs when, following the production of free radicals by the photoinitiator, acrylate double bonds are consumed in a free radical chain polymerisation reaction. The assessment of cure is, however, both variable and subjective, with the term 'fully cured' being applied to a product that has met its performance and resistance requirements rather than having achieved some actual quantitative cure state.

Cure testing is most often based on a series of physical tests designed to assess surface cure (the achievement of a tack-free state), through cure (the thumb twist test) and product resistance (scratch test)⁵⁷. These tests have the advantage of being quick and easy, but are subjective and not particularly differentiating, so a side by side comparison is often done using both the test formulation and a standard formulation. Various other physical tests such as tape adhesion, solvent resistance and flexibility are also used, but their precise procedures vary between individuals and companies.

The relative insensitivity and low differentiating ability of physical tests means that instrumental methods giving accurate and reproducible quantitative results are desirable in order to achieve the aims of this work. Some instrumental techniques have been described which are designed for product testing, including the Ink-Cure Analyser™ which measures the evaporation profile of a ¹³C labelled solvent from a print sample¹³¹, the UV Curetester which measures the force required to move a stylus across a coating surface¹³², and the Fluorescence Probe Cure Tester¹³³ which measures the blue shift in the fluorescence emission spectrum of an additive compound as a result of changes in its local viscosity or microviscosity.

The most established techniques for measuring cure involve monitoring the change in some chemical or physical characteristic of the coating, such as the loss of acrylate double bonds^{134,135} or changes in the rheology/viscosity¹³⁶⁻¹³⁸. Certain properties of the cured film can also be used to give information about the cure efficiency, these include T_g^{139,140}, hardness¹⁴¹, solvent resistance¹⁴², extractables¹⁴³ and shrinkage¹⁴⁴.

1.7 References

- 1 P Dufour in *Radiation Curing in Polymer Science and Technology (Volume I - Fundamentals and Methods)*; J P Fouassier and J F Rabek (Eds), Elsevier Science Publishers Ltd, Barking, Essex, 1 (1993).
- 2 A J Bean and R W Bassemir in *UV Curing: Science and Technology*; S P Pappas (Ed), Technology Marketing Corporation, Connecticut, USA, 185 (1978).
- 3 J P Fouassier in *Radiation Curing in Polymer Science and Technology (Volume I - Fundamentals and Methods)*; J P Fouassier and J F Rabek (Eds), Elsevier Science Publishers Ltd, Barking, Essex, 49 (1993).
- 4 G K Noren, A J Tortorello, J T Vandeburg; *Proc. Conf. RADTECH*, Chicago, Illinois, USA, 2, 201 (1990)
- 5 C G Roffey; *Photopolymerisation of Surface Coatings*, John Wiley & Sons Ltd (1982)
- 6 R Holman (Ed); *UV & EB Curing Formulation for Printing Inks, Coatings and Paints*, SITA-Technology (1984).
- 7 J J Shulman; *North American Tag and Label*, Sept/Oct, 14 (1994).
- 8 R W Stowe; *Proc. Conf. RADTECH*, Orlando Florida, 353 (1994).
- 9 A J Bean; *Proc. Conf. TAPPI*, Orlando, Florida, 317 (1989).
- 10 P G Schessler; *American Ink Maker*, 65 (8), 36 (1987).
- 11 J D Visser; *TAPPI Journal*, Feb (1989).
- 12 D C Armbruster and D E Fergesen; *Proc. Conf. TAPPI*, San Francisco, USA (1987).
- 13 P Elliott; *Radiation Curing in Coates: An Overview*, Coates Lorilleux internal document (1988).
- 14 S J Bett, P A Bwarjany and J L Garnet; *Proc. Conf. RADTECH*, Boston, USA, 122 (1992).
- 15 U V Läuppi; *Proc. Conf. RADTECH*, Boston, USA, 668 (1992).
- 16 A J Bean in *Radiation Curing: Science and Technology*; S P Pappas (Ed), Plenum Press, New York, 301 (1992).
- 17 P Dufour; *Polymers Paint and Colour Journal*, Jan, 23 (1995).
- 18 H R Ragin in *Radiation Curing: Science and Technology*; S P Pappas (Ed), Plenum Press, New York, 273 (1992).
- 19 G W Gruber in *UV Curing: Science and Technology*; S P Pappas (Ed), Technology Marketing Corporation, Connecticut, USA, 171 (1978).
- 20 C H Williams; *Polymers Paint and Colour Journal*, 185 (4369), S2 (1995)
- 21 V Gianinetto; *Proc. Conf. RADTECH*, Orlando, Florida, 293 (1994).
- 22 P G Garratt; *Proc. Conf. RADTECH*, Orlando, Florida, 658 (1994).
- 23 H Rubin; *Proc. Conf. TAGA*, 279 (1976).
- 24 P K T Oldring in *Chemistry and Technology of UV and EB Formulation of Coatings, Inks and Paints (Volume 3 - Photoinitiators for Free Radical and Cationic Polymerisation)*; P K T Oldring (Ed), SITA Technology Ltd, 1(1991).

- 25 N S Allen, M Edge; *Degradation and Stabilization of Polymers* - Lecture Course, Manchester Polytechnic, Manchester.
- 26 J G Calvert, J N Pitts; *Photochemistry*, John Wiley and Sons (1966).
- 27 R Phillips; *Sources and Applications of Ultraviolet Radiation*, Academic Press Inc., London (1983).
- 28 B Schaeffer, S Jönsson and M R Amin; *Proc. Conf. RADTECH*, Orlando, Florida, 314 (1994).
- 29 A Gilbert, J Baggot; *Essentials of Modern Photochemistry*, Blackwell Scientific Publications (1991).
- 30 N J Turro; *Modern Molecular Photochemistry*, The Benjamin/Cummings Publishing Co. Ltd, Philippines (1978).
- 31 J D Coyle; *Introduction to Organic Photochemistry*, J Wiley & Sons Ltd (1986).
- 32 J A Barltrop, J D Coyle; *Excited States in Organic Photochemistry*, John Wiley and Sons Ltd (1975).
- 33 J D Coyle in *Photochemistry in Organic Synthesis*; J D Coyle (Ed.), Royal Society of Chemistry, London, 1 (1986)
- 34 W Rutsch, G Berner, R Kirchmayr, R Hüsler, G Rist and N Bühler; *Proc. Xth Int. Conf. in Organic Coatings Science and Technology*; Athens, Greece, 241 (1984).
- 35 K Dietliker, M W Rembold, G Rist, W Rutsch and F Sitek; *Proc. Conf. RADTECH*; Florence, 37 (1987).
- 36 J P Fouassier and D Burr; *Eur. Polym. J.*, **27** (7), 657 (1991).
- 37 J P Fouassier and D Ruhlmann; *Proc. Conf. RADTECH*, Edinburgh, 499 (1991).
- 38 V L Ermolaev and A N Terenin; *J Chim. Phys.*, **55**, 698 (1958).
- 39 J N Pitts, Jr, R L Letsinger, R P Taylor, J M Patterson, G Recktenwald and R B Martin; *J. Amer. Chem. Soc.*, **81**, 1068-1077 (1959).
- 40 A Beckett, G Porter; *Trans. Faraday Soc.*, **59**, 2038 (1963).
- 41 N S Allen, D Mallon, I Sideridov, A Green, A Timms, F Catalina; *Eur. Polym. J.*, **28** (6), 647 (1992).
- 42 J P Fouassier, D J Lougnot; *Polymer Communications*, **31** (11), 418 (1990).
- 43 M Sander and C C Osborn; *Tetrahedron Lett.*, 415 (1974).
- 44 P J Flory; *Principles of Polymer Chemistry*, Cornell University Press, Ithaca and London (1953).
- 45 E Selli, I R Bellobono in *Radiation Curing in Polymer Science and Technology (Volume III - Polymerisation Mechanisms)*; J P Fouassier and J F Rabek (Eds), Elsevier Science Publishers Ltd, Barking, Essex, 1 (1993).
- 46 C E Hoyle in *Radiation Curing: Science and Technology*; S P Pappas (Ed), Plenum Press, New York, 57 (1992).
- 47 G R Tryson, A R Shultz; *Journal of Polymer Science: Polymer Physics Edition*, **17**, 2059 (1979).

- 48 A T Doornkamp, Y Y Tan; *Polymer Communications*, **31**, 362 (1990).
- 49 K Dietliker in *Radiation Curing in Polymer Science and Technology (Volume II - Photoinitiating Systems)*; J P Fouassier and J F Rabek (Eds), Elsevier Science Publishers Ltd, Barking, Essex, 155 (1993).
- 50 I Hargreaves in *The Printing Ink Manual - 5th Edition*; R H Leach, R J Pierce (Eds), Blueprint, London, 636 (1993).
- 51 Z W Wicks Jr, W Kuhhirt; *J. Paint Technology*, **47** (610), 49 (1975).
- 52 L R Gatechair; *Proc. Conf. RADTECH*, New Orleans, USA, 28 (1988).
- 53 L R Gatechair; A M Tiefenthaler; *ACS Symposium Series No.417*, 27 (1990).
- 54 E Beck, E Keil, M Lokai, J Schröder; *Radcure Letter*, **5**, 67 (1994).
- 55 K Dorfner in *Radiation Curing of Polymers II*; D R Randell (Ed), Royal Society of Chemistry, London, 216 (1991).
- 56 L Cataliz and J P Fouassier; *Die Angewandte Makromolekulare Chemie*, **218** (3813), 81 (1994).
- 57 R W Bassemir and A J Bean; *Proc. Conf. TAGA*, St Paul, Minnesota, 133 (1974).
- 58 A Green, A Timms, P Green; *Polymers Paint and Colour Journal*, **182** (4299), 40 (1992).
- 59 G Hencken; *American Ink Maker*, **March**, 57 (1978).
- 60 H J Hageman in *Photopolymerisation and Photoimaging Science and Technology*; N S Allen (Ed), Elsevier Science Publishers Ltd, Barking, Essex, 1 (1989).
- 61 H F Gruber; *Prog. Polym. Sci.*, **17**, 953 (1992).
- 62 C H Chang, A Mar, A Tiefenthaler, D Wostratzky in *Handbook of Coatings Additives, Volume 2*; L J Calbo (Ed.), Marcel Dekker Inc., New York, USA, 1 (1992).
- 63 B M Monroe, G C Weed; *Chem. Rev.*, **93**, 435 (1993).
- 64 R S Davidson; *J. Photochem. Photobiol. A: Chem.*, **73**, 81 (1993).
- 65 V D McGinniss in *Developments in Polymer Photochemistry - 3*; N S Allen (Ed), Applied Science Publishers Ltd, Barking, Essex (1982).
- 66 S C Lapin in *Radiation Curing: Science and Technology*; S P Pappas (Ed), Plenum Press, New York, 241 (1992).
- 67 J V Crivello in *Radiation Curing in Polymer Science & Technology (Volume II - Photoinitiating Systems)*; J P Fouassier, J F Rabek (Eds), Elsevier Science Publishers Ltd, Barking, Essex, 435 (1993).
- 68 J V Crivello, K Dietliker in *Chemistry and Technology of UV and EB Formulation for Coatings, Inks and Paints (Volume 3 - Photoinitiators for Free Radical and Cationic Polymerisation)*; P K T Oldring (Ed), SITA Technology Ltd, London, 327 (1991).
- 69 H G Heine, H J Rosenkrantz, H Rudolph; *Angew. Chem. Internat. Edit.*, **11**, 974 (1972)
- 70 G Li Bassi, L Cadona, F Broggi; *Proc. Conf. RADTECH*, Dearborn Michigan, USA, 4-27 (1986)
- 71 A Ajayaghosh, S Das, M V George; *Journal of Polymer Science: Part A: Polymer Chemistry*; **31**, 653 (1993).

- 72 W Kern, K Hummel; *Makromol. Chem.*, **194**, 2641 (1993).
- 73 R Awad, W Kern, K Hummel; *Farbe und Lack*, **99** (12), 991 (1993).
- 74 P Bosch, F del Monte, J L Mateo, R S Davidson; *J. Photochem. Photobiol. A: Chem.*, **73**, 197 (1993).
- 75 P Bosch, F del Monte, J L Mateo, R S Davidson; *J. Photochem. Photobiol. A: Chem.*, **78**, 79 (1994).
- 76 F Morlet-Savary, J P Fouassier, H Tomioka; *Polymer*, **33** (19), 4202 (1992).
- 77 N S Allen, S J Hardy, A F Jacobine, D M Glaser, B Yang, D Wolf, F Catalina, S Navaratnam, B J Parsons; *J. Applied Polymer Science*, **42**, 1169 (1991).
- 78 H A Gaur, C J Groenenboom, H J Hageman, G T Harkvoort, P Oosterhoff, T Overeem, R J Polman, S Van der Werf; *Makromol. Chem.*, **185**, 1795 (1984).
- 79 H J Hageman, L G J Jansen; *Makromol. Chem.*, **189**, 2781 (1988)
- 80 N S Allen, F Catalina, P N Green, W A Green; *Eur. Polym. J.*, **21** (10), 841 (1985).
- 81 P J Wagner; *Topics in Current Chemistry*, **66** (1), 1 (1976).
- 82 J C Scaiano; *J. Photochem.*, **2**, 81 (1973).
- 83 M Hoshino, H Shizuka in *Photo-induced Electron Transfer, Part C: Photo-induced Electron Transfer Reactions: Organic Substrates*, M A Fox and M Chanon (Eds), Elsevier, Amsterdam (1988).
- 84 J Mattay; *Synthesis*, **4**, 233 (1989).
- 85 P S Mariano, J L Stavinoha in *Synthetic Organic Photochemistry*; W M Horspool (Ed), Plenum Press, New York (1984).
- 86 J P Fouassier, S K Wu; *J. Applied Polymer Science*, **44**, 1179 (1992).
- 87 J L R Williams, D P Specht, S Farid; *Polymer Engineering and Science*, **23** (18), 1022 (1983).
- 88 D Braun, R Gehrish; *Polymer Photochemistry*, **6**, 415 (1985).
- 89 Hitachi Chemical Co. Ltd; *European Patent EP0503076A1* (1991).
- 90 P Di Battista, G Li Bassi, M Cattaneo; *Proc. Conf. RADTECH*, Maastricht, 223 (1995).
- 91 G Wehner, J Ohngemach; *Proc. Conf. RADTECH*, Chicago, Illinois, **2**, 1 (1990)
- 92 R S Davidson; *Proc. Conf. Aspects of Photoinitiation*, Egham, England, 97 (1993).
- 93 L Angiolini, D Caretti, E Corelli, C Carlini; *J. Applied. Polym. Sci.*, **55**, 1477 (1995).
- 94 A Dias; *PhD Thesis*, The University of Kent at Canterbury (1994).
- 95 L Angiolini, D Caretti, C Carlini, N Lelli, P Rolla; *Journal of Applied Polymer Science*, **48**, 1175 (1993).
- 96 F Catalina, C Peinado, R Sastre, J L Mateo, N S Allen; *J. Photochem. Photobiol. A*, **47**, 365 (1989).
- 97 X T Phan, M B Grubb; *J. Macromol. Sci-Chem.*, **A25** (2), 143 (1988).
- 98 S Göthe; *Proc. Conf. FATIPEC (17th)*, 13 (1984).
- 99 J L Mateo, P Bosch, A E Lozano; *Macromolecules*, **27**, 7794 (1994).

- 100 G Berner, R Kirchmayr, G Rist; *J. of Oil Col. Chem. Assoc.*, **61**, 105 (1978).
- 101 P C Adair; *Proc. Conf. RADTECH*, Orlando, Florida, 564 (1994).
- 102 V D McGinniss; *Photogr. Sci. Eng.*, **23** (3), 124 (1979).
- 103 N S Allen, E Lam, E M Howells, P N Green, A Green, F Catalina, C Peinado; *Eur. Polym. J.*, **26** (12), 1345 (1990).
- 104 C Peinado, F Catalina, T Corrales, R Sastre, F Amat-Guerri, N S Allen, *Eur. Polym. J.*, **28** (10), 1315 (1992).
- 105 J L Mateo, P Bosch, F Catalina, R Sastre; *J. Polym. Sci: Part A*, **28**, 1445 (1990).
- 106 C Decker, A D Jenkins; *Macromolecules*, **18**, 1241 (1985).
- 107 R S Davidson, K R Trethewey; *J. Chem. Soc. Chem. Commun.*, 674 (1975).
- 108 R S Davidson, K R Trethewey; *J. Chem. Soc. Perkin Trans. 2*, 167 (1977).
- 109 C L Osborn; *J. Radiat. Curing*, **3**, 2 (1976).
- 110 C R Morgan, D R Kyle; *J. Radiat. Curing*, **10**, 4 (1983)
- 111 D A Bolon, K K Webb; *J. Appl. Polym. Sci.*, **22**, 2543 (1978).
- 112 V D McGinniss in *UV Curing: Science and Technology*; S P Pappas (Ed), Technology Marketing Corporation, 96 (1980).
- 113 R Phillips in *Radiation Curing: Science and Technology Vol.II*; S P Pappas (Ed), Technology Marketing Corporation, 29 (1985).
- 114 R A Cundall, A Gilbert; *Photochemistry*, Nelson (1970).
- 115 J Fleischer; *Radtech Reports*, March/April, 19 (1995).
- 116 J E Eby, R E Levin in *Applied Optics and Optical Engineering VII*; R R Shannon, J C Wyant (Eds), Academic Press, New York (1979).
- 117 J F Rabek; *Experimental Methods in Photochemistry and Photophysics - Part I*, J Wiley & Sons (1982).
- 118 D Skinner; *Polymers Paint and Colour Journal*, **184** (4361), 566 (1994).
- 119 C H Chang, A Mar, H Evers III, D Wostratsky; *Proc. Conf. RADTECH*, Boston, USA, 16 (1992).
- 120 P J Gardner, J C Morris, W R Watson, H G Silver, J A Scholtz; *J. Illum. Eng. Soc.*, **5**, 45 (1975).
- 121 U Kogelschatz, B Eliasson, H Esrom; *Materials and Design*, **12** (5), 251 (1991).
- 122 B Gellert; *Proc. Conf. RADTECH*, Meditterano, 710 (1993).
- 123 R Diehl, A Roth; *Proc. Conf. RADTECH*, Maastricht, 48 (1995).
- 124 R Garlick; *Lithoweek*, **1**, 29 (1989).
- 125 J F Rabek in *Radiation Curing in Polymer Science and Technology, Vol.I: Fundamentals and Methods*; J P Fouassier, J F Rabek (Eds), Elsevier Science Publishers Ltd, Barking, Essex, 329 (1993).
- 126 R E Knight in *Radiation Curing of Polymers*, D R Randell (Ed), Royal Society of Chemistry, London, 1 (1987).

- 127 J F Brown, K Lau in *The Printing Ink Manual - 5th Edition*; R H Leach, R T Pierce (Eds), Blueprint, London, 86 (1993).
- 128 K McLaren; *The Colour Science of Dyes and Pigments*, J W Arrowsmith Ltd, Bristol (1993).
- 129 A M Munsell; *Munsell Book of Colour*, G P Putnam and Sons, London (1905).
- 130 N S Allen, M A Johnson, P K T Oldring, S Salim in *Chemistry and Technology of UV and EB Formulation for Coatings, Inks & Paints (Volume 2 - Prepolymers and Reactive Diluents for UV and EB Curable Formulations)*; P K T Oldring (Ed), SITA Technology Ltd (1991).
- 131 J L Anderson, R F Russell, C C Slover; *J. Radiation Curing*, **12**, 10 (1985).
- 132 J N Nobbs, J T Guthrie, D Duerden, P K T Oldring; *Proc. Conf. Radiation Curing Asia*, Tokyo, Japan (1988).
- 133 J C Song, Z J Wang, R Bao, D C Neckers; *Proc. ACS Polym. Mat. Sci. Eng*, **72**, 591 (1995).
- 134 C Decker; *Macromolecules*, **23**, 5217 (1990).
- 135 J E Moore, S H Schroeter, A R Schultz, L D Stang; *J. Radiation Curing*, **25**, 90 (1976).
- 136 S A Khan, I M Plitz, R A Frantz; *Rheologica Acta*, **31**, 151 (1992).
- 137 M S Cheema, M Leppard; *J. Radiation Curing*, **182**, 68 (1992).
- 138 M Toalson, T Richards; *Proc. Conf. RADTECH*, Orlando, Florida, USA, 333 (1994).
- 139 S Paul; *Surface Coatings International*, **8**, 336 (1994).
- 140 A Prioloa, G Gozzelino, F Ferrero; *Proc. 18th Int. Conf. in Organic Coatings Science and Technology*, Athens, Greece, 353 (1992).
- 141 B de Ruitter, F Molenaar, T Agterberg; *Proc. Conf. Aspects of Photoinitiation*, Egham, England, 209 (1993).
- 142 W Mahon; *Proc. Conf. RADTECH*, Edinburgh, Scotland, 201 (1991).
- 143 J G Kloosterboer, H P N van Genuchten, G M M Van de Hei, G P Melis, G J M Lippits; *Org. Coat. Plast. Chem.*, **48**, 445 (1983).
- 144 J G Kloosterboer, G M M Van de Hei, R G Gossink, G C M Dortant, *Polymer Communications*, **25**, 322 (1984)

CHAPTER 2

Outline of the study

2.1 Introduction

When formulating a new ink or coating, there are a number of properties not related to the photoinitiator that are key to its commercial success. The most important of these are properties such as colour, rheology, adhesion, gloss, flexibility and, where applicable, lithographic performance. Although some photoinitiators and synergists will themselves also affect these properties, the extent to which this occurs is not great, so the design of a photoinitiator package to cure the formulation is nearly always addressed as a separate issue once the remainder of the formulation is finalised.

2.2 Selection of photoinitiators

The large number and diverse nature of UV curing applications in use today means that the selection of a photoinitiator package is not straightforward. There is no ideal photoinitiator or combination of photoinitiators suitable for all applications, with selection based on a series of weighted factors and considerations often involving the sacrifice of one property in order to gain another. The main factors and considerations involved in the selection of a photoinitiator package can be summarised as¹⁻⁵:

- Required cure speed
- Type and level of pigmentation
- Film thickness
- Cost
- Colour and extent of yellowing on cure
- Odour of cured material
- Tainting characteristics of cured material
- Toxicology of photoinitiators and their decomposition products
- Volatiles and thermal stability
- Stability (shelf life)
- Solubility in the formulation
- Water/fount solubility
- Extractables/migratables

This benefit analysis approach, whether applied formally or informally, usually results in the best compromise of properties based on the constraints at the time, and nearly always involves the use of two or more photoinitiators and one or more amine synergists^{6,7}.

The ideal photoinitiator would clearly be fast curing, not affected by pigmentation, non-yellowing, non-toxic, non-odorous, easily solubilised, cheap to manufacture and with no decomposition products. Such a product does not exist, with every photoinitiator and synergist having its own strengths and weaknesses which dictate where it is used. For example, benzophenone is by far the most widely used photoinitiator^{1,8}, having reasonable reactivity and good solubility, but

more importantly having a much lower price in relation to most other photoinitiators. For these reasons, benzophenone is used almost exclusively in price-sensitive varnish formulations, but its weak absorption band in the near UV region means that other photoinitiators such as thioxanones must also be used to achieve satisfactory curing in pigmented formulations. In contrast, another widely used photoinitiator is 2,4,6-trimethylbenzoyl diphenylphosphine oxide (Lucerin TPO), which has very high reactivity and shows absorbance bands that extend into the far visible region making this, and other acylphosphine oxide photoinitiators, ideal for curing thick white pigmented coatings⁹⁻¹³. However, in many applications, its benefits are not sufficient to justify the high cost of this material.

2.3 The need for a broad study into the factors that affect photoinitiator efficiency

The field of radiation curing in inks and coatings has, particularly over the past 5 or 10 years, become an established technology, viewed as a commodity product as much as a specialist one, but still maintaining a growth rate of 8-10% per year¹⁴. However, the increased competition from a greater number of suppliers and the general acceptance of the technology as a commodity product have also forced down profit margins for manufacturers. This has been particularly noticeable in some sectors of the market such as the manufacture of inks for printed circuit boards.

Radiation curable coating manufacturers have well defined photoinitiator and synergist combinations for most products. Although these have served well for a number of years, they are now proving to be one of the major limiting factors in the effort to achieve the higher cure speeds being demanded by printers. Newer, more efficient photoinitiators are available and continue to be developed, but are increasingly complex molecules with their higher synthesis, development and toxicological testing costs, typically £0.5million or more, being passed on to customers, such that few developmental materials are now being offered for sale below £40/kg. In the effort to achieve the required technical advances these new photoinitiators have to be used carefully in order to retain cost effectiveness, with even the current generation of materials accounting for the second greatest portion of the formulation costs after the pigment.

Although at present acrylate based radiation curable products are not approved for direct food packaging use, they are often used in indirect contact applications, and concern is growing within the industry about the type and levels of materials available to extract or migrate into the food causing odour and taint problems. European Community directives exist that set guidelines for migration and residual content limits of food contact materials as low as 50ppb¹⁵, although some customers set their own limits even lower than this. The subject of extractable material from radiation cured films is one that receives relatively little attention, although it is known that a significant quantity of unreacted monomer, photoinitiator, synergist and photoinitiator derived decomposition products are available to extract and migrate^{1,16-18}. The quantitative measurement of extractables and migratables is

complicated by the significant variations due to cure conditions. As such, misleading results can be obtained if laboratory prepared samples are used in place of 'real samples' taken from the end of a printing press. Care should also be taken to ensure that the analysis method and extraction solvents used are appropriate for the materials being analysed, as these too may have a significant effect on the results. The nature of the materials likely to be available for extraction and migration can be identified both through a consideration of the raw materials used and by studies on model systems to determine a photoinitiator's reaction mechanism and photo-decomposition products.

Although, as a result of experience, a formulator in the printing ink industry would know that effective through-curing of a cyan ink requires the presence of a thioxanthone photoinitiator, the reason behind this necessity is not well understood. Similarly, some colour blends cure significantly slower than any of the individual inks for no obvious reason. A detailed study of the literature would hint at answers to these and other similar problems, but many studies are focused on only a few materials, concentrating particularly on aspects such as quantum efficiency of photoinitiators in model systems far removed from the materials that constitute a coating formulation. The information generated in these studies is ideal for aiding the development of new photoinitiators, but far from ideal for showing their curing effectiveness in a range of coatings applications. In addition, the high theory content in current literature discourages an in-depth investigation by those who may not have the background to fully interpret it in terms of their own practical observations.

A need exists for a broad ranging study into the factors that affect photoinitiation efficiency which is aimed at the printing ink industry. This should include a wide range of photoinitiators and synergists, including all those commercially available, and should generate information that is simple and easy to interpret using model systems and experimental conditions as close to those used in the industry as possible. The overall aim is to understand more fully how factors such as pigmentation and film thickness affect the choice of photoinitiator, allowing a fully optimised photoinitiator package to be quickly developed for any application. Through a better understanding of the reaction mechanisms of available photoinitiators, possible taint and odour problems due to specific photodecomposition products can also be anticipated and avoided. Legal claims cases in these instances tend to use large amounts of company resource and are expensive to contest.

2.4 Outline of the project

In order to fully understand the factors that affect photoinitiation efficiency, it is necessary to study both the overall cure reaction and a number of individual processes which contribute to it, since the observed cure is only as effective as the weakest link in the chain of events that lead to it. An example of this would be a photoinitiator with a high quantum efficiency for radical generation which, by virtue of producing initiating radicals not particularly reactive towards acrylate bonds, may not cure a coating effectively. Similarly, if a photoinitiator absorbs light in a spectral region where the lamp output is weak, or where a pigment absorbs much of the incident light, then cure efficiency will also be reduced. The factors affecting photoinitiator efficiency in the UV curing of acrylate based systems can be identified through a consideration of the chain of events that occurs during a cure reaction, and can be divided into four phases; as shown below and in Figure 2.1.

Phase

- I Photoinitiator physical properties
- II UV Light utilisation
- III Generation of active radicals
- IV Polymerisation of acrylate bonds

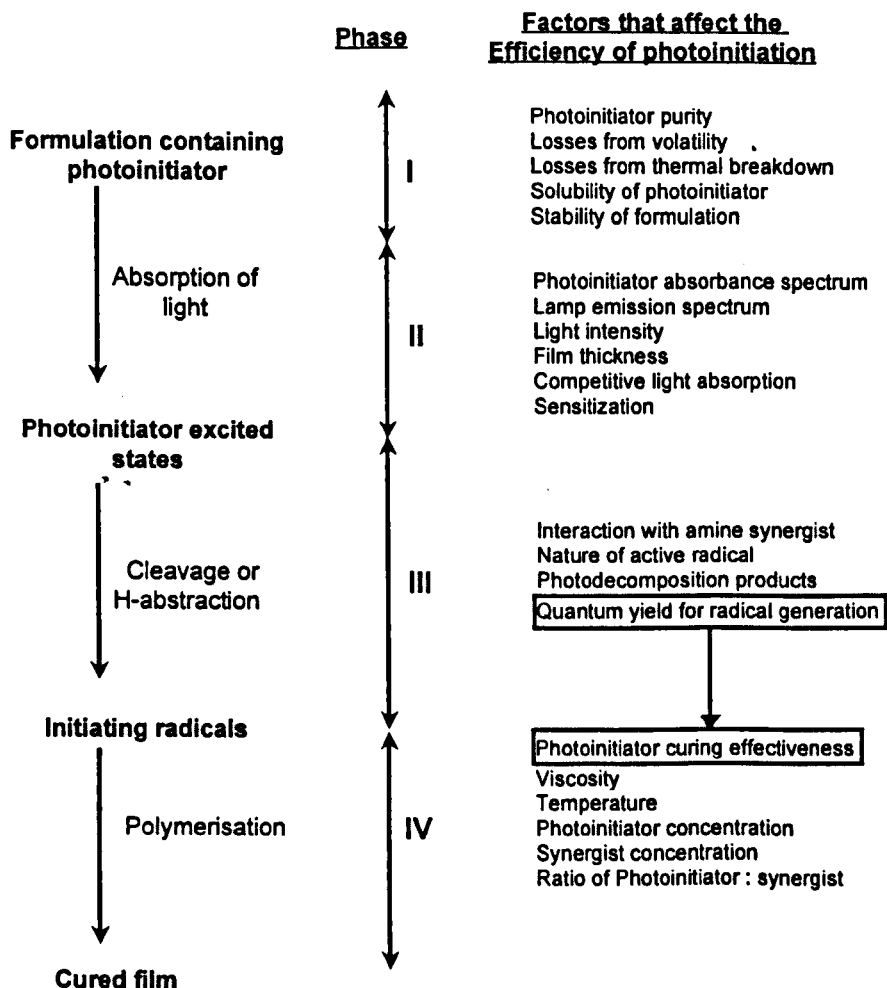


Figure 2.1 *The chain of events that occurs during a UV curing reaction, and factors which may affect its efficiency*

Whilst the initiation efficiencies (quantum yields for radical generation) for photoinitiators are important, they are beyond the scope of this work as they tend to have little practical applicability. A similar, more useful parameter is the curing effectiveness, which relates closely to the quantum yield of polymerisation Φ_p and is an overall measure of the efficiency of light absorption, radical generation and reactivity of derived radicals towards acrylate double bonds. Curing effectiveness is most easily determined by following the polymerisation reaction through the loss of acrylate double bonds. This is possible using established instrumental techniques such as real-time infra-red spectroscopy (RTIR)¹⁹ which monitors changes in the IR spectrum due to the loss of acrylate double bonds and differential photo-calorimetry (DPC) which measures the heat evolved as the exothermic curing reaction progresses²⁰.

One of the principle aims of this project is to use techniques such as RTIR and DPC to investigate the factors that affect photoinitiation efficiency. Since no RTIR instruments are currently manufactured commercially this involves custom building one and fully validating both it and the technique; this is detailed in chapter 6.

The contents of this thesis are specific to acrylate based free radical curing, and are arranged such that each of the chapters covers one of the phases of the cure reaction as outlined in Figure 2.1 and studies the factors that affect the processes occurring in that phase, with a final chapter serving to summarise the information.

Chapter 3	Photoinitiator physical properties
Chapter 4	UV light utilisation
Chapter 5	Photoinitiator reaction mechanisms and photodecomposition products
Chapter 6	Factors affecting the polymerisation reaction
Chapter 7	General conclusion

2.5 References

1. C Armstrong, S Herlihy; *Proc. Conf. Aspects of Photoinitiation*, Egham England, 1 (1993).
2. S J Wilson in *Radiation Curing of Polymers II*; D R Randell (Ed), The Royal Society of Chemistry, London, 124 (1991).
3. G Li Bassi in *Radiation Curing in Polymer Science and Technology (Volume II - Photoinitiating Systems)*; J P Fouassier, J F Rabek (Eds), Elsevier Science Publishers Ltd, Barking, Essex, 239 (1993).
4. G Robins in *Radiation Curing of Polymers*; D R Randell (Ed), The Royal Society of Chemistry, London, 78 (1987).
5. P K T Oldring, C Lowe in *Chemistry and Technology of UV and EB Formulation for Coatings, Inks and Paints (Volume 4 - Formulation)*; P K T Oldring (Ed), SITA Technology Ltd., 1 (1991).
6. R S Davidson, P K T Oldring, M S Salim in *Chemistry and Technology of UV and EB Formulation for Coatings, Inks and Paints (Volume 4 - Formulation)*; P K T Oldring (Ed), SITA Technology Ltd., 215 (1991).
7. R Holman in *Chemistry and Technology of UV and EB Formulation for Coatings, Inks and Paints (Volume 4 - Formulation)*; P K T Oldring (Ed), SITA Technology Ltd., 325 (1991).
8. W D Arendt; *RadTech Report*, 5, 6, 14 (1991).
9. W Rutsch, H Angerer, V Desobry, K Dietliker, R Hüsler; *Proc. Conf. 16th Int. Conf. in Organic Coatings Science & Technology*, Athens, Greece, 423 (1990).
10. K Dorfner in *Radiation Curing of Polymers II*; D R Randell (Ed), The Royal Society of Chemistry, London, 216 (1991).
11. M Jacobi, A Henne; *Polymers Paint and Colour Journal*; 175 (4150), 636 (1985).
12. E Beck, E Keil, M Lokai, J Schröder; *RadCure Letter*, 5, 67 (1994).
13. L Misev, K Dietliker, G Hug, M Koehler, D Leppard, A Litzler, W Rutsch; *Proc. Conf. Aspects of Photoinitiation*, Egham, England, 299 (1993).
14. P Dufour in *Radiation Curing in Polymer Science and Technology (Volume I - Fundamentals and Methods)*; J P Fouassier, J F Rabek (Eds), Elsevier Science Publishers Ltd, Barking Essex, 1 (1993).
15. E C Measurement and Testing Project: Directive 90/128/EEC (1990) and 92/39/EEC (1992).
16. W Baeumer, M Koehler, J Ohngemach; *Proc. Conf. RADTECH*, Baltimore, Maryland, USA, 4-43 (1986).
17. D L Easterby; *Proc. Conf. Aspects of Analysis*, Egham, England (1994).
18. C Renson, J M Loutz; *Proc. Conf. Radiation Curing Asia*, Tokyo, Japan, 356 (1988).
19. C Decker; *Macromolecules*, 23, 5217 (1990).
20. J E Moore, S H Schroeter, A R Schultz, L D Stang; *J. Radiation Curing*, 25, 90 (1976).

CHAPTER 3

Photoinitiator physical properties

3.1 INTRODUCTION

As outlined in chapter 2, when considering UV photoinitiated free radical curing applications a large number of factors are important in the choice of photoinitiator, particularly its technical suitability in terms of light absorption characteristics and reactivity (see chapters 4 and 6 respectively). However, the physical properties are also important and may be a deciding factor in the choice of a suitable material. Although the exact requirements vary greatly because of the wide range of coating methods and end use applications in the field of UV curing, properties such as solubility and volatility / thermal stability are important.

The subject of photoinitiator volatility / thermal stability is particularly relevant in application areas such as the manufacture of printed circuit boards, where a heating stage may be included in the processing to remove solvent prior to photo-imaging, or to improve resistance properties through a thermal cure reaction, typically at 70-100°C and 120-160°C respectively. By their very nature these coatings will also be exposed to molten solder at a temperature of around 260°C. Clearly a photoinitiator which is volatile under these conditions could be of no use in this application because it may evaporate and be unavailable for the intended reaction.

Concerns over photoinitiator volatility are also present for less obvious applications such as printing inks for food packaging. In this case, as well as the need for low odour and low volatility materials at room temperature, packaging for foods that are microwaved in a box or packet can reach temperatures of up to 200-220°C and increases the likelihood of food contamination by the photoinitiator as a result of vapour phase migration¹. Also, a certain amount of care is required with inks for label printing since these are subjected to laser printing and can cause problems due to the redeposition of sublimed / volatilised material on the print head.

Although it has been reported that the majority of the volatiles from cured coatings are unreacted photoinitiator and monomer², only Beck et. al³ have published any significant work on the volatility / thermal stability of photoinitiators. Their investigations included both the analysis of volatile material emitted from a cured film at 75°C (8 hours) and the weight losses of 7 photoinitiators and 1 synergist over a period of 72 hours at 75°C. They found that it is the volatility of the photoinitiators and their breakdown products that mainly determines the extent to which they are released into the atmosphere, the degree to which the film has been cured having relatively little influence. The photoinitiators isopropyl thioxanthone (Quantacure ITX), 2,4,6-trimethylbenzoyl diphenylphosphine oxide (Lucerin TPO) and 2,4,6-trimethylbenzoyl phenylphosphinic acid ethyl ester (Lucerin TEPO) were identified as having low volatility under these conditions, with 1-phenyl-2-hydroxy-2-methyl propan-1-one (Darocure 1173) in particular showing high volatility.

In this chapter the properties of a large number of photoinitiators and synergists have been investigated using thermogravimetric analysis (TGA). This simple technique very accurately records the weight of a sample as a function of the applied temperature / time program, providing information on the volatility and thermal decomposition temperatures. The information then allows decisions to be made regarding the suitability of particular materials for applications involving heating stages.

The principal limitation of a stand-alone TGA instrument is that the results have to be interpreted through experience as no chemical information is afforded. The use of specific detectors for analysing the evolved gases from the TGA has been widely reported in the literature and most often involves the coupling of TGA and Fourier transform infrared spectrometers (FTIR)⁴⁻⁷, termed TGA-FTIR. The coupling of a TGA to a mass spectrometer (TGA-MS)⁸⁻¹² and to both infrared and mass spectrometers (TGA-FTIR-MS)¹³⁻¹⁴ has also been reported, but in these cases the engineering considerations are far more complex because both TGA and FTIR instruments operate at atmospheric pressure with an air carrier gas, whereas a mass spectrometer operates under high vacuum with a helium carrier gas. Solutions to this problem vary greatly from relatively expensive concentration equipment such as jet separators and molecular leaks^{8,10-12} to a length of GC capillary column sufficient both to preserve the vacuum in the mass spectrometer and to increase sensitivity by sucking sample into the open-ended column near the TGA sample^{9,13-14}. One other reported solution¹⁴ has been to run the TGA off-line and substitute it as a source of evolved gases with a temperature programmable injection port fitted to gas chromatograph (GC) which then runs the same temperature program as the TGA. The advantage of this pseudo-TGA-MS setup is that it is a sealed system with a helium carrier gas, giving very high sensitivity and the option of running the experiment in continuous mode; evolved gases transferred immediately to the mass spectrometer, or batch mode; cold trapping all the evolved gases from a sample and then separating and analysing them using the GC-MS. This technique was fully validated against a true TGA-MS setup and found to give excellent results. It also has been used in this chapter to investigate the evolved gases from a small number of photoinitiators in order to learn more about whether they decompose or merely volatilise.

Within the printing ink industry the photoinitiator and synergist is often added to a formulation either as a liquid blend to a pigmented concentrate / otherwise fully formulated ink, or, particularly with low solubility materials, is dispersed directly along with the pigment. The latter process is known to be inefficient, with some undissolved material being lost in the filtration stage. Low solubility materials also tend to precipitate out with time, requiring the ink to be reworked or disposed of. For these reasons the solubility of photoinitiators and synergists is an important consideration that has not been well covered in the literature. Where such information does exist it typically involves evaluating solubilities in acrylate monomers such as 1,6-hexanediol diacrylate

(HDDA) or trimethylolpropane triacrylate (TMPTA)¹⁵. Although neither of these monomers are used within the U.K. printing ink industry, this approach is a reasonable comparison for low viscosity formulations such as overprint varnishes and flexographic inks which contain high monomer concentrations, but is a poor comparison for lithographic inks which contain predominantly oligomer and only a few percent of monomer. In this chapter the relative solubilities and subsequent formulation stabilities of a number of photoinitiators in an oligomer / monomer blend is investigated.

The type of printing process employed may also be a consideration when choosing a suitable photoinitiator system. For example, the lithographic printing process, which involves an aqueous fount solution to control the distribution of ink into the image and non-image areas of the printing plate¹⁶, precludes the use of most aliphatic amine and aminoacrylate type synergists because they are partially or completely water soluble, affecting both the printing quality through the ink / water balance, and the subsequent cure speed because of a lack of synergist¹⁷. Whilst a detailed examination of the fount solubilities of a range of photoinitiators is beyond the scope of this work, it is known that 4-(2-hydroxyethoxy)-phenyl 2-hydroxy-2-methyl-2-propanone (Darocure 2959) is suitable for use in waterbased UV applications because of a high water solubility¹⁸. It is therefore likely that this material will be unsuitable for lithographic applications for the reasons given above. Fount solubility is not a problem for most varnishes since the bulk of these are printed by in-line coater or dry offset methods which do not involve a fount solution. This is also true of the emerging technology of UV flexographic printing.

3.2 RESULTS AND DISCUSSION

3.2.1 Volatility and thermal stability of photoinitiators and synergists

In this section the volatility and thermal stability of a range of photoinitiators and synergists have been investigated using thermogravimetric analysis (TGA). The method used measured the sample weight as a function of temperature, increasing at a rate of 5°C / minute in an air purge.

TGA data of this type is generally displayed as a graph of percent of original sample weight vs. temperature, often including the first derivative curve (rate of change of sample weight as a function of temperature) which provides further information. A lack of space and the large number of samples involved precludes this type of presentation in favour of data in a tabular form. However, in order for this to be meaningful it is necessary to show the different types of weight loss curves found and how they have been interpreted;

1) *Photoinitiator evaporation*

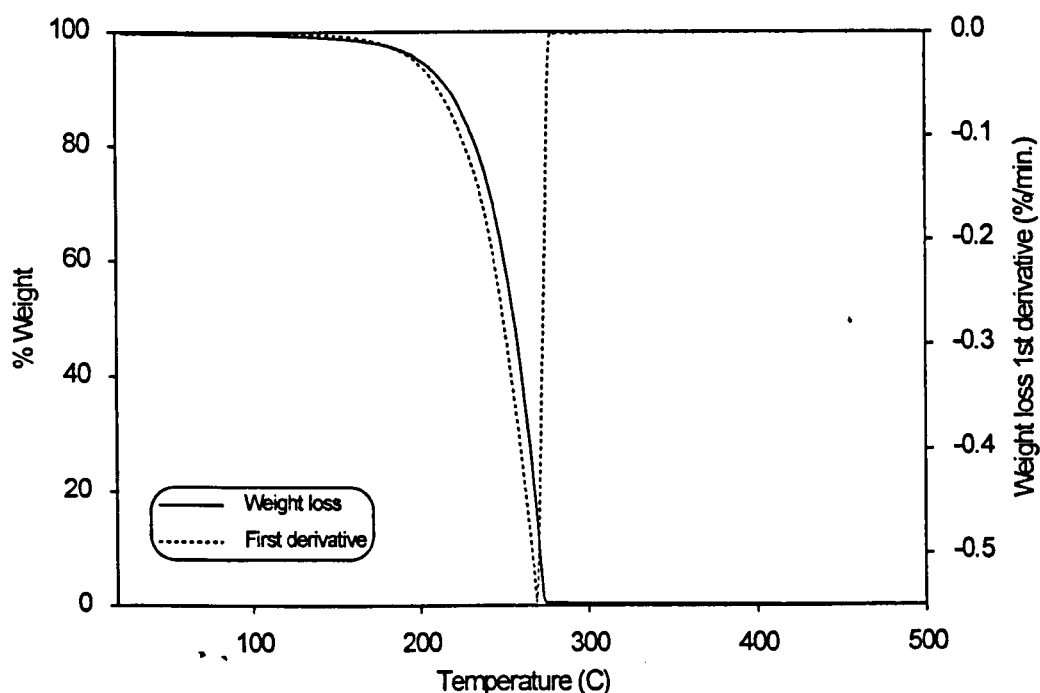


Figure 3.1 TGA data showing photoinitiator evaporation

Figure 3.1 shows results for the photoinitiator 4,4'-dimethoxybenzil, where as the sample temperature rises, the evaporation rate (1st derivative curve) shows a gradual numerical increase until no more material remains i.e. sample weight = 0%. At this point the first derivative curve quickly falls back to zero. The asymmetrical peak shape in the first derivative curve is characteristic of evaporation behavior.

2) *Photoinitiator evaporation with some thermal decomposition*

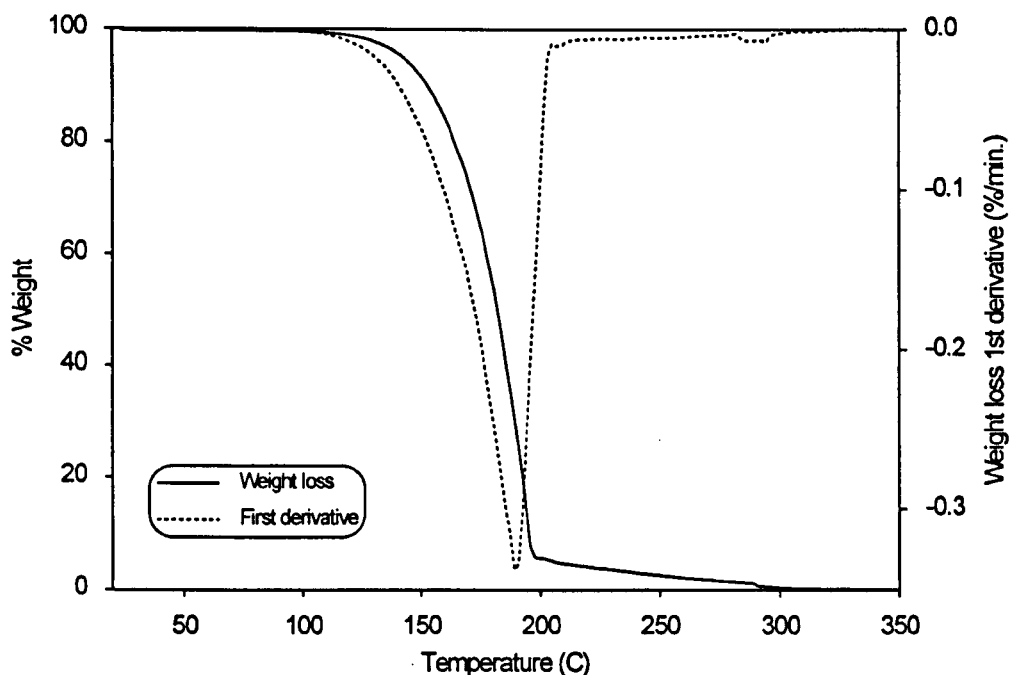


Figure 3.2 *TGA data showing mostly photoinitiator evaporation but with some thermal decomposition at higher temperatures*

Figure 3.2 shows results for the photoinitiator benzoin which displays both a gradual weight loss with increasing temperature, consistent with sample volatilisation, and a slow weight loss of several percent of residual material over a wide temperature range, often indicative of thermal decomposition. Most of the photoinitiators and synergists analysed showed this behavior, with the evidence suggesting that both evaporation and thermal decomposition may be important.

3) *Photoinitiator thermal decomposition*

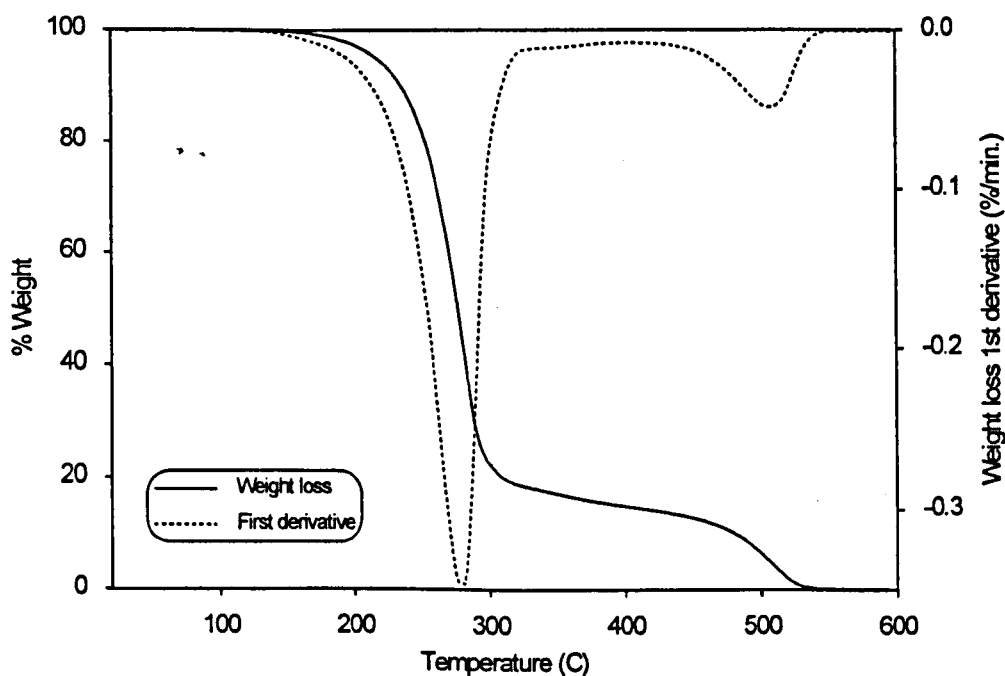


Figure 3.3 *TGA data showing photoinitiator thermal decomposition*

Figure 3.3 shows the results for the photoinitiator 2-benzyl-2-dimethylamino-1-(4-morpholinophenyl) butan-1-one (Irgacure 369), where a distinct two stage reaction is observed. Both the multi-stage reaction and the symmetrical shape of the peaks in the first derivative curve suggest that this is a thermal decomposition reaction with little contribution to the weight loss coming from evaporation. Several other photoinitiators showed this type of behavior.

4) *Photoinitiator evaporation and desublimation*

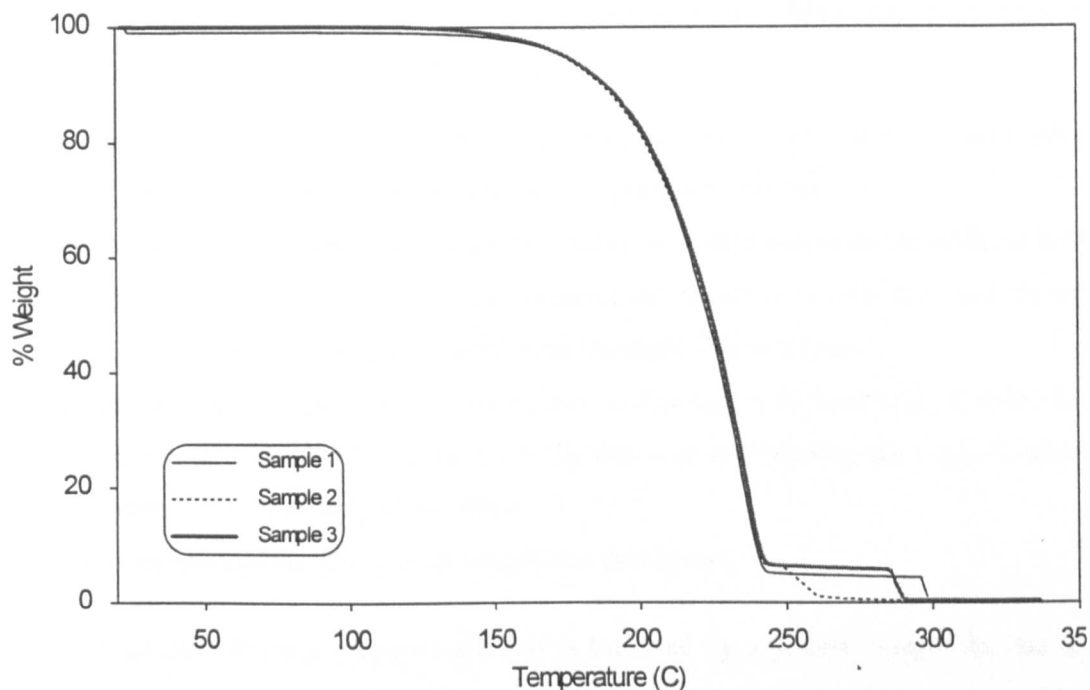


Figure 3.4 *TGA data showing photoinitiator evaporation and desublimation*

A material is said to sublime when it passes from the solid state to the vapour state without having melted. The reverse process is also possible and can still be termed sublimation, but is also known as desublimation¹⁹. Evidence for sublimation processes in TGA experiments is usually associated with a visual observation in the area around the sample during the run, but in some cases can be seen in the experimental data.

Figure 3.4 shows the results for duplicate experiments using the photoinitiator 2-ethyl anthraquinone, where it was observed that as the temperature increased the sample melted and volatilised, but desublimed from the vapour state back to the solid state, forming crystal strands both on the hangdown wire connecting the sample to the balance and on the furnace tube baffle assembly. Subsequently, as the temperature rose further the material on the hangdown wire volatilised and therefore registered a second weight loss. Despite the good reproducibility of the technique as shown by the first weight loss, the second weight loss is not reproducible because of the slight variations in the recondensation location.

Although none of the photoinitiators examined in this work have been reported to show sublimation behavior, anthraquinone itself is known to sublime²⁰. Other anthraquinone, xanthone, thioxanthone and benzophenone derivatives also showed evidence of sublimation and / or desublimation in this work. However, these assignments are by visual observation only since the experimental data showing secondary volatilisation of desublimed material can be easily confused with a slow thermal decomposition process.

Weight loss data for the photoinitiators and synergists investigated in this section is presented in tabular form with the following information included;

- Temperature (°C) at which 5% of the original sample weight has been lost, indicating the temperature region in which the sample shows significant volatility.
- Temperature (°C) of maximum weight loss rate; as determined from the peak in the first derivative curve. This indicates the temperature region in which the photoinitiator / synergist would be immediately volatilised or thermally decomposed.
- In a largely single weight loss process similar to that shown in figure 3.2, if observed, the amount of residual material (%) that thermally decomposes following the major weight loss.
- The number of distinct weight loss stages.
- Comments and description of other weight loss processes.

In experimental data where a major weight loss is followed by a gradual weight decline due to thermal decomposition, such as that shown in figure 3.2 for benzoin, the exact number and temperature of individual thermal decomposition processes can be difficult to determine. In the data reported here, with the exception of the major evaporative weight loss, all distinct weight losses have been detailed separately as a percentage weight loss at the highest weight loss rate temperature, with slow trailing weight losses, such as that shown in figure 3.2, reported merely as a residual weight loss.

The thermal stability of selected photoinitiators was investigated further using a pseudo thermogravimetric analysis-mass spectroscopy (TGA-MS) system, where the TGA weight loss profile is compared with the evolved material detected by a mass spectrometer as part of a gas chromatography-mass spectroscopy (GC-MS) instrument. The GC-MS was modified for this operation by the fitting of a temperature programmable injection port that runs the same temperature scan experiment as the TGA. The normal 25m long column was also replaced with a 1m narrow bore column, such that as material is evolved in the injection port it is passed to the mass spectrometer with almost no time delay whilst still preserving the vacuum in the mass spectrometer. The oven temperature was maintained at 280°C throughout to aid the rapid transfer of material, and MS data collected continuously, with the evolution profiles of the total ion current (TIC) or particular mass fragments being displayed against temperature / time.

3.2.1.1 Benzoin type photoinitiators

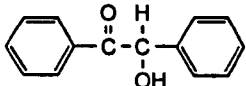
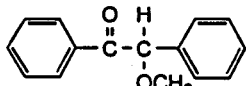
Photoinitiator	Temp. of 5% wt. loss (°C)	Max. rate of wt. loss (°C)	Residual wt loss (%)	No. of Wt. loss stages	Comments and other weight losses
 benzoin	144	188	5	1	
 benzoin methyl ether	130	190	8	1	
<i>Daitocure EE</i> benzoin ethyl ether	133	190	4	1	
<i>Daitocure IP</i> benzoin isopropyl ether	140	201	3	1	
<i>Esacure EB3</i> benzoin butyl / isobutyl ethers	121	178	-	> 3	4% at 25°C 10% at 235°C 3% at 410°C
benzoin isobutyl ether	123	202	3	2	3% at 25°C

Table 3.1 TGA weight loss data from benzoin ether type photoinitiators

The results in table 3.1 and the TGA raw data suggest that all the benzoin type photoinitiators largely volatilise on heating, with the type of ether substituent making little difference to their relative volatility. Esacure EB3 shows a slightly more complex weight loss profile than the other photoinitiators, although this is likely to be because it is a blend of both benzoin butyl and isobutyl ethers. For all the materials in this class, the residual weight losses following the major evaporative loss suggests that some thermal decomposition may be occurring at temperatures around 200°C, although their general level of volatility makes these materials unsuitable for many applications involving heating processes.

3.2.1.2 Hydroxyalkylphenone type photoinitiators

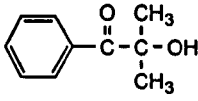
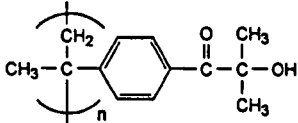
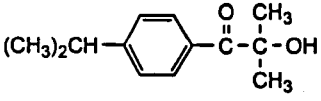
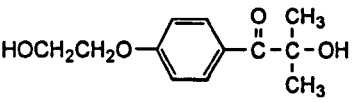
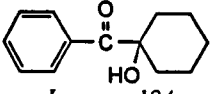
Photoinitiator	Temp. of 5% wt. loss (°C)	Max. rate of wt. loss (°C)	Residual wt. loss (%)	No. of Wt. loss stages	Comments and other weight losses
 <p><i>Darocure 1173</i> 1-phenyl-2-hydroxy-2-methyl propan-1-one</p>	84	138	-	1	1% at 25°C
 <p><i>Esacure KIP</i> polymeric 1-phenyl-2-hydroxy-2-methyl propan-1-one</p>	135	281		>4	main losses: 15% at 179°C 45% at 281°C 30% at 530°C
 <p><i>Darocure 1116</i> 4-isopropyl-phenyl-2-hydroxy-2-methyl-2-propan-1-one</p>	110	166	1	1	
 <p><i>Darocure 2959</i> 4-(2-hydroxyethoxy) phenyl-2-hydroxy-2-methyl-2-propan-1-one</p>	185	243	1	2	0.5% at 90°C
 <p><i>Irgacure 184</i> 1-hydroxycyclohexyl phenyl ketone</p>	127	180	2	2	1% at 300°C

Table 3.2 TGA weight loss data from hydroxyalkylphenone type photoinitiators

The results in table 3.2 and the TGA raw data show that the hydroxyalkylphenone photoinitiators are generally unsuitable for applications involving heating processes, and that with the exception of Esacure KIP appear to merely vaporise on heating. Darocure 1173 is the most volatile of these, with isopropyl substitution at the 4- position in the aromatic ring, Darocure 1116, showing only a slightly higher evaporation temperature. The polymeric form of Darocure 1173, Esacure KIP, was observed not to volatilise, but thermally decomposes in a multi-stage process between 100°C and 550°C, although the relatively low temperature for the onset of this decomposition also makes Esacure KIP unsuitable for applications involving heat. Only the 2-hydroxyethoxy substituted material, Darocure 2959, shows a high enough evaporation temperature to allow its use in applications involving heating processes. Both Irgacure 184 and Darocure 1173 have previously been reported to show significant volatility³.

3.2.1.3 Acylphosphine oxide type photoinitiators

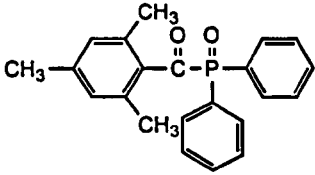
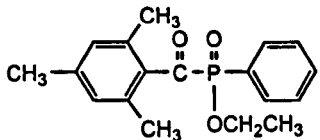
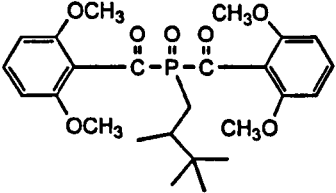
Photoinitiator	Temp. of 5% wt. loss (°C)	Max. rate of wt. loss (°C)	Residual wt. loss (%)	No. of Wt. loss stages	Comments and other weight losses
 <p><i>Lucerin TPO</i> 2,4,6-trimethylbenzoyl diphenylphosphine oxide</p>	223	259	-	3	56% at 259°C 38% at 315°C 1.5% at 491°C
 <p><i>Lucerin LR8893X (TEPO)</i> 2,4,6-trimethylbenzoyl phenylphosphinic acid ethyl ester</p>	163	227	2	1	
 <p><i>BDTPO</i> bis(2,6-dimethoxybenzoyl)-2,4,4-trimethylpentyl phosphine oxide</p>	232	283	-	4	44% at 283°C 34% at 305°C 4% at 497°C 4% at 755°C
Irgacure 1700	74	124	-	>4	weight losses as for BDTPO and Darocure 1173

Table 3.3 TGA weight loss data from acylphosphine oxide type photoinitiators

The results in table 3.3 and the TGA raw data show that acylphosphine oxide type photoinitiators are generally quite thermally stable and non-volatile. Although TEPO appears merely to vaporise on heating, the other two materials in this group, TPO and BDTPO show evidence of thermal decomposition in multi-stage processes extending up to temperatures as high as 750-800°C. BDTPO is however only commercially available as Irgacure 1700; a 1:3 blend with the volatile photoinitiator 1-phenyl-2-hydroxy-2-methyl propan-1-one (Darocure 1173).

The thermal stability of TPO was investigated further using thermogravimetric analysis-mass spectroscopy (TGA-MS), the results being shown in figure 3.5. In conjunction with reference mass spectra of TPO and the materials formed following UV irradiation (see chapter 5) these results indicate that the material evolved in the 220-300°C range (spectrum 1) is a combination of volatilised TPO and 2,4,6-trimethylbenzoic acid, the latter being indicated by the presence of the unique fragments m/z 146 and 164 in the correct ratio.

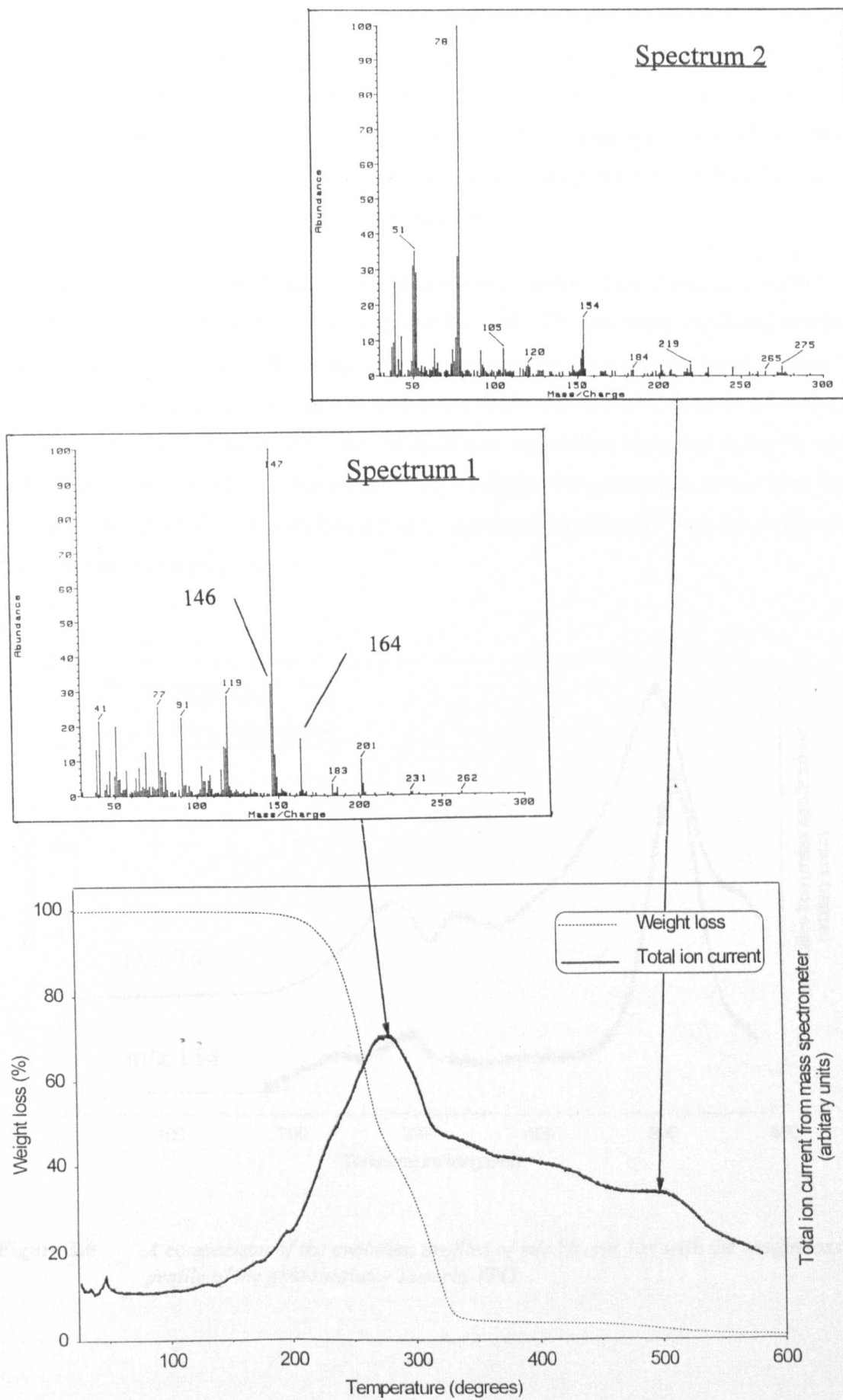


Figure 3.5 TGA-MS data for the photoinitiator Lucerin TPO

The presence of 2,4,6-trimethylbenzoic acid would suggest that thermal decomposition is occurring via an α -cleavage route, although the general similarity of the mass spectra involved makes this difficult to confirm since other known photocleavage products such as 2,4,6-trimethyl benzaldehyde (see chapter 5) could not be identified. Also, although the most likely explanation, insufficient data is available to confirm that the two weight loss processes in 220-300°C region are associated with evaporation and α -cleavage respectively.

The material evolved in the 500°C region is also shown in figure 3.5 (spectrum 2) and can be seen to be significantly different to that evolved at 220-300°C. The two most significant ions in this spectrum, m/z 78 and 154 are, following the lower temperature fragmentation reaction, most likely to be a consequence of further reactions of the remaining diphenyl phosphine based material to produce benzene, which has a strong m/z 78 molecular ion, and an additional unknown material with a significant m/z 154 ion. Further evidence to support this speculation comes from the fact that the evolution profiles of both ions are only associated significantly with the weight loss at 500°C, as shown in figure 3.6.

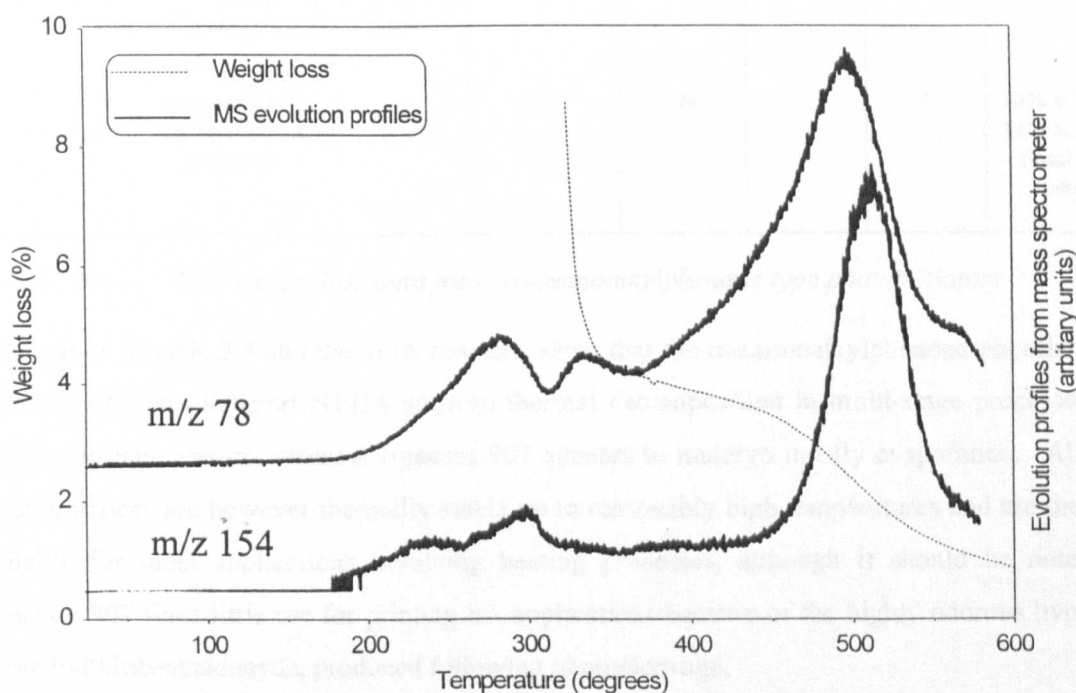


Figure 3.6 A comparison of the evolution profiles of m/z 78 and 154 with the weight loss profile of the photoinitiator Lucerin TPO

3.2.1.4 α -Aminoalkylphenone type photoinitiators

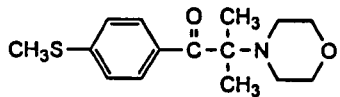
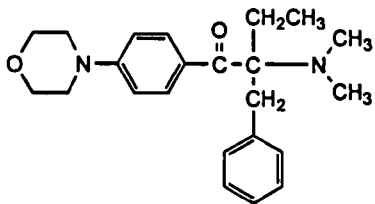
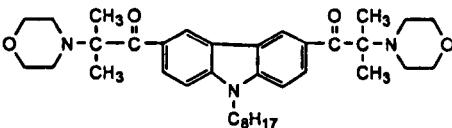
Photoinitiator	Temp. of 5% wt. loss (°C)	Max. rate of wt. loss (°C)	Residual wt. loss (%)	No. of wt. loss stages	Comments and other weight losses
 <p><i>Irgacure 907</i> 2-methyl-1-[4-(methylthio)phenyl]-2-morpholino propan-2-one</p>	175	235	-	2	1% at 459°C
 <p><i>Irgacure 369</i> 2-benzyl-2-dimethylamino-1-(4-morpholinophenyl) butan-1-one</p>	217	279	-	2	79% at 279°C 11% at 507°C
 <p><i>Radstart N1414</i> 3,6-bis(2-morpholino isobutyryl) N-octyl carbazole</p>	253	344	-	4	49% at 341°C 51% at 533°C (total of 3 losses)

Table 3.4 TGA weight loss data from α -aminoalkylphenone type photoinitiators

The results in table 3.4 and the TGA raw data show that the α -aminoalkylphenone photoinitiators Irgacure 369 and Radstart N1414 undergo thermal decomposition in multi-stage processes with increasing temperature, whereas Irgacure 907 appears to undergo mostly evaporation. All three photoinitiators are however thermally stable up to reasonably high temperatures and are therefore suitable for most applications involving heating processes, although it should be noted that Irgacure 907 finds little use for printing ink applications because of the highly odorous byproduct 4-methylthiobenzaldehyde, produced following photocleavage.

The photoinitiator Irgacure 369 was investigated further using TGA-MS, the results of which are shown in figure 3.7. In conjunction with reference mass spectra of Irgacure 369 and the materials formed following UV irradiation (see chapter 5) these results indicate that the material evolved in the 200-300°C range (spectrum 1) is, with the exception of the m/z 176 ion, consistent with the spectrum of the volatilised photoinitiator. However, the strongest ion, m/z 176, does not appear in either the photoinitiator reference spectrum or any of the byproducts found in chapter 5, including those which were not positively assigned. As such, two possibilities exist:

1. The weight loss is due to a combination of both photoinitiator evaporation and a thermal decomposition reaction giving different reaction product(s) to those observed on UV irradiation.
2. The weight loss is due entirely to a thermal decomposition reaction giving different reaction product(s) to those observed on UV irradiation, but with strong similarities to that of the unreacted photoinitiator.

In view of the general similarity of the mass spectra for many of the photodecomposition products associated with this photoinitiator the true situation cannot be ascertained without further work.

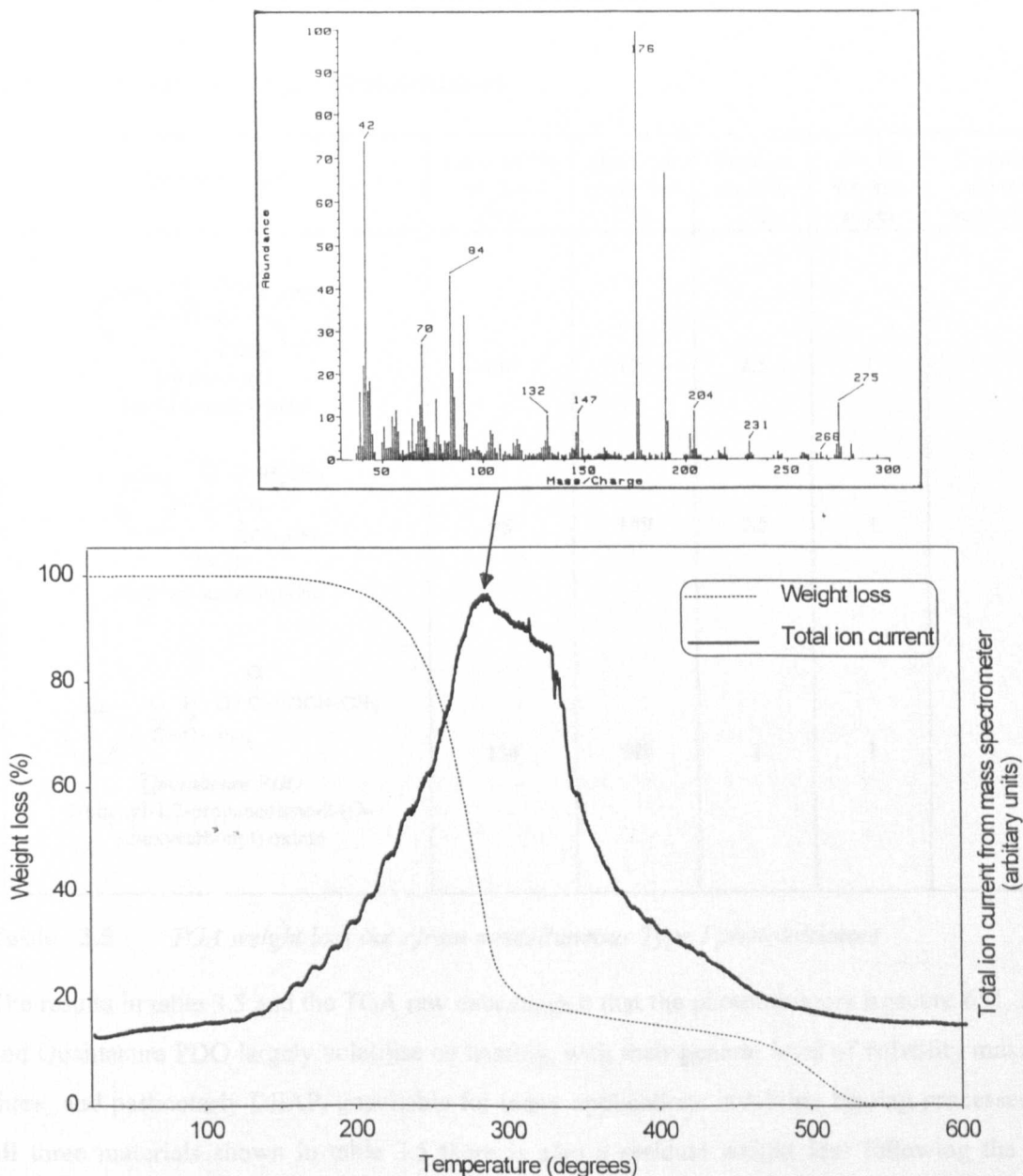


Figure 3.7 TGA-MS data for the photoinitiator Irgacure 369

Figure 3.7 also shows that no material was detected by the mass spectrometer during the weight loss in the 460-520°C region. The fact that the lower scan limit in this experiment was m/z 30 means that most carbon and nitrogen oxides would have been detected if complete thermal breakdown were occurring. As such, the only valid explanation for this observation is that the evolved material is too involatile to pass through the GC column.

The results and observations with regard to the photoinitiator Irgacure 369 suggest that the thermal decomposition products are not the same as the photodecomposition products (see chapter 5). As such, a more detailed investigation of the processes occurring during thermal decomposition of this photoinitiators would be an area worthy of further study.

3.2.1.5 Miscellaneous Type I photoinitiators

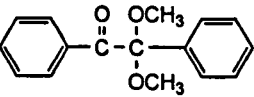
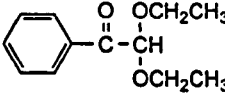
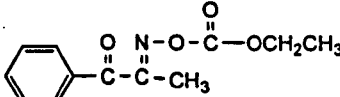
Photoinitiator	Temp. of 5% wt. loss (°C)	Max. rate of wt. loss (°C)	Residual wt. loss (%)	No. of Wt. loss stages	Comments and other weight losses
 <p><i>Irgacure 651</i> benzil dimethyl ketal</p>	140	193	2.5	1	
 <p><i>DEAP</i> diethoxy acetophenone</p>	98	159	2.5	1	
 <p><i>Quantacure PDO</i> 1-phenyl-1,2-propanedione-2-(O-ethoxycarbonyl) oxime</p>	134	187	2	1	

Table 3.5 TGA weight loss data from miscellaneous Type I photoinitiators

The results in table 3.5 and the TGA raw data suggest that the photoinitiators Irgacure 651, DEAP and Quantacure PDO largely volatilise on heating, with their general level of volatility making all three, and particularly DEAP, unsuitable for many applications involving heating processes. For all three materials shown in table 3.5 there is also a residual weight loss following the major evaporative loss, suggesting that some thermal decomposition may be occurring.

3.2.1.6 Xanthone and thioxanthone type photoinitiators

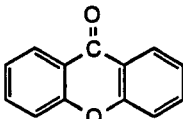
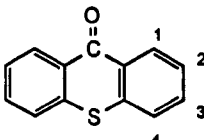
Photoinitiator	Temp. of 5% wt. loss (°C)	Max. rate of wt. loss (°C)	Residual wt. loss (%)	No. of Wt. loss stages	Comments
 xanthone	161	207	-	1	some desublimation
 thioxanthone	189	235	-	1	some desublimation
<i>Quantacure ITX</i> isopropyl thioxanthone	180	239	2.5	1	
<i>Speedcure DETX</i> 2,4-diethyl thioxanthone	206	264	-	2	4% at 507°C
2- <i>t</i> .butyl thioxanthone	195	259	1.5	1	
<i>Kayacure CTX</i> 2-chloro thioxanthone	190	250	-	1	some desublimation
<i>Quantacure PTX</i> 2-propoxy thioxanthone	205	268	8	1	
<i>Quantacure CPTX</i> 1-chloro-4-propoxy thioxanthone	231	296	3	1	

Table 3.6 TGA weight loss data from xanthone and thioxanthone type photoinitiators

The results in table 3.6 and the TGA raw data show that all the xanthone and thioxanthone type photoinitiators tested are non-volatile but evaporate when heated to sufficiently high temperatures. The thioxanthenes were all observed to be less volatile than xanthone, with several of the materials also showing desublimation behavior.

Quantacure PTX was chosen for further study by TGA-MS to characterise the nature of the weight loss, and in particular the nature of the residual weight loss which is quite significant for this photoinitiator. Using a reference spectrum for Quantacure PTX, TGA-MS results, shown in figure 3.8, indicate that in the temperature range 200-275°C it is volatilised Quantacure PTX that is evolved (spectrum 1). However, at temperatures above 300°C, associated with the residual weight loss, the spectrum of the evolved material (spectrum 2) shows both volatilised Quantacure PTX and a significant quantity of other hydrocarbon material caused by thermal decomposition. The prominence of this region in the total ion chromatogram is associated with the extensive mass spectral fragmentation shown by hydrocarbons resulting in high ion current and high sensitivity.

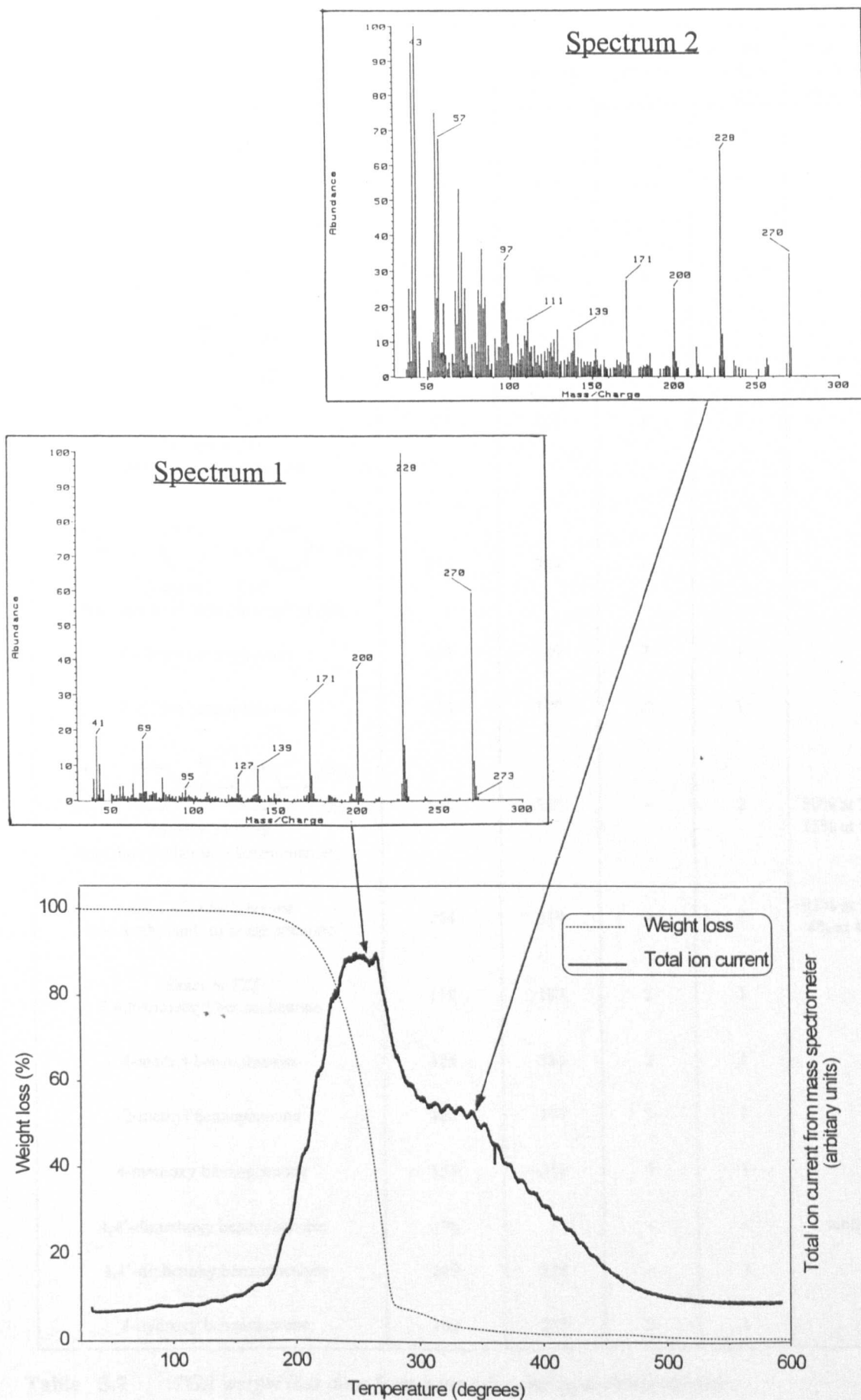


Figure 3.8 TGA-MS data for the photoinitiator Quantacure PTX

3.2.1.7 Benzophenone type photoinitiators

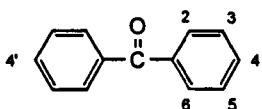
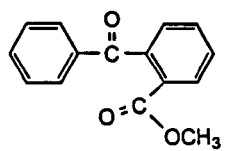
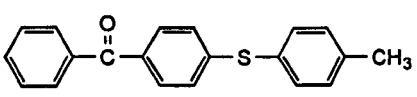
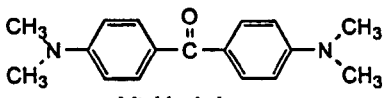
Photoinitiator	Temp. of 5% wt. loss (°C)	Max. rate of wt. loss (°C)	Residual wt. loss (%)	No. of Wt. loss stages	Comments and other weight losses
 benzophenone	118	175	2	1	
<i>Trigonal 12</i> 4-phenyl benzophenone	197	256	4	1	
 <i>Daitocure OB</i> 2-benzoyl methyl benzoate	154	211	4	1	
 <i>Quantacure BMS</i> 4-benzoyl-4'-methyl diphenyl sulfide	224	284	-	1	
4-chloro benzophenone	134	189	2	1	
2-chloro benzophenone	122	177	2	1	
 <i>Michler's ketone</i> 4,4-(dimethylamino) benzophenone	247	316	-	2	80% at 316°C 15% at 532°C
<i>Ethyl Michler's ketone</i> 4,4-(diethylamino) benzophenone	254	319	-	2	93% at 319°C 4% at 499°C
<i>Esacure TZT</i> 2,4,6-trimethyl benzophenone	119	187	2	1	
4-methyl benzophenone	125	181	2	1	
2-methyl benzophenone	123	177	2	1	
4-methoxy benzophenone	155	211	4	1	
4,4'-dimethoxy benzophenone	178	-	-	-	sublimes
4,4'-diphenoxy benzophenone	249	318	-	1	
4-hydroxy benzophenone	193	253	1	1	

Table 3.7 TGA weight loss data from benzophenone type photoinitiators

The results in table 3.7 and the TGA raw data show that the benzophenone type photoinitiators have a wide range of volatilities / thermal stabilities depending on the type and position of any substituent. Benzophenone itself is quite volatile and therefore unsuitable for many applications involving heating processes, as has previously been shown by Beck³ et al. This is also true of the methyl and chloro substituted benzophenones which show little advantage over benzophenone in this respect. Most other substituent types result in a significant reduction in volatility, this was seen particularly with materials such as 4,4'-diphenoxy benzophenone, 4-phenyl benzophenone and Quantacure BMS.

With the exception of the two dialkylamino benzophenones, Michler's ketone and Ethyl Michler's ketone, which show distinctly two stage thermal decomposition reactions, all the materials in this class appear to show weight loss through evaporation. However, most also show a residual weight loss following the major evaporative weight loss, indicating that some thermal decomposition may be occurring at higher temperatures. In addition, 4,4'-dimethoxy benzophenone was unusual in that it showed extensive desublimation behavior, forming a cotton wool like matrix around the hangdown wire that prevented further measurements being recorded.

3.2.1.8 Quinone type photoinitiators

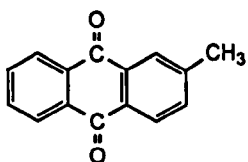
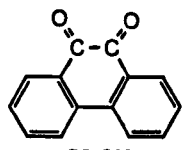
Photoinitiator	Temp. of 5% wt. loss (°C)	Max. rate of wt. loss (°C)	Residual wt. loss (%)	No. of Wt. loss stages	Comments and other weight losses
 2-methyl anthraquinone	183	236	-	1	some desublimation
2-ethyl anthraquinone	173	225	-	1	some desublimation
2- <i>t</i> .butyl anthraquinone	185	243	2	1	
 <i>PI-ON</i> phenanthrene-9,10 quinone	208	259	4	1	

Table 3.8 TGA weight loss data from quinone type photoinitiators

The results in table 3.8 and the TGA raw data show that despite some displaying desublimation behaviour, all the quinone type photoinitiators analysed show good thermal stability, losing weight principally through evaporation, although some thermal decomposition is also likely at higher temperatures.

3.2.1.9 Aromatic 1,2-diketone type photoinitiators

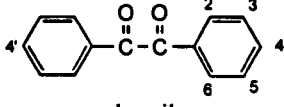
Photoinitiator	Temp. of 5% wt. loss (°C)	Max. rate of wt. loss (°C)	Residual wt. loss (%)	No. of Wt. loss stages	Comments and other weight losses
 benzil	144	198	1	1	
4,4'-dimethoxy benzil	203	268	-	1	
4,4'-dimethyl benzil	167	223	4	1	

Table 3.9 TGA weight loss data from aromatic 1,2-diketone type photoinitiators

The results in table 3.9 and the TGA raw data show that, as for the substituted benzophenones, benzil is reasonably volatile but is made less so by substitution, particularly with methoxy groups. All the photoinitiators in this class show principally evaporation on heating.

3.2.1.10 Miscellaneous Type II photoinitiators

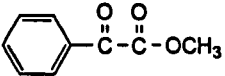
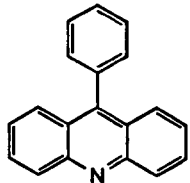
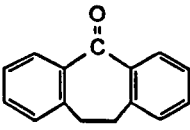
Photoinitiator	Temp. of 5% wt. loss (°C)	Max. rate of wt. loss (°C)	Residual wt. loss (%)	No. of Wt. loss stages	Comments and other weight losses
 <i>Nuvopol PI 3000</i> phenyl glyoxylic acid methyl ester	86	145	-	1	
 9-phenyl acridine	199	255	6	1	
 dibenzosuberone	180	248	3	1	

Table 3.10 TGA weight loss data from miscellaneous Type II photoinitiators

The results in table 3.10 and the TGA raw data show that both 9-phenyl acridine and dibenzosuberone have good thermal stability; losing weight on heating principally through evaporation, but with evidence for some thermal decomposition at higher temperatures. In contrast, Nuvopol PI3000 is very volatile and unsuitable for applications involving heating processes. In this case weight loss appears to be exclusively by evaporation, with no evidence of any thermal decomposition.

3.2.1.11 Aliphatic amine synergists

Photoinitiator	Temp. of 5% wt. loss (°C)	Max. rate of wt. loss (°C)	Residual wt. loss (%)	No. of Wt. loss stages	Comments and other weight losses
triethylamine	-	-	-	-	weight loss too fast to measure
triethanolamine	157	223	-	1	2% at 25°C
tri-isopropanolamine	137	187	-	1	
N,N-dimethyl propanolamine	40	87	-	1	
N-methyl diethanolamine	81	153	-	1	
N,N-dimethyl ethanolamine	40	90	-	1	
$\text{H}_2\text{C}=\text{CH}-\overset{\text{O}}{\parallel}{\text{C}}-\left(\text{OCH}_2\underset{\text{CH}_3}{\text{CH}}\right)_3-\overset{\text{O}}{\parallel}{\text{C}}\text{CH}_2\text{CH}_2-\text{N}\begin{matrix} \text{CH}_2\text{CH}_3 \\ \text{CH}_2\text{CH}_3 \end{matrix}$ <i>Ebecryl P115</i>	159	230	-	3	80% at 230°C 14% at 316°C 6% at 467°C

Table 3.11 TGA weight loss data from aliphatic amine synergists

The results in table 3.11 and the TGA raw data show that with the exception of triethanolamine, tri-isopropanolamine and Ebecryl P115, all the aliphatic amines investigated are volatile at low temperatures and completely unsuited to use in applications involving heating processes. Both triethanolamine and tri-isopropanolamine are volatile at comparatively low temperatures but could find use in some applications, as could Ebecryl P115, although this material loses weight in a distinctly 3 stage thermal decomposition process.

3.2.1.12 Aromatic amine synergists

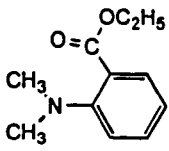
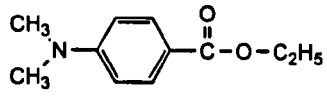
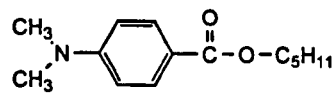
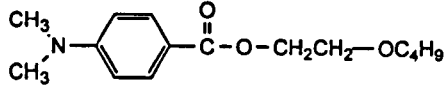
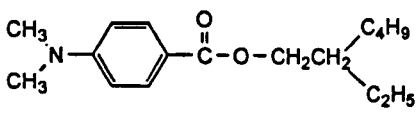
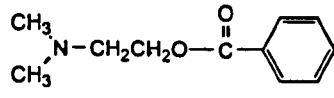
Photoinitiator	Temp. of 5% wt. loss (°C)	Max. rate of wt. loss (°C)	Residual wt. loss (%)	No. of Wt. loss stages	Comments and other weight losses
 2-N,N-dimethylamino benzoic acid ethyl ester	176	244	1.5	1	
 <i>Quantacure EPD</i> 4-N,N-dimethylamino benzoic acid ethyl ester	132	187	3	1	
 <i>Quantacure MCA</i> 4-N,N-dimethylamino benzoic acid amyl ester	171	233	1.5	1	
 <i>Speedcure BEDB</i> 4-N,N-dimethylamino benzoic acid (2-butoxy ethyl) ester	188	258	1	1	0.5% at 25°C
 <i>Quantacure EHA</i> 4-N,N-dimethylamino benzoic acid (2-ethyl hexyl) ester	184	248	0.5	1	
 <i>Quantacure DMB</i> (2-dimethylamino) ethyl benzoate	100	167	1	1	

Table 3.12 TGA weight loss data from aromatic amine synergists

The results in table 3.12 and the TGA raw data show that the aromatic amine synergists investigated are more suited to use in applications involving heating processes than aliphatic ones. The data suggests that the weight loss for these materials is principally through evaporation, although there is some evidence for thermal decomposition at higher temperatures.

For the 4-N,N-dimethylamino benzoic acid esters, volatility decreases with increasing chain length of the ester group such that the ethyl ester would be unsuitable for some applications (5% weight loss at 132°C) but the (2-ethylhexyl) ester would find more widespread use (5% weight loss at 184°C). In addition the substitution position appears to be important, with the 2-N,N-dimethylamino benzoic acid ethyl ester being significantly more thermally stable than the 4-N,N-dimethylamino benzoic acid ethyl ester. The synergist (2-dimethylamino) ethyl benzoate is significantly more volatile than any of the other materials in this class and would be unsuitable for most applications involving heating processes.

3.2.2 The solubility of photoinitiators in an oligomer / monomer blend

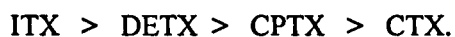
The results shown in table 3.13 show the relative solubilities of a wide range of photoinitiators at 2 %wt in an 80/20 blend of the aliphatic urethane diacrylate oligomer CN934 and the monomer TMPTA. Since the samples were subsequently used to investigate the reactivity of different photoinitiators (see chapter 6), they also contained 2 %wt of the amine synergist N-methyl diethanolamine (MDEA).

The classification of materials into different solubility bands was achieved for each photoinitiator type by observing the rate of dissolution of material in a small glass jar being stirred on a hot plate using a magnetic stirrer bar. From a rough knowledge of the temperature setting / time taken for dissolution of one or more materials from each structural type, an overview of the relative photoinitiator solubilities was then constructed for all the materials examined, as shown in table 3.13. This approach is far from being analytically accurate in terms of differentiating between materials of similar solubility, particularly if they are of a different structural type, but does clearly show larger solubility differences and trends within any structurally similar group of materials.

The information in table 3.13 shows that, whilst substitution in thioxanthone type photoinitiators results in increased solubility, substitution in aromatic 1,2 diketone and to a large extent benzophenone type photoinitiators results in decreased solubility. Insufficient information is available to make such comments about the other structural groups, although throughout all the materials investigated, alkyl groups tend to have a better solubilising effect than alkoxy groups.

It is also possible from the data presented in table 3.13 to hypothesize that, despite a large number of articles by Decker²¹⁻²³ concerning the cost and performance benefits of 4,4'-diphenoxy benzophenone over benzophenone, the UV curing industry has failed to show any significant interest in this photoinitiator because of its extremely poor solubility characteristics. When compared to the much more soluble derivatives Quantacure ITX and Speedcure DETX, Quantacure CPTX and Quantacure PTX may have found limited commercial success for the same reason. 2-Chloro thioxanthone, one of the first commercially available thioxanthone derivatives,

thioxanthone derivatives, is also now rarely used following the introduction of the much more soluble alkyl substituted thioxanthenes. Similar results have been reported by Rajamani et. al.¹⁵ who found thioxanthone derivatives to show the following order of solubility:



Although benzoin gelled during sample preparation, the benzoin ethers all dissolved but subsequently gelled on storage; the isopropyl and isobutyl ethers gelling within 2 days, the methyl ether and Esacure EB3 gelling within 1 week and the ethyl ether gelling within 2 months. The low storage stability of benzoin ether type photoinitiators is well known^{17,24}, having previously been attributed to the labile benzylic hydrogen²⁴. However, the relative levels of instability do not agree with the work of Berner et. al.²⁴ who reported that ethers with the shortest alkyl chains showed the lowest stability. This difference cannot readily be explained without further work, but could be related to the differing types and levels of free radical stabilizers in commercial grades of some benzoin ethers.

Photoinitiator type	highly soluble					soluble		low solubility		insoluble
	liquid	benzoin isobutyl ether	benzoin methyl ether benzoin ethyl ether	benzoin isopropyl ether	benzoin isobutyl ether	Darocure 2959	Lucerin TPO BDTPO		benzoin (gels)	
Benzoin	Esacure EB3									
Hydroxyalkyl phenone	Darocure 1173 Darocure 1116			Irgacure 184 Esacure KIP						
Acyl phosphine oxide	TEPO Irgacure 1700									
α -Aminoalkyl phenone										
Miscellaneous Type I	DEAP	Quantacure PDO		Irgacure 651						
Xanthone / thioxanthone				Speedcure DETX Quantacure ITX	t. butyl thioxanthone			Quantacure PTX Quantacure CPTX	Kayacure CTX** xanthone**	thioxanthone*
Benzophenone	Esacure TZT 2-methyl benzophenone		benzophenone Daitocure OB 2-chloro benzophenone 4-chloro benzophenone 4-methyl benzophenone 4-methoxy benzophenone		Quantacure BMS 4-hydroxy benzophenone			4-phenyl benzophenone ethyl Michler's ketone 4,4'-dimethoxy benzophenone		4,4'-diphenoxy benzophenone* Michler's ketone**
Quinone					t. butyl anthraquinone			ethyl anthraquinone		methyl anthraquinone** PI-ON**
Aromatic 1, 2 diketone			benzil		4,4'-dimethyl benzil			4,4'-dimethoxy benzil**		
Miscellaneous Type II	Nuvopol PI3000	dibenzosuberone							9-phenyl acridine	

Table 3.13 Relative solubilities of photoinitiators in an 80/20 blend of the oligomer CN934 and the monomer TMPTA

* Precipitates on cooling

**Precipitates on standing (1-2 weeks)

3.3 CONCLUSIONS

Thermogravimetric analysis (TGA) and thermogravimetric analysis-mass spectroscopy (TGA-MS) have been used to investigate the volatility / thermal stability of a wide range of photoinitiators and amine synergists in order to determine whether they are suitable for use in application areas that involve the use of heating processes, particularly before any UV irradiation occurs.

The results suggest that for most photoinitiators and synergists evaporation is the dominant weight loss process, although for many materials some thermal decomposition is evident at higher temperatures. A few materials such as the photoinitiators Esacure KIP, Irgacure 369 and Michler's ketone show clear evidence of multistage thermal decomposition reactions. Where these were investigated in more detail for specific photoinitiators using TGA-MS, it was evident that the decomposition products were not the same as those seen by a photodecomposition reaction mechanism.

For the photoinitiators investigated a wide range of behaviour was found; from Darocure 1173 which showed significant evaporative weight loss at only 84°C, to ethyl Michler's ketone which started to thermally decompose at temperatures above 254°C. Amine synergists showed an equally wide stability range; from triethylamine which has a weight loss at room temperature too fast to accurately measure, to Quantacure EHA which is non-volatile up to 184°C. This wide range of behaviour is such that careful consideration is required regarding photoinitiator selection for applications involving heating processes, with accurate information needed about temperature conditions within the process before the most appropriate choice can be made.

Several thioxanthone and quinone type photoinitiators showed desublimation behavior on heating, with the vapour condensing directly into the solid phase. This may lead to potential printing and contamination problems in some applications, particularly those which involve food.

The relative solubility of a range of photoinitiators was assessed in an oligomer / monomer blend with the results being used to speculate that some new materials, claimed in the literature to be highly reactive, have failed to gain significant commercial sales by virtue of their low solubility.

3.4 EXPERIMENTAL

3.4.1 Volatility and thermal stability of photoinitiators and synergists

Thermogravimetric analysis (TGA)

A Perkin-Elmer (Beaconsfield, Bucks.) TGA7 thermogravimetric analyser was used. Samples of approximately 2-4 mg were heated at 5°C per minute in a 5 cm³ per minute air purge.

Thermogravimetric analysis-mass spectroscopy (TGA-MS)

A Hewlett-Packard (Bracknell Berks.) GC-MS system comprising a 5890 gas chromatograph (GC) and 5970 mass selective detector (MSD) was modified for use in this procedure. A temperature programmable injection port was fitted to the GC oven by GC² Chromatography (Altrincham, Cheshire) and connected through the oven directly to the MSD inlet using a 1 metre length of 0.1 mm internal diameter non-polar capillary column. The oven temperature and MSD inlet temperature were maintained at 280°C throughout, and the temperature of the injection port, containing a few milligrams of sample in a glass liner, raised from 25°C to 600°C at 10°C per minute. The MSD was operated in scan mode between m/z 30 and 400. A helium purge gas at a pressure of 10 psi. was used throughout.

The total ion current recorded by the MSD was plotted and compared on a similar temperature axis as the TGA data for the same material. A faster temperature ramp was used for the TGA-MS experiment in order to minimise the run time since problems due to sample overloading were common and resulted in reruns being required.

3.4.2 Solubility of photoinitiators in an oligomer / monomer blend

Formulations based on an 80/20 blend of the oligomer CN934 and the monomer TMPTA, containing 2 %wt photoinitiator and 2 %wt of the synergist N-methyl diethanolamine (MDEA) were prepared on a hot plate-stirrer. Materials from each structural group were classified into different solubility bands based on their visual rate of dissolution and / or the hot plate temperature setting.

3.5 REFERENCES

1. S M Johns, J W Gramshaw, L Castle, S M Jickells; *Deutsche Lebensmittel-Rundschau*, **91** (3), 69 (1995)
2. S A Sharma, A J Tortorello; *J. Applied Polym. Sci.*, **43**, 699 (1991)
3. E Beck, M Lokai, E Keil H Nissler; *Proc. Conf. RADTECH*, Nashville, USA, 160 (1996)
4. R Kinoshita, Y Teramoto, T Nakano, H Yoshida; *Journal Of Thermal Analysis*, **38**, 1891 (1992)
5. V Berbenni, A Marini, G Bruni, T Zerlia; *Thermochemica Acta.*, **258**, 125 (1995)
6. B J McGrattan in *ACS Symposium Series 581*; T Provder, M W Urban, H G Barth (Eds.), Washington D.C., USA, 103 (1994)
7. D A Compton; *BIO-RAD FTS/IR Application Note 47*, May (1987)
8. E Kaisersberger, E Post, J Janoschek in *ACS Symposium Series 581*, 75 (1994)
9. M S Chace, *Finnigan Mat Application Report Number 218* (1988)
10. E L Charsley, S B Warrington, G K Jones, A R McGhie; *American Laboratory*, Jan. (1990)
11. S B Warrington in *Thermal Analysis-Techniques and Applications*, E L Charsley, S B Warrington (Eds.), Royal Society Of Chemistry, Cambridge, England, 84 (1992)
12. J P Redfern; *Polymer International*, **26**, 51 (1991)
13. W H McClennen, R M Buchannan, N S Arnold, J P Dworzanski, H L C Meuzelaar; *Analytical Chemistry*, **65**, 2819 (1993)
14. S L Herlihy; *Thermogravimetric Analysis-Mass Spectroscopy: Its Development And Use In The Surface Coatings Industry*, Coates Lorilleux Internal Report (1991)
15. N Rajamani, J S Bowers Jr.; *Proc. Conf. RADTECH*, Nashville, USA, 74 (1996)
16. J W Birkenshaw in *The Printing Ink Manual -5th Edition*, R H Leach, R J Pierce (Eds.), Blueprint, London, 14 (1993)
17. S J Wilson in *Radiation Curing of Polymers II*; D R Randell (Ed.), The Royal Society of Chemistry, Cambridge, England, 124, (1991)
18. M Kohler, J Ohngemach; *Proc. Conf. RADTECH*, New Orleans, USA, 150 (1988)
19. *Perry's Chemical Engineers' Handbook (6th Edition)*, R H Perry, D W Green, J O Maloney (Eds.), McGraw-Hill Inc., 17-12 (1984)
20. *Kingzett's Chemical Encyclopedia (3rd Edition)*, D H Hey (Ed.), Bailliere, Tindall and Cassell Ltd., London (1966)
21. C Decker, K Moussa; *Journal of Polymer Science: Part C: Polymer Letters*, **27**, 347 (1989)
22. C Decker, K Moussa; *Proc. Conf. RADTECH*, Boston, USA, 260 (1992)
23. C Decker, K Moussa; *Journal of Coatings Technology*, **65** (819), 49 (1993)
24. G Berner, R Kirchmayr, G Rist; *J. Oil and Col. Chem. Assoc.*, **61**, 105 (1978)

CHAPTER 4

UV light utilisation

4.1 INTRODUCTION

A UV curing reaction can only proceed effectively if a photoinitiator present in the formulation absorbs light of an appropriate wavelength and generates the free radicals necessary to initiate the chain polymerization reaction. One of the principal factors that governs the efficiency of this process is the amount of light the photoinitiator absorbs. This is defined for any point within the coating by the Beer-Lambert Law (1), which states that the amount of light absorbed decreases exponentially per unit thickness from the exposed surface¹⁻⁵.

$$A = \epsilon \cdot c \cdot d \quad (1)$$

ϵ = molar extinction coefficient ($\text{mol dm}^{-3}\text{cm}^{-1}$), c = concentration (mol dm^{-3}), d = path length (cm)

4.1.1 Competitive light absorption

UV curing formulations almost always contain more than one material that absorbs light in the UV region. The cumulative nature of absorbance means that, under ideal conditions, equation (1) can be modified to express the total absorbance as a function of all the materials present²⁻⁵ i.e.

$$A = d (\epsilon_1 c_1 + \epsilon_2 c_2 + \dots + \epsilon_n c_n) \quad (2)$$

In these situations, the individual components compete for the available incident light, with photoinitiator efficiency being reduced if light is absorbed by a component other than a photoinitiator or sensitizer. Competitive light absorption, often termed the 'inner filter effect', or 'screening', can lead to both a reduction in cure speed and a loss of physical properties, with the extent of any problem being related simply by equation (2) to the identity and concentration of the materials involved. Pigments are known to present the biggest problem in this respect⁵⁻⁹, since as well as having absorption bands in the visible region, defining the coating colour to the observer, pigments also contain absorption bands in the UV region that compete with the photoinitiator for incident light. The detrimental effect of pigments on the curing of inks was first rationalised by Bassemir and Bean⁶, and then more firmly established by Hencken⁷, where the curing efficiency for a series of inks was empirically related to the UV transmission spectra of the pigments used. It was shown that, for a fixed photoinitiator combination, inks containing weakly UV absorbing pigments cured faster than those containing strongly UV absorbing pigments. This effect has subsequently been shown by a number of other authors, particularly with reference to the relative ease of curing for yellow and magenta inks compared to cyan and black¹⁰⁻¹².

Hencken argued that, in order to achieve optimum curing efficiency, a photoinitiator should be chosen which has its absorption maximum in the same spectral region as the pigment spectrum's absorption minimum⁷. Although this theory was widely accepted, the few photoinitiators commercially available meant that it was of limited practical significance at the time. In contrast,

the wide variety of photoinitiators available in today's market means that Hencken's theories are far more relevant and applicable.

Plews and Phillips¹³ more firmly established the link between the photoinitiator absorbance spectrum and the pigment type, using two differently absorbing photoinitiator systems to cure magenta, cyan and non-pigmented inks at increasing film thicknesses. They clearly showed the need for photoinitiators that absorb strongly in the 300-400 nm region to effectively cure pigmented inks, and that although weakly absorbing photoinitiators were effective at low film thicknesses, their effectiveness decreases rapidly as film thickness increased.

Relatively few other references are available that investigate pigmentation on the UV curing efficiency of printing inks. However, there are a large number which concentrate on thick white pigmented coatings¹⁴⁻²⁰; a testament to the size of the wood coatings and paint industries. Whilst this work has often shown the importance of particular photoinitiator types, long UV wavelengths, choice of curing lamp and the type of white pigment used, white is not a well used colour for printing inks and the work is therefore of limited practical significance in the printing ink industry.

Competitive light absorption can also result from light absorption by oligomers, monomers, amine synergists and other photoinitiators. To the author's knowledge, the extent of their influence in this respect has not been investigated.

4.1.2 Extent of UV light absorption

The incidence of competitive light absorption in a coating can result in a lack of UV radiation reaching the lower layers. In many cases this leads to poorer cure in this area, manifesting itself as the physical problems of poor "through cure", when the coating appears to be soft in its lower layers, or shows a lack of adhesion to the substrate. In severe cases, when virtually no light reaches the base of the coating, this region remains liquid. If this occurs, surface wrinkling is also likely due to the differential shrinkage between the cured upper layers and the uncured lower layers. In very thin printing inks, these cure problems are less pronounced, but through cure is often the limiting factor in the curing of cyan or black inks¹⁰.

The nature of absorbance is such that under ideal conditions the Beer-Lambert Law (1) can be used to quantify the percent of incident light transmitted to the bottom of a specified coating, and a prediction made of any likely through cure problems. A number of authors have done work in this area, the most informative being that of Seko²¹ and Gatechair^{22,23}, who also calculated an index of radical concentration as a function of film thickness. More complex calculations have also been made by other authors²⁴⁻²⁶, attempting to quantify the extent of surface reflection, scattering by pigment particles and absorption by the substrate of the incident light. However, the complex single wavelength calculations and the problems associated with light scattering by the pigment

have meant that these models have not been well used by the ink industry, which at best, still uses qualitative spectral comparison in its formulation and development work.

It has been suggested that the optimum photoinitiator concentration will be characterised by an absorbance value of 0.43, resulting in the maximum available light being absorbed by the bottom 1% of the coating²⁶⁻²⁸. However, practical problems such as the large variations in molar extinction coefficient with wavelength for most photoinitiators and the use of polychromatic light sources are known to limit the potential of this formulating approach^{5,22}.

Within this chapter a simple model for quantifying light absorption and transmission is presented and validated for use in non-pigmented and some pigmented systems.

4.1.3 Wavelength of light absorption

The probability of a photoinitiator molecule absorbing UV or visible light is reflected by its absorbance spectrum, with each of the broad bands being associated with an individual electronic transition within the molecule. This information cannot be used in isolation to determine whether a photoinitiator will be effective in a given situation, since only light that is available can be absorbed. The emission spectrum of the curing lamp used must also therefore be considered. Within the coatings industry this is almost always the medium pressure mercury lamp.

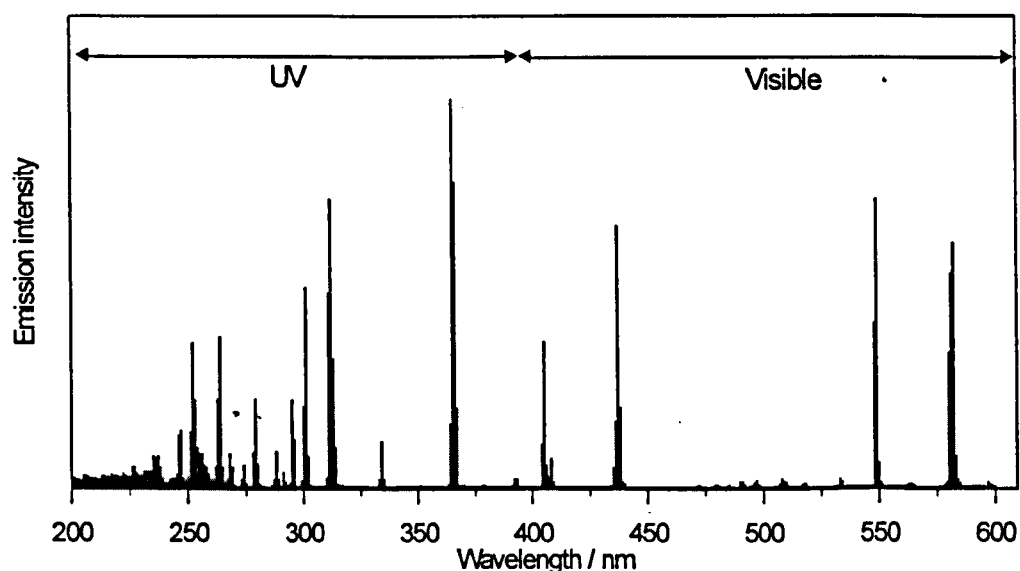


Figure 4.1 *Representation of the emission spectrum of a typical medium pressure mercury lamp.*

The emission spectrum of the medium pressure mercury lamp, shown in figure 4.1, extends throughout the UV, visible and IR regions of the electromagnetic spectrum. Although the UV region only extends to 390 nm, the presence of two prominent near visible lamp emission bands at 405 nm and 436 nm, where many photoinitiators still absorb light, means that the spectral region of interest in this project covers the UV region and visible region up to 450 nm.

For a typical photoinitiator such as benzophenone, it is well known that the photochemically active first excited triplet state is formed following inter system crossing from the first excited singlet state^{1,3,4}. It is also known that the singlet state can be formed either directly from the ground state following absorption of light in the (n-π*) spectral region, or via the second excited singlet state following light absorption in the (π-π*) spectral region and internal conversion to dissipate excess energy^{1,3,4}. Despite speculation by Rubin²⁴ that absorption of light in either the (n-π*) or (π-π*) spectral regions for benzoin ethyl ether will result in the generation of free radicals, this does not appear to have been practically demonstrated in the literature for this or any similar photoinitiator. In particular, very little work has been published that relates the lamp emission wavelengths and photoinitiator absorbance spectra to cure efficiency. The exception is the work of de Ruiter, de Vlieger and Bouwma³⁰, who showed using a series of interference filters that the curing effectiveness of two photoinitiators was both photoinitiator absorbance spectrum and lamp emission intensity dependent.

The work of de Ruiter, de Vlieger and Bouwma³⁰ suggests that in order to choose the most appropriate photoinitiator(s) to cure a given ink, it is necessary to know how effective photoinitiators are as a result of irradiation with each of the principal lamp emission wavelengths, and how they are affected by the addition of pigments. This subject has been investigated in this chapter.

4.1.4 Sensitization

The sensitization process involves an energy transfer reaction whereby a sensitizer molecule (S) absorbs light, generating an excited state, and then transfers this energy to a ground state photoinitiator molecule (P). The excited photoinitiator molecule then goes on to form free radicals and initiate the cure process^{3,4} i.e.:



The two principal advantages of sensitization are that;

1. Excited state photoinitiator molecules can be produced which may not otherwise be attained because of low direct initiation efficiency.
2. Light can be utilised by the sensitizer which may not be absorbed by the photoinitiator, or available to it by virtue of competitive light absorption by other materials.

Although the term sensitization relates particularly to energy transfer reactions, it is more commonly used to describe a number of processes that lead to a higher observed reactivity from a combination of photoinitiators than would be expected based on their individual reactivities.

These are summarised below, with 2) and 3) being more accurately described as synergistic processes.

1) *Energy transfer reactions*

Energy is transferred directly from the triplet state sensitizer to the ground state photoinitiator with conservation of angular momentum. Generally, the sensitizer must have a higher triplet energy than the photoinitiator, allowing the reaction to be thermodynamically favourable.

e.g. the sensitization of 2-methyl-1-[4-(methylthio)phenyl]-2-morpholino-propan-1-one (Irgacure 907) by isopropyl thioxanthone (Quantacure ITX)^{19,31}

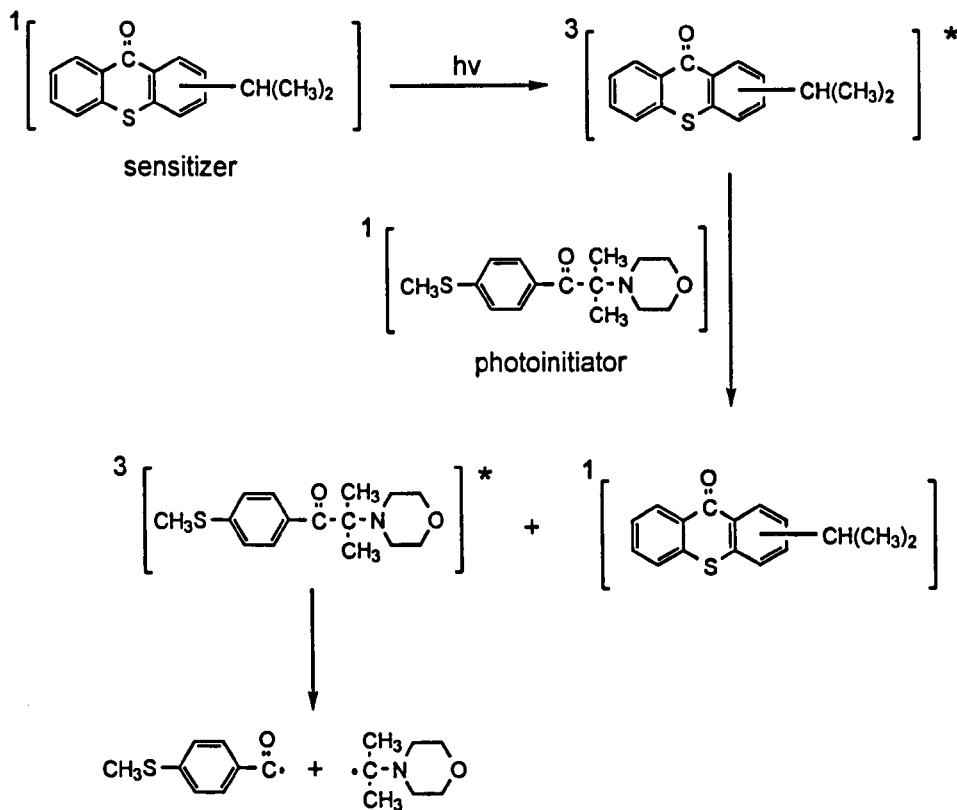


Figure 4.2 *Energy transfer sensitization of Irgacure 907 by Quantacure ITX*

It has been suggested that the reaction mechanism for the combination of Irgacure 907 and thioxanthone derivatives is a combination of an energy transfer sensitization process and an electron / proton transfer process involving the nitrogen lone pair, with the relative balance of these processes dependent on the structure of the thioxanthone and the polarity of the medium³². The sensitization activity of a series of thioxanthone and acetophenone type photoinitiators has been reported and the energy transfer process shown to provide greater curing activity³³.

2) Electron transfer followed by proton transfer

The formation of an excited state complex (exciplex) which can be populated by excitation of either molecule. Electron and then proton transfer results in the formation of a reactive alkylamino radical and a relatively unreactive ketyl radical.

e.g. the benzophenone and 4,4'-(dimethylamino)benzophenone (Michler's ketone) system^{5,34-36}

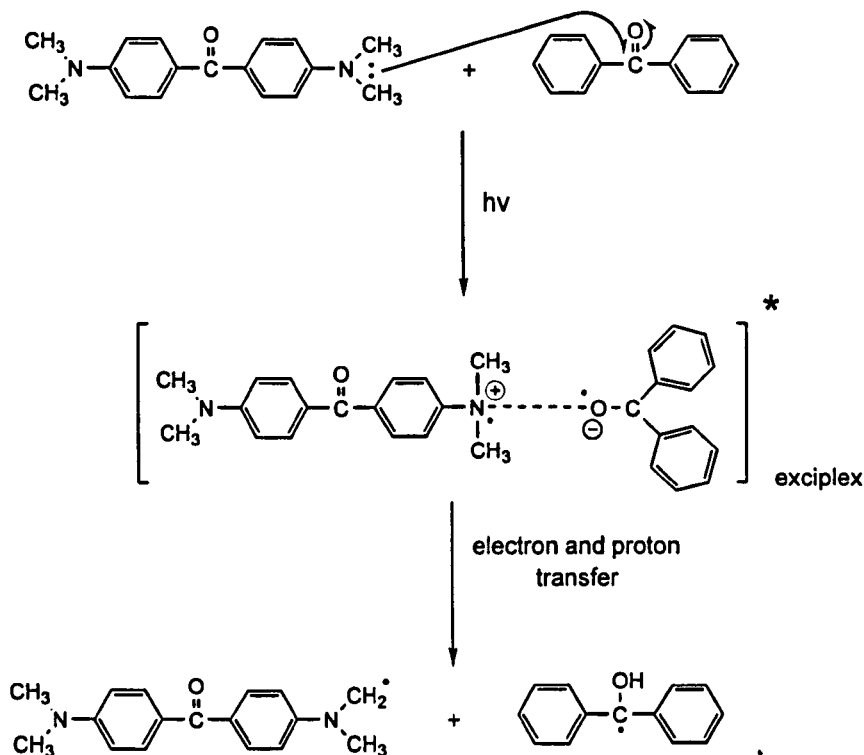


Figure 4.3 *Electron and proton transfer sensitization involving Michler's ketone and benzophenone*

3) Chemical reaction with the radical formed in the primary process

Radicals produced by the cleavage of some photoinitiators are easily scavenged by oxygen to give relatively unreactive peroxy radicals, which then abstract hydrogens from amines or other donors to form hydroperoxides. The hydroperoxides then react with the excited state of a second photoinitiator, possibly via an energy transfer reaction, to give a hydroxyl and alkoxy radical, both of which are efficient polymerisation initiators.

e.g. The reaction of 1-hydroxycyclohexyl acetophenone (Irgacure 184) or 1-phenyl-2-hydroxy-2-methyl propan-1-one (Darocure 1173) with benzophenone³⁷.

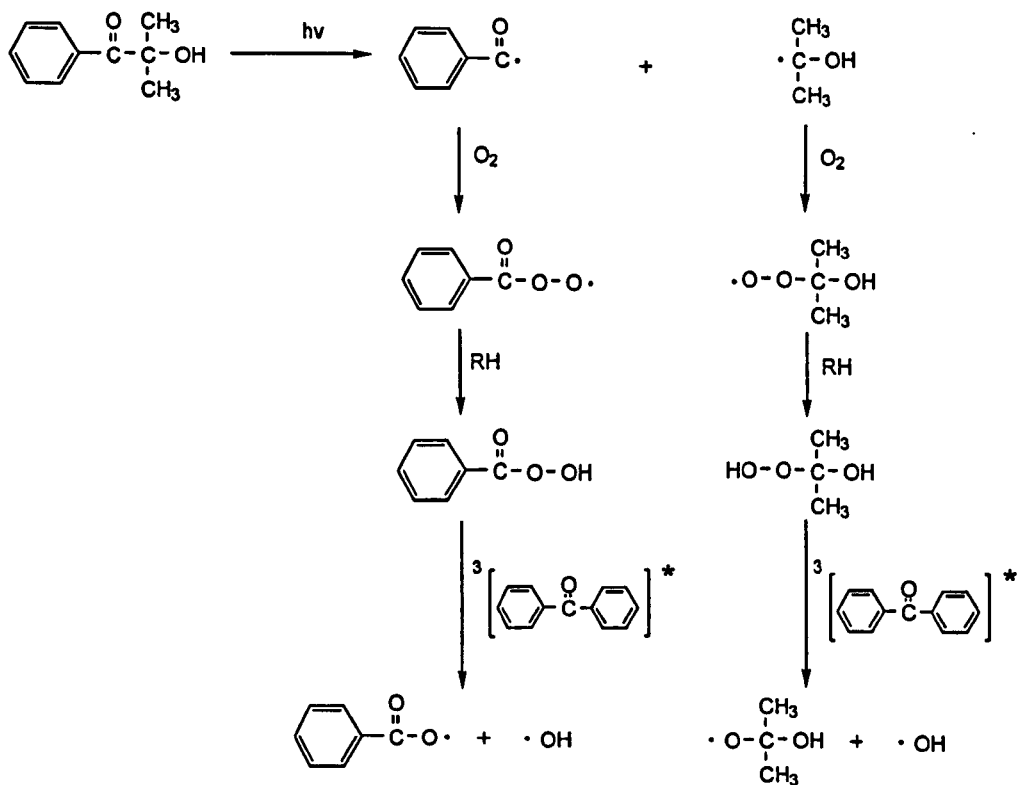


Figure 4.4 Chemical reaction sensitization involving Darocure 1173 and benzophenone

In practice, sensitization is sought mostly to increase reactivity through use of a wavelength region in which the photoinitiator itself does not absorb light, but a sensitizer does. Thioxanones are very useful in this respect since they absorb light into the near visible region with a significant molar extinction coefficient. A number of commercial photoinitiators have been investigated for potential sensitization by Quantacure ITX, but with the exception of the α -aminoalkylphenones Irgacure 907 and Irgacure 369, none have shown any sensitization activity. Based on their triplet energies, other materials were also speculated by Dietliker et al. not to show any sensitization activity in conjunction with ITX^{33,38}.

A simple and practical Differential Photocalorimetry (DPC) method has been described³³ which allows a rapid and effective determination of any sensitization activity to be made by irradiating a potential photoinitiator / sensitizer combination with light absorbed only by the sensitizer. In this chapter, the DPC method described is modified slightly and used to investigate sensitization within a wider range of materials than has previously been published.

4.2 RESULTS AND DISCUSSION

4.2.1 UV light absorption

UV light is absorbed by many of the components in an ink formulation. In this section, the effect of light absorption is discussed in terms of how the reactivity of a formulation is affected by the combination of photoinitiator type, irradiation wavelength and the presence of other materials in the formulation that compete for the incident light.

4.2.1.1 Most effective curing wavelengths of photoinitiators

The curing effectiveness of different photoinitiators was assessed in an 80:20 ratio combination of the urethane diacrylate oligomer CN934 and the monomer TMPTA by Differential Photocalorimetry (DPC). Samples were irradiated using monochromatic light from a medium pressure mercury short arc lamp at each of the principal lamp emission wavelengths; 302, 313, 334, 365, 405 and 436 nm, and the weight normalized exotherm peak height (Wg^{-1}) used as a measure of reactivity. In this way the wavelength regions providing the greatest contribution to the cure performance can be identified for each photoinitiator, including the influence of the varying lamp emission intensity at these wavelengths. The emission intensities at the irradiation wavelengths investigated are similar to those shown in figure 4.1 except that the 334 nm emission band from the short arc lamp is slightly enhanced, having an intensity similar to that of the 302 nm emission band.

Information on cure performance at wavelengths below 300 nm is not available, both because the short arc lamp used does not emit below 280 nm, and because the light absorbance by the oligomer in these thick films at wavelengths below 300 nm would prove to be too great an influence on the observed reactivity³⁹.

The photoinitiator concentration was optimised at 0.2 %wt for these experiments to eliminate self-screening effects, with 0.2 %wt MDEA used as a synergist in all formulations. Also, for reasons of time, not all the photoinitiators of interest in this project were investigated. Materials thought to behave similarly to others, and some materials of limited commercial importance were not tested.

All results are presented on the same scale to allow a comparison of curing efficiency in any wavelength region for any combination of photoinitiators.

The absorbance spectra of the photoinitiators were acquired in methanol solution at a concentration of 0.02 g dm^{-3} .

Hydroxyalkylphenones

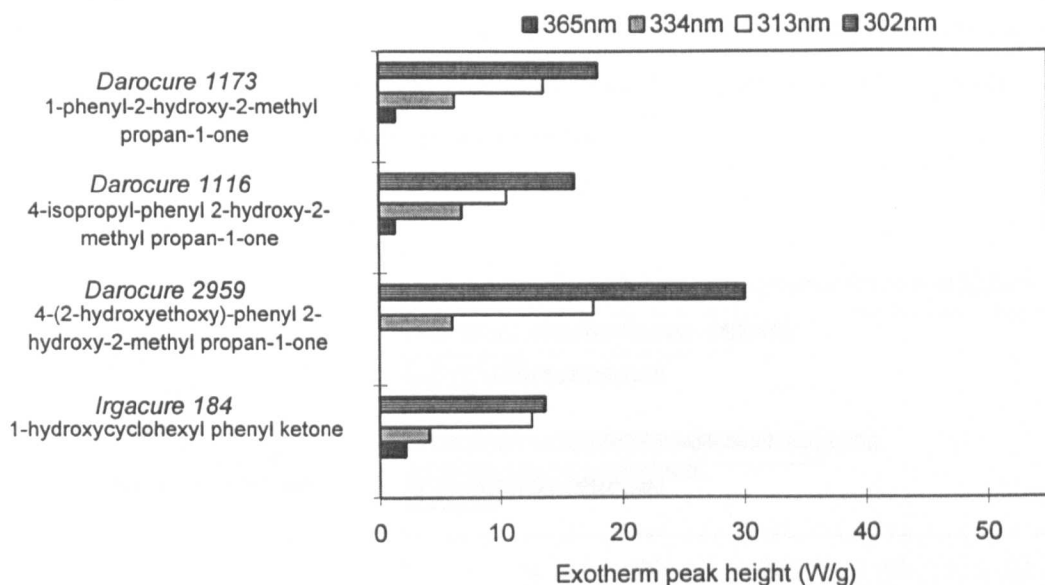


Figure 4.5 *Most effective curing wavelengths by DPC for hydroxyalkylphenone photoinitiators*

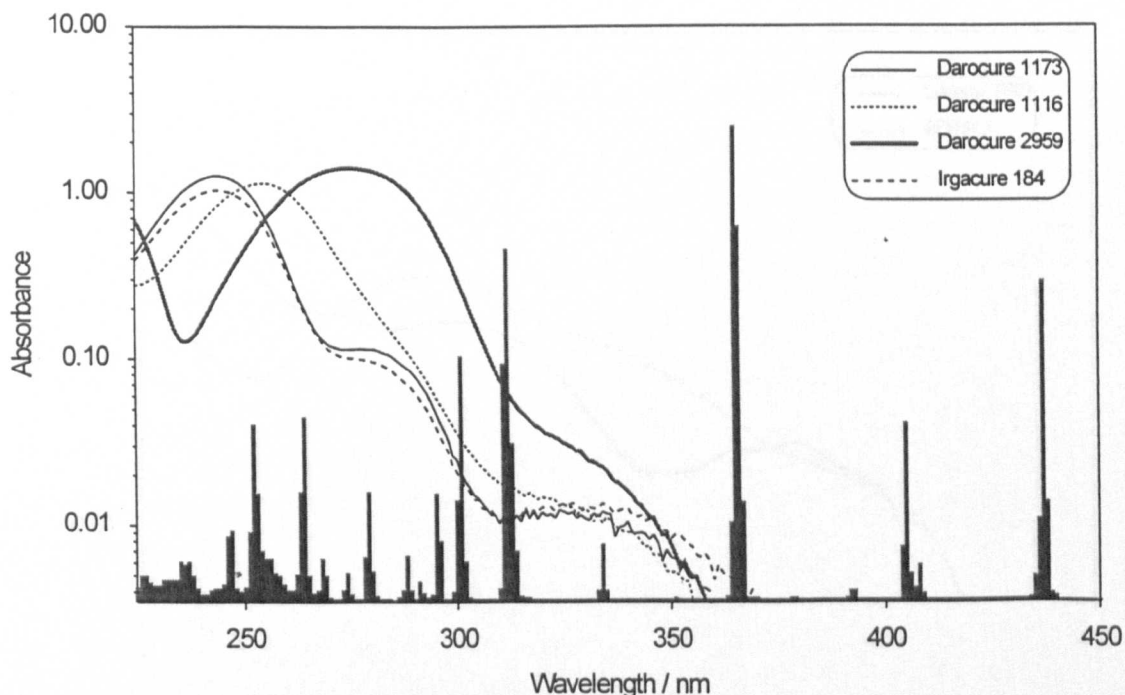


Figure 4.6 *The relationship between the medium pressure mercury lamp emission spectrum and the absorption spectra of hydroxyalkylphenone photoinitiators*

The results in figure 4.5 show that for hydroxyalkylphenone photoinitiators, it is the light from the lamp emission bands at 302 nm and 313 nm that provide the greatest contribution to the observed cure. Despite the high intensity of the 365 nm lamp emission band, its importance in the curing process for this class of photoinitiator is very low because they either fail to absorb light, or do so very weakly at this wavelength.

Another photoinitiator in this class is the oligomeric form of 1-phenyl-2-hydroxy-2-methyl propan-1-one, Esacure KIP, which has a similar reactivity (see chapter 6) and absorption spectrum to Darocure 1116. It would therefore be reasonable to expect it to show similar curing effectiveness at each of the lamp emission wavelengths.

Acylphosphine oxides

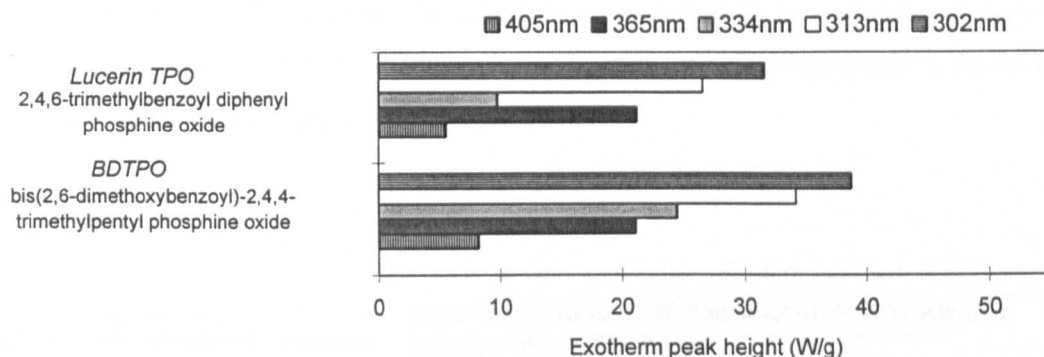


Figure 4.7 Most effective curing wavelengths by DPC for acylphosphine oxide photoinitiators

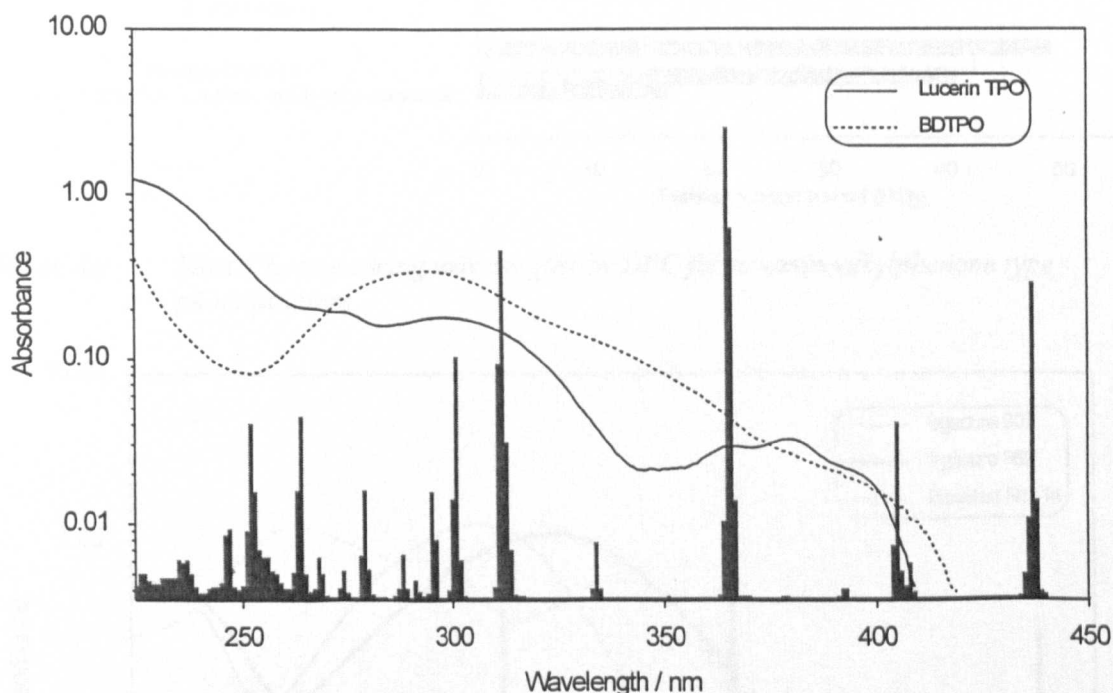


Figure 4.8 The relationship between the medium pressure mercury lamp emission spectrum and the absorption spectra of acylphosphine oxides

The results in figures 4.7 and 4.8 show that for acylphosphine oxide photoinitiators, it is the light from the lamp emission wavelengths at 302 nm and 313 nm that provide the greatest contribution to the observed cure, with relatively little contribution to the overall cure coming from the 405 nm emission band. These results are somewhat surprising in view of the general literature acceptance that this class of photoinitiator is very responsive to wavelengths of around 400 nm, such that it is particularly suitable for curing white pigmented coatings⁴⁰. In fact, the results shown here suggest that acylphosphine oxides would be of even greater use in yellow and magenta pigmented

coatings, where the extent of the UV light absorption by the pigment is considerably less than in white pigmented coatings⁶⁻⁸.

An additional photoinitiator in this class is 2,4,6-trimethylbenzoyl phenylphosphinic acid ethyl ester (TEPO) which is structurally similar and has a similar absorption spectrum to Lucerin TPO. It would be reasonable to expect TEPO to show similar curing effectiveness at each of the lamp emission wavelengths to TPO, although its generally lower reactivity (see chapter 6) would be reflected by a lower curing effectiveness at each of the lamp emission wavelengths, particularly 405 nm where TEPO shows a very weak absorption.

α -Aminoalkylphenones

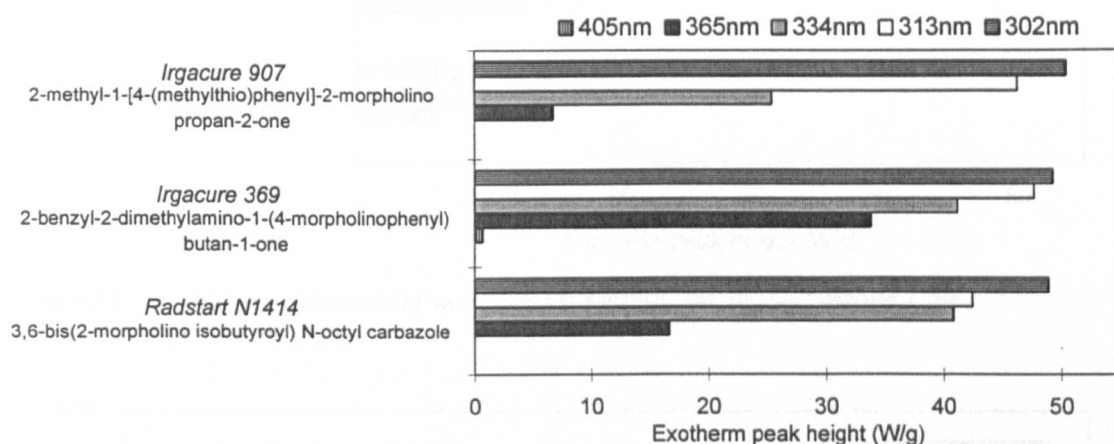


Figure 4.9 Most effective curing wavelengths by DPC for α -aminoalkylphenone type photoinitiators

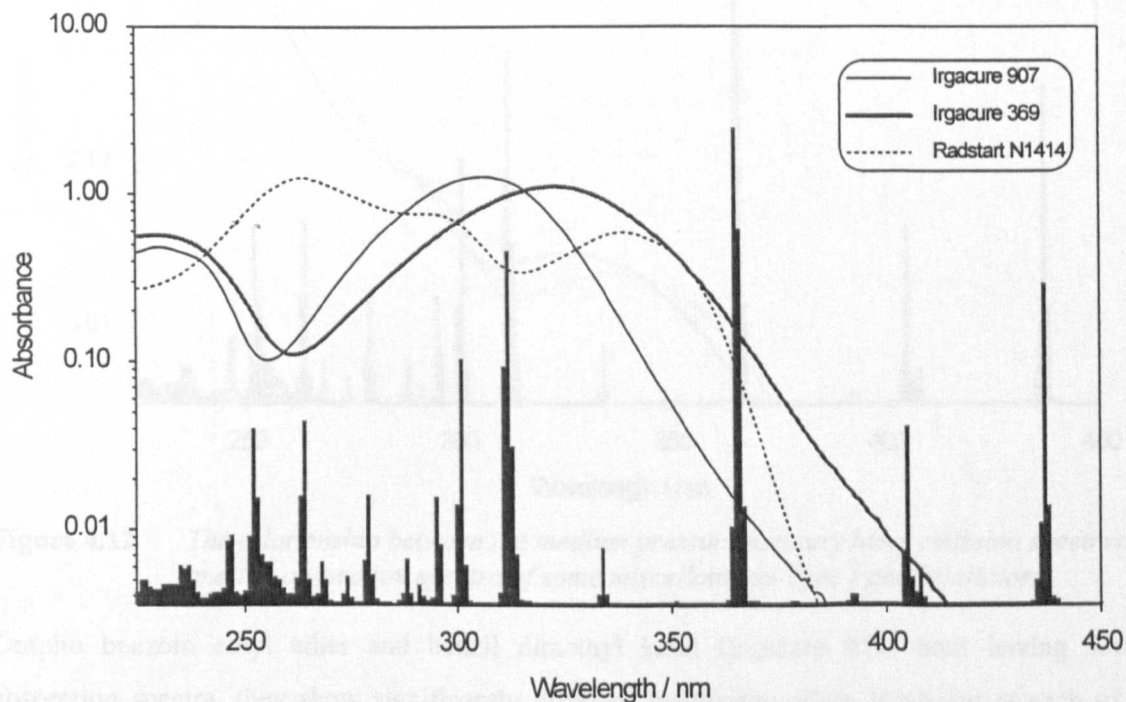


Figure 4.10 The relationship between the medium pressure mercury lamp emission spectrum and the absorption spectra of α -aminoalkylphenone photoinitiators

The results in figures 4.9 and 4.10 show that for the three α -aminoalkylphenone photoinitiators investigated, exceptionally high reactivity at the 302 and 313 nm lamp emission bands is observed. These photoinitiators show strong absorbance bands in this region, and in the case of Irgacure 369, the long trailing nature of the charge transfer character ($\pi-\pi^*$) band means that it shows a similarly high level of reactivity at 334 and 365 nm, with a low level of reactivity at 405 nm. Both Irgacure 907 and Radstart N1414 show a much lower reactivity at 365 nm, where their absorbance intensities are lower.

Miscellaneous Type I photoinitiators

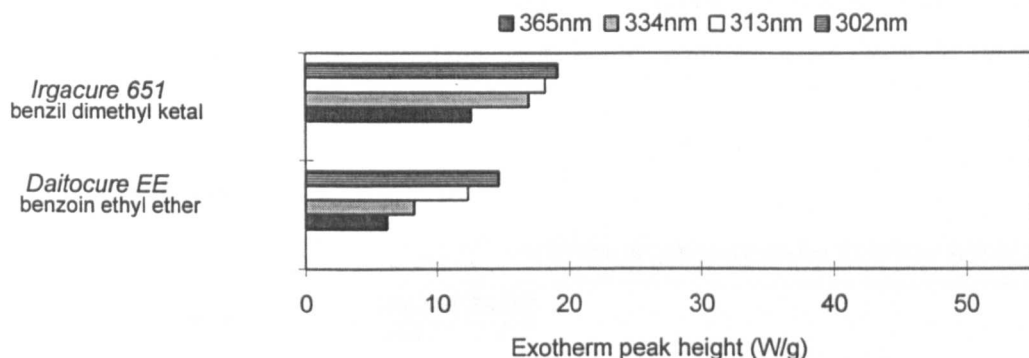


Figure 4.11 Most effective curing wavelengths by DPC for miscellaneous Type I photoinitiators

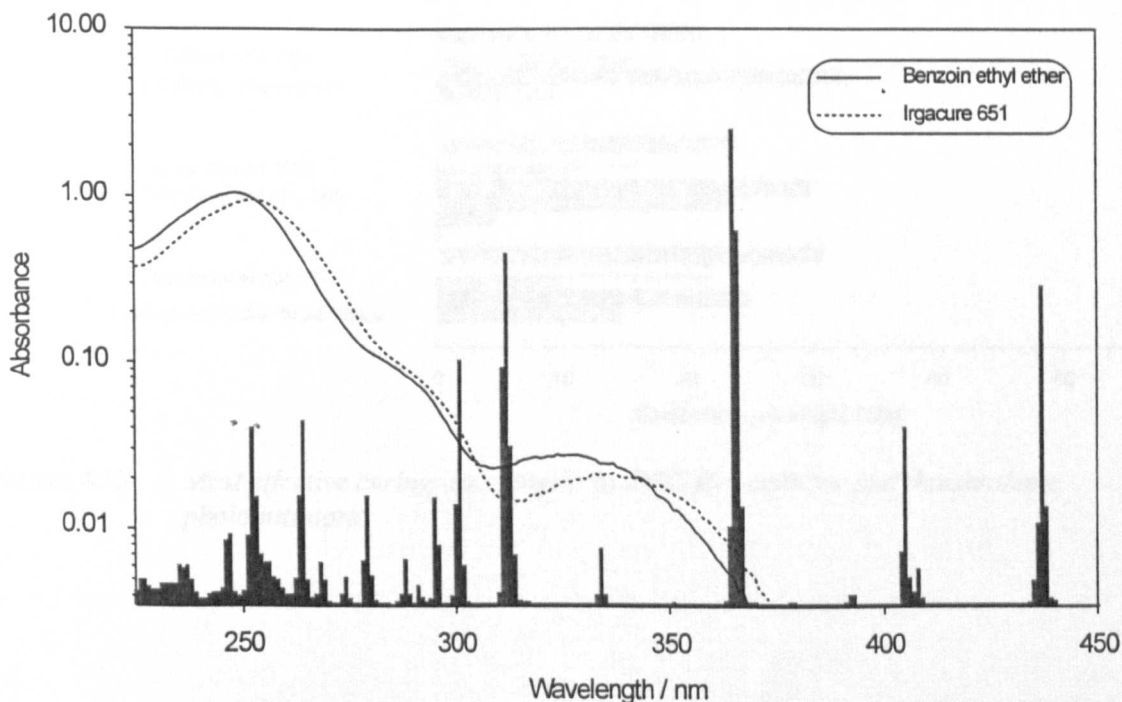


Figure 4.12 The relationship between the medium pressure mercury lamp emission spectrum and the absorption spectra of some miscellaneous Type I photoinitiators

Despite benzoin ethyl ether and benzil dimethyl ketal (Irgacure 651) both having similar absorption spectra, they show significantly different reactivities when irradiated at each of the principal lamp emission wavelengths, as shown in figure 4.11. Benzoin ethyl ether displays a reactivity profile similar to that observed with many other of the photoinitiators examined as part

of this work, with reactivity increasing when irradiated with shorter, more energetic wavelengths. However, Irgacure 651 appears to have a reactivity much less dependent on the irradiation wavelength. This observation cannot be accounted for by spectral examination alone since the hydroxyalkylphenone photoinitiators Darocure 1173 and Irgacure 184 have very similar absorption spectra to Irgacure 651 and benzoin ethyl ether in the 300-380 nm region, but show an even more significant reactivity decrease with increasing wavelength (see figures 4.5 and 4.6). It is speculated that these observations may relate to the quantum efficiencies of the photoinitiators involved, with Irgacure 651 having the highest quantum yield (0.55)⁴¹ followed by benzoin ethyl ether (0.39-0.44)⁴², and Irgacure 184 and Darocure 1173 having the lowest values (0.2-0.3)⁴³. Further work on a larger series of compounds with known quantum yield values is required to clarify this hypothesis.

Xanthone / thioxanthenes

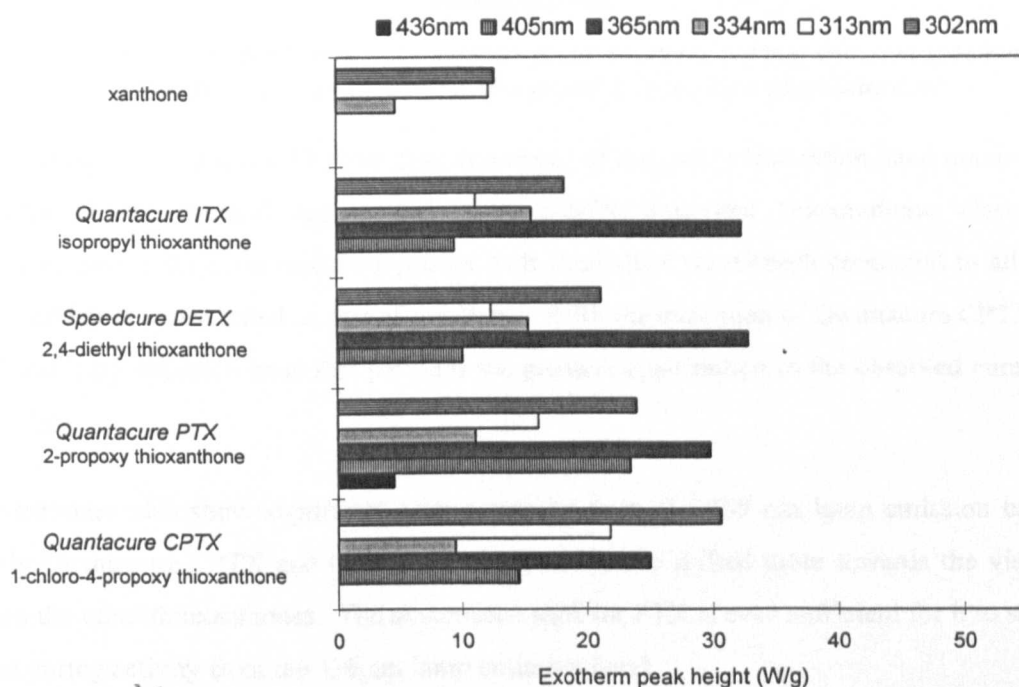


Figure 4.13 Most effective curing wavelengths by DPC for xanthone and thioxanthone photoinitiators

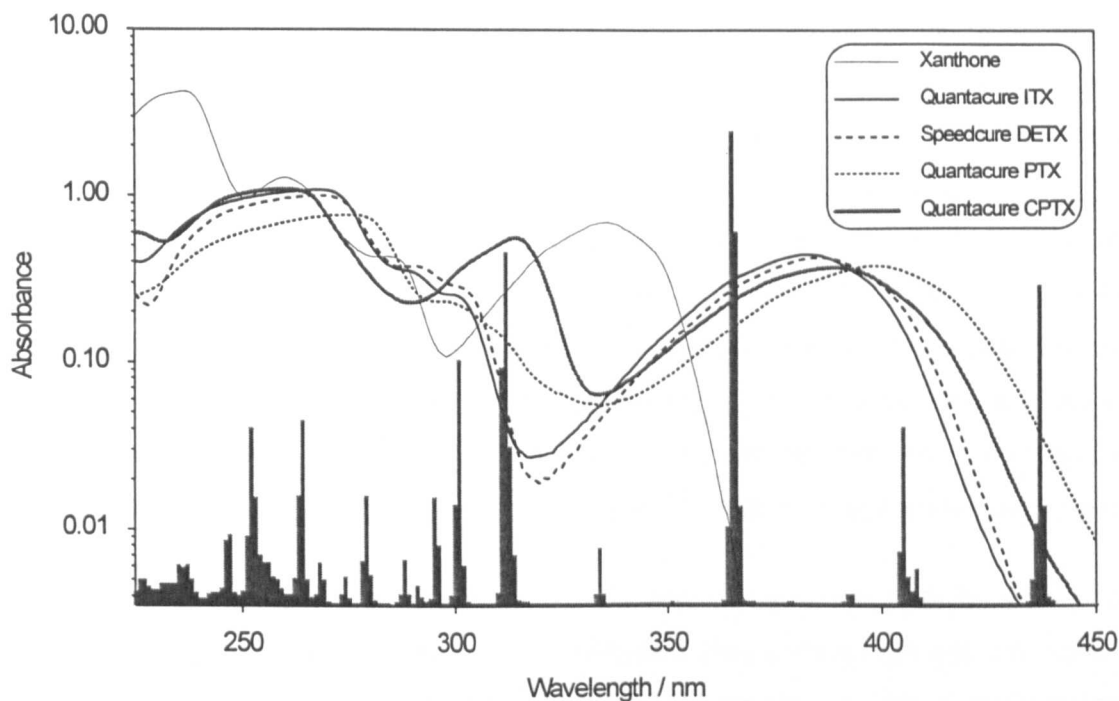


Figure 4.14 *The relationship between the medium pressure mercury lamp emission spectrum and the absorption spectra of xanthone and thioxanthone photoinitiators*

The results in figures 4.13 and 4.14 show that, as a result of the ($n-\pi^*$) absorption band maximum in the 370-380 nm spectral region, the commercially important thioxanthone class of photoinitiators have a different reactivity profile with irradiation wavelength compared to all the other photoinitiators investigated as part of this work. With the exception of Quantacure CPTX, it is the 365 nm lamp emission band that provides the greatest contribution to the observed cure for these materials.

The thioxanthenes also show significant curing activity from the 405 nm lamp emission band, particularly Quantacure CPTX and Quantacure PTX which are shifted more towards the visible region than the other thioxanthenes. The absorbance shift for PTX is even sufficient for it to show significant curing activity from the 436 nm lamp emission band.

Xanthone, lacking a sulfur atom conjugated to the chromophore, has its ($n-\pi^*$) absorption band centered at 340 nm, and consequently shows much lower reactivity (see chapter 6) than the thioxanthenes. It also shows curing activity only from the lamp emission bands at 302, 313 and 334 nm.

The observation of significant reactivity in a distinctly ($\pi-\pi^*$) spectral region, as shown by all the thioxanthenes at 302 nm, is evidence to support Rubin's speculation that initiation will occur following ($n-\pi^*$) or ($\pi-\pi^*$) transitions²⁴. As a result of these observations it is reasonable to expect that the thioxanthenes will all show good reactivity in the 250-265 nm region where they have a strong ($\pi-\pi^*$) absorption, and where there are two significant lamp emission bands.

The slight drop in the reactivity of PTX at 365 nm relative to ITX and DETX can be accounted for because of its lower molar extinction coefficient at this wavelength. However, despite a similar extinction coefficient to ITX and DETX at 365 nm, CPTX displays a significantly lower reactivity than the 3 other thioxanthenes tested. The reason behind this observation is speculated to be a lower quantum efficiency for CPTX relative to the other thioxanthenes as a result of the slight steric hinderance of the carbonyl group from the 1-chloro substituent. Although the reactivity of CPTX would also be expected to be lower at the other lamp emission wavelengths, the strong absorption band at 314 nm for this photoinitiator allows better light utilisation and therefore much higher reactivity in this spectral region. In fact, this additional light utilisation is so significant that CPTX displays the highest overall reactivity within this class of photoinitiator (see chapter 6).

Other photoinitiators in the thioxanthone class include 2-*t*.butyl thioxanthone and 2-chloro thioxanthone (Kayacure CTX). These materials both have absorption spectra and reactivities (see chapter 6) similar to ITX, and can therefore be reasonably expected to show a similar reactivity profile with lamp emission wavelength.

Benzophenones

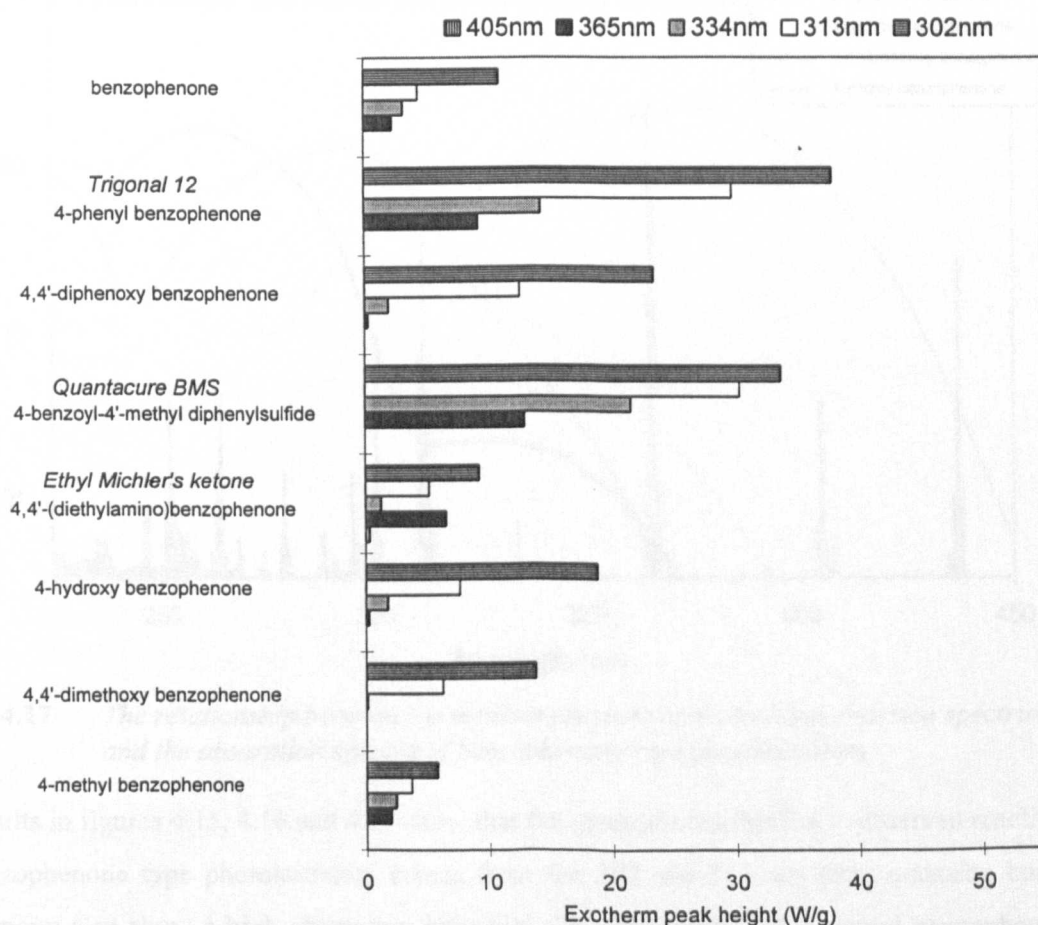


Figure 4.15 Most effective curing wavelengths by DPC for benzophenone photoinitiators

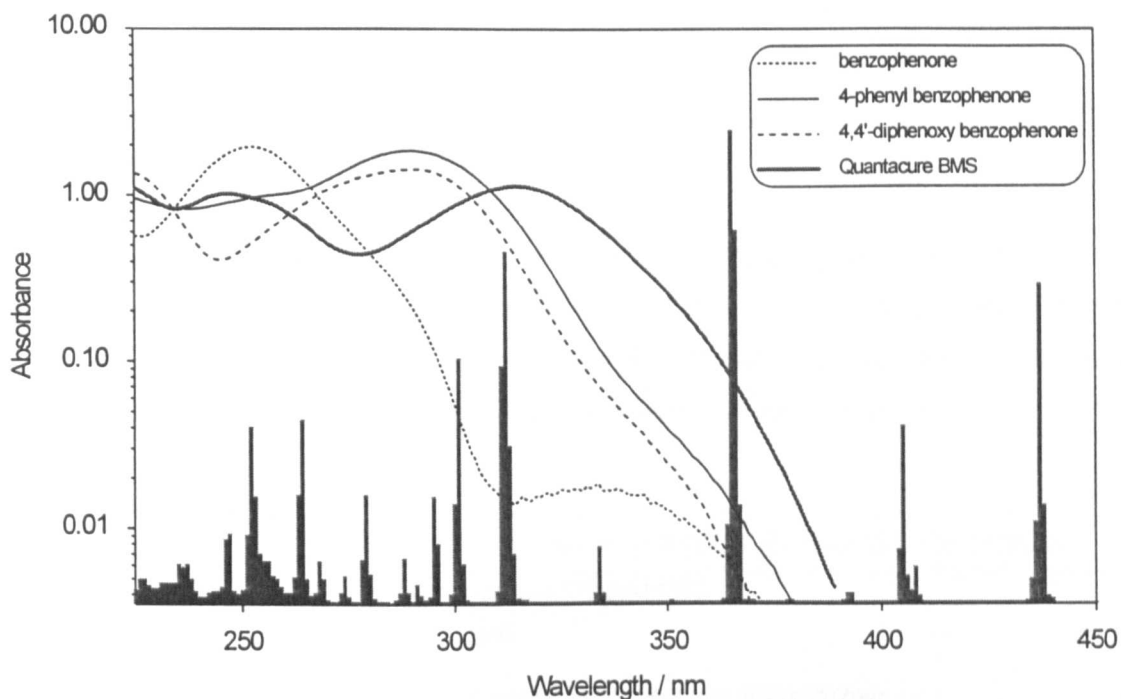


Figure 4.16 *The relationship between the medium pressure mercury emission spectrum and the absorption spectra of benzophenone type photoinitiators*

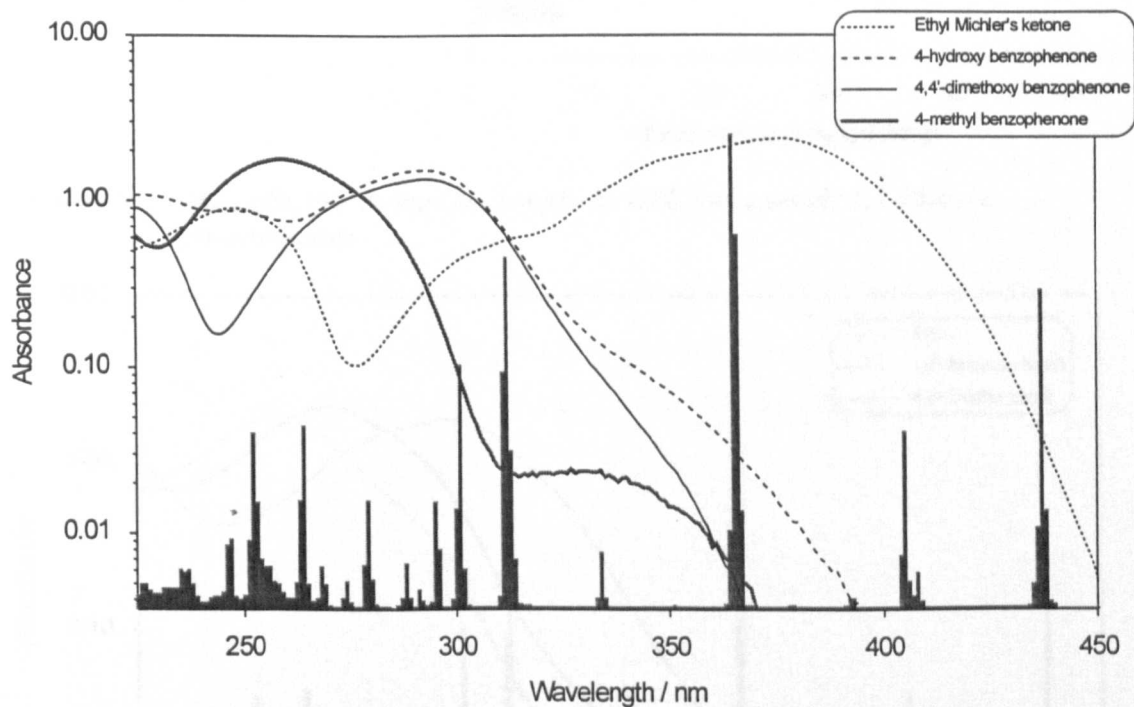


Figure 4.17 *The relationship between the medium pressure mercury lamp emission spectrum and the absorption spectra of benzophenone type photoinitiators*

The results in figures 4.15, 4.16 and 4.17 show that the greatest contribution to observed reactivity for benzophenone type photoinitiators comes from the 302 and 313 nm lamp emission bands, where many also show a high absorption intensity. The photoinitiators 4-phenyl benzophenone and Quantacure BMS were seen to be particularly reactive in this region, although some reactivity was also gained from the 365 nm lamp emission band.

Ethyl Michler's ketone displays a strong absorption band centered around 375 nm, but shows only a weak curing activity. However, this photoinitiator and the structurally similar Michler's ketone are known to be relatively ineffective when used on their own, but show greatly increased reactivity when used in combination with benzophenone^{5,34-36}.

Other commercial photoinitiators within this class include 2-benzoyl methyl benzoate (Daitocure OB) and 2,4,6-trimethyl benzophenone (Esacure TZT), both of which show similar absorption spectra and reactivity (see chapter 6) to benzophenone. As such, it is reasonable to expect that their reactivity profile with wavelength will be similar to that of benzophenone.

Aromatic 1,2 diketones

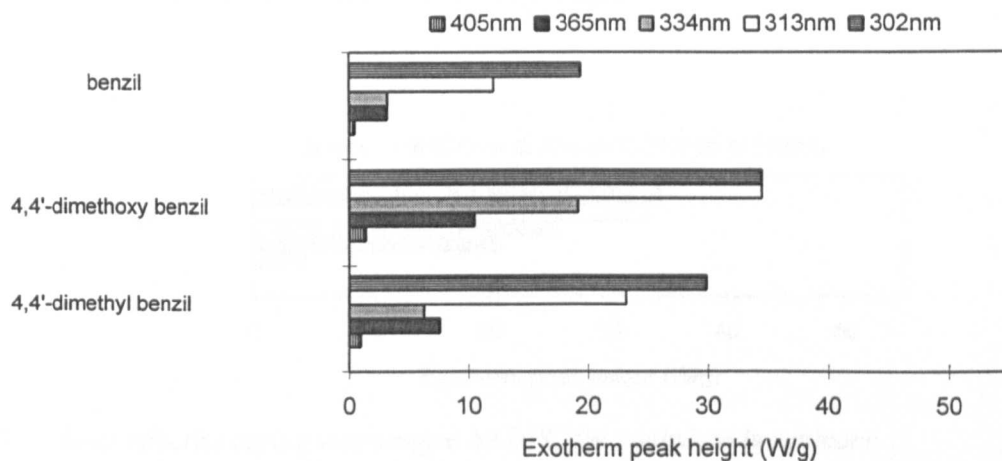


Figure 4.18 *Most effective curing wavelengths by DPC for aromatic 1,2 diketone photoinitiators*

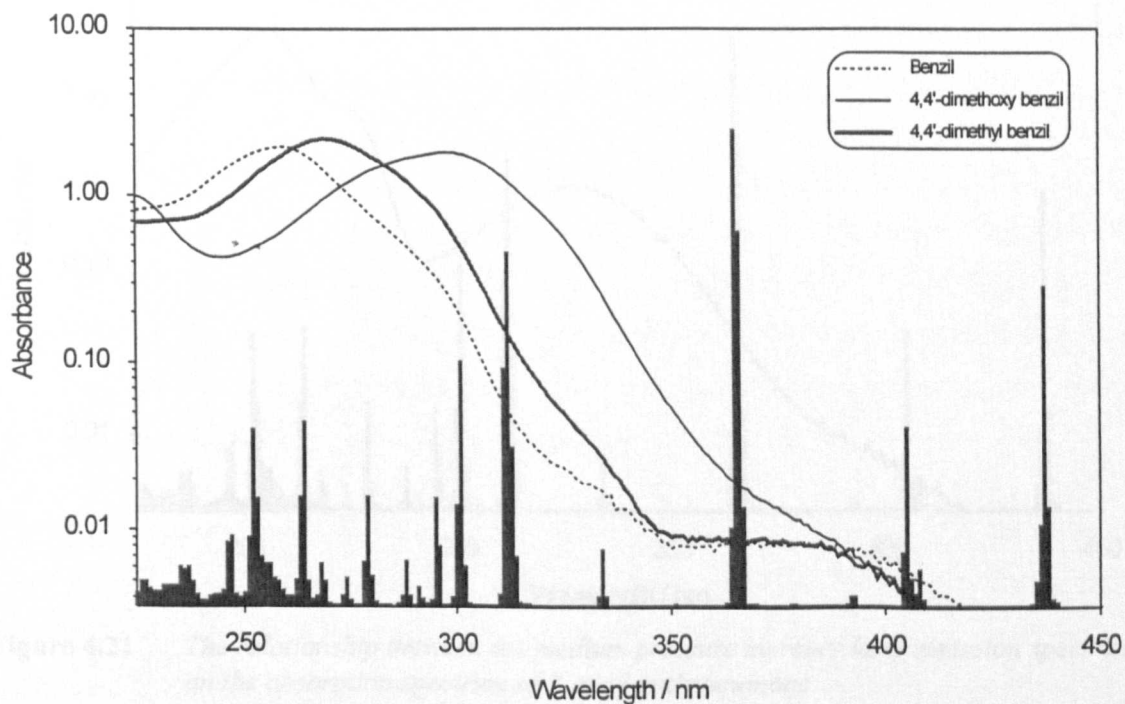


Figure 4.19 *The relationship between the medium pressure mercury lamp emission spectrum and the absorption spectra of aromatic 1,2 diketones*

The results in figures 4.18 and 4.19 show that the aromatic 1,2-diketone type photoinitiators derive most of their curing activity from the 302 and 313 nm lamp emission bands. Their long wavelength (n- π^*) transition at around 375 nm also allows them to show a low level of reactivity from the 405 nm lamp emission band.

The two substituted materials, 4,4'-dimethyl benzil and 4,4'-dimethoxy benzil, would appear to show a higher reactivity than the unsubstituted benzil. This can be partially attributed to the greater light utilisation of the two substituted materials at each of the lamp emission wavelengths, but the higher reactivity of 4,4'-dimethyl benzil at 365 nm, where both it and benzil have very similar absorption intensities, means that it is likely that both 4,4'-dimethyl benzil and 4,4'-dimethoxy benzil have a greater quantum efficiency than benzil.

Quinones

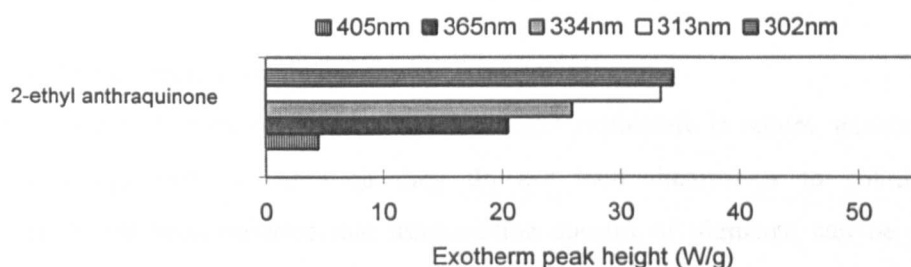


Figure 4.20 *Most effective curing wavelengths by DPC for 2-ethyl anthraquinone*

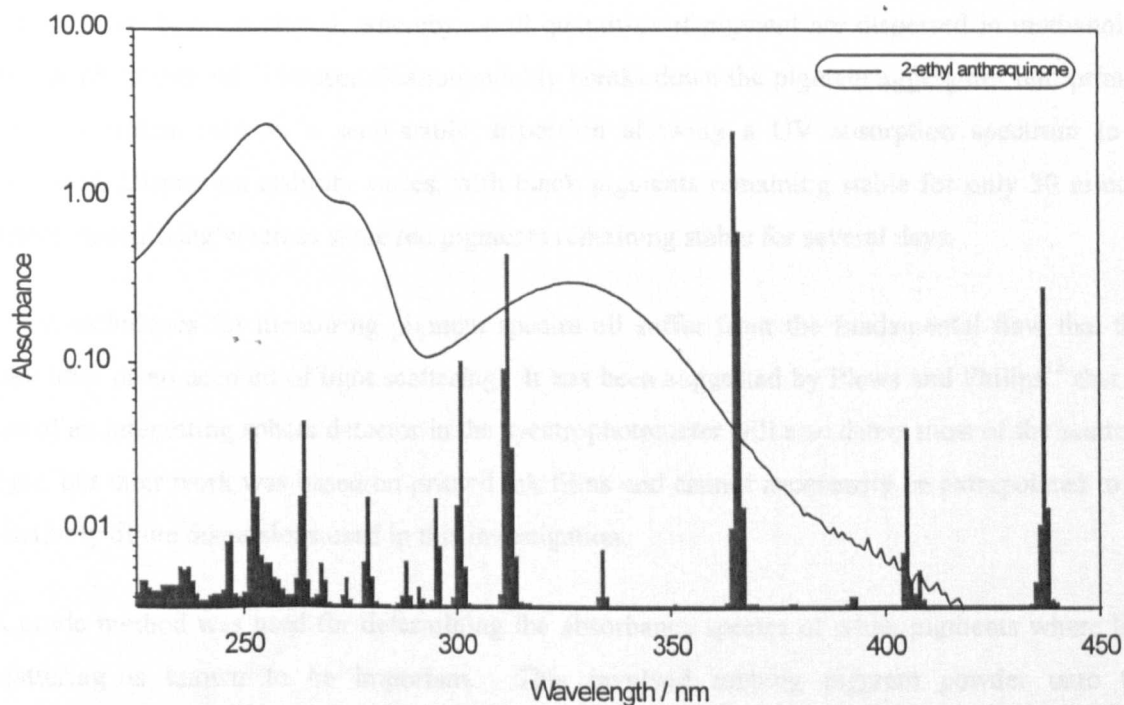


Figure 4.21 *The relationship between the medium pressure mercury lamp emission spectrum on the absorption spectrum of 2-ethyl anthraquinone*

The results in figures 4.20 and 4.21 show that as a result of the long trailing ($n-\pi^*$) absorption band centered at 330 nm, 2-ethyl anthraquinone shows good reactivity across a wide wavelength range. Although the most effective curing wavelengths are 302 nm and 313 nm, significant curing activity is still observed from the 405 nm lamp emission band.

Other photoinitiators in this class include the 2-methyl and 2-*t*.butyl anthraquinone derivatives and phenanthrene-9,10-quinone. The 2-methyl and 2-*t*.butyl anthraquinones have similar reactivity (see chapter 6) and absorption spectra to the 2-ethyl anthraquinone and can therefore be reasonably expected to show similar reactivity profiles with lamp emission wavelength. The reactivity of phenanthrene-9,10-quinone is also similar to the three anthraquinone derivatives, although its absorption spectrum contains an additional weak ($n-\pi^*$) band centered around 420 nm. This low energy spectral region is not expected to change its reactivity profile significantly, although the 405 nm lamp emission wavelength may become slightly more important.

4.2.1.2 UV light absorption by pigments

The pigments used in UV curing inks are insoluble and particulate in nature, existing as crystal aggregates and agglomerates, as such they do not lend themselves to solution spectral determination. It has been reported that transmission spectra of pigments can be obtained by dispersing small quantities of pigments into mineral oil using a 'Red Devil' shaker⁶, or by dispersing into a water / glycol mix with a stabilizing surfactant⁷. In this work an alternative approach has been employed, whereby small quantities of pigment are dispersed in methanol by the use of ultrasound. Ultrasonification quickly breaks down the pigment aggregates into primary particles which exist in a semi-stable dispersion allowing a UV absorption spectrum to be measured. Dispersion stability varies, with black pigments remaining stable for only 30 minutes before flocculating whereas some red pigments remaining stable for several days.

These techniques for measuring pigment spectra all suffer from the fundamental flaw that they take little or no account of light scattering. It has been suggested by Plews and Philips¹³ that the use of an integrating sphere detector in the spectrophotometer will also detect most of the scattered light, but their work was based on printed ink films and cannot necessarily be extrapolated to the relatively dilute dispersions used in this investigation.

A crude method was used for determining the absorbance spectra of white pigments where light scattering is known to be important. This involved rubbing pigment powder onto thin polyethylene film and blowing away the excess to give a 'stained' film which was taped across the light beam in the spectrophotometer. This technique was fast and reasonably effective but was limited by its non-quantitative nature.

The photoreactivity of printing inks has previously been investigated by Abadie and Carrera¹² using Differential Photocalorimetry (DPC), but their work produced exotherms that were both weak and highly asymmetrical in shape. It is the view of the author that the relatively thick samples used for their DPC experiments ($> 80\mu\text{m}$) was causing significant screening of the incident light and therefore anomalous results. In this work DPC is also used as a measure of photoreactivity for pigmented systems, but the concentration of all the components is reduced by a factor of 40 in a reactive matrix, since the DPC sample thickness is approximately $80\ \mu\text{m}$ whereas the intended ink application thickness is only $2\ \mu\text{m}$. This concentration adjustment leads to a similar degree of competition for incident light through the sample as would be found in a thin printing ink film, but without any complications due to screening.

Samples were irradiated at 45°C in an air atmosphere using either monochromatic light from a medium pressure mercury short arc lamp at each of the principal lamp emission wavelengths (302, 313, 334, 365, 405 and 436 nm), or the full lamp emission spectrum. The weight normalised exotherm peak height (Wg^{-1}) was used as a measure of reactivity. As has been previously mentioned, information at wavelengths below 300 nm is not available since the short arc lamp design does not emit radiation below 280 nm and the oligomer / monomer combination used also absorbs significant amounts of light below 300 nm.

Yellow pigments

Although there are nearly 200 yellow pigments classified, the monoarylide and particularly the diarylide types, such as Yellow 13, are highly dominant within the inks industry. Inorganic yellows such as iron oxides, lead chromates and cadmium sulfides are also available but no longer used because of their toxicity.

The structural similarity of most frequently used yellow pigments means that they all have similar UV absorption spectra, as shown in figure 4.22, with an absorption minimum somewhere between 300 and 350 nm. However, the absorption band which provides the colouristic properties of yellow pigments is between 400 and 500 nm. Although in the visible part of the spectrum, this band is significant when choosing an appropriate photoinitiator system for yellow inks, since, as shown in figure 4.23, it competes effectively with a photoinitiator for the incident light in this region and severely reduces the contribution of the lamp emission band at 405 nm to the overall cure efficiency.

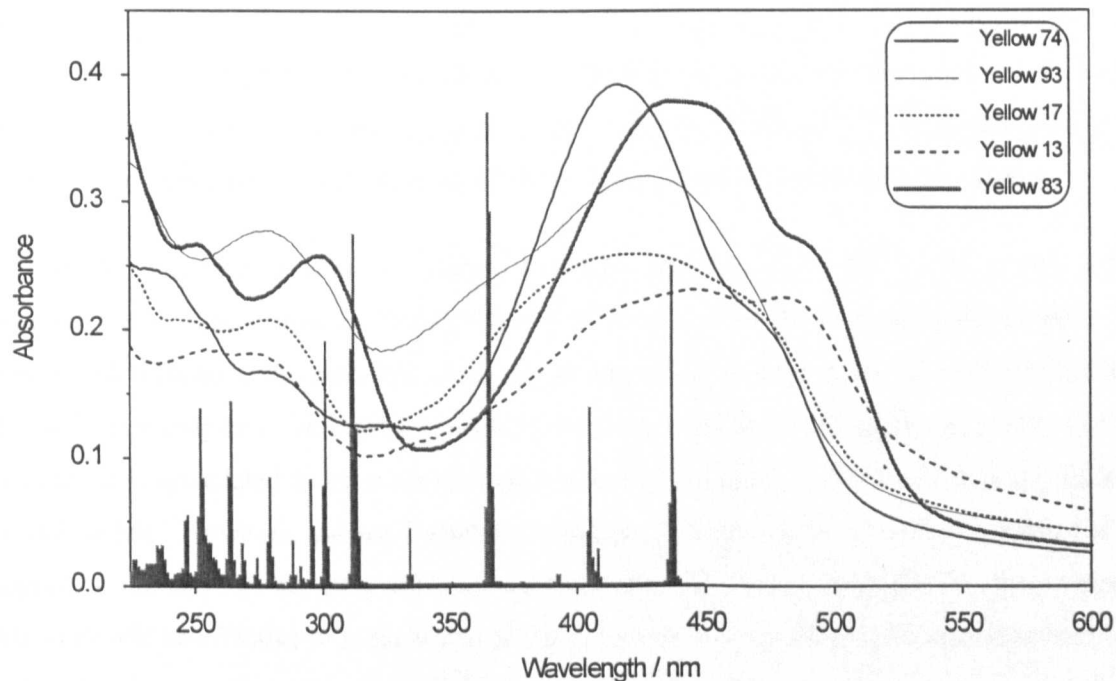
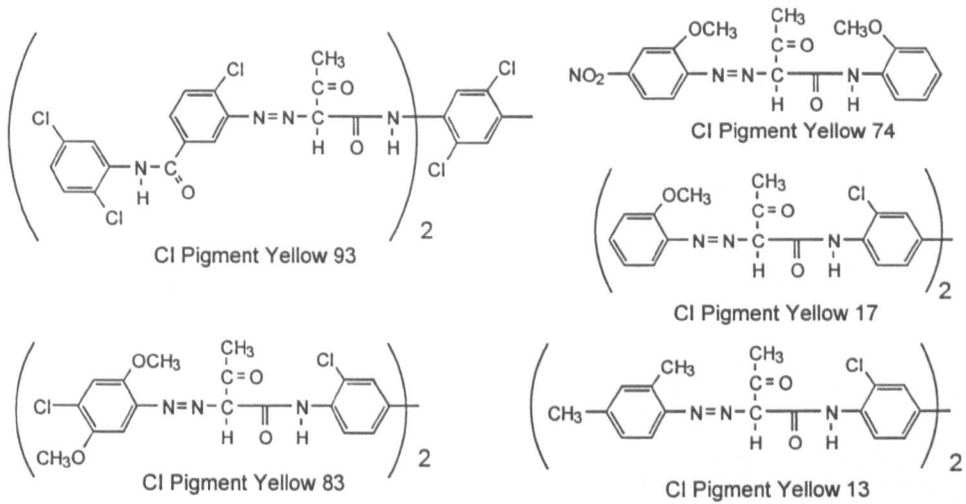


Figure 4.22 The relationship between absorption spectra of yellow pigments and the emission spectrum of a medium pressure mercury curing lamp

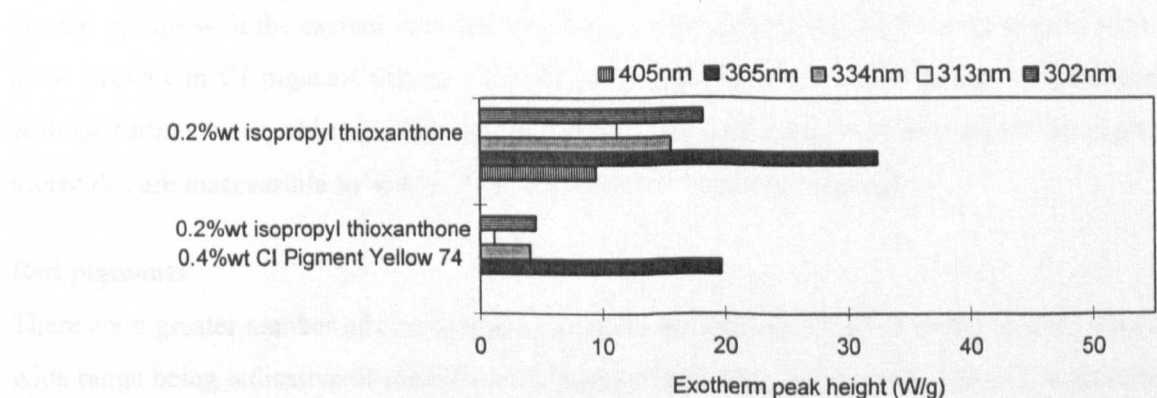


Figure 4.23 The influence of the yellow pigment CI Yellow 74 on the most effective curing wavelengths of isopropyl thioxanthone, as measured by DPC



Photoinitiator type and level	Exotherm peak height (Wg ⁻¹)	
	unpigmented	0.4 %wt CI Yellow 74
0.2 %wt isopropyl thioxanthone (ITX)	20.82	8.26
0.2 %wt 4-phenyl benzophenone	19.76	8.06
0.2 %wt benzil dimethyl ketal	10.57	1.19

Table 4.1 *The influence of the pigment CI Yellow 74 on the overall reactivity of three differently absorbing photoinitiators as measured by DPC*

The results in table 4.1 show how the overall reactivity of three different photoinitiators is affected by the presence of a yellow pigment. They indicate that despite gaining their reactivity from different parts of the lamp emission spectrum, the strongly absorbing photoinitiators isopropyl thioxanthone and 4-phenyl benzophenone are similarly affected by the presence of yellow pigment. In contrast, benzil dimethyl ketal, which has only a weak ($n-\pi^*$) absorption band in the 300-380 nm region, has its reactivity significantly reduced by the presence of the pigment.

The results suggest that a photoinitiator which absorbs strongly in the region of the yellow pigment's absorption minimum (300-360 nm) will be most effective for curing yellow inks. The α -aminoalkylphenone Irgacure 369 has a strong absorption maximum at 323 nm and has been shown in this chapter to be highly reactive at the lamp emission wavelengths 302, 313, 334 and 365 nm. It is speculated that this photoinitiator will prove to be most effective for curing all types of yellow ink. However, the weak absorption intensity displayed by all yellow pigments at the important 302 and 313 nm lamp emission bands means that all the photoinitiators investigated in this work will be effective to some degree in curing yellow inks, justifying the generally held view that yellow inks are the easiest to cure¹⁰⁻¹².

Yellow pigments may also reduce the overall cure efficiency due to energy transfer reactions of the azo groups with the excited state photoinitiator, or radical scavenging by nitro groups, such as those present in CI pigment yellow 74. The magnitude of these effects cannot be determined without further work, although they are speculated not to be great because most of the pigment molecules are inaccessible by virtue of the pigment particle crystal structure.

Red pigments

There are a greater number of commercially available red pigments than any other colour, with the wide range being indicative of their diverse chemical structures. Pigments based on azo chemistry are however still the most common. Although there are no inorganic red pigments, there are a wide variety that are metal salts, such as the barium salt Red 53:1 and the calcium salt Red 57:1. Pigment red 57:1, commonly termed a 'calcium 4B' is the most widely used process magenta.

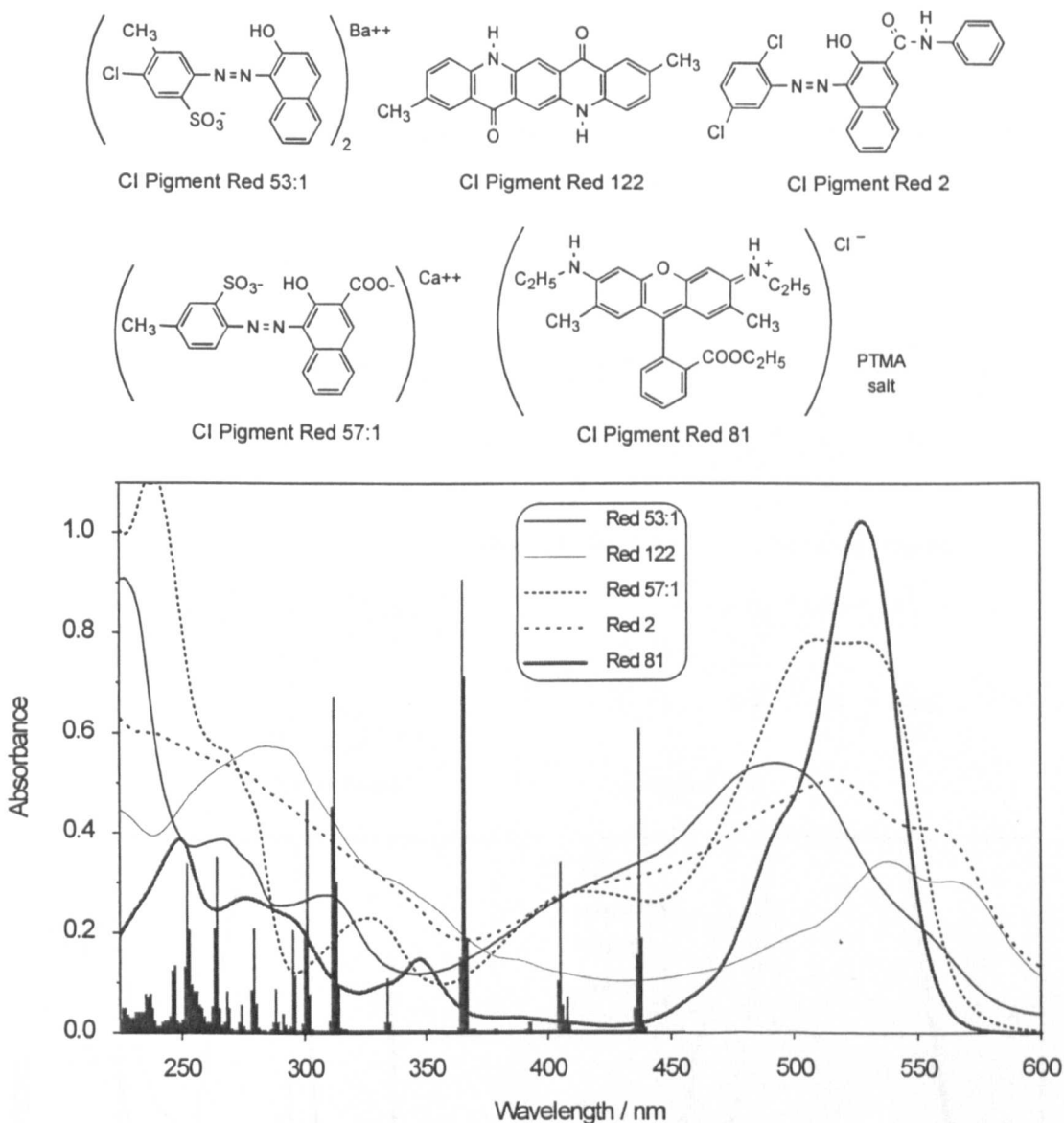


Figure 4.24 *The relationship between the absorption spectra of red pigments and the emission spectrum of a medium pressure mercury curing lamp*

The data in figure 4.24 shows that although all red pigments are characterized by their absorption in the 450-575 nm region, their diverse chemical structures result in very different absorption characteristics in the UV region. It could be generalised that each shows either a minimum or weak absorbance in the 365 nm region, making them particularly suitable for curing with thioxanthone type photoinitiators. However, at all the other important lamp emission wavelengths the different pigment types show a wide range of absorption intensities. For this reason it is important to consider the absorption spectrum of the actual pigment being used when formulating a red ink and not to generalise them as 'red pigments'.

Blue pigments

In comparison with yellow and red pigments there are relatively few blue pigments classified, with the phthalocyanine blues being universally dominant in the printing ink industry, particularly as a

process colour. The β copper phthalocyanine, CI Pigment Blue 15:3, is the most widely used, being cheap, light fast, easy to disperse and with excellent resistance properties. However, their high tinctorial strength means that Blue 1 and Blue 61 both still find significant use. The copper free phthalocyanine CI Blue 16 is often used in applications such as food wrappers, where Blue 15:3 would be the most appropriate pigment choice but a metal free system is required.

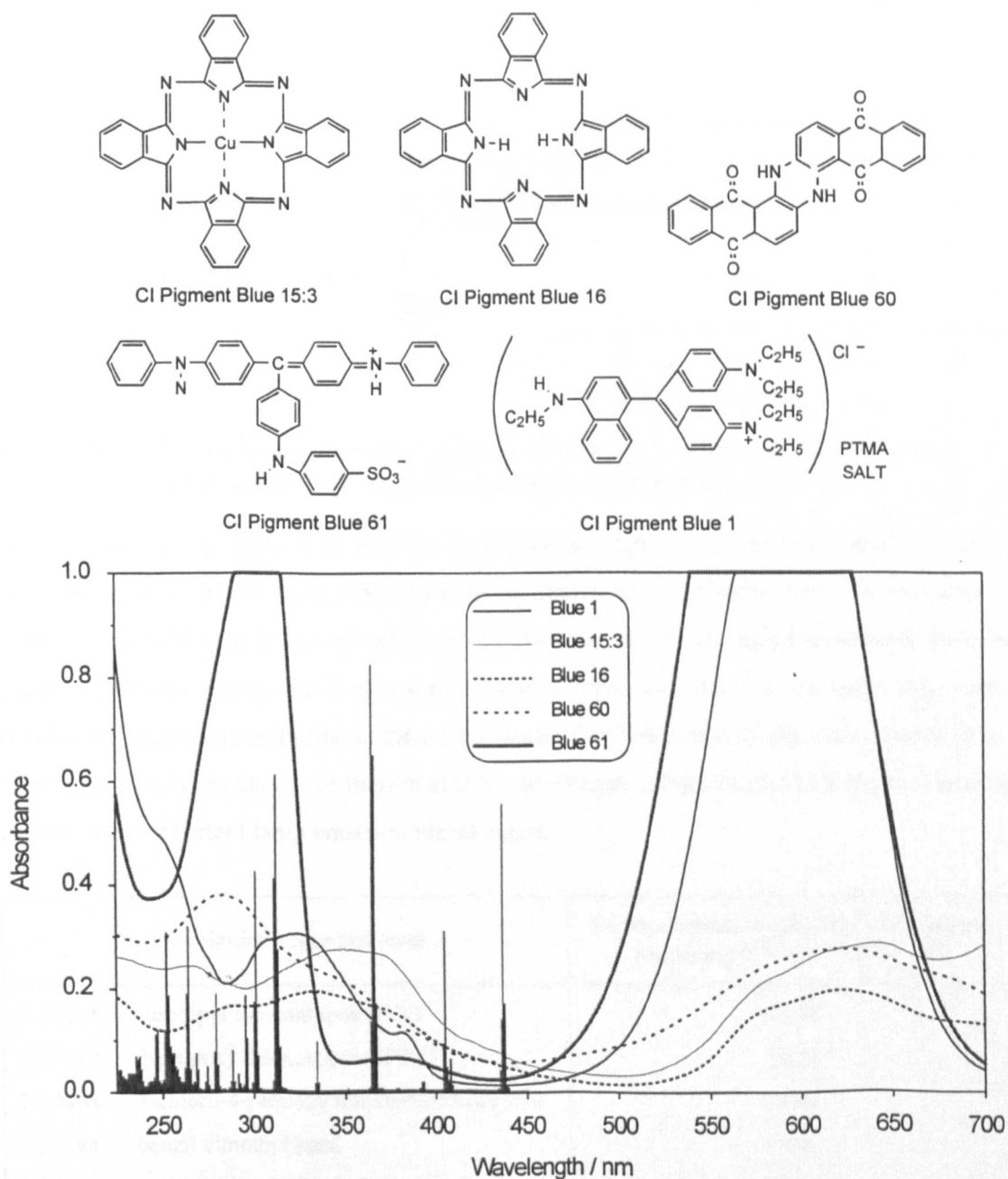


Figure 4.25 *The relationship between the absorption spectra of blue pigments and the emission spectrum of a medium pressure mercury curing lamp*

The data in figure 4.25 shows that although blue pigments are characterized by their absorption in the 500-700 nm region, their diverse chemical structures result in a range of UV and visible absorption characteristics. Of particular note is the extremely high absorption intensities of Blue 1 and Blue 61, reflecting their high tinctorial strengths.

Blue pigments by their nature appear this colour because they do not absorb light in the 390-500nm region. This is an important consideration when choosing an appropriate photoinitiator system to cure a blue ink, with photoinitiators that utilise the 405 nm lamp emission band likely to be the most effective, especially since most blue pigments also absorb strongly at all wavelengths below 390 nm. This is demonstrated in figure 4.26, where the most effective curing wavelengths of isopropyl thioxanthone are compared in the presence and absence of the commonly used β copper phthalocyanine pigment, Blue 15:3.

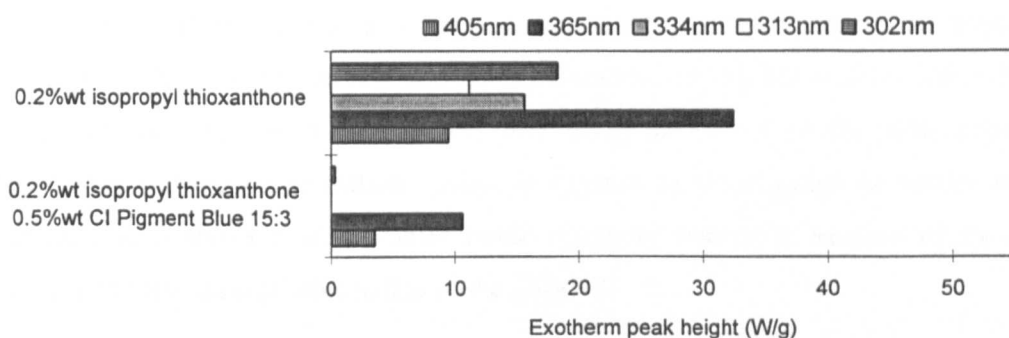


Figure 4.26 *The influence of the blue pigment CI Blue 15:3 on the most effective curing wavelengths of isopropyl thioxanthone, as measured by DPC*

It can be seen from figure 4.26 that the absorption of light by the pigment leads to the lamp emission bands at 302, 313 and 334 nm providing almost no contribution to the overall cure. The incident light at 365 nm is also absorbed by the pigment, but the strong photoinitiator absorbance at this wavelength means that it competes relatively effectively for the available light, and still provides the greatest contribution to the overall cure. The low extent of pigment absorption at 405 nm has resulted in the cure contribution at this wavelength being affected to a much lesser extent than the other important lamp emission wavelengths.

Photoinitiator type and level	Exotherm peak height (Wg^{-1}) for samples containing 0.5 %wt CI Blue 15:3
0.2 %wt isopropyl thioxanthone (ITX)	12.38
0.2 %wt 2-propoxy thioxanthone (PTX)	16.36
0.2 %wt 1-chloro-4-propoxy thioxanthone (CPTX)	11.42
0.2 %wt benzil dimethyl ketal	0.4
0.2 %wt 4-phenyl benzophenone	7.11
0.1 %wt Irgacure 369	17.09

Table 4.2 *The influence of the pigment CI Blue 15:3 on the overall reactivity of a number of photoinitiators, as measured by DPC*

The results in table 4.2 show how effective various photoinitiators are in curing blue inks containing CI Blue 15:3. (Note that the numerical values of these results cannot be directly compared with others in this chapter due to a DPC bulb change during this work). They

demonstrate that PTX has a significantly higher reactivity than both ITX and CPTX under these conditions, supporting earlier observations that this photoinitiator better utilises the lamp emission bands at 405 and 436 nm. Although CPTX also showed better utilisation of the 405 nm lamp emission band, its lower efficiency at 365 nm more than offsets this benefit. CPTX has been claimed by Green et al.⁴⁴ to be particularly beneficial for the curing of blue inks, but the results presented here, together with the observation that the pigment used by Green was not Blue 15:3, suggests that this is not necessarily the case.

It can be seen that benzil dimethyl ketal, which absorbs weakly in the region of the pigment absorption maximum, shows almost no cure activity in this procedure, but Irgacure 369, which absorbs strongly in the same region, displays the best curing activity of all the photoinitiators tested, even at only half the concentration. Also, in contrast to the situation in yellow inks, 4-phenyl benzophenone shows a significantly lower reactivity than ITX because of its less favourable absorption spectrum relative to that of the pigment.

Clearly the competitive light absorption effect by pigments is more of an issue in blue inks than for yellow and possibly magenta inks, requiring a more in-depth consideration of the most suitable photoinitiators. However, it would still appear that Irgacure 369 represents the most effective photoinitiator for this application. Although it is generally accepted in the literature that thioxanthone derivatives are desirable in order to effectively cure a blue ink^{13,44,45} the effectiveness of Irgacure 369 has been reported⁴⁶.

Black pigments

Although black iron oxide, CI Black 11, is sometimes used in the inks and coatings industry, its brown shade makes its use extremely rare. Carbon black pigments, CI Black 7, are used almost exclusively and are classified further according to their method of manufacture as channel, furnace or lamp blacks. Furnace blacks are the most common in printing ink applications, but variations in shade and colour strength still exist. In practice, some of the more brown shade Black 7's are used with a blue toning pigment to make them appear more jet black.

The data in figure 4.27 shows that, as well as absorbing all light in the visible region of the electromagnetic spectrum, defining them as black to an observer, black pigments absorb continuously throughout the UV region. However, the large variations in absorbance intensities for the different pigments investigated was unexpected in view of their known similar colour strengths when made into inks. It is speculated that these variations are related to the dispersion stability of the black pigments in methanol, which was considerably lower than for other 'coloured' pigments. The Black 7 pigments represented in figure 4.27 are all furnace blacks, but correspond to different supply grades.

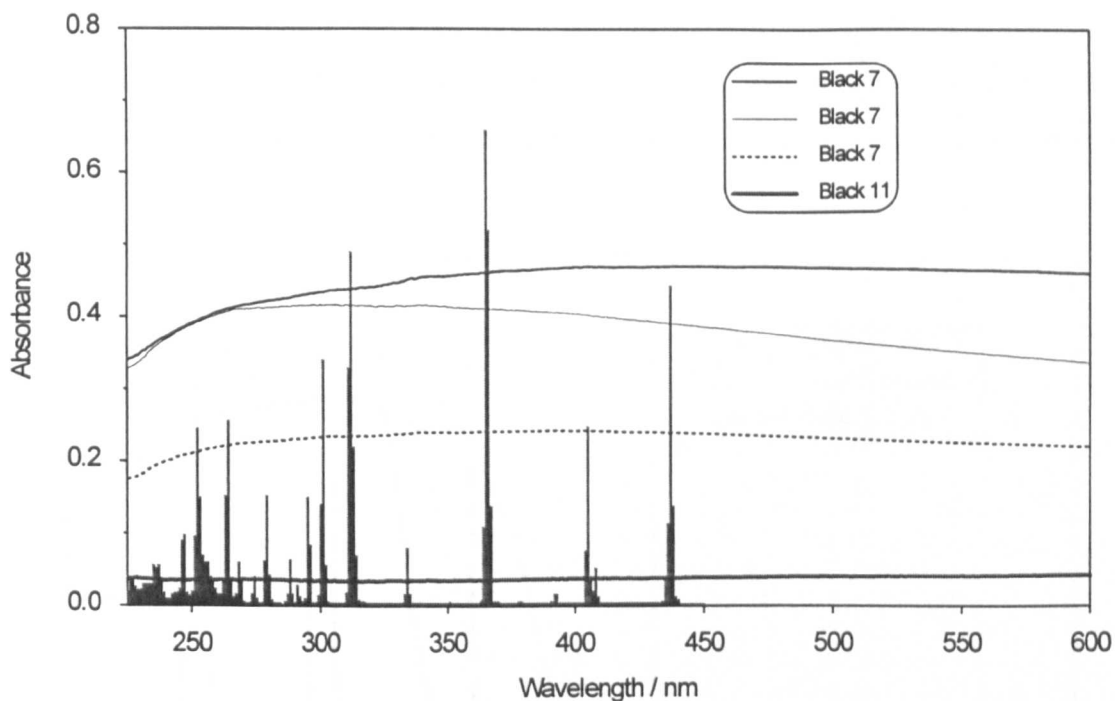


Figure 4.27 *The relationship between the absorption spectrum of black pigments and the emission spectrum of a medium pressure mercury curing lamp*

With no pigment absorption minima around which to optimise photoinitiator choice, the curing of black inks is achieved by selecting a highly reactive and strongly absorbing photoinitiator such as Irgacure 369, although the limited amount of available light may mean it is necessary to use a number of photoinitiators that absorb strongly across the entire useful range of the medium pressure mercury lamp. e.g. Irgacure 369, Quantacure ITX and 4-phenyl benzophenone.

White pigments

In contrast to all the other colours, white pigments are exclusively inorganic in nature. Although there are many white pigments classified, most, such as calcium carbonate, talc and silica have refractive indices similar to the oligomers and monomers used in UV curing inks and therefore appear transparent when dispersed. Only pigments such as zinc sulfide, White 7, and the two forms of titanium dioxide, White 6, have refractive indexes sufficiently high to show a white colouration when dispersed.

The data in figure 4.28 shows that all three of the commonly used white pigments show a continuous absorbance across the visible spectral region which can be associated with losses due to scattering. The white pigments investigated also show light absorption in the UV region, with the spectra in figure 4.28 suggesting that zinc sulfide based white UV inks would be the easiest to cure and should find the most widespread use because the 365 nm lamp emission band in this case is not being screened by the pigment. However, in practice the rutile form of titanium dioxide is the only white pigment used in printing inks for the very practical reason that the lower refractive indices of anatase titanium dioxide and zinc sulfide would necessitate a much higher pigment

concentration leading to inks with very poor flow. The thicker films involved in screen printing inks ($\sim 10 \mu\text{m}$) means that the pigment concentrations in this application are generally lower, so anatase titanium dioxide is often used, but zinc sulfide still suffers the same disadvantage and finds limited use.

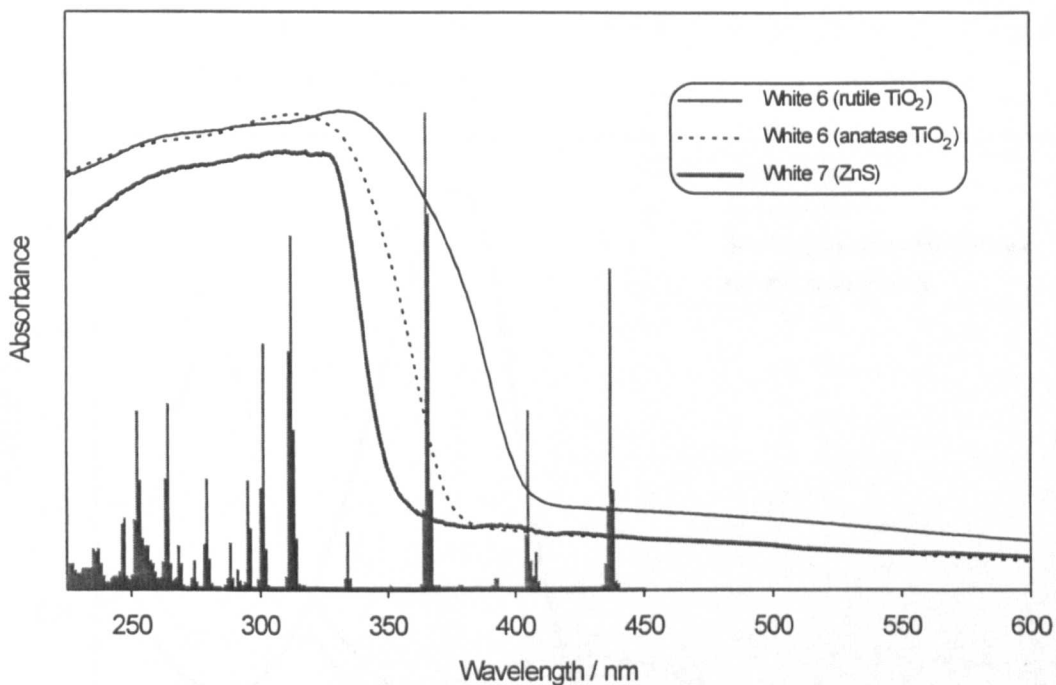


Figure 4.28 *The relationship between the absorption spectra of white pigments and the emission spectrum of a medium pressure mercury curing lamp*

In general terms, the UV and far visible absorbance spectra of rutile titanium dioxide is similar to that of the β copper phthalocyanine Blue 15:3, such that similar photoinitiator combinations would be effective. However, thioxanthenes cannot be used in white inks above 0.1-0.2 %wt because of the yellow colour they impart by absorbing in the visible region. This problem also restricts the use of other effective photoinitiators such as Irgacure 369 because of its significant yellowing on cure. As has been widely reported, acylphosphine oxides are the most suitable photoinitiators for curing white inks because they have only a weak absorbance in the visible region, photobleach on reaction and gain significant reactivity from the 405 nm lamp emission band¹⁹⁻²⁰. In practice acylphosphine oxides are currently far too expensive for use as a principal photoinitiator in printing inks, which can be effectively formulated using mostly benzophenone and hydroxyalkylphenone photoinitiators, with only low levels of either acylphosphine oxides or thioxanthone photoinitiators as required.

4.2.1.3 UV light absorption by amine synergists

In UV curing applications, amine synergists provide both a source of abstractable hydrogens for Type II photoinitiators and lessen the effect of oxygen inhibition at the surface by a scavenging chain reaction^{47,48}. Aromatic amine synergists, typically esters of 4-N,N-dimethylamino benzoic

acid, are of particular importance in the printing ink industry since they are insoluble in water and can therefore be used in lithographic applications, although they are also known to absorb light strongly in the UV region^{13,49}.

The extent of UV light absorption for several synergists relative to the photoinitiator benzophenone is shown in figure 4.29, with the effect they have on benzophenone's curing ability as measured by RT-FTIR shown in table 4.3.

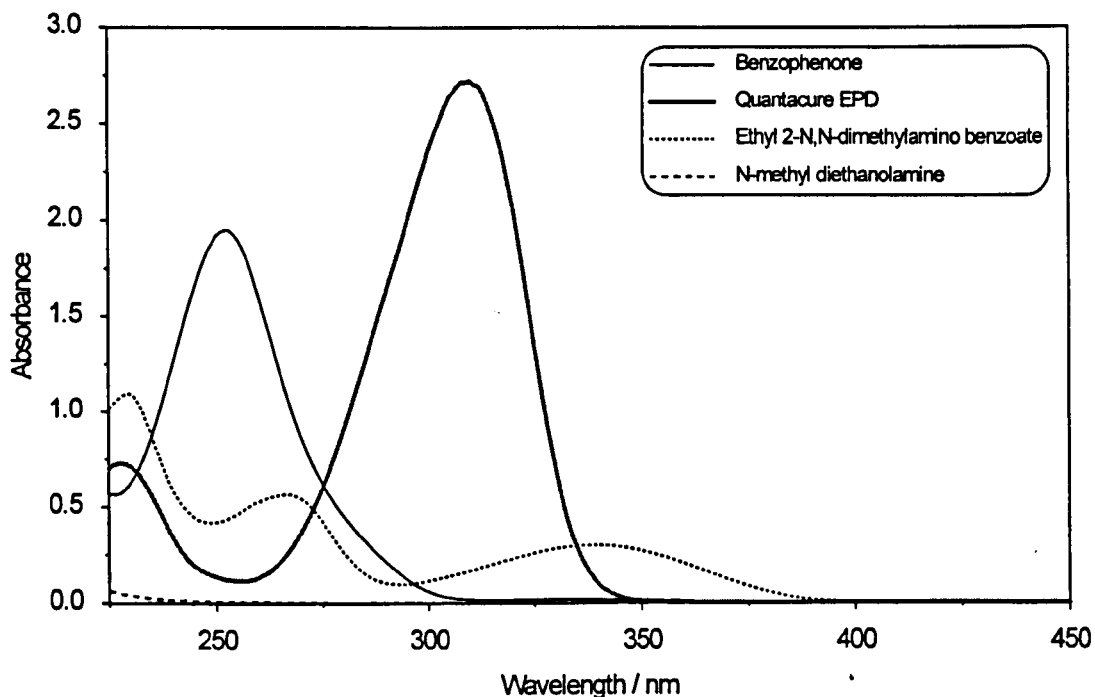


Figure 4.29 The absorption spectra of benzophenone and various amine synergists

Amine type	Initial reaction rate (%s ⁻¹)
none	17.5
MDEA N-methyl diethanolamine	31.3
<chem>CN(C)c1ccc(cc1)C(=O)OCC</chem> Quantacure EPD 4-N,N-dimethylamino benzoic acid ethyl ester	21.0
<chem>CN(C)c1ccccc1C(=O)OCC</chem> 2-N,N-dimethylamino benzoic acid ethyl ester	28.15

Table 4.3 The influence of competitive light absorption by amine synergists on the cure efficiency of benzophenone by RT-FTIR

The data in figure 4.29 shows that Quantacure EPD has a very strong absorption band at 308 nm which competes for light with benzophenone at the important curing wavelengths previously identified. This is also true of a number of other commercial examples of 4-dimethylamino benzoic acid esters, including the (2-ethyl)hexyl, pentyl, iso-pentyl and (2-butoxy)ethyl esters. Although it extends over a longer wavelength range, the extent of the light absorption is considerably less for the ethyl 2-N,N-dimethylamino benzoate, accounting for its higher reactivity under these conditions. N-methyl diethanolamine shows almost no competitive light absorption and displays the highest curing reactivity.

4.2.2 UV light utilisation through a film

It has been shown in 4.2.1 that the loss of reactivity resulting from competitive light absorption can be significant, but with careful choice of raw materials the reactivity loss can be minimised. It is also important to consider a further aspect of this problem; film thickness. The Beer-Lambert law (5) is very useful in this respect since it relates absorbance, A, to concentration and film thickness (path length) but also defines the percentage of transmitted light^{2,50}.

$$A = \epsilon \cdot c \cdot d = \log \frac{I_0}{I_T} \quad (5)$$

ϵ = molar extinction coefficient ($\text{mol dm}^{-3}\text{cm}^{-1}$), c = concentration (mol dm^{-3}), d = path length (cm), I_0 = incident light intensity, I_T = transmitted light intensity

4.2.2.1 Extrapolation of the Beer-Lambert law to thin films

UV absorbance spectra for materials such as photoinitiators are generally measured at low concentrations ($\sim 1 \times 10^{-4}\text{M}$) in cells of 1 cm path length. These conditions are far removed from those of the end use, where concentrations of 1-8 %wt are used at film thicknesses of only a few microns. However, it is possible to introduce scaling factors to compensate for this difference, such that the absorbance value obtained under a standard set of conditions A_{standard} can be scaled to show the value under another specified set of conditions $A_{\text{specified}}$.

$$A_{\text{specified}} = A_{\text{standard}} \times \frac{Y}{0.002} \times \frac{Z}{10000} \quad (6)$$

where $A_{\text{specified}}$ is the absorbance value under a specified set of conditions (Y and Z), A_{standard} is the absorbance value under a standard set of conditions (0.002 %wt, 1 cm /10000 μm path length), Y = specified weight percent level in the formulation, Z = specified path length (μm)

Using a typical computer spreadsheet program it is possible to do these calculations simultaneously for all the absorbance values in a spectral data file. This process generates a new absorbance spectrum which is visually identical to the original, but has a scale appropriate to the specified values of film thickness and %wt in the formulation. The advantage of such a procedure

is that at any wavelength the extent of competitive light absorption can be judged more accurately because the scaled spectra will reflect the actual amount of light being absorbed by each component in the formulation. In order for the spectra to be scalable according to their %wt composition in this way it is necessary to have acquired the spectra at a standard %wt level, and not, as is more usual, at a standard molar concentration.

The use of absorbance measurements in this way is of limited use because of their intangible nature relative to a printed ink film. It is however possible to use a % transmission scale since the Beer-Lambert law (5) can also be expressed as;

$$\% \text{ Transmission} = \frac{100}{\exp(2.303 \times A)} \quad (7)$$

Therefore, by substitution using (6) we obtain the % transmission under a specified set of conditions % Transmission_{specified}.

$$\% \text{ Transmission}_{\text{specified}} = \frac{100}{\exp\left(2.303 \times A_{\text{standard}} \times \frac{Y}{0.002} \times \frac{Z}{10000}\right)} \quad (8)$$

where % Transmission_{specified} is the percentage of incident light transmitted through the sample under a specified set of conditions (Y and Z), A_{standard} is the absorbance value under a standard set of conditions (0.002 %wt, 1 cm /10000 μm path length), Y = specified weight percent level in the formulation, Z = specified path length (μm)

Again, this transformation can be done as a single operation on a computer spreadsheet to generate a % transmission UV spectrum for an individual component in an ink formulation from a standard absorbance data file of that material. An example of this is shown in figure 4.30, showing the absorbance spectrum of a 0.002 %wt solution of isopropyl thioxanthone in methanol in a 1 cm path length cell, and the calculated % transmission spectrum in a 2 μm thick ink film at a formulated level of 3.0 %wt (Y=3, Z=2).

The use of % transmission spectra in this way is more informative than absorbance because it provides a tangible image of the light utilisation through a film, with the value of % transmission at any wavelength corresponding to the amount of incident light reaching the bottom of the coating. It can also serve as a warning of screening in particular wavelength regions resulting from excessive concentrations of one or more materials. Screening can be said to occur if the % transmission value at any wavelength is close to zero.

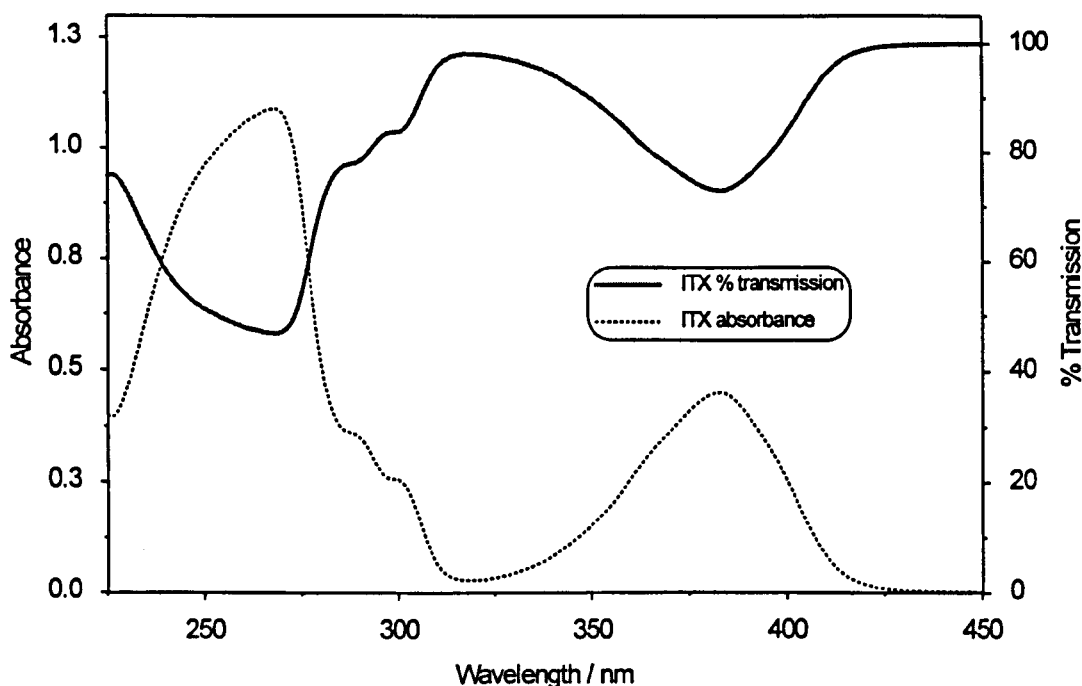


Figure 4.30 Use of a modified form of the Beer-Lambert law to predict the UV transmission spectrum of 3 %wt Quantacure ITX in a 2 μm thick ink film

Similar calculations have been made by Seko²¹, who ratioed the transmission under standard conditions to that under a specified set of conditions. Calculations were necessary for each individual wavelength, but the measured and calculated values were in good agreement.

The work of Gatechair^{22,23} has been most widely referenced on this subject. For individual lamp emission wavelengths, this involved the calculation of the fraction of incident light absorbed and transmitted at various points within a coating, leading to an estimate of the relative radical concentration as a function of coating thickness, which was then successfully correlated to experimental results about cure performance.

4.2.2.2 Validation of the modified Beer-Lambert law

Although the mathematical manipulation of the Beer-Lambert law (5) to express it in the form shown in equation (8) involves no major assumptions, the practical use of (8) does, with the major errors and unknowns being;

1. Conformity to the Beer-Lambert law under the conditions the spectra are acquired
2. Conformity to the Beer-Lambert law under conditions found in a typical ink film
3. The consequences of light scattering by the pigment
4. The effect of differences in the refractive index of an oligomer / monomer blend and methanol, in which the standard spectra were acquired

It is therefore necessary to prove that data extrapolated to typical ink film conditions from low concentration long path length measurements is a valid procedure. This is most easily shown, as

in figure 4.31, by comparing, at a single wavelength for a film thickness range, the calculated % transmission values with the values measured directly from a series of prints in the film thickness range of interest. The latter is achieved by printing known area and weights of a formulation onto a thin grade polyethylene substrate and directly measuring the transmission spectrum through the substrate. An unprinted sample of the substrate is also placed across the reference window in the spectrophotometer, although strictly speaking this is not necessary because the substrate used does not absorb light at wavelengths longer than 225 nm.

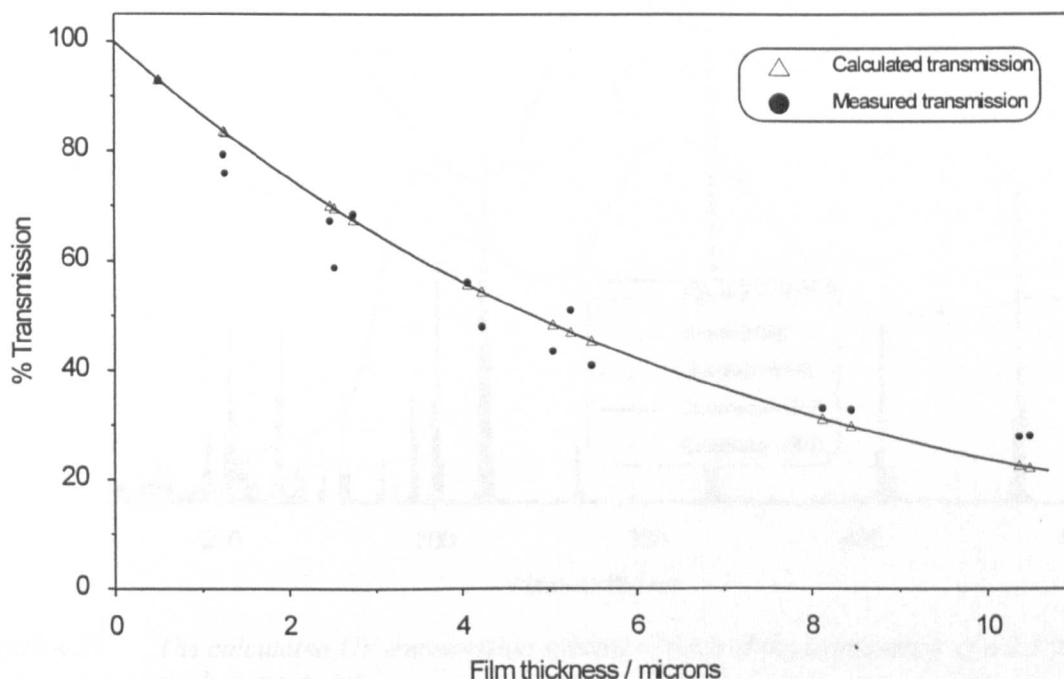


Figure 4.31 *A comparison of measured and calculated values for the % transmission of 3 wt 2-hydroxy benzophenone at 340 nm*

Although it is not a photoinitiator, 2-hydroxy benzophenone was used in this procedure both because it has an absorption intensity at 340 nm similar to isopropyl thioxanthone's ($n-\pi^*$) band maximum, and more importantly, because unlike photoinitiators it does not cause gelation problems on the printing rollers during sample preparation in daylight.

The data in figure 4.31 shows that, within the film thickness range 0-10 μm , the measured and calculated values of % transmission are in good agreement. It is therefore possible to use equation (8) to generate the transmission spectra of components within an ink film.

The procedure described can be used to model, and more effectively optimise, an entire ink formulation, giving the individual UV transmission spectra of each UV absorbing component. An example of this is shown in figure 4.32 for a magenta ink based on the materials listed below. Other materials such as the oligomers and monomers are not included since their UV absorbance in very thin films is not significant.

16.2%	CI Pigment Red 57:1	
1.8%	Irgacure 369	2-benzyl-2-dimethylamino-1-(4-morpholinophenyl) butan-1-one
2.25%	Quantacure ITX	isopropyl thioxanthone
1.125%	Quantacure EHA	4-N,N-dimethylamino benzoic acid (2-ethylhexyl) ester
1.125%	Quantacure EPD	4- N,N dimethylamino benzoic acid ethyl ester

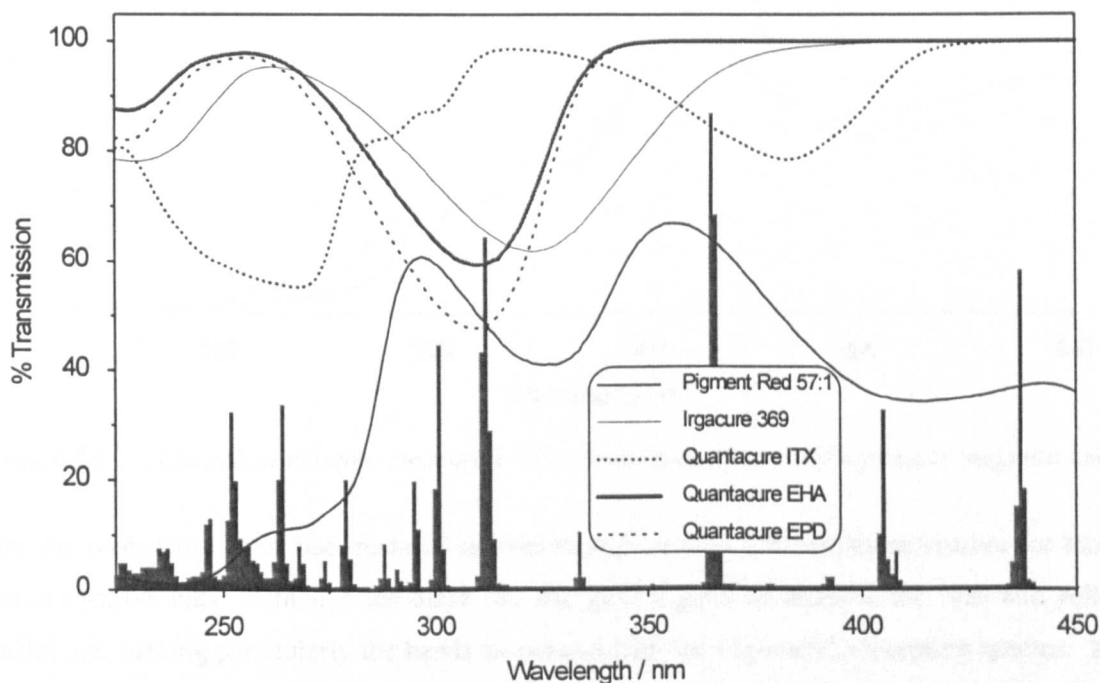


Figure 4.32 *The calculated UV transmission spectra of each of the components of a 2.1 μm thick magenta ink*

Figure 4.32 shows that, in the ink described, the pigment is the dominant factor in determining the extent to which UV light is transmitted through the film. Although the spectrum of ITX is optimal in relation to both the pigment absorption and the lamp emission spectrum at 365 nm, the spectrum of Irgacure 369 is not, absorbing principally in a region where both the pigment and aminobenzoate synergists EPD and EHA absorb strongly. In fact, as shown earlier, this should not cause a major loss in reactivity because the strong absorption of this photoinitiator competes effectively for the incident light.

If the procedure described in this section is valid, it should also be possible to predict the transmission spectrum of an entire ink based on the sum of its parts. This cannot be achieved directly since transmission spectra are not additive. However, it can be achieved by scaling the absorbance for all the UV absorbing materials using equation (6) and then using equation (7) to generate the transmission spectrum. Using this procedure for the magenta ink detailed above, the calculated and measured ink transmission spectra for a 2.1 μm film thickness are shown in figure 4.33, where it is demonstrated that there is good agreement between the theoretical and measured transmission spectra.

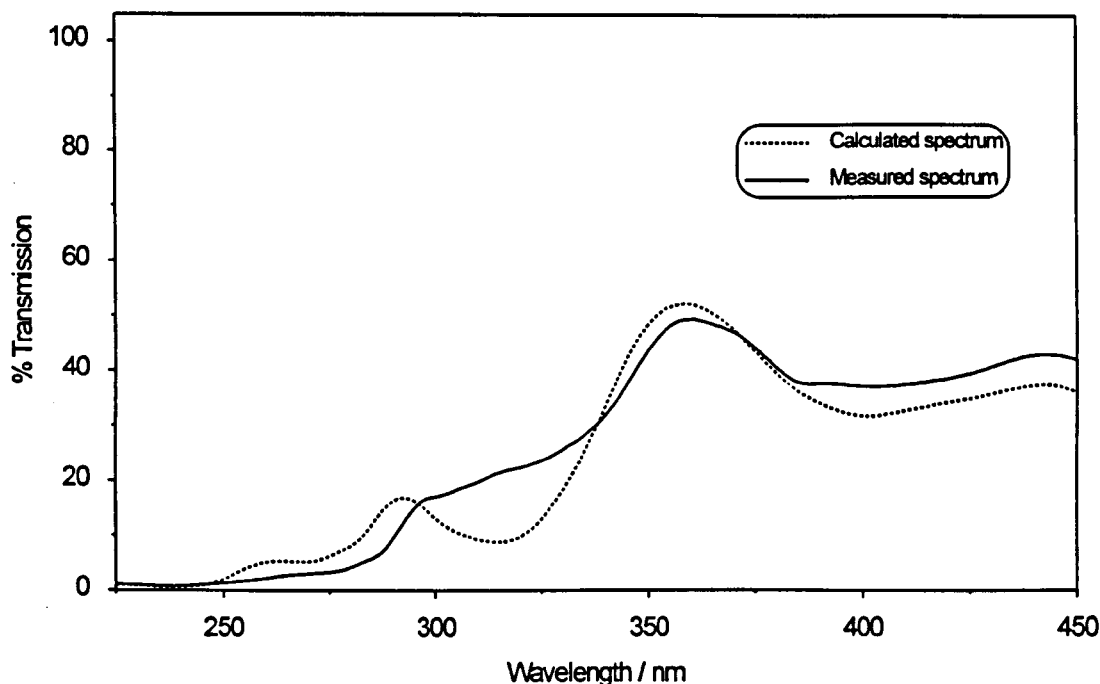


Figure 4.33 *The calculated and measured UV transmission spectra of a process magenta ink*

A similar comparison was also made of calculated and measured transmission spectra for black, cyan and yellow inks. Although the black ink also gave a good correlation, the cyan and yellow inks did not, lacking particularly the bands associated with the pigments' absorption spectra. It is speculated that the ultrasonification dispersion process used in acquiring the pigment spectra does not necessarily break down the pigment particles to the same extent in every case. This is not unexpected in view of the differing stabilities of the dispersions and the large variations in absorbance intensity observed with black pigments. Light scattering may also be important in some of the dispersions, where for example, the white pigments all failed to show any absorption in the UV region when dispersed using the ultrasonification method, but did show their known characteristic spectra¹⁴⁻²⁰ when acquired using the more crude "stained polyethylene film" technique previously referred to.

These results suggest that, in contrast to soluble materials, the absorption spectra of pigments acquired using the ultrasonification method cannot in all cases be reliably scaled to predict spectra under other conditions. Scalable pigment spectra could be obtained by one of two techniques:

1. Printing equivalent pigmented and non-pigmented ink samples containing no photoinitiators or synergists onto polyethylene at the same film weight, and using a spectral subtraction procedure to obtain the pigment spectra.
2. Mechanically disperse pigments at a low percentage level in mineral oil as has previously been reported⁶, and measure the absorbance spectra in 1cm path length cells.

Although the latter could result in stability problems due to the non-polar medium, both methods suffer from their time consuming nature, making them beyond the scope of this work. However, pigment spectra obtained using the ultrasonification method can still be used as an unscaled reference spectrum, providing information on the areas of strong or weak absorption without attempting to quantify these further.

4.2.2.3 UV transmission spectra of printed ink films

The UV transmission spectra of a typical set of process inks (yellow, magenta, cyan and black) were acquired by printing them onto a thin grade of polyethylene substrate at their normal application thickness ($\sim 2 \mu\text{m}$) and measuring the transmission spectrum through the print. Unprinted substrate was used as a reference although it absorbs almost no light in the 225-450 nm wavelength range.

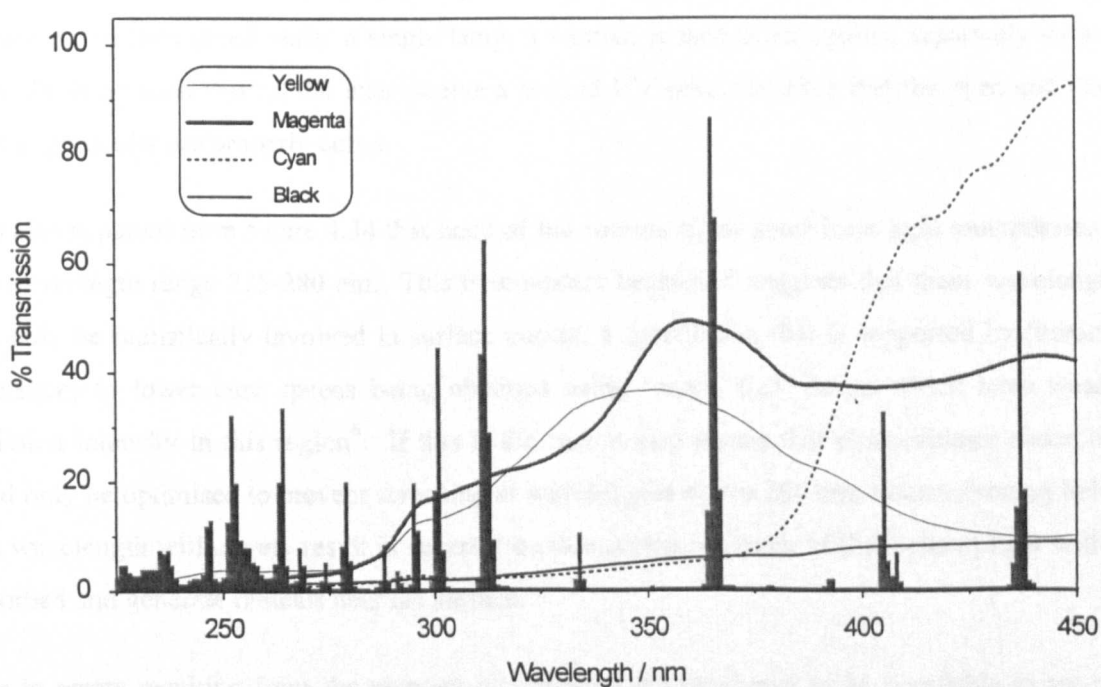


Figure 4.34 The UV transmission spectra of a set of process inks relative to the emission spectrum of a medium pressure mercury curing lamp

The UV transmission spectra shown in figure 4.34 illustrates some of the reasons behind the large amounts of empirical data known to the printing ink industry, but often not reported, about the relative ease of curing of process colours. In particular, the generally known rule of thumb that yellow and magenta inks are easy to cure whereas cyan and particularly black inks are not^{6,10-12} can be related to the amount of UV light reaching the bottom of the film, as has previously been speculated by other authors^{6,7}. Figure 4.34 shows that the yellow and magenta inks allow significant UV transmission in the 280-450 nm region, such that the photoinitiator molecules at the bottom of the film are still able to absorb sufficient light to initiate the cure reaction effectively, and provide a balanced and robust cure. In contrast, the cyan and black inks transmit almost no light across the entire UV region, depriving the photoinitiator molecules near the bottom of the

film of sufficient light to initiate the cure reaction fully. The effect of this is to make the through cure relatively inferior to the surface cure, such that the film can be completely removed in a thumb twist test if the light intensity is too low or the line speed too fast. Cyan inks are not as bad as blacks in this respect, particularly if thioxanthone type photoinitiators are used in the formulation, since these provide cure from the 405 nm lamp emission band in the visible region which is not strongly absorbed by the pigment. However, black inks have no 'pigment window' and are notoriously difficult to cure, particularly if a dense colour is applied through either a high film weight or a high pigment concentration. Printers have developed measures which sometimes help in these situations such as printing the black first so that with "inter-deck drying" the black ink goes under at least four lamps. This approach is often not practical because the printing rollers for the lighter colours become contaminated with uncured black ink. Another approach is used for the more common "wet-trapping" printing technique. In this case all the colours are applied in sequence and then cured under a single lamp, a varnish is then often applied separately with its own UV lamp such that all the inks receive a second UV dose, ensuring that the cyan and black inks in particular are properly cured.

It is also apparent from figure 4.34 that none of the colours allow significant light transmission in the wavelength range 225-280 nm. This is important because it suggests that these wavelengths can only be realistically involved in surface curing, a speculation that is supported by literature references to lower cure speeds being obtained using 'ozone free' lamps which have weaker emission intensity in this region⁶. If this is the case it also means that photoinitiator absorption need only be optimised to prevent screening at wavelengths above 280 nm, since screening below this wavelength will merely result in superior surface curing, as much of the incident light will be absorbed and generate radicals near the surface.

Due to errors resulting from the pigment contribution it was shown to be unreliable to try and model the UV transmission spectrum of an entire ink based on the sum of its parts. However, it is possible to print a series of inks onto polyethylene at different film weights and study the measured transmission spectra as a function of film thickness using 3 dimensional graphs. Figures 4.35, 4.36, 4.37 and 4.38 show such graphs for typical yellow, magenta, cyan and black process inks respectively, providing information about how far into the film light of any wavelength will penetrate.

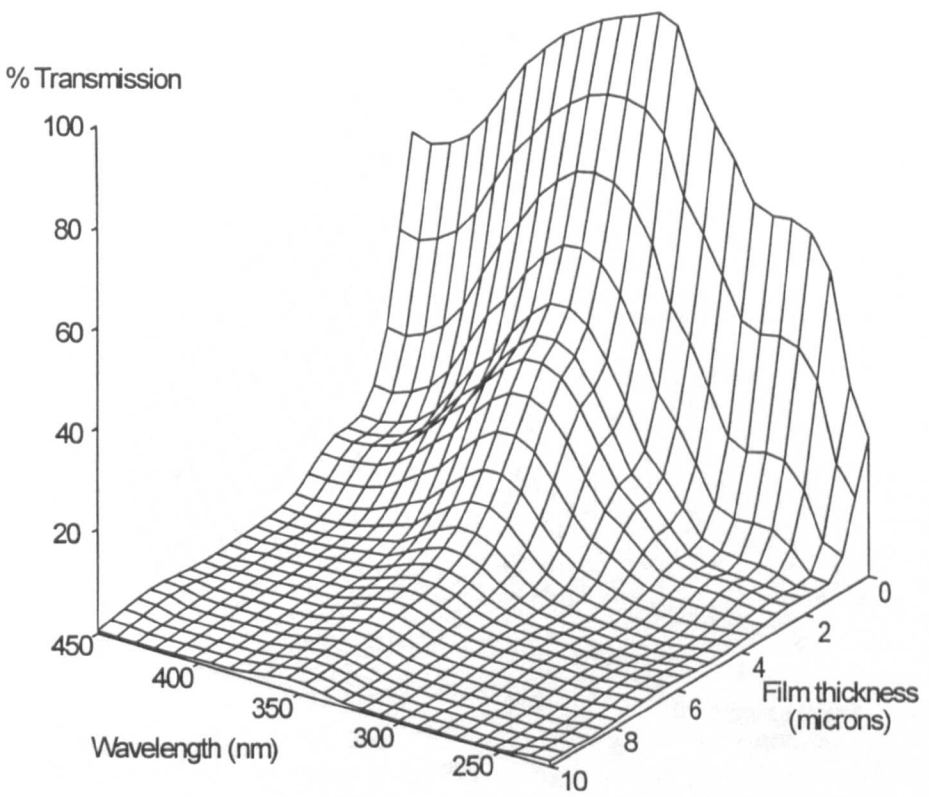


Figure 4.35 *The UV transmission spectrum of a typical process yellow ink as a function of film thickness*

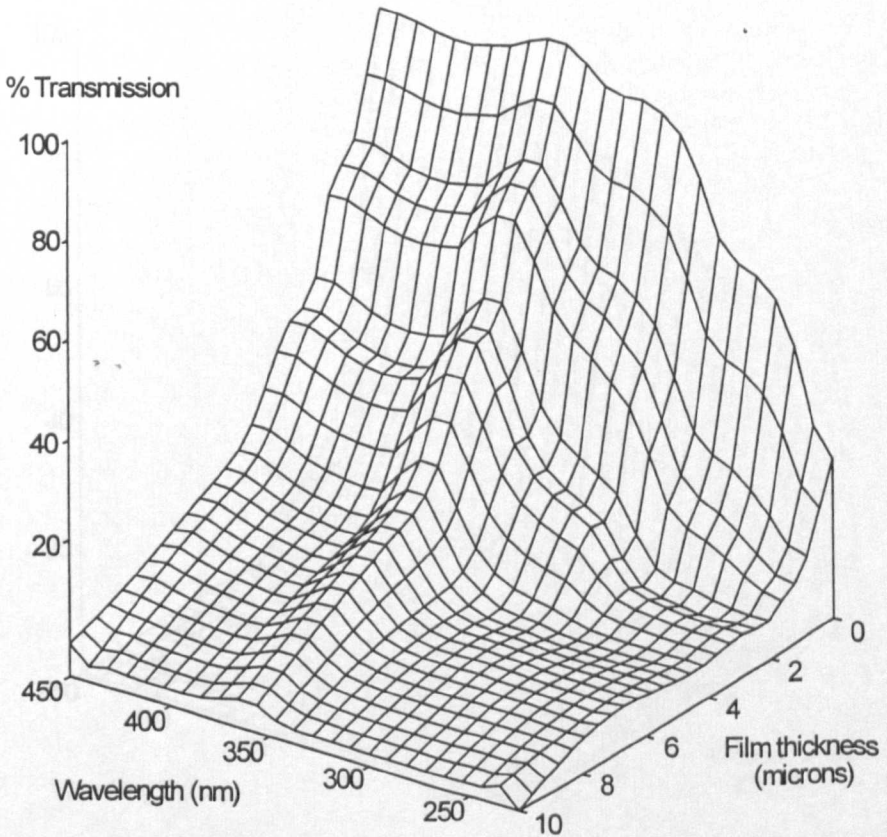


Figure 4.36 *The UV transmission spectrum of a typical process magenta ink as a function of film thickness*

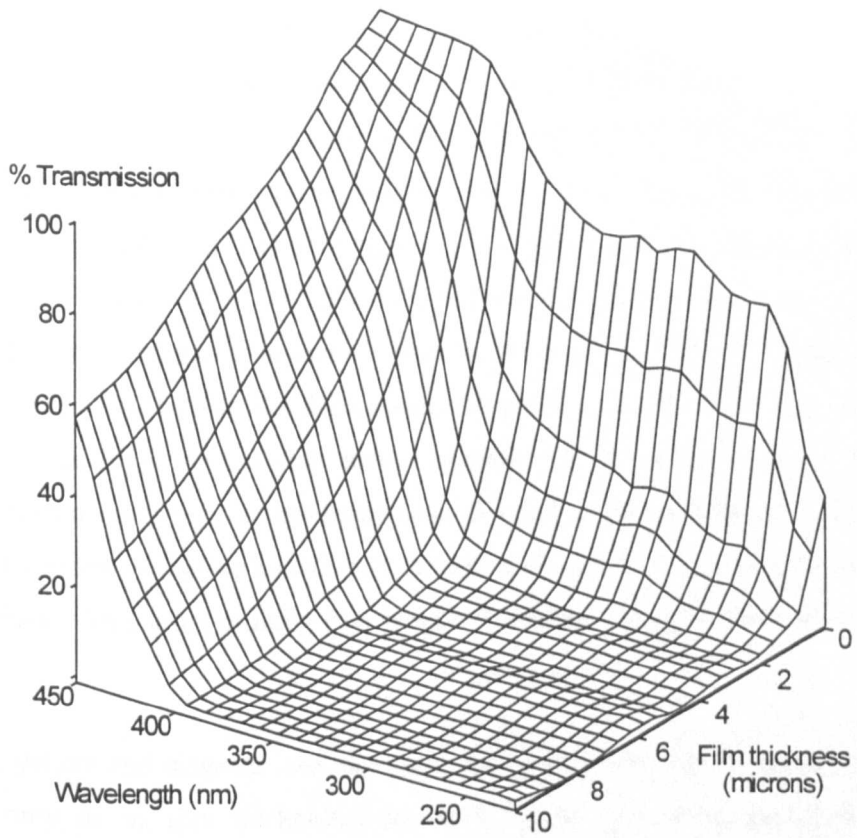


Figure 4.37 *The UV transmission spectrum of a typical process cyan ink as a function of film thickness*

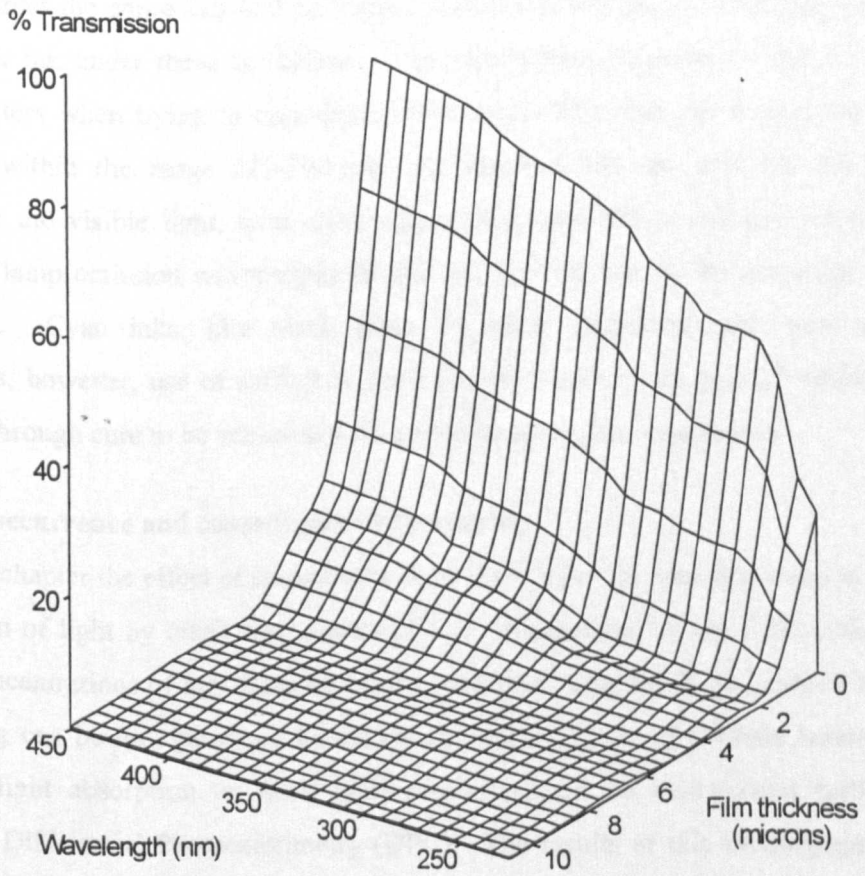


Figure 4.38 *The UV transmission spectrum of a typical process black ink as a function of film thickness*

The graphs in figures 4.35-4.38, and the individual spectra from which they are constructed, show that both the yellow and magenta inks have significant light transmission in the range 225-450 nm for film thicknesses up to 1.5-2.0 μm . Since this is the typical printing ink thickness range for lithographic inks, it means that all the emission bands from the curing lamp are potentially involved in providing both surface and through cure with these colours. Pigment windows exist in the region 300-370 nm and 300-450 nm for the yellow and magenta inks respectively, with the inks being sufficiently transparent in these regions to allow greater than 10% of the incident light to reach the bottom of the film at film thicknesses as high as 5 μm for the yellow and 5.5-8 μm for the magenta. The high transmission levels suggest that as long as these inks contain a photoinitiator such as isopropyl thioxanthone (as in this case), which absorbs strongly in the region of the pigment window, achieving satisfactory through cure should not be a problem for the yellow and magenta inks with normal printing film weight variations, although line speed will also have some effect.

In contrast to yellow and magenta inks, the cyan and black show significant transmission at all wavelengths only up to film thicknesses of 0.6-1.3 μm . As such, the wavelength region 225-280nm cannot be involved in providing any cure near the bottom of the film. In fact, for the black ink printed at film thicknesses above 2.75 μm , less than 10% of the incident light is transmitted across the entire 225-450 nm range, such that it will prove to be almost impossible to cure the black ink under these conditions. This observation accounts for the severe problems found by printers when trying to cure dense black inks. The cyan has a similarly low level of transmission within the range 225-390 nm, but between 390 nm and 450 nm it is largely transparent to the visible light, with observed through cure almost certainly coming from the utilisation of lamp emission wavelengths at 365 nm and 405 nm by the isopropyl thioxanthone photoinitiator. Cyan inks, like black inks, are often associated with poor through cure characteristics, however, use of sufficient quantities of thioxanthone type photoinitiators should enable good through cure to be achieved with a wide range of film thicknesses.

4.2.2.4 The occurrence and consequences of screening

So far in this chapter the effect of competitive light absorption has been discussed in terms of how the absorption of light by other components affects the reactivity of the photoinitiator, and how excessive concentrations of any material can be predicted using the Beer-Lambert law. The fact that screening can be brought about by excessive concentrations of a single material leading to competitive light absorption by itself (self screening) can be investigated further using the technique of Differential Photocalorimetry (DPC). The results of this investigation can also be used to validate the theories put forward within this chapter. DPC is ideal for this investigation because of the sensitivity of the technique, its versatility in terms of use of different atmospheres, exposure temperatures, light sources/wavelengths and the relatively high film thicknesses

involved. A DPC experiment typically involves a 0.80-0.85 mg sample used over an area that corresponds to a film thickness of 80 μm ; approximately 40 times as thick as the printing ink it is used to model. On that basis, a 3.0 %wt concentration of a photoinitiator such as Irgacure 369 would result in severe self screening in a DPC experiment. This is illustrated in figure 4.39 where the UV transmission spectrum under these conditions has been calculated for Irgacure 369. Also shown is the transmission spectrum for a 0.25 %wt Irgacure 369 formulation, indicating that in the absence of other UV absorbing materials this is the highest concentration that can be used in a DPC experiment without causing self screening.

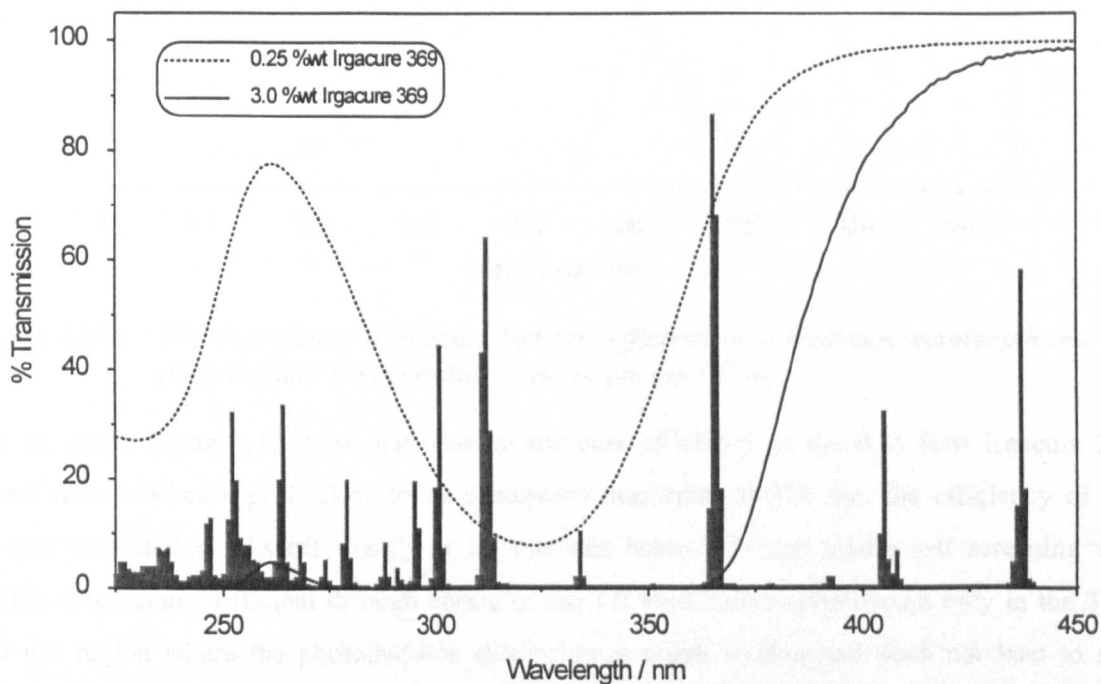


Figure 4.39 *The calculated UV transmission spectra for formulations containing 0.25 %wt and 3.0 %wt Irgacure 369 in an 80 μm thick film*

The results in figure 4.39 lead to the speculation that self screening by Irgacure 369 in a 3.0 %wt formulation will occur at all wavelengths below 375 nm, where the transmitted light falls to below 10% of the incident light intensity. This can be demonstrated by irradiating both formulations with successive monochromatic wavelengths in the region 300-420 nm and observing their cure exotherms, as shown in figure 4.40. Experiments used 0.85 mg samples in an air purge at 45°C, exposed to monochromatic light from a 150W Xenon lamp, with the weight normalised exotherm partial peak area at maximum cure rate (Jg^{-1}) used as a measure of reactivity.

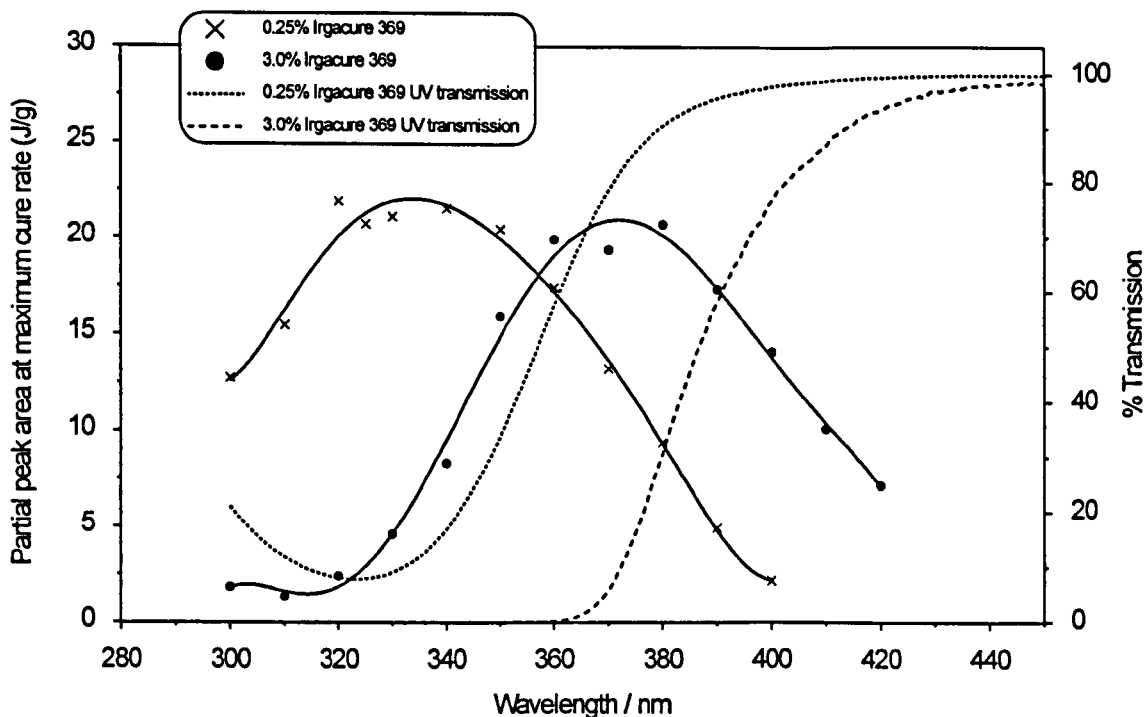


Figure 4.40 *The dependency of Irgacure 369 cure efficiency on irradiation wavelength and photoinitiator concentration in an 80 μm thick film*

The results in figure 4.40 show that whereas the cure efficiency of the 0.25 %wt Irgacure 369 formulation reaches a peak close to its absorption maximum at 323 nm, the efficiency of the 3.0%wt formulation falls off sharply at wavelengths below 375 nm, where self screening was predicted to occur. Efficient through curing of the 3.0 %wt formulation occurs only in the 375-420 nm region where the photoinitiator absorption is much weaker and does not lead to self screening. Although some curing also occurs in the 375-420 nm region with the 0.25 %wt formulation, it is considerably less efficient because of the lower photoinitiator concentration.

These results and observations are entirely consistent with those predicted based on the UV transmission spectra of the two formulations, adding weight to the validity of the spectral prediction procedure. However, the emission spectrum of the xenon lamp, although continuous and smooth in this experimental region, does decline in intensity with decreasing wavelength⁵¹, such that the data in figure 4.40 is more comparative than absolute. Based on other work in this chapter it is thought that the curve for the 0.25 %wt formulation is reflecting this intensity decrease as a slight shift of 5-10 nm in the efficiency maximum towards longer wavelengths, and a more significant drop in cure efficiency at wavelengths below the absorption maximum than would be expected. No other significant changes are thought likely to result from this intensity variation.

Due to the exotherm distortion that accompanies screening in DPC experiments, where screening is known or suspected to occur it is particularly important to measure reactivity using either the

exotherm peak height or the integrated partial area at the exotherm peak maximum. The choice between these two parameters is based largely on the type of experiment, with peak height measurements producing better data over a wider reactivity range and with pigmented samples, whereas the integrated partial area at the peak maximum provides better data in low-medium reactivity range situations. When screening occurs, the normally symmetrical exotherm peak becomes smaller and asymmetrical, with a sharp leading edge and a long trailing back edge. This distorted peak shape reflects both the rapid curing near the surface, where most of the light is absorbed (sharp leading edge), and the slower curing near the bottom (long trailing back edge), where the probability of light absorption is very low. An example is shown on a slightly expanded scale in figure 4.41 for the exotherms associated with 0.25 %wt and 3.0 %wt Irgacure 369 formulations irradiated at 340 nm. In this case the integrated peak area over the total exposure time is the same for both samples, although the 3.0 %wt formulation shows severe exotherm distortion due to screening. As a result of this exotherm distortion it is not appropriate to use total peak area as a measure of curing activity since misleading results may be produced³⁹.

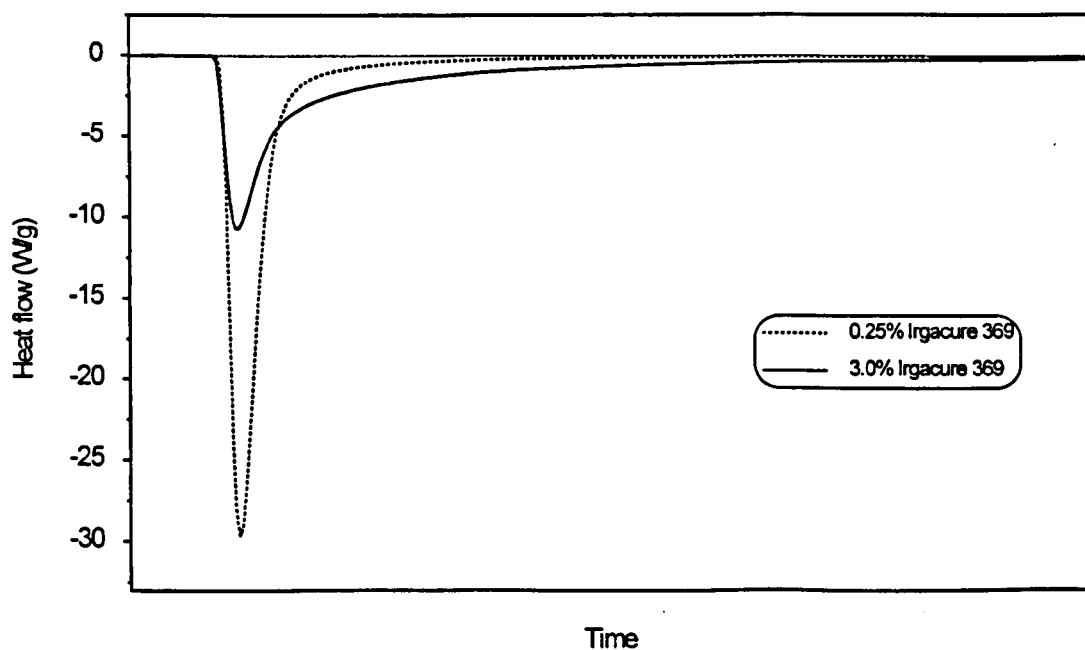


Figure 4.41 *The observation of exotherm distortion in DPC experiments resulting from photoinitiator self screening*

These experiments show the effect of screening on the DPC exotherm peak shape using a monochromatic light source. In practice, with a polychromatic light source such as a medium pressure mercury lamp, the effect of screening is quite different and significantly more difficult to identify. Figure 4.42 shows DPC exotherm peak height results for samples containing increasing levels of either the strongly absorbing photoinitiator Irgacure 369 or the weakly absorbing 2,4,6-trimethylbenzoyl diphenylphosphine oxide (Lucerin TPO) irradiated with the full lamp emission spectrum from a medium pressure mercury short arc lamp at 40°C in an air purge.

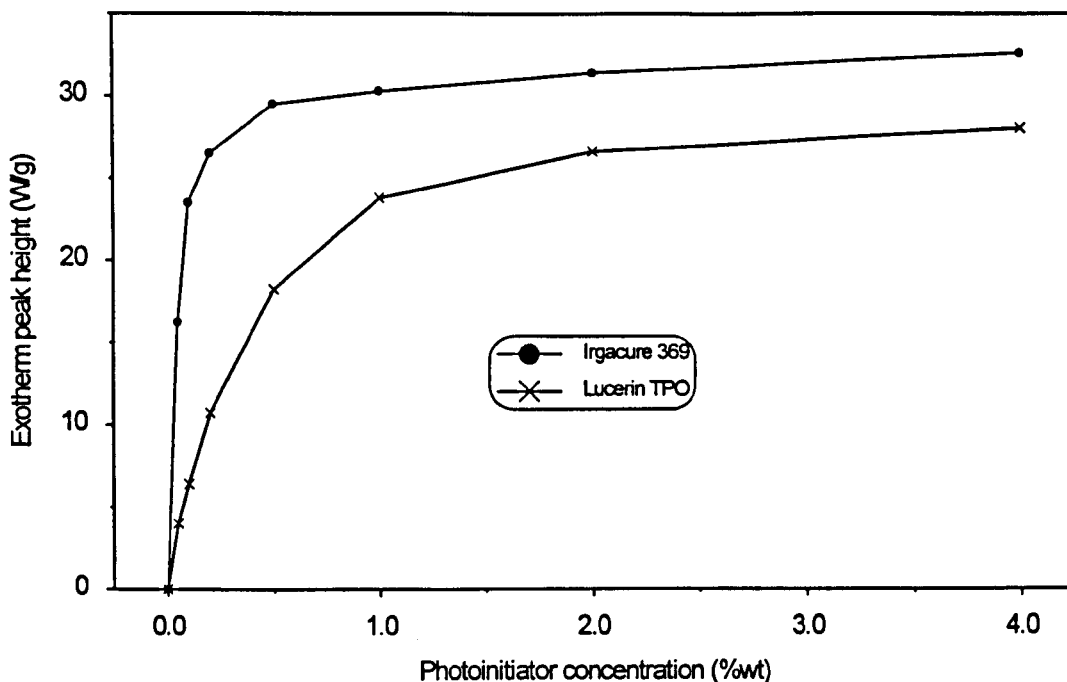


Figure 4.42 *The effect of photoinitiator concentration on reactivity due to the onset of screening*

The data in figure 4.42 shows that for formulations containing Irgacure 369, the cure speed increases sharply with photoinitiator concentration up to 0.2-0.5 %wt. As the concentration increases further there is little or no benefit in terms of cure speed because self screening is occurring in the region of the photoinitiator absorption maximum. Unlike with a monochromatic light source, screening does not then decrease the cure speed because the curing is increasingly provided by the longer wavelengths which absorb less strongly, although the lower efficiency in this region also results in very little additional cure speed. In contrast, Lucerin TPO absorbs much less strongly and doesn't self screen in the 300-450 nm range at concentrations below 2.0 %wt, consequently it shows a more continuous reactivity increase as a function of concentration, and despite being inherently much less reactive than Irgacure 369, at 2 %wt can provide almost as fast a cure speed under these experimental conditions.

Although self screening due to excessive photoinitiator concentrations is unlikely in thin printing ink films of around 2 μm thickness, the much thicker films applied in the screen printing process (~10 μm) could well give rise to this problem when strongly UV absorbing photoinitiators are used. As such it is important to be able to recognise and circumvent the problem. Figure 4.43 shows the DPC exotherm peak height measurements for both black and yellow pigmented formulations containing increasing levels of the photoinitiator Irgacure 369, exposed under the full emission spectral output of a medium pressure mercury short arc lamp at 45°C in an air purge.

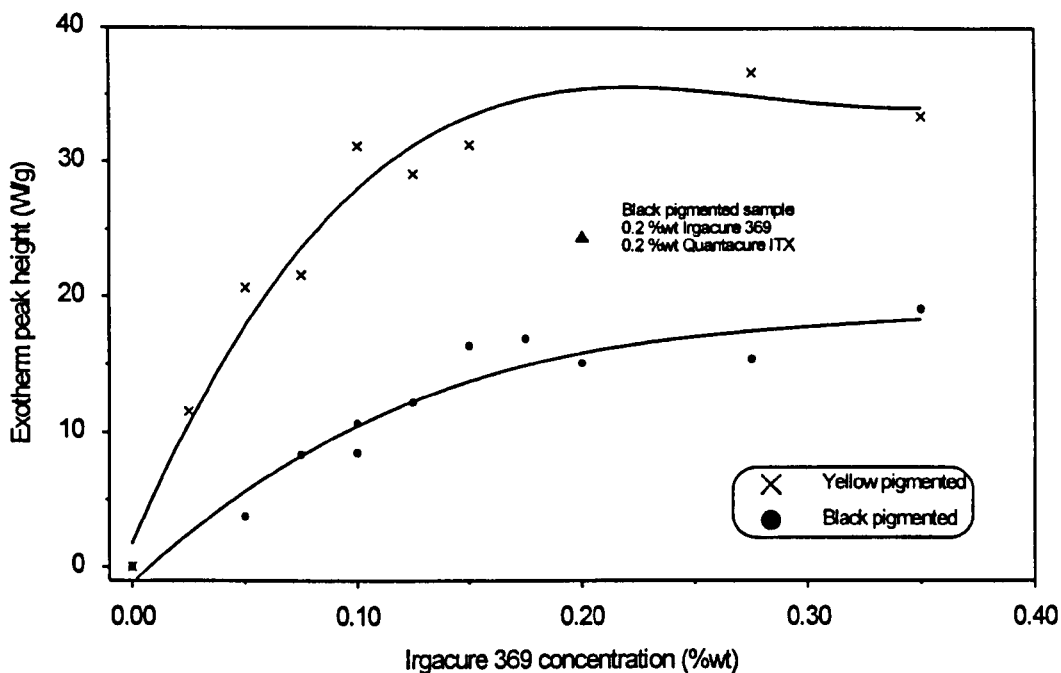


Figure 4.43 *The effect of photoinitiator concentration and self screening on the cure reactivity of pigmented formulations*

In a non-pigmented formulation containing Irgacure 369, cure reactivity was previously shown to plateau at a photoinitiator concentration of around 0.25 %wt. However, the data in figure 4.43 shows that for a black pigmented formulation, the presence of the additional UV absorbing black pigment leads to a reactivity plateau at a concentration of only 0.15-0.20 %wt, with additional Irgacure 369 having little or no beneficial effect on cure. Also, the indicated point on the graph shows how an additional 0.2 %wt of a different photoinitiator (Quantacure ITX) dramatically increases the reactivity of the black pigmented formulation containing 0.2 %wt Irgacure 369. This effect can be ascribed to the ITX absorbing light at much longer wavelengths than Irgacure 369, in a spectral region where screening is not occurring, and leads to more efficient curing than could be obtained by the use of Irgacure 369 alone.

It is also apparent from figure 4.43 that the yellow pigmented formulation shows a much higher reactivity than the black at all photoinitiator concentrations, almost certainly due to the low pigment absorption in the region of the photoinitiator absorption maximum. This lower extent of competitive light absorption by the yellow pigment results in reactivity increasing with photoinitiator concentration up to 0.2-0.25 %wt, although above this level reactivity appears to decrease rather than merely to plateau. It was previously identified that when self screening occurs using the photoinitiator Irgacure 369, much of the through cure comes from the weakly absorbing wavelengths in the region 375-450 nm. Since the yellow pigment absorbs strongly in this region, it is speculated that the decrease in reactivity is a result of increased competitive light absorption as these wavelengths. A similar effect is not observed with the black pigmented sample because black pigments have a continuous absorbance in the UV and visible regions, such that competitive light absorption suppresses through curing at all wavelengths.

4.2.3 Sensitization

4.2.3.1 Energy transfer reactions

Although the energy transfer sensitization of 2-methyl-1-[4-(methylthio)phenyl]-2-morpholino propan-2-one (Irgacure 907) by isopropyl thioxanthone (ITX) has been reported³¹ and widely accepted, relatively little work has been reported on the influence of thioxanthone type. Also, the use of ITX as a potential sensitizer of other common photoinitiators has not been well investigated.

The results in figure 4.44 show the extent to which the photoinitiator Irgacure 907 is sensitized by various thioxanthone derivatives in a Differential Photocalorimetry procedure similar to one previously reported by Dietliker et al.³³. In this case, the samples are based on an oligomer / monomer blend containing 2 %wt of the photoinitiator Irgacure 907 and 0.2 %wt of a thioxanthone sensitizer, and were irradiated with 405 nm monochromatic light which is absorbed by the sensitizer but not by the photoinitiator. Care was taken to ensure that no screening occurred at the irradiation wavelength. The exotherm peak height (Wg^{-1}) for these formulations was then compared with the exotherms from samples containing only the photoinitiator or only the sensitizer in order to establish the extent of the sensitization. Amine synergist was omitted from the formulation to suppress cure activity from the thioxanthone reacting by a type II mechanism.

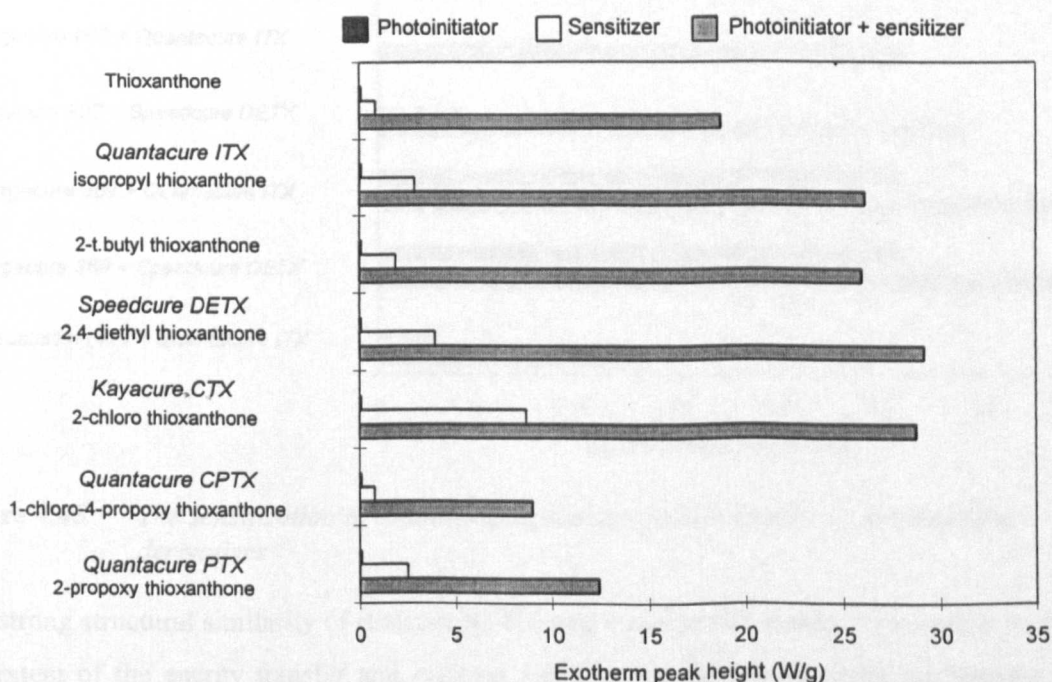


Figure 4.44 The sensitization of Irgacure 907 by thioxanthone derivatives

The results in figure 4.44 show that Irgacure 907 is sensitized to some extent by all the thioxanthenes tested, with the isopropyl, 2-*t*.butyl, 2,4-diethyl and 2-chloro derivatives showing the greatest efficiency.

The lower reactivity of the thioxanthone / Irgacure 907 combination could be accounted for by the weak absorption of thioxanthone at 405 nm compared to its derivatives. The low sensitizing activity of CPTX and PTX is more surprising, particularly in view of literature claims that both are efficient sensitizers of Irgacure 907^{44,45}. This lower efficiency cannot be accounted for by the extent of UV light absorption alone because the (n- π^*) bands for CPTX and PTX are red shifted even further than those of the alkyl and chloro derivatives, allowing them to absorb more light at the 405 nm irradiation wavelength. The fact that triplet energies have only been published for Irgacure 907 and the isopropyl and 2-chloro thioxanthenes makes it difficult to speculate too much about the reasons behind this observation, although the long wavelength absorptions of CPTX and PTX implies that the excitation energy, and consequently the triplet energy level, is lower. If this were the case, then the energy transfer to Irgacure 907 would be less favourable and a lower reactivity would be observed. It is also possible that for CPTX and PTX, the balance of the two possible sensitization mechanisms favours the less reactive electron / proton transfer mechanism.

Figure 4.45 shows the results of similar experiments using other α -aminoalkylphenone photoinitiators. These demonstrate that both Radstart N1414 and Irgacure 369 are sensitized by thioxanthenes, but at a lower efficiency than Irgacure 907.

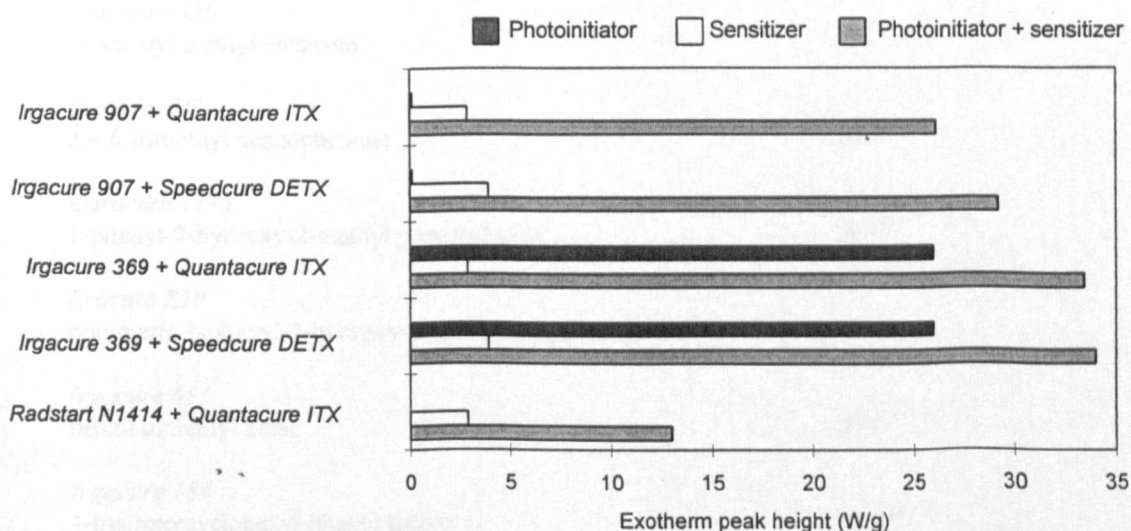


Figure 4.45 *The sensitization of α -aminoalkylphenone photoinitiators by thioxanthone derivatives*

The strong structural similarity of Radstart N1414 and Irgacure 907 makes it reasonable to expect the extent of the energy transfer and electron / proton transfer sensitization mechanisms to be similar when using the same sensitizer. However, despite similar reactivities for the two photoinitiators (see chapter 6) the reactivity of a Radstart N1414 / ITX combination is significantly lower than a Irgacure 907/ ITX combination, suggesting that other factors are important in defining the reactivity of any photoinitiator / sensitizer combination.

It has been reported that Irgacure 369 shows high reactivity at 405 nm without the use of a sensitizer, making the sensitization process difficult to study³¹. This effect was also observed here, but a clear improvement in reactivity of Irgacure 369 was observed when it was used in conjunction with either ITX or DETX. Triplet energies have been published for Irgacure 369, but the values of 252 kJ mol⁻¹³¹ and 257-266 kJ mol⁻¹⁵² are ambiguous since the former suggests that Irgacure 369 can be sensitized by energy transfer using ITX ($E_{\text{triplet}}=254.8 \text{ kJ mol}^{-1}$ ³⁸), whereas the latter suggests it cannot.

A series of other commercial photoinitiators was also investigated for possible sensitization by ITX. These are given below, along with their triplet energies where known;

	E_{triplet} (kJ mol ⁻¹)
<i>Quantacure BMS</i> 4-benzoyl-4'-methyl diphenyl sulphide	-
<i>Trigonal 12</i> 4-phenyl benzophenone	254 ⁵³
benzophenone	289 ⁵³
4-methyl benzophenone	-
<i>Daitocure OB</i> 2-benzoyl methyl benzoate	-
<i>Esacure TZT</i> 2,4,6-trimethyl benzophenone	285 ⁵⁴
<i>Darocure 1173</i> 1-phenyl-2-hydroxy-2-methyl propan-1-one	295 ³³
<i>Esacure KIP</i> polymeric 1-phenyl-2-hydroxy-2-methyl propan-1-one	-
<i>Irgacure 651</i> benzil dimethyl ketal	275 ¹⁹
<i>Irgacure 184</i> 1-hydroxycyclohexyl phenyl ketone	277 ¹⁹
benzil	227 ⁵³

Despite benzil and 4-phenyl benzophenone reportedly having triplet energies lower than that of ITX ($E_{\text{triplet}}=254.8 \text{ kJ mol}^{-1}$ ³⁸), none of the above photoinitiators showed any sensitization activity. Clearly energy transfer sensitization is more complicated than it is often portrayed, and is a subject worthy of additional research, particularly in the area of α -aminoalkylphenone sensitization by thioxanthone derivatives.

4.2.3.2 Electron / proton transfer reactions

The results in figure 4.46 show the extent to which the photoinitiator benzophenone is sensitized by 4,4'-(dimethylamino) benzophenone (Michler's ketone) and 4,4'-(diethylamino) benzophenone (ethyl Michler's ketone) in a Differential Photocalorimetry procedure similar to one previously reported by Dietliker et al.³³. In this case the samples were based on an oligomer / monomer blend containing 2 %wt of benzophenone and 0.2 %wt of sensitizer and were irradiated with 405 nm monochromatic light, absorbed only by the sensitizer but to an extent insufficient to cause screening. The weight normalized exotherm peak area (Wg^{-1}) was used as a measure of reactivity

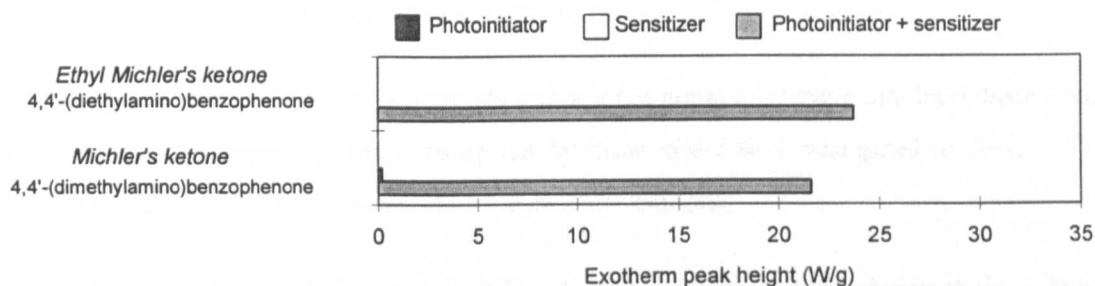


Figure 4.46 The sensitization of benzophenone by 4,4'-(dialkylamino)benzophenones

The combination of benzophenone and Michler's ketone has been known for a long time to be particularly reactive^{7,34,35,55}, with excitation of either material leading to radical formation³⁵. This is demonstrated in figure 4.46 for both Michler's ketone and ethyl Michler's ketone, with the observed reactivity being close to that of the highly reactive Irgacure 907/isopropyl thioxanthone combination. These results demonstrate that as well as being a synergistic combination with benzophenone, 4,4'-(dialkylamino) benzophenones used at low levels can provide a significant cure contribution. The mechanism of reaction for this combination has been widely reported and is generally accepted as an electron / proton transfer process, with energy transfer sensitization having been discounted because the triplet energy of Michler's ketone is below that of benzophenone⁵⁶.

Whilst Michler's ketone is suspected of having carcinogenic activity⁵⁷, preventing its continued use in printing inks, ethyl Michler's ketone is not, and could therefore still have considerable potential as a photoinitiator or sensitizer.

4.3 CONCLUSIONS

The reactivity of a large number of photoinitiators has been investigated at each of the principal wavelength emission bands from a medium pressure mercury arc lamp. This has identified that, with the exception of thioxanthone based photoinitiators, which derive much of their curing activity from the strong 365 nm lamp emission band, most commercial photoinitiators derive much of their observed reactivity from the shorter more energetic wavelengths around 300 nm. Although wavelengths below 300 nm were not accessible in these experiments, some evidence suggests that the strong ($\pi-\pi^*$) transitions for many photoinitiators at wavelengths below 300 nm are also capable of providing significant curing activity.

The absorption spectra of amine synergists and a large number of pigments have been measured and the effect of competitive light absorption by these materials investigated in detail. This has been correlated with data and observations from other authors.

By printing a number of different inks at known film weights and measuring their transmission spectra it has proved possible to identify spectral regions involved in providing both surface and through cure for each colour in a process ink set. Their ease of cure has also been rationalised in terms of the amount of incident light reaching various points in the film, and predictions made of the photoinitiator combinations likely to prove most effective in curing them.

Based on absorbance spectral data obtained in dilute solution and long path length cells, the Beer-Lambert law has been modified to allow calculation of the transmission spectra of individual components in an ink formulation of only a few microns thickness. The advantage of this procedure is that a prediction can then easily be made as to when any individual material or combination of materials absorb excessive amounts of light near the surface of a given film, such that no light reaches the lower layers and results in poor through cure. This has been validated both directly and indirectly for non-pigmented systems and some pigmented systems. Although, as a result of inadequate dispersion, pigment spectra could not be 'scaled' in the same way as photoinitiator and synergist spectra, a procedure has been suggested which could overcome this.

The energy transfer sensitization of a large number of photoinitiators by thioxanthone derivatives has been investigated. Whilst most commercial photoinitiators showed no sensitization activity, all three of the α -aminoalkylphenone type photoinitiators tested did show sensitization by isopropyl thioxanthone. The type of thioxanthone derivative was also shown to have a significant influence on the effectiveness of the sensitization process.

The information presented here can be effectively used to aid the development of cost effective and technically robust photoinitiator systems for the curing of a wide range of inks and coatings.

4.4 EXPERIMENTAL

4.4.1 UV / vis absorption spectra

UV/vis absorption spectra were measured using a Perkin-Elmer (Beaconsfield, Bucks.) Lambda 6 UV/vis spectrophotometer at a scan rate of 60 nm/min. with 1 cm path length cells and an integrating sphere detector.

Photoinitiators and synergists

Photoinitiator and synergist spectra were measured at a concentration of 0.02 gdm⁻³ in spectroscopic grade methanol.

Pigments

Yellow, magenta, cyan and black pigment spectra were measured at a concentration of 0.02 gdm⁻³ following the dispersion of 0.5 mg pigment in 25 ml of spectroscopic grade methanol using a Lucas Dawe Ultrasonics, ultrasonic cleaning bath. The spectra of white pigments were measured directly through a polyethylene film after rubbing pigment powder onto the film and blowing away the excess to give a thin pigment layer impregnated into the film surface.

4.4.2 Determining the most effective curing wavelengths for photoinitiators by DPC

A Perkin-Elmer (Beaconsfield, Bucks.) Differential Scanning Calorimeter (DSC7) fitted with a Differential Photocalorimetry Accessory (DPA7) was used. Formulations were prepared by dissolving 0.2 %wt photoinitiator and 0.2 %wt of the synergist N-methyl diethanolamine in an 80/20 blend of the aliphatic urethane diacrylate oligomer CN934 and the monomer TMPTA. Separate samples of approximately 0.8 mg were irradiated at 45°C in air with each of the principal lamp emission bands (302, 313, 334, 365, 405 and 436 nm) from an Osram HBO 100W/2 medium pressure mercury short arc lamp using a prism monochromator. Care was taken to ensure no self-screening occurred at any of the irradiation wavelengths. Sample weight normalized exotherm peak height measurements (Wg⁻¹) were used as a measure of reactivity.

For the analysis of pigmented samples, a similar procedure to that described above was used, with pigment being introduced by blending 39 parts of the formulation containing 0.2 %wt photoinitiator / amine with 1 part of a Coates Lorilleux electron beam (EB) curable lithographic process ink. The EB ink contains no photoinitiator or synergist and therefore merely provides 1/40th of the normal pigment concentration for a DPC sample that is used at a thickness 40 times greater than a typical lithographic ink. As such, the extent of UV absorption through the 80 µm DPC sample should be similar to that found in a printed lithographic ink.

4.4.3 The effect of competitive light absorption by amine synergists

Formulations were based on an 80/20 blend of the aliphatic urethane diacrylate oligomer CN934 and the monomer TMPTA, containing 3 %wt of the photoinitiator benzophenone and 3 %wt of the amine synergist. These were analysed according to the Real-Time Fourier Transform Infrared (RT-FTIR) spectroscopy method described in detail in chapter 6.

Transmission spectra of printed films

The transmission spectra of a formulation containing 3 %wt of 2-hydroxy benzophenone in a CN934/ TMPTA blend at different film thicknesses was measured by printing the formulation onto a thin grade of low density polyethylene using an IGT print tester. The specific gravity of the formulation was determined gravimetrically to be 1.16 gcm^{-3} . The print area was constant for this application method, with the deposited film weight being calculated from the weight difference of the print roller before and after printing. Film thickness (μm) was therefore given by:

$$\frac{1}{\text{specific gravity (gcm}^{-3}\text{)}} \times \frac{\text{mass deposited (g)}}{\text{print area (m}^2\text{)}}$$

The wet print sample was covered either with a layer of unprinted substrate or another piece of wet print (face to face), producing an easy to handle single or double layer thickness.

A similar procedure was used for printing the yellow, magenta, cyan and black inks from the Coates Lorilleux Unicure CL ink process set.

4.4.4 The occurrence and consequences of screening

The dependency of cure efficiency on photoinitiator concentration and irradiation wavelength

Formulations were prepared based on an 80/20 blend of the aliphatic urethane diacrylate oligomer CN934 and the monomer TMPTA, containing 0.25 %wt and 3.0 %wt of the photoinitiator 2-benzyl-2-dimethylamino-1-(4-morpholinophenyl)butan-1-one, (Irgacure 369). These were analysed using a Perkin-Elmer (Beaconsfield, Bucks.) Differential Scanning Calorimeter (DSC7) fitted with a Differential Photocalorimetry Accessory (DPA7) by irradiating the 0.85 mg samples with monochromatic light at 10 nm increments between 300 and 420 nm from an Osram XBO 150 Watt xenon short arc lamp at 45°C in an air purge. The weight normalized exotherm partial peak area at the peak maximum (Jg^{-1}) was used as a measure of reactivity.

The effect of photoinitiator concentration on reactivity of an unpigmented formulation

Formulations were prepared based on an 80/20 blend of the aliphatic urethane diacrylate oligomer CN934 and the monomer TMPTA, containing 0, 0.1, 0.2, 0.5, 1.0, 2.0 and 4.0 %wt of the photoinitiators 2-benzyl-2-dimethylamino-1-(4-morpholinophenyl)butan-1-one (Irgacure 369) and 2,4,6-trimethylbenzoyl diphenylphosphine oxide (Lucerin TPO). The curing activity of the formulations was measured using a Perkin-Elmer (Beaconsfield, Bucks.) Differential Scanning

Calorimeter (DSC7) fitted with a Differential Photocalorimetry Accessory (DPA7). Samples of approximately 0.8 mg were irradiated through a 10% neutral density filter at 40°C in an air purge with the full emission spectrum of an Osram HBO 100W/2 medium pressure mercury short arc lamp. The weight normalized exotherm peak height (Wg^{-1}) was used as a measure of reactivity.

The effect of photoinitiator concentration on reactivity of pigmented formulations

Formulations were prepared based on an 80/20 blend of the aliphatic urethane diacrylate oligomer CN934 and the monomer TMPTA, containing the photoinitiator 2-benzyl-2-dimethylamino-1-(4-morpholinophenyl)butan-1-one (Irgacure 369) at levels between 0.025 %wt and 0.35 %wt. These formulations were subsequently blended with a yellow or black Coates Lorilleux EB curing lithographic ink in a 39:1 ratio to provide a similar extent of absorption through the 80 μm DPC sample as would be found in a 2 μm thick lithographic ink film. The curing activity of these formulations was measured using a Perkin-Elmer (Beaconsfield, Bucks.) Differential Scanning Calorimeter (DSC7) fitted with a Differential Photocalorimetry Accessory (DPA7). Samples of approximately 0.8 mg were irradiated with the full emission spectrum of an Osram HBO 100W/2 medium pressure mercury short arc lamp at 45°C in an air purge. The weight normalized exotherm peak height (Wg^{-1}) was used as a measure of reactivity.

4.4.5 Sensitization

Formulations were prepared based on an 80/20 blend of the aliphatic urethane diacrylate oligomer CN934, and the monomer TMPTA. Various levels of photoinitiators were added, typically being 0.2 %wt of a thioxanthone derivative (sensitizer) and 2 %wt of an α -aminoalkylphenone type photoinitiator. The sensitization activity of the photoinitiator / sensitizer combination was measured using a Perkin-Elmer (Beaconsfield, Bucks.) Differential Scanning Calorimeter (DSC7) fitted with a Differential Photocalorimetry accessory (DPA7). Samples of approximately 0.8 mg were irradiated using 405 nm monochromatic light from an Osram HBO 100W/2 medium pressure mercury short arc lamp at 40°C in an air purge. The weight normalized exotherm peak height (Wg^{-1}) was used as a measure of reactivity.

4.5 REFERENCES

1. J G Calvert, J N Pitts; *Photochemistry*, John Wiley & Sons (1966)
2. R Phillips; *Sources And Applications Of Ultraviolet Radiation*, Academic Inc., London (1983)
3. A Gilbert, J Baggot; *Essential Modern Photochemistry*, Blackwell Scientific Publications (1991)
4. N J Turro; *Modern Molecular Photochemistry*, The Benjamin/Cummings Publishing Co. Ltd., Philippines (1978)
5. K Dietliker in *Radiation Curing In Polymer Science And Technology (Volume II- Photoinitiating Systems)*; J P Fouassier, J F Rabek (Eds.), Elsevier Science Publishers Ltd., Barking, Essex; 155 (1993)
6. R W Bassemir and A J Bean; *Proc. Conf. TAGA*, St Paul, Minnesota, 133 (1974).
7. G Hencken; *American Ink Maker*, March, 57 (1978).
8. K Dorfner in *Radiation Curing Of Polymers II*; D R Randell (Ed), The Royal Society Of Chemistry, 216 (1991)
9. Z W Wicks Jr, S P Pappas in *Radiation Curing: Science And Technology*; S P Pappas (Ed), Technology Marketing Corporation, Norwalk, Connecticut, USA, 78 (1978)
10. D Skinner; *Polymers Paint and Colour Journal*, 184 (4361), 566 (1994).
11. L Misev; *Proc. Conf. RADTECH-ASIA*, Osaka, Japan, 404 (1991)
12. M J M Abadie, L C Carrera; *European Coatings Journal*, 6, 330 (1992)
13. G Plews, R Phillips; *Journal Of Coatings Technology*, 51 (648), 69 (1979)
14. P G Garratt in *Radiation Curing Of Polymers II*; D R Randell (Ed.), Royal Society Of Chemistry, London, 103 (1991)
15. A D Aldridge, P D Francis, J Hutchinson; *Journal Of The Oil And Colour Chemists Association*, 67 (2), 33 (1984)
16. B E Hulme, J J Marron; *Paint And Resin*, 54 (1), 31 (1984)
17. N Pietschmann; *Journal Of Radiation Curing*, 21 (4), 2 (1994)
18. S Göthe; *Proc. Conf. FATIPEC*, (17th), 13 (1984).
19. W Rutsch, G Berner, R Kirchmayr, R Hüsler, G Rist, N Bühler; *Proc. 10th Int. Conf. Org. Coat. Sci. Tech.*, Athens, Greece, 241 (1984)
20. E Beck, E Keil, M Lokai, J Schröder; *Radcure Letter*, 5, 67 (1994)
21. K Seko; *Proc. Conf. RADTECH-ASIA*, Tokyo, Japan, 331 (1986)
22. L R Gatechair; *Proc. Conf. RADTECH*, New Orleans, USA, 28 (1988)
23. L R Gatechair, A M Tiefenthaler; *ACS Symposium Series No. 417*, 27 (1990)
24. H Rubin; *Proc. Conf. TAGA*, 279 (1976)
25. Z W Wicks Jr., W Kuhhirt; *Journal Of Paint Technology*, 47 (610), 49 (1975)
26. J H Nobbs, P K T Oldring; *ACS Symposium Series No. 417*, 43 (1990)
27. S P Pappas; *Proc. Conf. RADTECH*, Edinburgh, Scotland, 393 (1991)

28. G A Thomas, V J Webers; *J. Imaging Sci.*, **29**, 112 (1985)
29. A R Gutierrez, R J Cox; *Polm. Photochem.*, **7**, 517 (1986)
30. B de Ruitter, J J de Vlieger, J Bouwma; *Proc. Conf. RADTECH*, Edinburgh, Scotland, 597 (1991)
31. K Dietliker in *Chemistry and Technology of UV and EB Formulations for Coatings Inks and Paints (Volume 3-Photoinitiators for Free Radical and Cationic Polymerization)*; P K T Oldring (ed), SITA Technology Ltd., London, 58 (1991)
32. J P Fouassier, D Burr; *European Polymer Journal*, **27**, 657 (1990)
33. K Dietliker, M W Rembold, G Rist, W Rutsch, F Sitek; *Proc. Conf. RADTECH*, Florence, Italy, 3/37 (1987)
34. D F Eaton in *Photoinduced Electron Transfer I; J Mattay (ed.); Topics in Current Chemistry*, **156**, Springer Verlag, Berlin, 218 (1990)
35. G S Hammod, C C Wamser, C T Chang, C J Baylor; *J. Amer. Chem. Soc.*, **92**, 6362 (1970)
36. V D McGinniss, T Provder, C Kuo, A Gallopo; *Macromolecules*, **11**, 405 (1978)
37. S P Pappas; *Radiat. Phys. Chem.*, **25**, 633 (1985)
38. V Desobry, K Dietliker, Rüsler, W Rutsch, H Loeliger; *Polymers Paint And Colour Journal*, **178** (4227), 913 (1988)
39. S L Herlihy, G C Battersby; *Proc. Conf. RADTECH*, Florida, USA, 156 (1994)
40. M Jacobi, A Henne; *Polymers Paint And Colour Journal*, **175** (4150), 636 (1985)
41. H Fischer, R Baer, H Roland, I Verhoolen, M Walbiner; *J. Chem. Soc. Perkin Trans. 2*, 787 (1990)
42. F D Lewis, R J Lauterbach, H G Heine, W Hartmann, H Rudolph; *J. Am. Chem. Soc.*, **97**, 1519 (1975)
43. J Eichler, C P Herz, I Naito, W Schnabel; *J. Photochem.*; **12** 225 (1980)
44. W A Green, A Timms; *Proc. Conf. RADTECH*, Boston, USA, 33 (1992)
45. A Green, A Timms, P Green; *Polymer Paint and Colour Journal*; **182** (4299), 40 (1992)
46. C H Chang, A Mar, H Evers III, D Wostratzky; *Proc. Conf. RADTECH*, Boston, USA, 16 (1992)
47. G Berner, R Kirchmayr, G Rist; *J. Oil and Col. Chem. Assoc.*, **61**, 105 (1978)
48. C L Osborn; *J. Radiation Curing*, **3**, 2 (1976)
49. J E Christensen, W L Wooten, P J Whitman; *J. Radiation Curing*, **July**, 35 (1987)
50. J F Rabek in *Radiation Curing In Polymer Science And Technology (Volume 1-Fundamentals And Methods)*; J P Fouassier, J F Rabek (Eds), Elsevier Science Publishers Ltd., Barking, Essex, 329 (1993)
51. J F Rabek in *Radiation Curing In Polymer Science And Technology (Volume 1-Fundamentals And Methods)*; J P Fouassier, J F Rabek (Eds), Elsevier Science Publishers Ltd., Barking, Essex, 453 (1993)

52. C H Chang, D Wostratzky, A Mar; *Proc. Conf. RADTECH*, Northbrook, Illinois, USA, 1 (1990)
53. S L Murov, I Carmichael, G L Hug; *Handbook of Photochemistry (2nd Edition)*, Marcel Dekker Inc., New York (1993)
54. Y Ito, Y Umehara, K Nakamura, Y Yamada, T Matsuura, F Imshiro; *J. Org. Chem.*, **46**, 4359 (1981)
55. J F Ackerman, J Weisfield, R G Savageau, G Beerli; *US Patent 3,673,140* (1972)
56. S P Pappas, V D McGinnis in *UV Curing: Science and Technology*; S P Pappas (Ed.), Technology Marketing Corporation, Norwalk, Connecticut, USA, 2 (1980)
57. G Li Bassi; *Double Liason-Chimie de Peintures*, **32** (361), 17 (1985)

CHAPTER 5

Photoinitiator reaction mechanisms and photodecomposition products

5.1 INTRODUCTION

It has been suggested that photoinitiated free radical polymerisation reactions occur in three successive stages¹;

1. *Photophysical processes*

UV light is absorbed by a photoinitiator to yield a ($n-\pi^*$) or ($\pi-\pi^*$) lowest excited singlet state, followed by intersystem crossing (ISC) to yield the lowest excited triplet state.

2. *Photochemical processes*

The deactivation of an excited triplet state resulting in the formation of free radicals, either by a fragmentation reaction or the abstraction of a hydrogen atom from a suitable donor molecule; termed Type I and Type II processes respectively.

3. *Ground state free radical processes*

The primary radicals formed in the photochemical process undergo reactions typical of free radicals i.e. initiation, chain transfer and chain termination.

Although photoinitiators and photoinitiated free radical polymerisation have been the focus of an enormous amount of research over the last 20-30 years, much of this has been in the study of photophysical and photochemical processes. Of particular interest to many research groups has been the use of techniques such as laser flash photolysis to provide information on the nature and lifetimes of excited states for newly synthesised photoinitiators²⁻¹¹. The structure / reactivity relationships identified in these investigations have aided the development of new materials by the photoinitiator manufacturers.

Although seldom studied in isolation or in great detail, a great deal of information has also been reported about the ground state free radical processes of photoinitiators. The exceptions to this are the photoinitiators benzil dimethyl ketal¹²⁻¹⁹ and diethoxy acetophenone¹⁸⁻²⁵, which by virtue of a number of secondary reactions, have been studied extensively and a great deal of information is known about their reaction mechanisms and photodecomposition products.

In contrast to the photoinitiator manufacturers, the printing ink industry is under increasing pressure regarding the identity and levels of extractable / migratable material in its products, having to comply both with EC legislative restrictions requiring migration into food to be less than 50 ppb, and limits imposed by major customers which are often even more demanding. As such, the needs of the printing ink manufacturers are very different from the photoinitiator manufacturers. For example, information on the identity and lifetimes of excited states is of little direct use, since by definition, if the photoinitiator is commercially available it is effective to at least some degree. Much more important is the need to identify the by-products of the photoinitiation process, both to allow compliance with the imposed limits and to minimise any risk of taint and odour problems associated with their use. This involves a great deal of analytical

work, often with studies using actual printed material which necessitates large areas of print having to be extracted and analysed because of the small quantities involved and the low film weights applied. Although some work of this type has been published²⁷⁻²⁹, it is not a common occurrence since no-one has a vested interest to do so; printing ink manufacturers could not easily publish without disclosing their formulations to competitors, and photoinitiator manufacturers do not want to raise concerns about their products which could result in a loss of sales. In addition the results of these investigations tend to be very system specific, varying considerably as a result of factors such as:-

- Photoinitiator type and concentration
- Synergist type and concentration
- Pigmentation type and level
- Line speed and lamp power
- Cross link density
- Type of extracting solvent

Acrylate based coatings which cure by a free radical mechanism have not yet been approved by the regulatory bodies for direct food contact applications, although a large part of the existing market is in indirect food contact applications, such as the outside of boxes which contain foodstuffs. Although a box represents a physical barrier and no migration into the food would be expected, some work has been reported to show that this is possible^{30,31}. This type of data justifies both the industry concerns and the work being done because, for example, if a taint problem is not discovered until a product is on the supermarket shelf, the legal claim can be several hundred thousand pounds or more, with the ink and substrate being prime suspects. As a direct consequence of these types of problem, the photoinitiator benzil dimethyl ketal (Irgacure 651) is now largely avoided for applications involving food³². In this case, and as a result of the large amount of mechanistic information available for this photoinitiator, the material found to be responsible for the taint and odour problems was the photodecomposition product methyl benzoate.

The general mechanism of reaction of photoinitiators is covered in chapter 1 and in a number of excellent texts^{1,33,34} where it is accepted that most photoinitiators function by either a cleavage mechanism (Type I) or by a bimolecular hydrogen abstraction mechanism, typically involving a tertiary amine (Type II). Two notable exceptions to this situation have been reported; Ledwith found that the cleavage photoinitiator benzoin also shows an ability to abstract reactive hydrogens³⁵, and Fouassier found that 4-benzoyl-4'-methylphenyl sulphide (Quantacure BMS) undergoes both a cleavage reaction in the absence of amine synergist and a Type II reaction in the presence of amine².

Whilst it has been reported that cleavage photoinitiators such as benzil dimethyl ketal, diethoxy acetophenone and 2,4,6-trimethylbenzoyl diphenylphosphine oxide show a considerable cure speed increase when used with tertiary amine synergists^{12,19}, this behavior has been attributed to a radical chain process^{18,19} which reduces radical scavenging by oxygen. However, more recently it was suggested that the reactivity increase of 1-phenyl-2-hydroxy-2-methyl propan-1-one (Darocure 1173) could not be attributed to this mechanism alone³⁶.

The aim of this chapter is to more fully investigate the possible by-products of a wide range of photoinitiators by studying their photolysis in a simple model system. In an ideal situation this would be using a single photoinitiator in an otherwise fully formulated coating, but the amount of sample preparation time involved and the complications of coeluting acrylate monomers makes this beyond the scope of this work. Here, photoinitiator photolysis takes place in dilute solution, where depriving the primary radicals of any double bonds with which to react encourages the likely by-product reactions. Samples were also irradiated in the presence of the amine synergist N-methyl diethanolamine (MDEA) to investigate its involvement in the cure process and in the formation of any photodecomposition products. The identification of photodecomposition products from these photoinitiators may also allow the mechanism of reaction to be clarified for certain materials.

The large amount of literature data available on the subject of photoinitiator by-products means that for reasons of space and repetition, known literature will be discussed alongside the results in section 5.2.

5.1.1 Radical trapping techniques

A common method for studying the reaction mechanism of photoinitiators involves the use of radical trapping to identify the primary radicals formed. The use of a number of different radical traps and identification procedures has been reported.

2.2.6.6-Tetramethyl piperidin-1-oxyl (TMPO)

TMPO is a stable nitroxyl radical which does not dimerise, but reacts with other free radicals to give a neutral species which can be isolated and analysed, typically by Gas Chromatography-Mass Spectroscopy (GC-MS)

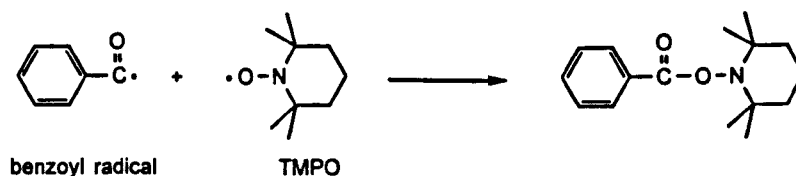


Figure 5.1 Radical trapping using 2,2,6,6-tetramethyl piperidin-1-oxyl (TMPO)

This technique has been successfully applied to identify the primary radicals formed from for the photoinitiators 2,4,6-trimethylbenzoyl diphenylphosphine oxide (Lucerin TPO)³⁷, benzoin³⁸ and diethoxy acetophenone¹. Although it has also been used to study 2-methyl-1-[4-(methylthio)phenyl]-2-morpholino propan-2-one (Irgacure 907)³⁹ it was found that one of the trapped primary radicals was unstable, hydrolysing during the workup procedure.

2-Methyl-2-nitroso propane (MNP)

MNP is used to create a stable nitroxyl radical which can then be analysed using Electron Spin Resonance spectroscopy (ESR).

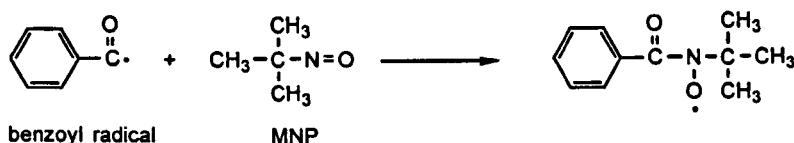


Figure 5.2 *Radical trapping using 2-methyl-2-nitroso propane (MNP)*

This technique is not widely used but has been reported for the study of benzoin³⁵ and a benzophenone / triethylamine system⁴⁰.

Methyl α .t.butyl acrylate (MTBA)

As with any acrylate monomer, the photoinitiator primary radicals react with the MTBA, but the steric bulk of the *t*.butyl group prevents the propagation reaction occurring. In the presence of a hydrogen donor the radical then abstracts a hydrogen atom and becomes a stable neutral molecule capable of being analysed by techniques such as GC-MS.

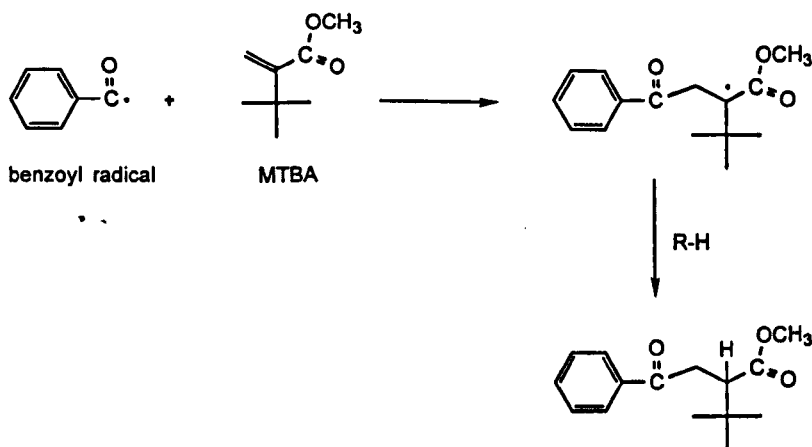


Figure 5.3 *Radical trapping using methyl α .t.butyl acrylate (MTBA)*

This trapping technique has an advantage over the other techniques described in that being an acrylate material, the tendency of the primary radicals to react with it will be similar to their tendency to react with conventional acrylate monomers. As such, quantitative analysis of the adducts under specific conditions could provide information on the relative reactivity of particular free radicals towards acrylate bonds.

Radical trapping using MTBA has not been well used, but results have been reported for 2-benzyl-2-dimethylamino-1-(4-morpholinophenyl) butan-1-one (Irgacure 369)⁴¹. It has been used in this chapter to help investigate the reaction mechanism of some photoinitiators.

5.1.2 Identification of photolysis products

Although most reported work on photoinitiator photolysis mechanisms utilises techniques such as Chemically Induced Dynamic Nuclear Polarisation (CIDNP)^{13,41-44} and Electron Spin Resonance (ESR)^{13,45,46} to identify the reaction by-products, a Gas Chromatograph fitted with a Mass Spectrometer detector (GC-MS) has also been used to separate and identify unknown materials^{2,12,47,48}. GC-MS systems typically operate by an electron impact ionisation principle (EI), where a highly energetic electron beam impinges on the sample at low pressure (10^{-2} Pa) to produce positive ions of the sample molecule (the molecular ion) and a number of fragment ions which are all focused and separated according to their mass:charge ratio. The fragmentation patterns for particular molecules are both consistent and capable of being searched on commercial mass spectral libraries, aiding the identification of unknowns. There are two problems with this approach, often resulting in not all of the photolysis products being identified:-

1. Many photoinitiators and most of their photolysis products are not present on commercial mass spectral libraries.
2. Most photoinitiators and many of their photodecomposition products contain the benzoyl group. Analysing these materials using electron impact ionisation tends to give weak or absent molecular ions and little fragmentation data other than the stable benzoyl (m/z 105) and phenyl (m/z 77) fragments, resulting in the spectra being difficult to interpret.

A 'softer' ionisation technique is Chemical Ionisation (CI), where a reagent gas, typically ammonia, methane or iso-butane, present in the ionisation chamber at a large excess ($\sim 10^4:1$) and at high pressure (~ 100 Pa) is ionised by the high energy electron beam to produce a reagent gas molecular ion. This can then react with further reagent gas (R) to produce reactive ion species capable of reacting with the sample molecule (M)⁴⁹, as shown in figure 5.4.

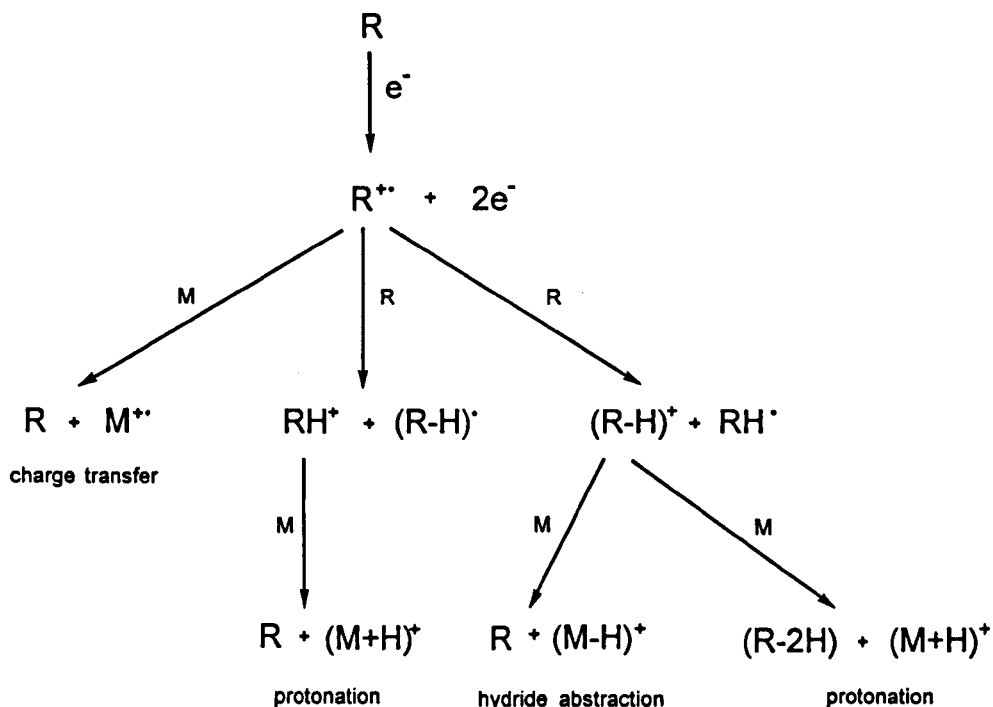


Figure 5.4 *The chemical ionisation process in mass spectroscopy*

Of the possible processes outlined in figure 5.4, protonation is most common and produces a strong protonated molecular ion with relatively little fragmentation. Where fragment ions do appear they are a result of the small amount of electron impact ionisation that still occurs.

Chemical ionisation mass spectroscopy clearly has an advantage over the more usual electron impact ionisation for the identification of photolysis products, with some work of this type having been previously reported⁴⁷. In the work reported here, both techniques have been used to help identify unknown materials, with the advantage over either technique used independently that although fragment ions appear at the same masses, under CI conditions protonation results in the molecular ion being conspicuous by its appearance at 1 amu higher than under EI conditions.

5.2 RESULTS AND DISCUSSION

5.2.1 Photolysis in the absence of amine synergist

In this section photoinitiators representative of a number of structural types were dissolved in dichloromethane, methanol or toluene and irradiated in a shallow metal dish using a medium pressure mercury arc lamp. Any precipitate formed during irradiation was re-dissolved by the addition of a second solvent. Samples of the photoinitiator solutions before and after irradiation were then analysed using GC-MS operating in electron impact ionisation (EI) mode. Some samples were also analysed with the GC-MS operating in chemical ionisation mode (CI) using methane as the reagent gas. All of the solvents used were also investigated before and after irradiation but found to give no byproducts. This was a particular concern with the use of dichloromethane, although in this case any solvent reaction would give rise to a chlorinated product, conspicuous by a 3:1 ratio of the 35 and 37 amu chlorine isotopes.

The identification of photolysis products for a particular photoinitiator provides information about both the extractable / migratable materials that could be present in a UV cured coating after cure, and the reaction mechanism of that photoinitiator. A large number of photoinitiators were analysed in this way but a lack of space prevents a detailed discussion of them all. Those chosen for discussion represent a range of structural types and in general are either commercially important materials or allow a detailed discussion of their mechanism in relation to work reported in the literature. In addition, of the GC peaks observed, only those which could be identified have been numbered and discussed in detail.

5.2.1.1 Benzoin type photoinitiators

Benzoin

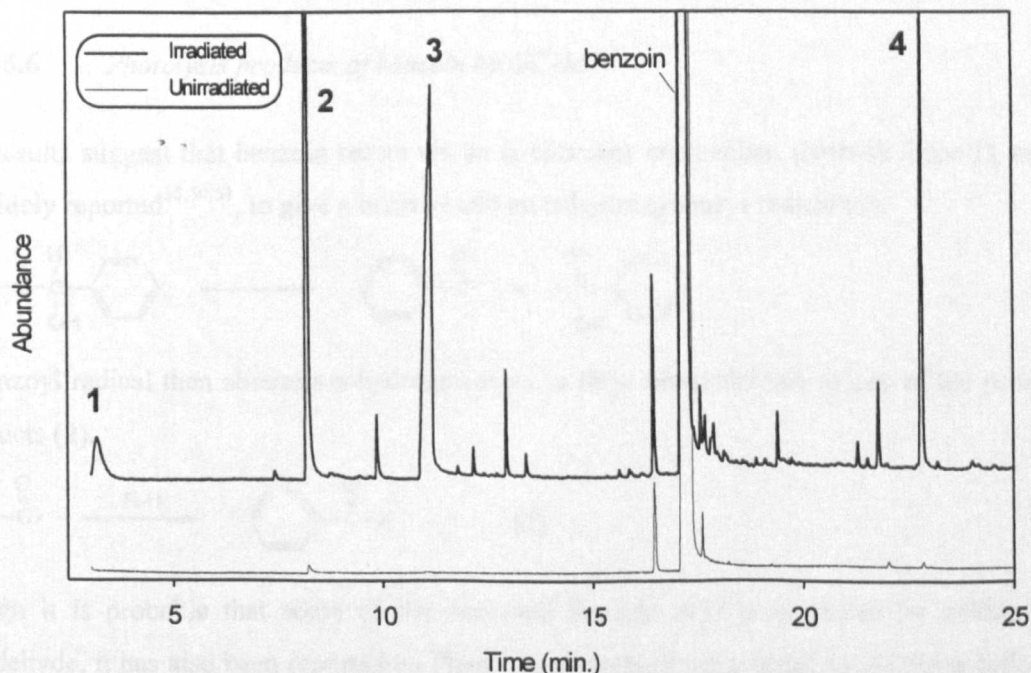


Figure 5.5 GC chromatogram of benzoin solution before and after irradiation in dichloromethane

Figure 5.5 shows the GC chromatograms of an unirradiated and irradiated solution of the photoinitiator benzoin in dichloromethane. The chromatogram peaks 1-4 identified each have an associated mass spectrum. These have been interpreted and the results given in figure 5.6.


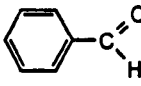
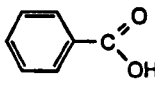
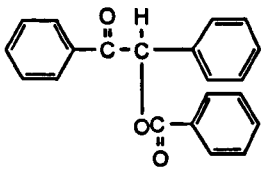
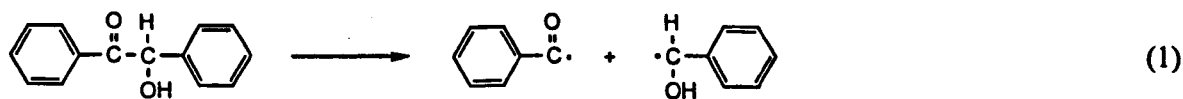
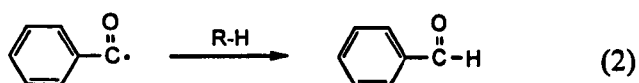
Peak 1	 Benzene	Retention time (min.)	m/z	I	Identity
		3.26	78	100	M.+
Peak 2	 Benzaldehyde	Retention time (min.)	m/z	I	Identity
		8.23	106 105 77	95 100 85	M.+ PhCO+ Ph+
Peak 3	 Benzoic acid	Retention time (min.)	m/z	I	Identity
		11.18	122 105 77	88 100 62	M.+ PhCO+ Ph+
Peak 4	 Benzoin benzoate	Retention time (min.)	m/z	I	Identity
		22.82	316 211 105 77	0.4 21 100 31	M.+ [M-PhCO]+ PhCO+ Ph+

Figure 5.6 Photolysis products of benzoin by GC-MS

These results suggest that benzoin reacts via an α -cleavage mechanism (Norrish Type I), as has been widely reported^{35,50,51}, to give a benzoyl and an α -hydroxybenzyl radical (1).



The benzoyl radical then abstracts a hydrogen atom to form benzaldehyde as one of the principal byproducts (2).



Although it is probable that some of the observed benzoic acid is produced by oxidation of benzaldehyde, it has also been reported by Phan¹⁴ to be formed via a series of reactions following quenching of the benzoyl radical by atmospheric oxygen, as shown in figure 5.7.

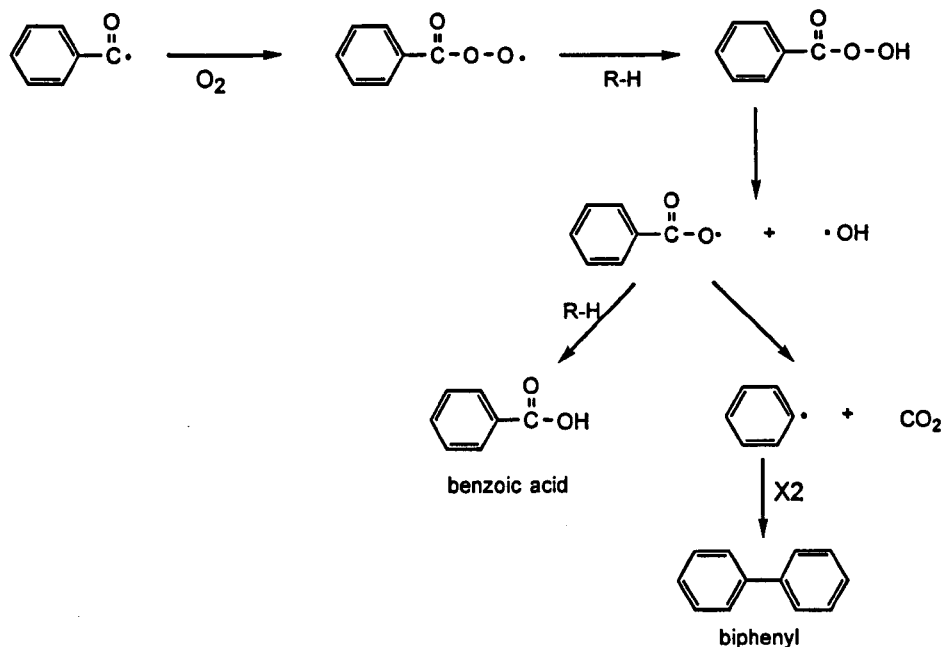


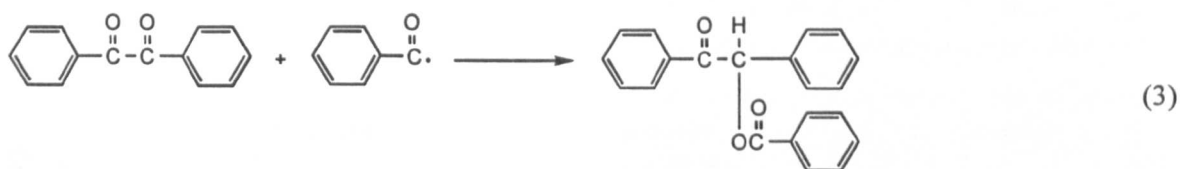
Figure 5.7 *Reported mechanism of formation of benzoic acid*¹⁴

Phan's proposed mechanism also involved the formation of biphenyl, but although a peak was found at the retention time corresponding to this material under the experimental conditions used (13.42 minutes), the mass spectrum contained principally the benzoyl group ions m/z 77 and 105, with none of the characteristic m/z 154 ion indicative of biphenyl. Phan's speculated mechanism is supported by the significant quantities of benzene detected in these experiments, with its formation most likely to be due to the phenyl radical abstracting a hydrogen atom. Benzene was not detected as a byproduct by Phan because benzene itself was used as a solvent for the photolysis experiments. In fact, the reaction of the phenyl radical with the benzene solvent is speculated to be a more likely route to the formation of biphenyl than the radical-radical termination reaction proposed by Phan. It is also possible that benzene is produced by a β -cleavage reaction of the benzoin or by decarbonylation of the benzoyl radical. However, these pathways are thought to be much less favourable than the reported decarboxylation mechanism¹⁴.

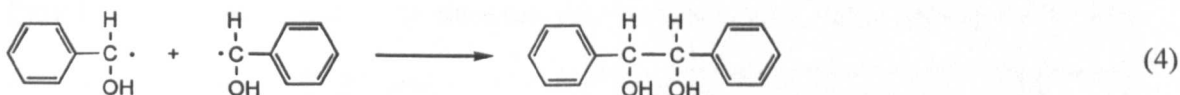
Benzil is a frequently reported byproduct of reactions involving benzoyl radicals^{13,14,47,52}, but was not seen as a distinct peak in this experiment because under the conditions used it coelutes with benzoin at 17.13 minutes. However, analysis of the leading edge of the benzoin chromatogram peak for the irradiated sample shows an abnormally strong m/z 210 signal relative to the unirradiated sample. Since m/z 210 corresponds to the molecular ion for benzil, it is speculated that benzil is formed during the irradiation procedure.

The occurrence of benzoin benzoate may be a consequence of a reaction between benzoin and the benzoyl radical. However, benzoin benzoate has also been reported as a byproduct of both 1-hydroxycyclohexyl phenyl ketone (Irgacure 184)¹⁴ and benzil⁵⁴. Since benzil itself is one of the

principal byproducts of the benzoyl radical, it is likely that benzoin benzoate is formed by a reaction between benzil and an additional benzoyl radical (3), as speculated by Phan¹⁴. Assuming this is the case, benzoin benzoate would be a characteristic byproduct of all photoinitiators that generate benzoyl radicals. It should also be pointed out that the mass spectrum assigned as benzoin benzoate is also consistent with the 2- and 4-isomers of benzoyl benzoin. These materials could also conceivably be formed by the reaction of benzil and a benzoyl radical, but are felt to be less likely than benzoin benzoate. Further work is required to clarify this assignment.



The results in figures 5.5 and 5.6 show principally products derived from the benzoyl radical, with products derived from the α -hydroxybenzyl radical notable by their absence. In particular, the reported dimerisation byproduct of the α -hydroxybenzyl radical (4)⁵⁵ was not identified.



Benzoin ethyl ether (Daitocure EE)

Figure 5.7 shows the GC chromatograms of an unirradiated and irradiated solution of the photoinitiator benzoin ethyl ether in dichloromethane. The chromatogram peaks 1-9 each have an associated mass spectrum. These and supporting GC-CI-MS data from experiments in methanol solution have been interpreted, with the results given in figure 5.8.

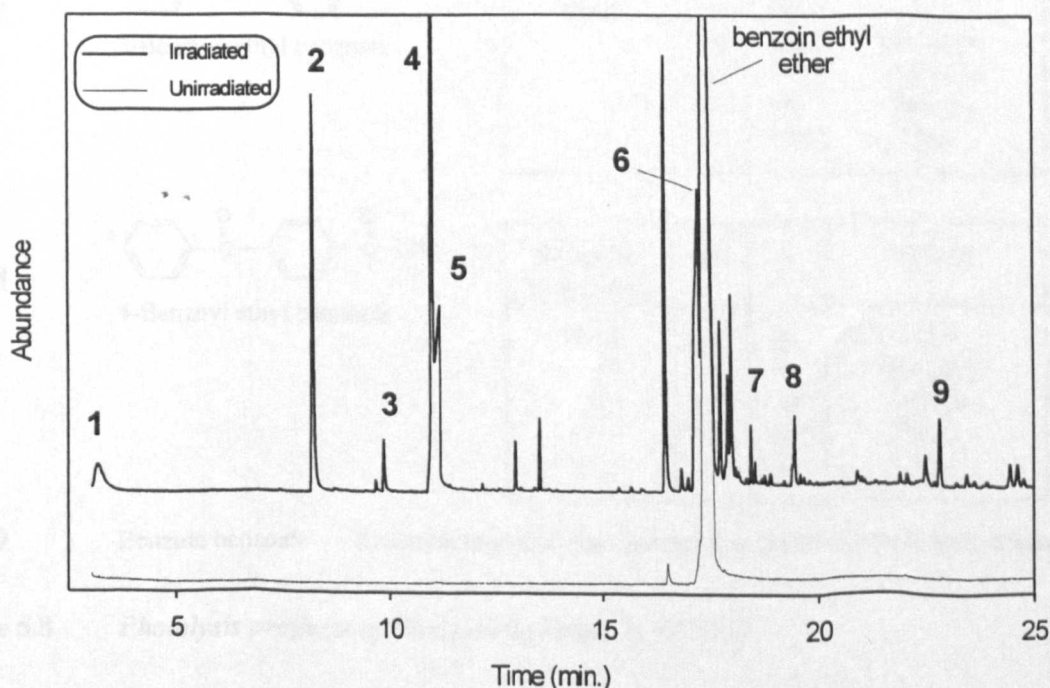
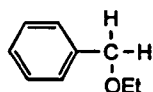


Figure 5.7 GC chromatogram of benzoin ethyl ether solution before and after irradiation in dichloromethane

Peak 1 Benzene Retention time and mass spectrum as found for photolysis of benzoin

Peak 2 Benzaldehyde Retention time and mass spectrum as found for photolysis of benzoin

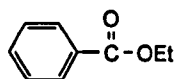
Peak 3



Benzyl ethyl ether

Retention time (min.)	m/z	I	Identity
9.824	136	9	M.+
	107	19	[M-Et]+
	92	88	unknown
	91	100	[M-OEt]+
	77	29	Ph+

Peak 4

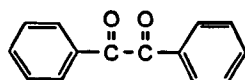


Ethyl benzoate

Retention time (min.)	m/z	I	Identity
11.03	150	17	M.+
	105	100	PhCO+
	77	57	Ph+

Peak 5 Benzoic acid Retention time and mass spectrum as found for photolysis of benzoin

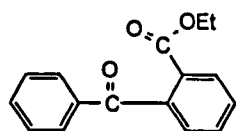
Peak 6



Benzil

Retention time (min.)	m/z	I	Identity
17.22	210	7	M.+
	105	100	PhCO+
	77	51	Ph+

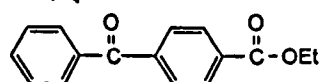
Peak 7



2-Benzoyl ethyl benzoate

Retention time (min.)	m/z	I	Identity
18.42	254	100	M.+
	209	43	[M-OEt]+
	177	53	[M-Ph]+
	105	90	PhCO+
	77	53	Ph+

Peak 8



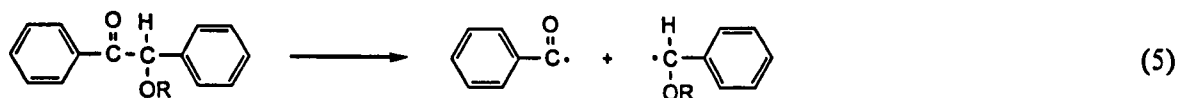
4-Benzoyl ethyl benzoate

Retention time (min.)	m/z	I	Identity
19.43	254	57	M.+
	209	46	[M-OEt]+
	177	54	[M-Ph]+
	105	100	PhCO+
	77	41	Ph+

Peak 9 Benzoin benzoate Retention time and mass spectrum as found for photolysis of benzoin

Figure 5.8 Photolysis products of benzoin ethyl ether by GC-MS

The results in figures 5.7 and 5.8 show that, as has been widely reported^{35,47,55} benzoin ethyl ether reacts via an α -cleavage mechanism (Norrish Type I) to give a benzoyl and a benzyl radical (5)



The benzoyl radical can be seen to undergo similar reactions to those observed for benzoin, producing benzene, benzaldehyde and benzoic acid as significant byproducts. The fate of the α -substituted benzyl radical itself is more controversial, with Osborn and Sandner²¹ having suggested that some secondary fragmentation could take place to give benzaldehyde and an alkyl radical (6), whereas Carlblom and Pappas⁵⁶ showed by using ¹⁴C studies that this was not important, with supporting evidence for this from ESR studies by Steenken et al.⁵⁷.



Whilst the α -ethoxy benzyl radical was shown to abstract a hydrogen from a suitable donor molecule to give benzoin ethyl ether, the widely reported dimerisation product of this was not observed. This was despite the additional use of CI-MS which would have clearly shown a m/z 270 molecular ion in the mass spectrum of an unknown GC peak.

In the case of benzoin and the benzoin ethers, benzil could be formed, as shown in figure 5.9, either by the termination reaction of two primary benzoyl radicals or by abstraction of the labile benzylic hydrogen. The latter is thought to be unlikely since benzil has also been reported as a byproduct of many other Type I photoinitiators which do not possess benzylic hydrogens^{12,14,52}.

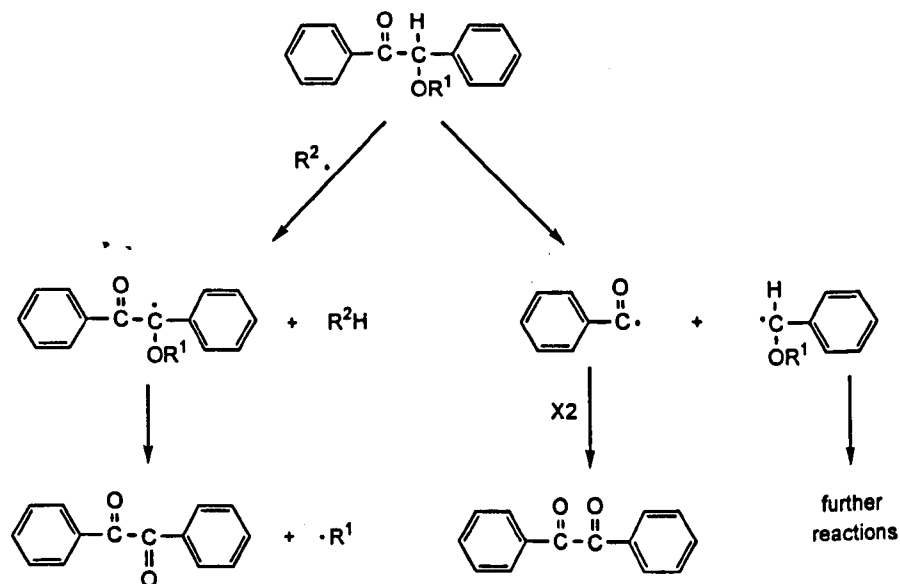


Figure 5.9 Possible routes to the formation of benzil from benzoin and benzoin ethers^{12,14,52}

Abstraction of labile benzylic hydrogens in benzoin ethers has also been reported to be involved in the formation of the alkyl benzoate byproducts via a hydroperoxide intermediate^{20,53} as shown in figure 5.10. However, as speculated for the production of benzil by benzylic hydrogen abstraction,

this is unlikely to be a major reaction pathway and could not realistically be involved in the formation of such large quantities of the alkyl benzoate, as has been observed here. It would appear to be more likely that the alkyl benzoate is formed from the substituted benzyl radical. Hagemann⁴⁷ also speculated that the methyl benzoate detected following the photolysis of benzoin methyl ether was formed by an undisclosed oxidation reaction of the α -methoxy benzyl radical. A possible reaction scheme for the formation of alkyl benzoate from a substituted benzyl radical is shown in figure 5.11.

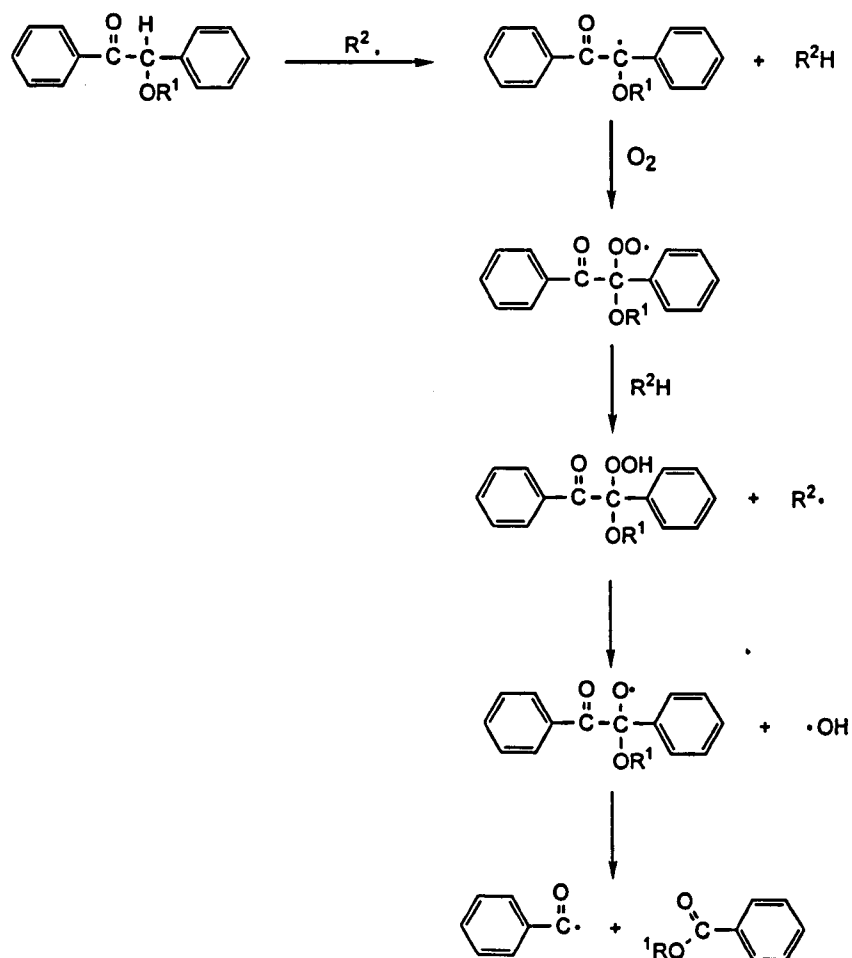


Figure 5.10 *Reported mechanism of formation of alkyl benzoate from benzoin alkyl ethers^{20,53}*

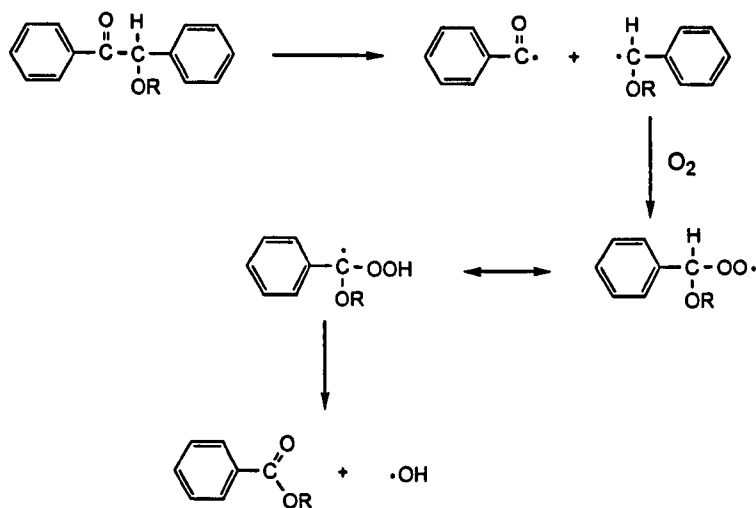
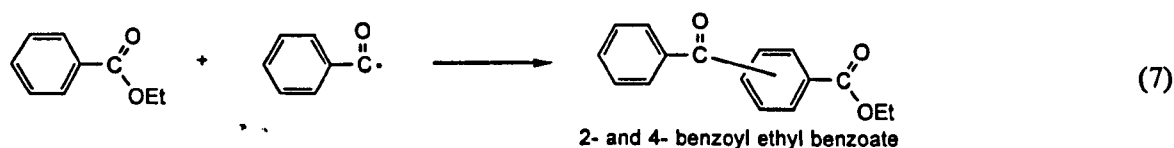


Figure 5.11 *Speculated mechanism of formation of alkyl benzoate from the substituted benzyl radical generated by benzoin alkyl ethers*

The mass spectrum of the large chromatogram peak at retention time 16.42 minutes in figure 5.7 was shown to contain the ions m/z 135, 107 and 77, indicating that it is a byproduct of the α -ethoxy benzyl radical. However, despite a molecular weight assignment of 224, based on a strong protonated molecular ion at m/z 225 in the CI spectrum, the structure could not be identified positively.

The occurrence of benzoin benzoate as a byproduct of benzoin ethyl ether serves to show that this material is a byproduct associated with the benzoyl radical itself, as previously speculated, and is possibly formed by the reaction of benzil with an additional benzoyl radical.

The occurrence of the 2 and 4 substituted forms of benzoyl ethyl benzoate is speculated to be a consequence of the reaction between ethyl benzoate and a primary benzoyl radical (7).



A number of other commercial benzoin alkyl ethers are available which are speculated to undergo similar reactions and processes to those found here for benzoin ethyl ether. e.g. benzoin isopropyl ether (Daitocure IP) and benzoin butyl ethers (Esacure EB3).

5.2.1.2 Hydroxyalkyl phenone type photoinitiators

1-Phenyl-2-hydroxy-2-methyl propan-1-one (Darocure 1173)

Figure 5.12 shows the GC chromatograms of an unirradiated and irradiated solution of the photoinitiator 1-phenyl-2-hydroxy-2-methyl propan-1-one (Darocure 1173) in dichloromethane. The chromatogram peaks 1-7 identified each have an associated mass spectrum. These and supporting GC-CI-MS data from experiments in methanol solution have been interpreted, with the results given in figure 5.13.

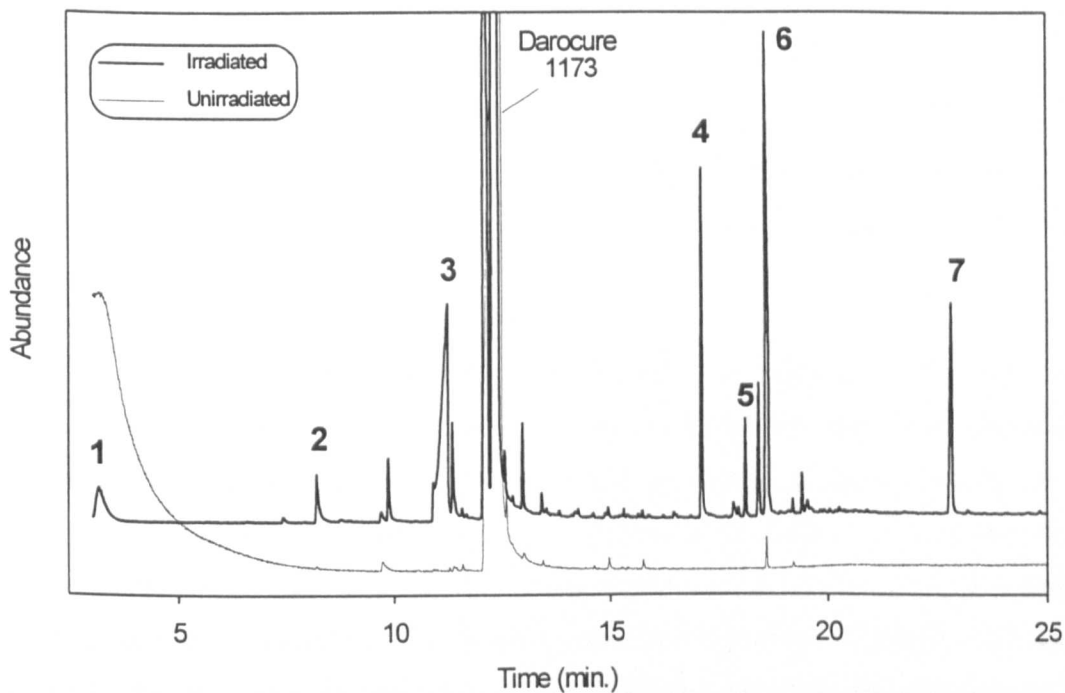


Figure 5.12 GC chromatograms of Darocure 1173 solution before and after irradiation in dichloromethane

- Peak 1** Benzene Retention time and mass spectrum as found for photolysis of benzoin
- Peak 2** Benzaldehyde Retention time and mass spectrum as found for photolysis of benzoin
- Peak 3** Benzoic acid Retention time and mass spectrum as found for photolysis of benzoin
- Peak 4** Benzil Retention time and mass spectrum as found for photolysis of benzoin ethyl ether

Peak 5

Benzoyl butyrophenone

Retention time (min.)	m/z	I	Identity
18.11	252	4	M.+
	209	0.3	M.+ -C ₃ H ₇
	105	100	PhCO+
	77	32	Ph+

Peak 6

2,2-Dibenzoyl propane

Retention time (min.)	m/z	I	Identity
18.62	252	30	M.+
	105	100	PhCO+
	77	82	Ph+

- Peak 7** Benzoin benzoate Retention time and mass spectra as found for photolysis of benzoin

Figure 5.13 Photolysis products of Darocure 1173 by GC-MS

Note that the high baseline in the GC chromatogram for the unexposed Darocure 1173 and in various other experiments throughout this chapter is a consequence of an intermittent air leak in the GC-MS transfer line which is self-sealing as the oven temperature rises and the sealing ferrule expands. Also, the material which elutes just before Darocure 1173 in the chromatogram is the impurity 2-hydroxy-2-methyl-2-phenyl acetic acid, identified by a search against a large commercial mass spectral library.

Previous literature⁵² has indicated that Darocure 1173 reacts via a Norrish Type I, α -cleavage mechanism. However, the results in figures 5.12 and 5.13 suggest that when irradiated in dichloromethane cleavage occurs in both the α and β positions, giving the byproducts 2,2-dibenzoyl propane and benzoyl butyrophenone in significant quantities. The observation of benzene, benzaldehyde, benzoic acid, benzil and benzoin benzoate confirms that a significant amount of α -cleavage is occurring. These processes are represented in figure 5.14 but are complicated by the observation that both 2,2-dibenzoyl propane and benzoyl butyrophenone were not observed as byproducts when the experiment was repeated using methanol as the solvent (GC-MS experiment). Although it is well known that solvent polarity can cause both a shift in the absorbance wavelength and inversion of the lowest excited states⁵⁸, no published work could be found that described a change in the solvent type leading to a change in reaction mechanism.

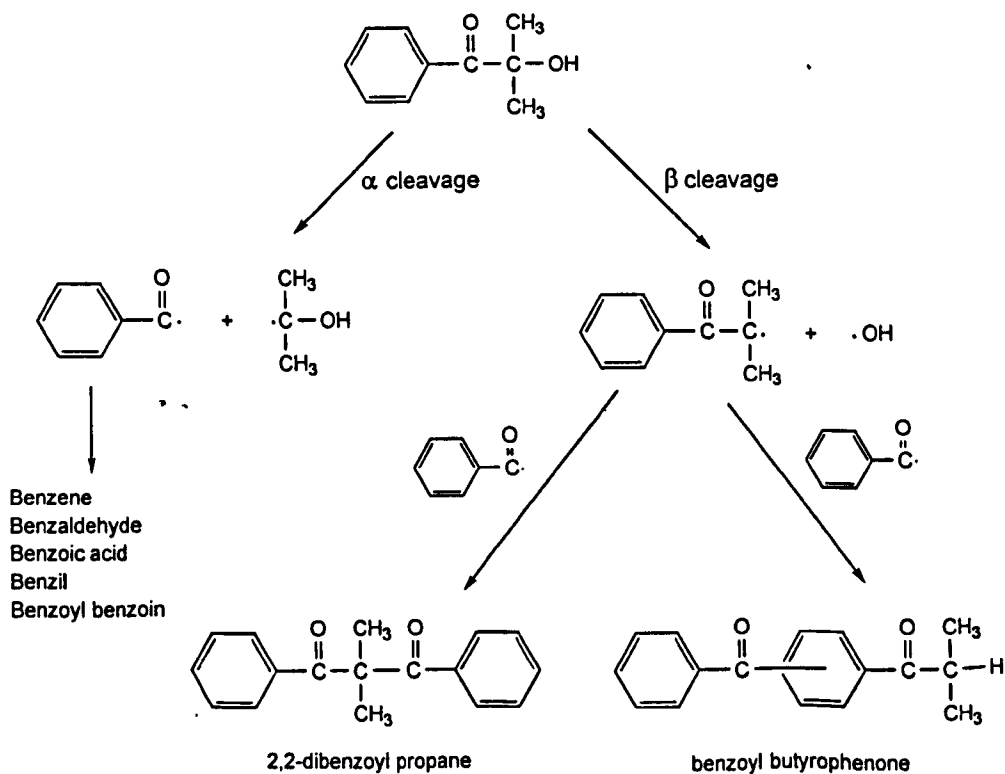
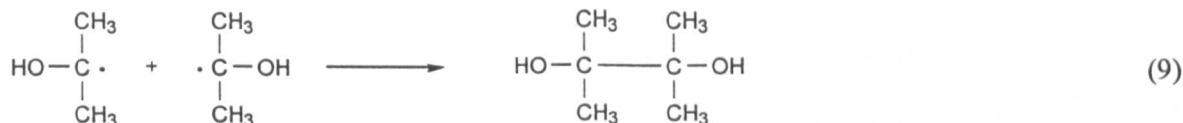
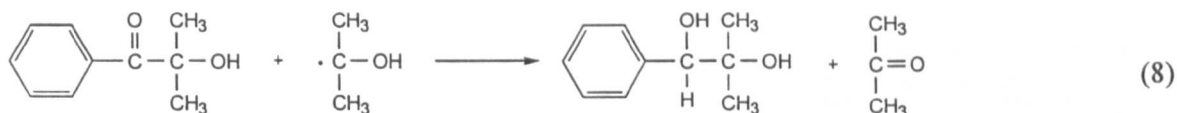


Figure 5.14 α and β -cleavage photolysis products of Darocure 1173

It has been claimed⁵² that the aliphatic ketyl radical produced by the α -cleavage reaction abstracts a hydrogen atom to give acetone; this was not observed in these experiments although it would coelute with the reaction solvent. It was also claimed⁵² that this ketyl radical both reduces the starting material (8) and undergoes dimerisation to give a pinacol product (9), no evidence for either of these processes was observed in these experiments.



Other structurally similar photoinitiator molecules include the p-isopropyl and p-(2-hydroxyethoxy) derivatives of Darocure 1173 (Darocure 1116 and Darocure 2959 respectively). Both these and the oligomeric equivalent of Darocure 1173 (Esacure KIP) are expected to show similar reactions and processes, although the para substitution will clearly prevent the formation of the p-substituted analogues of 4-benzoyl butyrophenone and benzoyl benzoil.

1-Hydroxycyclohexyl acetophenone (Irgacure 184)

Figure 5.15 shows the GC chromatograms of an unirradiated and irradiated solution of the photoinitiator 1-hydroxycyclohexyl acetophenone (Irgacure 184) in dichloromethane. The chromatogram peaks 1-7 each have an associated mass spectrum. These and supporting GC-MS data from experiments in methanol have been interpreted, with the results given in figure 5.16.

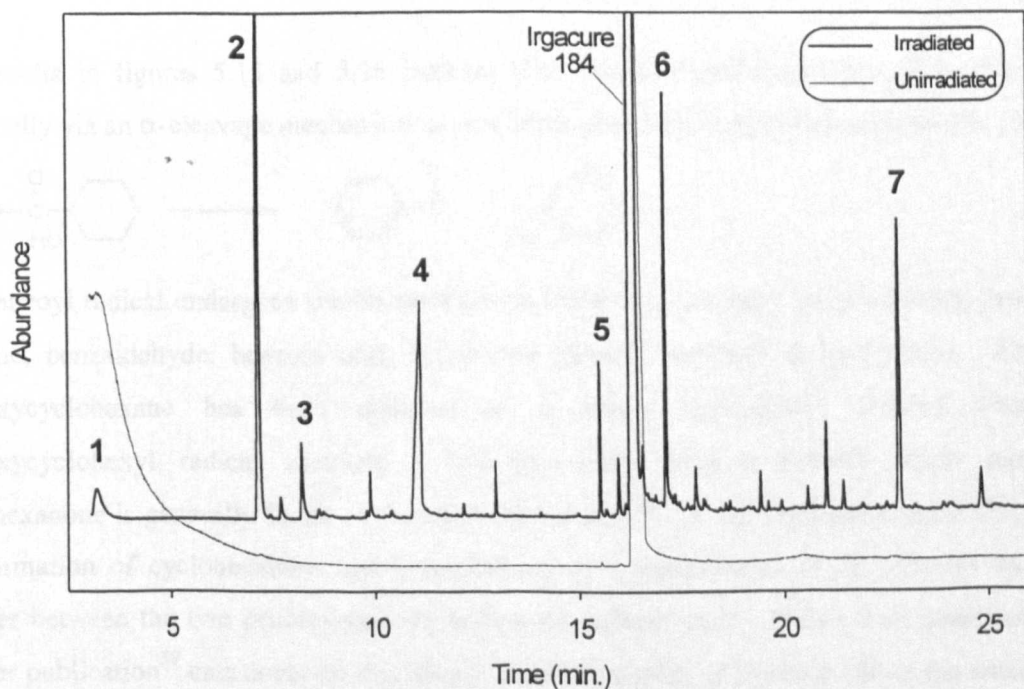
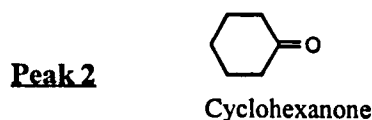

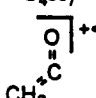


Figure 5.15 GC chromatograms of Irgacure 184 solution before and after irradiation in dichloromethane

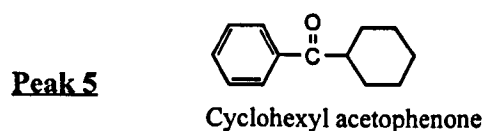
Peak 1 Benzene Retention time and mass spectrum as found for photolysis of benzoin



Retention time (min.)	m/z	I	Identity
7.16	98	44	M.+
	70	2	
	55	88	C ₄ H ₇ +.
	42	100	

Peak 3 Benzaldehyde Retention time and mass spectrum as found for photolysis of benzoin

Peak 4 Benzoic acid Retention time and mass spectrum as found for photolysis of benzoin



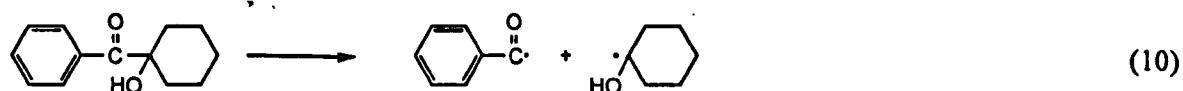
Retention time (min.)	m/z	I	Identity
15.50	188	28	M.+
	105	100	PhCO+
	77	30	Ph+

Peak 6 Benzil Retention time and mass spectrum as found for photolysis of benzoin ethyl ether

Peak 7 Benzoin benzoate Retention time and mass spectrum as found for photolysis of benzoin

Figure 5.16 *Photolysis products of Irgacure 184 by GC-MS*

The results in figures 5.15 and 5.16 indicate that 1-hydroxycyclohexyl phenyl ketone reacts principally via an α -cleavage mechanism to give benzoyl and hydroxycyclohexyl radicals (10).



The benzoyl radical undergoes similar reactions to those seen for other photoinitiators, producing benzene, benzaldehyde, benzoic acid, benzil and benzoin benzoate as byproducts. Although hydroxycyclohexane has been reported as a minor byproduct¹⁴, formed when the hydroxycyclohexyl radical abstracts a hydrogen atom from a suitable donor molecule, cyclohexanone is generally found as the main byproduct^{14,28}. It has been claimed by Phan¹⁴ that the formation of cyclohexanone and benzaldehyde is a consequence of an efficient hydrogen transfer between the two primary radicals within the solvent cage. Phan's own observations in another publication⁵⁹ cast doubt on this theory, since irradiation of Irgacure 184 in the presence of monomer produced no observable cyclohexanone, with initiation speculated to be via the

hydroxycyclohexyl radical. However, if cyclohexanone formation was an in-cage process it would be a major product regardless of the presence or absence of reactive monomer. Also, if the photoinitiator was so inefficient as to produce high levels of non-reacting byproducts within the solvent cage in a low viscosity solvent medium¹⁴, its ability to produce significant quantities of initiating radicals in a high viscosity coating formulation could be expected to be very poor. This is clearly not the case, with Irgacure 184 being a widely used and highly reactive photoinitiator. As such it is speculated that the cyclohexanone is produced by a rearrangement reaction outside the solvent cage, either before or after abstraction of a hydrogen atom from a donor molecule.

As with Darocure 1173, a β -cleavage reaction is occurring to some extent in dichloromethane solution, indicated by the presence of the byproduct cyclohexyl acetophenone, but the reaction is exclusively via an α -cleavage mechanism in methanol solution (GC-CI-MS experiment).

5.2.1.3 Benzil ketal type photoinitiators

Benzil dimethyl ketal (Irgacure 651)

Figure 5.17 shows the GC chromatograms of an unirradiated and irradiated solution of the photoinitiator benzil dimethyl ketal (Irgacure 651) in dichloromethane. The chromatogram peaks 1-11 each have an associated mass spectrum. These and supporting GC-CI-MS data from experiments in methanol solution have been interpreted, with the results given in figure 5.18.

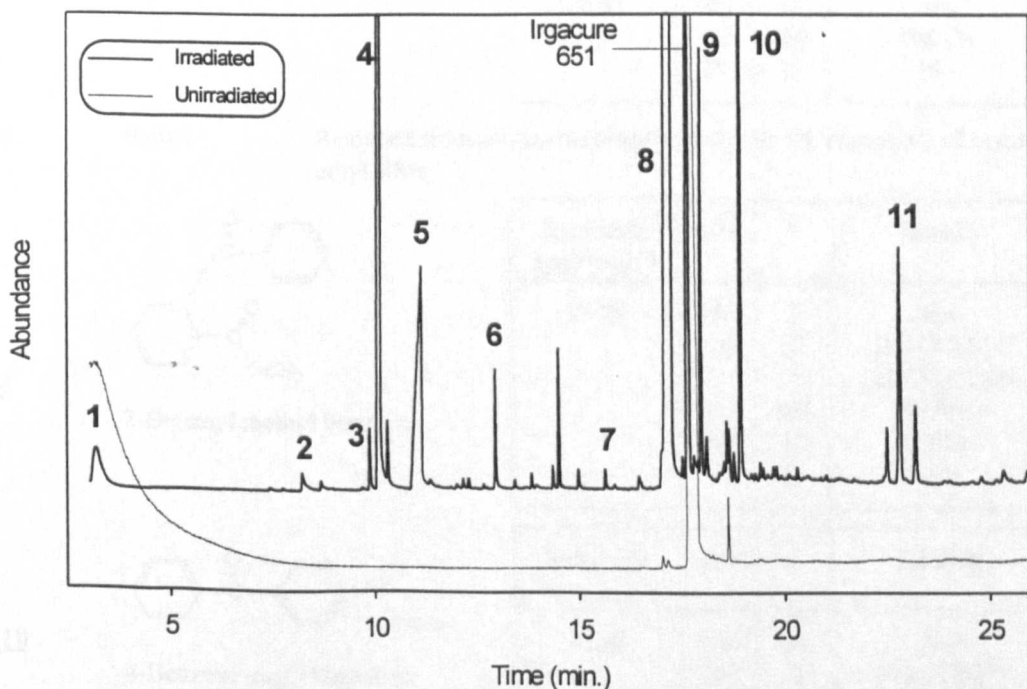
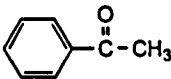


Figure 5.17 GC chromatogram of benzil dimethyl ketal solution before and after irradiation in dichloromethane

Peak 1 Benzene Retention time and mass spectrum as found for photolysis of benzoin
Peak 2 Benzaldehyde Retention time and mass spectrum as found for photolysis of benzoin

Peak 3

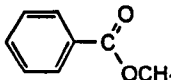


Acetophenone

CI spectrum

Retention time (min.)	m/z	I	Identity
9.8	121	100	M.+ (protonated) PhCO+
	105	7	

Peak 4

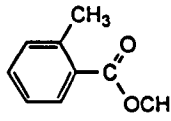


Methyl benzoate

Retention time (min.)	m/z	I	Identity
10.14	136	33	M.+ PhCO+ Ph+
	105	100	
	77	70	

Peak 5 Benzoic acid Retention time and mass spectrum as found for photolysis of benzoin

Peak 6

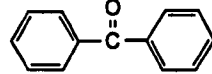


Methyl anisoate

CI spectrum

Retention time (min.)	m/z	I	Identity
12.96	151	100	M.+ (protonated) [M-OCH ₃] ⁺ [M-CO ₂ CH ₃] ⁺
	119	45	
	91	11	

Peak 7

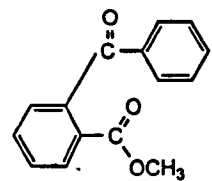


Benzophenone

Retention time (min.)	m/z	I	Identity
15.65	182	43	M.+ PhCO+ Ph+
	105	100	
	77	51	

Peak 8 Benzil Retention time and mass spectrum as found for photolysis of benzoin ethyl ether

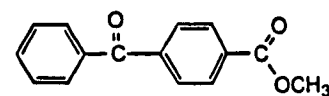
Peak 9



2-Benzoyl methyl benzoate

Retention time (min.)	m/z	I	Identity
17.98	240	3	M.+ [M-OCH ₃] ⁺ [M-CO ₂ CH ₃] ⁺ [M-Ph] ⁺ PhCO+ Ph+
	209	22	
	181	7	
	163	100	
	105	52	
	77	48	

Peak 10



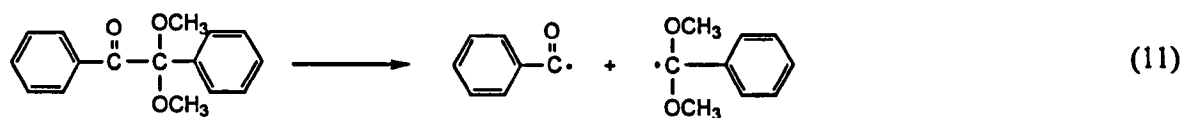
4-Benzoyl methyl benzoate

Retention time (min.)	m/z	I	Identity
18.93	240	56	M.+ [M-OCH ₃] ⁺ [M-CO ₂ CH ₃] ⁺ [M-Ph] ⁺ PhCO+ Ph+
	209	2	
	181	21	
	163	64	
	105	100	
	77	52	

Peak 11 Benzoyl benzoin Retention time and mass spectrum as found for photolysis of benzoin

Figure 5.18 Photolysis products of benzil dimethyl ketal by GC-MS

The photoinitiator benzil dimethyl ketal (Irgacure 651) has been well studied over the last 20 years, mostly because of its interesting secondary fragmentation reaction. The results shown in figures 5.17 and 5.18 largely support reported data, with fragmentation occurring exclusively by an α -cleavage mechanism to produce a benzoyl and a dimethoxy benzyl radical (11).



The benzoyl radical was seen to undergo its characteristic reactions, giving benzene, benzaldehyde, benzoic acid, benzil and benzoin benzoate as byproducts.

The dimethoxybenzyl radical has been widely reported^{13,14,16} to undergo a secondary fragmentation reaction to give methyl benzoate and a methyl radical as shown in figure 5.19. More recently this has been shown⁴⁶ to be via either a fast photochemical reaction following the absorption of a second photon, or a slow thermal fragmentation which occurs at room temperature. Methyl benzoate was also observed in high yield in the experiments reported here.

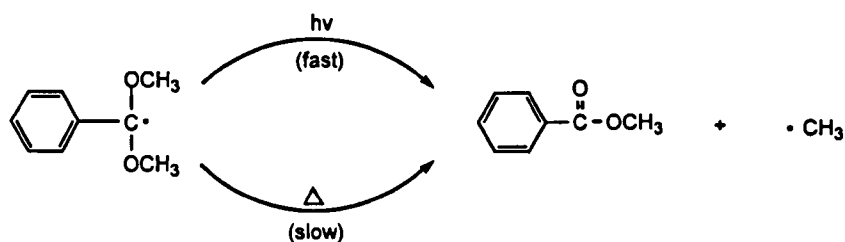
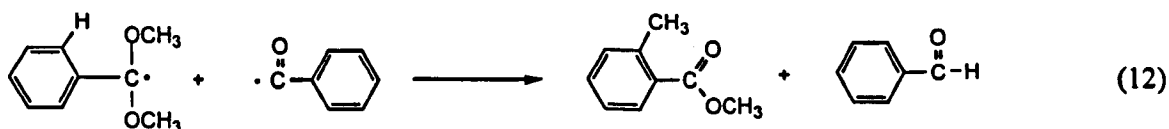


Figure 5.19 Secondary fragmentation reaction of the benzil dimethyl ketal derived dimethoxybenzyl radical⁴⁶

Other previously reported reaction products formed by radical-radical termination reactions and observed at low level in these experiments include acetophenone^{2,14,17} (structure assigned by CI mass spectrum only) and benzophenone¹², the latter involving the phenyl radical produced following the oxygen quenching of the primary benzoyl radical¹⁴. Methyl anisoate was also detected at low level (structure assigned by CI mass spectrum only) and has been speculated by McGinniss¹⁷ to be formed by a reaction between the benzoyl and dimethoxybenzyl primary radicals (12).



2-Benzoyl methyl benzoate and 4-benzoyl methyl benzoate were observed in these experiments in significant quantities, the 4-isomer being slightly more abundant. These byproducts have been observed by other workers^{12,13} and have been reported to be formed via the mechanism shown in figure 5.20. The two semibenzene intermediates have also been reportedly isolated^{17,22}, but these have easily abstractable hydrogen atoms and are readily converted to the benzoyl methyl benzoate esters.

Methane has also been reported as a byproduct by Fischer et al.¹³ following hydrogen abstraction by the methyl radical. Whilst this is a possibility in a non-reactive system, it is unlikely to be formed in a system containing acrylate double bonds because of the methyl radical's high reactivity. Methane was not detected in the experiments reported here since in the unlikely event it had not evaporated prior to the GC analysis it would coelute with the solvent.

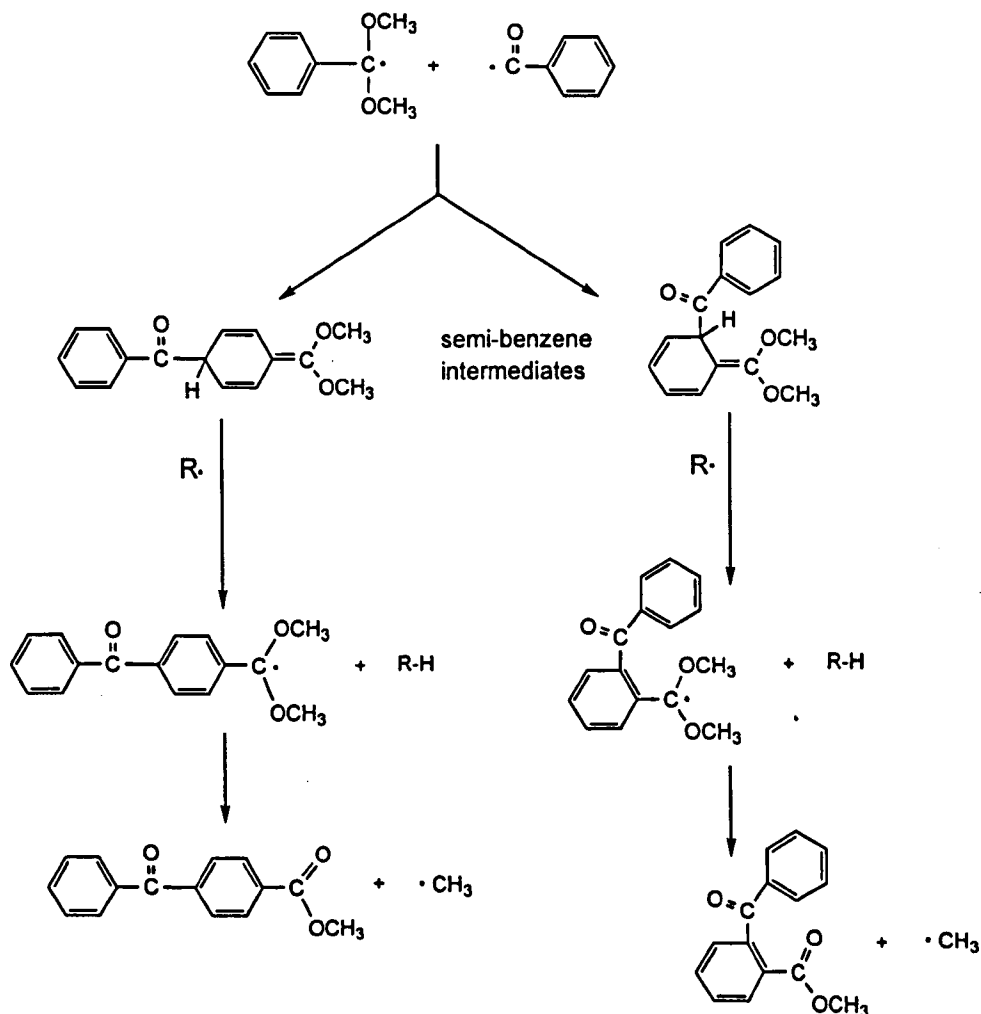


Figure 5.20 *The formation of 2 and 4-benzoyl methyl benzoate esters from benzil dimethyl ketal by recombination of the two primary radicals*

5.2.1.4 Acylphosphine oxide type photoinitiators

2,4,6-Trimethylbenzoyl diphenyl phosphine oxide (Lucerin TPO)

Figure 5.21 shows the GC chromatograms of an unirradiated and irradiated solution of the photoinitiator 2,4,6-trimethylbenzoyl diphenyl phosphine oxide (Lucerin TPO) in methanol. The chromatogram peaks 1-7 each have an associated mass spectrum. These and supporting GC-MS data from experiments in methanol solution have been interpreted, with the results given in figure 5.22.

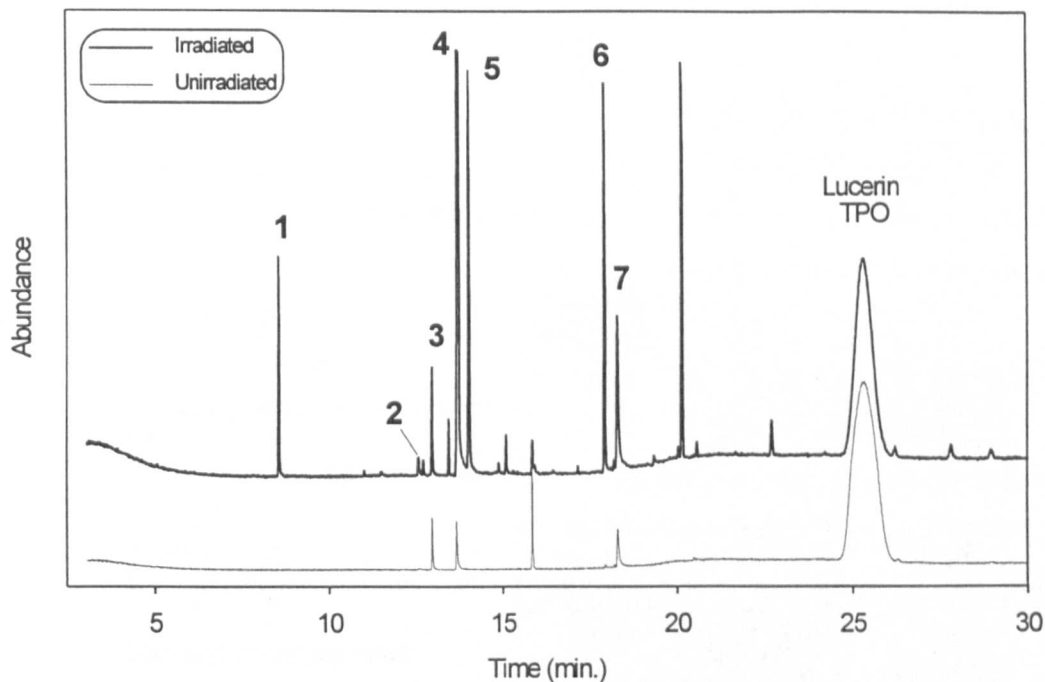


Figure 5.21 GC chromatograms of Lucerin TPO solution before and after irradiation in methanol

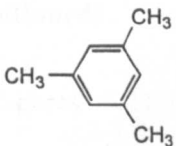
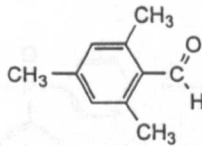
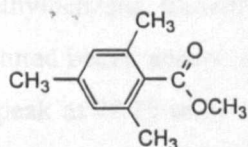
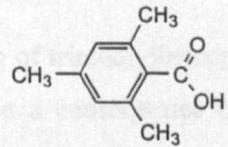
<p>Peak 1</p>  <p>2,4,6-Trimethyl benzene</p>	Retention time (min.)	m/z	I	Identity
	8.56	120 105	48 100	M.+ [M-CH ₃] ⁺
<p>Peak 2</p>  <p>2,4,6-Trimethyl benzaldehyde</p>	Retention time (min.)	m/z	I	Identity
	12.57	148 147 119	74 100 44	M.+ [M-H] ⁺ [M-CHO] ⁺
<p>Peak 3</p>  <p>2,4,6-Trimethyl benzoic acid methyl ester</p>	Retention time (min.)	m/z	I	Identity
	12.97	178 163 147 146 119	52 7 100 90 31	M.+ [M-CH ₃] ⁺ [M-OCH ₃] ⁺ [M-MeOH] ⁺ [M-CO ₂ CH ₃] ⁺
<p>Peak 4</p>  <p>2,4,6-Trimethyl benzoic acid</p>	Retention time (min.)	m/z	I	Identity
	13.73	164 147 146 119	62 28 100 29	M.+ [M-OH] ⁺ [M-H ₂ O] ⁺ [M-CO ₂ H] ⁺

Figure 5.22 Photolysis products of Lucerin TPO by GC-MS

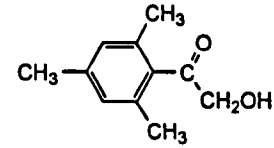
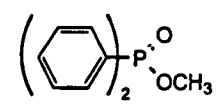
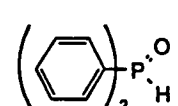
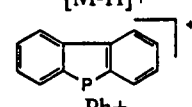
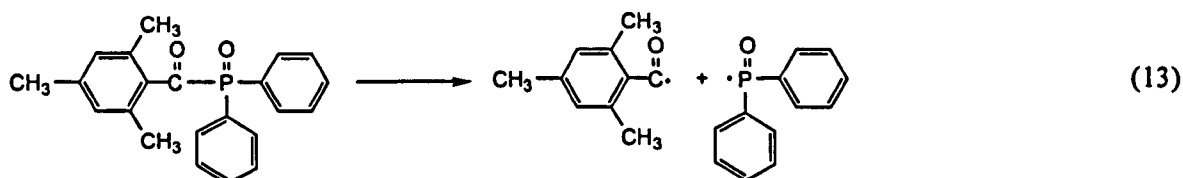
Peak 5	 2,4,6-Trimethyl benzoyl methanol CI spectrum	Retention time (min.)	m/z	I	Identity
		14.04	179 161 147	88 100 32	M.+ (protonated) [M-OH] ⁺ [M-CH ₂ OH] ⁺
Peak 6	 Diphenyl phosphinic acid methyl ester CI spectrum	Retention time (min.)	m/z	I	Identity
		17.93	233 201 155	100 100 32	M.+ (protonated) [M-OCH ₃] ⁺ [M-Ph] ⁺
Peak 7	 Diphenyl phosphine oxide	Retention time (min.)	m/z	I	Identity
		18.29	202 201 183 77	38 100 16 20	M.+ [M-H] ⁺  Ph ⁺

Figure 5.22 (continued) *Photolysis products of Lucerin TPO by GC-MS*

The data in figures 5.21 and 5.22 shows that, as has previously been reported^{37,60}, 2,4,6-trimethylbenzoyl diphenylphosphine oxide undergoes an α -cleavage reaction to yield a trimethylbenzoyl and a phosphonyl radical (13).



The trimethylbenzoyl radical undergoes similar processes to the unsubstituted benzoyl radical, producing trimethylbenzene, trimethylbenzaldehyde and trimethylbenzoic acid as byproducts. The trimethyl substituted benzil analog was not identified positively, although it is suspected to be the chromatogram peak at 20.15 minutes, which even under CI conditions contains largely only the m/z 147 ion corresponding to the trimethylbenzoyl fragment. The presence of the m/z 147 ion in both the EI and CI spectra of this material confirms that it is not the molecular ion, but insufficient data is available to confirm the assignment.

The observation of trimethylbenzoic acid and diphenylphosphine oxide in the unirradiated sample is thought to be a consequence of some reaction taking place under artificial laboratory light during the weighing procedure.

Although not positively identified in this work, the primary phosphonyl radical has been reported to yield diphenylphosphinic acid as the major byproduct^{12,61}, with Baxter et. al.¹² also reporting

methyldiphenylphosphinate and methyldiphenylphosphine oxide as products formed by an unknown mechanism. In the experiments reported here, methyldiphenylphosphine oxide was also identified when methanol was used as an irradiation solvent but not when dichloromethane was used. This suggests that a reaction has taken place between the methanol solvent and either the phosphonyl radical or one of its principal byproducts. This speculation is not unreasonable when the reported sensitivity of the carbon-phosphorus bond to solvolytic cleavage by nucleophilic compounds such as water, alcohols or amines is considered⁶². Supporting evidence is also provided by Baxter's analysis procedure which involves the use of methanol as a solvent in the preparation of samples for HPLC analysis¹², suggesting that the methanol reacts with one of the principal photoinitiator byproducts rather than the primary phosphonyl radical. Additional reactions of the methanol solvent occurred in these experiments, generating 2,4,6-trimethylbenzoic acid methyl ester and 2,4,6-trimethylbenzoyl methanol. Neither of these byproducts was observed when dichloromethane was used as the irradiating solvent.

Bis-(2,6-dimethoxybenzoyl)-2,4,4-trimethylpentyl phosphine oxide (BDTPO)

Bis-(2,6-dimethoxybenzoyl)-2,4,4-trimethylpentyl phosphine oxide (BDTPO) is a new photoinitiator marketed by Ciba-Geigy under the trade name Irgacure 1700 as a 1:3 blend with Darocure 1173. Figure 5.23 shows the GC chromatogram of an irradiated solution of BDTPO (no Darocure 1173) in methanol, which shows only the photolysis products detected, since BDTPO itself is too involatile to pass through the non-polar GC capillary column used. The chromatogram peaks 1-4 each have an associated mass spectrum which have been interpreted and the results shown in figure 5.24. Note that this photoinitiator was analysed using GC-CI-MS only.

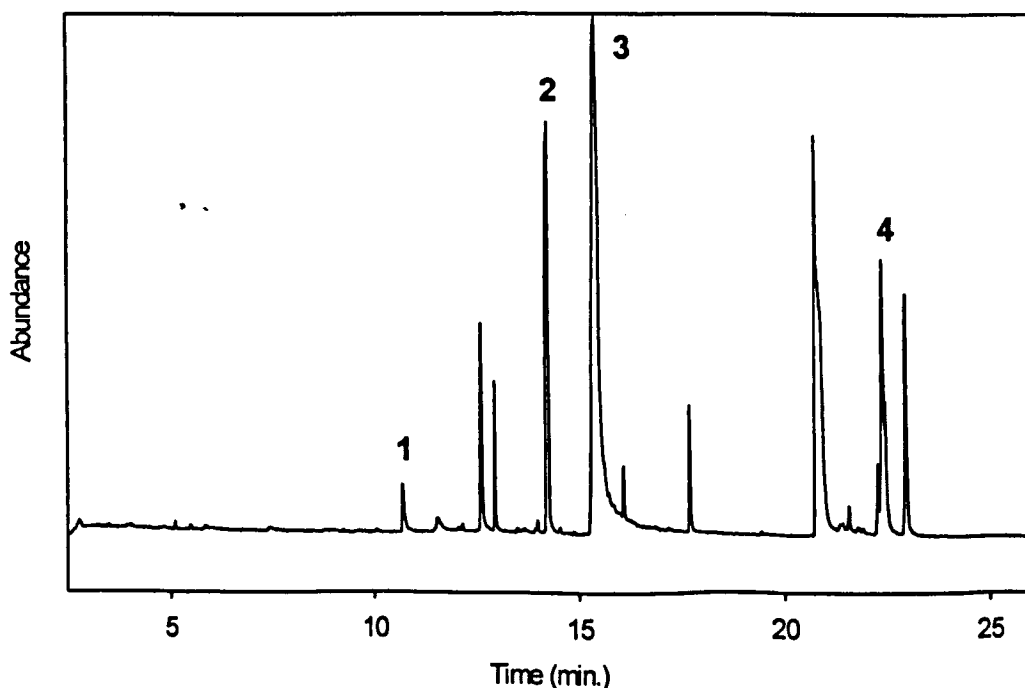


Figure 5.23 *GC chromatogram of Bis-(2,6-dimethoxybenzoyl)-2,4,4-trimethylpentyl phosphine oxide (BDTPO) after irradiation in methanol*

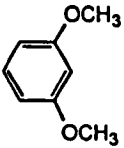
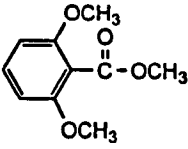
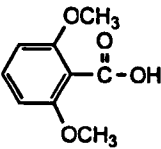
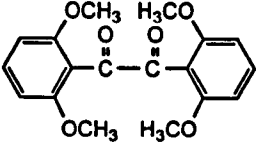
Peak 1	 2,6-Dimethoxy benzene	Retention time (min.)	m/z	I	Identity
		10.71	139	100	M.+ (protonated)
Peak 2	 2,6-Dimethoxy benzoic acid methyl ester	Retention time (min.)	m/z	I	Identity
		14.24	197 167 165	26 66 100	M.+ (protonated) unknown [M-OCH ₃] ⁺
Peak 3	 2,6-Dimethoxy benzoic acid	Retention time (min.)	m/z	I	Identity
		15.4	183 165	57 100	M.+ (protonated) [M-OH] ⁺
Peak 4	 2,2',6,6'-Tetramethoxy benzil	Retention time (min.)	m/z	I	Identity
		22.38	331 165	22 100	M.+ (protonated) Ph(OCH ₃) ₂ CO +

Figure 5.24 Photolysis products by GC-CI-MS of Bis-(2,6-dimethoxybenzoyl)-2,4,4-trimethylpentyl phosphine oxide (BDTPO)

Few literature references are available concerning the photoinitiator BDTPO, although CIDNP experiments have led to the suggestion that the molecule fragments to produce a total of 4 initiating radicals⁶³ (two substituted benzoyl radicals and a phosphorus centered diradical). Experiments as part of this work have shown that an α -cleavage reaction takes place giving 2,6-dimethoxy benzene, 2,6-dimethoxy benzoic acid and 2,2',6,6'-tetramethoxy benzil as byproducts.

As with the photoinitiator 2,4,6-trimethylbenzoyl diphenylphosphine oxide (Lucerin TPO) it is speculated that the formation of 2,6-dimethoxy benzoic acid methyl ester is a consequence of a reaction of the primary substituted benzoyl radical with the methanol irradiating solvent.

A number of other significant byproducts were formed as a result of irradiating BDTPO, however GC-CI-MS data alone provided insufficient fragmentation detail to allow their identification.

Another commercially available acylphosphine type photoinitiator is 2,4,6-trimethylbenzoyl phenylphosphinic acid ethyl ester (Lucerin LR8893X or TEPO). This is structurally similar to Lucerin TPO and would therefore be reasonably expected to react in a similar way.

5.2.1.5 α -Aminoalkylphenone type photoinitiators

2-Methyl-1-[4-(methylthio)phenyl]-2-morpholino propan-2-one (Irgacure 907)

Figure 5.25 shows the GC chromatograms of an unirradiated and irradiated dichloromethane solution of the photoinitiator 2-methyl-1-[4-(methylthio)phenyl]-2-morpholino propan-2-one (Irgacure 907). The chromatogram peaks 1-8 each have an associated mass spectrum. These and supporting GC-CI-MS data from experiments in methanol solution have been interpreted with the results given in figure 5.26.

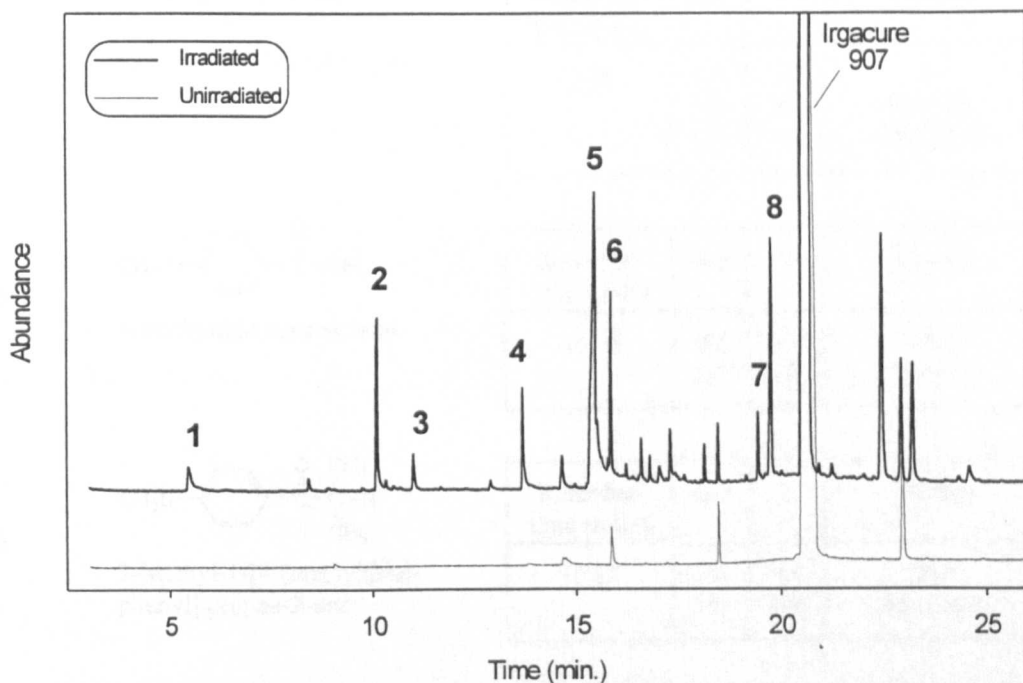
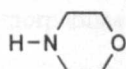


Figure 5.25 GC chromatograms of Irgacure 907 solution before and after irradiation in dichloromethane

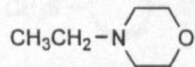
Peak 1



Morpholine

Retention time (min.)	m/z	I	Identity
5.46	87	76	M.+
	86	39	[M-H]+
	57	100	[M-CH ₂ O]+

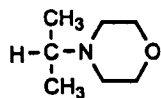
Peak 2



N-ethyl morpholine

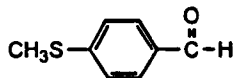
Retention time (min.)	m/z	I	Identity
10.11	115	100	M.+
	100	73	[M-CH ₃]+
	86	42	[M-C ₂ H ₅]+
	57	76	unknown
	29	89	C ₂ H ₅ +

Figure 5.26 Photolysis products of Irgacure 907 by GC-MS

Peak 3

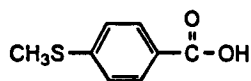
N-isopropyl morpholine

Retention time (min.)	m/z	I	Identity
11.01	129	67	M.+
	114	49	[M-CH ₃]+
	86	73	[M-C ₃ H ₇]+
	57	100	unknown
	43	84	C ₃ H ₇ +

Peak 4

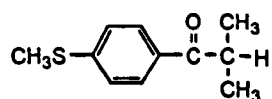
4-Methylthio benzaldehyde

Retention time (min.)	m/z	I	Identity
13.69	152	100	M.+
	151	90	[M-H]+
	123	11	[M-CHO]+

Peak 5

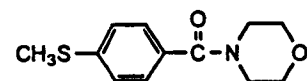
4-Methylthio benzoic acid

Retention time (min.)	m/z	I	Identity
15.45	168	100	M.+
	151	44	[M-OH]+

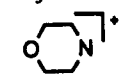
Peak 6

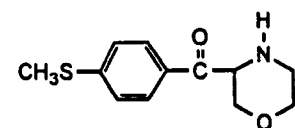
2-Methyl-1-[4-(methylthio)phenyl] propan-2-one

Retention time (min.)	m/z	I	Identity
15.85	194	15	M.+
	151	100	[M-C ₃ H ₇]+

Peak 7

N-[4-(methylthio)benzoyl] morpholine

Retention time (min.)	m/z	I	Identity
19.44	237	16	M.+
	151	100	CH ₃ SPhCO +
	86	69	 +
	58	39	unknown

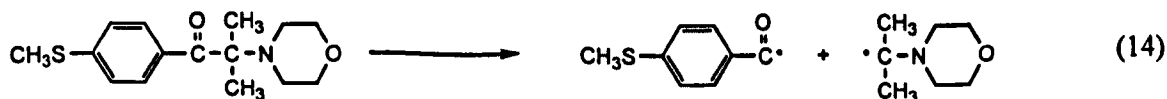
Peak 8

2-[4-(methylthio)benzoyl] morpholine

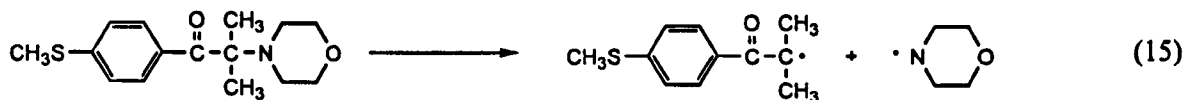
Retention time (min.)	m/z	I	Identity
19.75	237	18	M.+
	236	16	[M-H]+
	151	100	CH ₃ SPhCO +

Figure 5.26 (continued)*Photolysis products of Irgacure 907 by GC-MS*

The photoinitiator Irgacure 907 has been well studied in the literature and found by techniques such as CIDNP^{42,43,64} and radical trapping^{65,66} to operate via an α -cleavage mechanism, generating a methylthio substituted benzoyl radical and an aminoalkyl radical (14).



In the experiments reported here, the observation of 4-methylthio benzaldehyde and N-isopropyl morpholine largely confirms this mechanism, although observation of the byproducts morpholine and 2-methyl-1-[4-(methylthio)phenyl] propan-2-one suggests that a β -cleavage mechanism may be important (15). The byproducts morpholine and 2-methyl-1-[4-(methylthio)phenyl] propan-2-one have also been observed by Leopold and Fischer⁴² and in a commercial coating formulation⁶⁷ following irradiation.



It has been suggested⁶⁸ that 2-methyl-1-[4-(methylthio)phenyl] propan-2-one and morpholine could be formed following the reduction of the photoinitiator triplet state by N-methyl diethanolamine, although in the experiment reported here an amine synergist was not present.

The substituted benzoyl radical undergoes some of the reactions observed for the benzoyl radical, producing 4-methylthio benzaldehyde and 4-methylthio benzoic acid as byproducts. 4-Methylthio benzene and 4,4'-methylthio benzil were not identified, although the latter has been previously reported⁶⁴.

The presence of such large quantities of N-ethyl morpholine cannot be explained in terms of a breakdown mechanism of Irgacure 907. However, although not reported in detail here N-ethyl morpholine was also observed as a major byproduct of the photoinitiator 3,6-bis-(2-morpholinoisobutyroyl) N-octyl carbazole (Radstart N1414) which is structurally similar to Irgacure 907.

N-[4-(methylthio)benzoyl] morpholine and 2-[4-(methylthio)benzoyl] morpholine were also detected in this work and are speculated to result from the termination reactions of the substituted benzoyl radical and the morpholine radical, produced by the α and β -cleavage reactions respectively.

2-Benzyl-2-dimethylamino-1-(4-morpholinophenyl) butan-1-one (Irgacure 369)

Figure 5.27 shows the GC chromatograms of an unirradiated and irradiated solution of the photoinitiator 2-benzyl-2-dimethylamino-1-(4-morpholinophenyl) butan-1-one (Irgacure 369). The photoinitiator was irradiated in toluene solution since it had only a limited solubility in methanol and appeared to be unstable in dichloromethane, giving rise to a number of GC peaks prior to irradiation. The precipitate formed following irradiation was redissolved by the addition of methanol. The chromatogram peaks 1-12 each have an associated mass spectrum. These and supporting GC-CI-MS data from experiments also in toluene solution have been interpreted with the results given in figure 5.28.

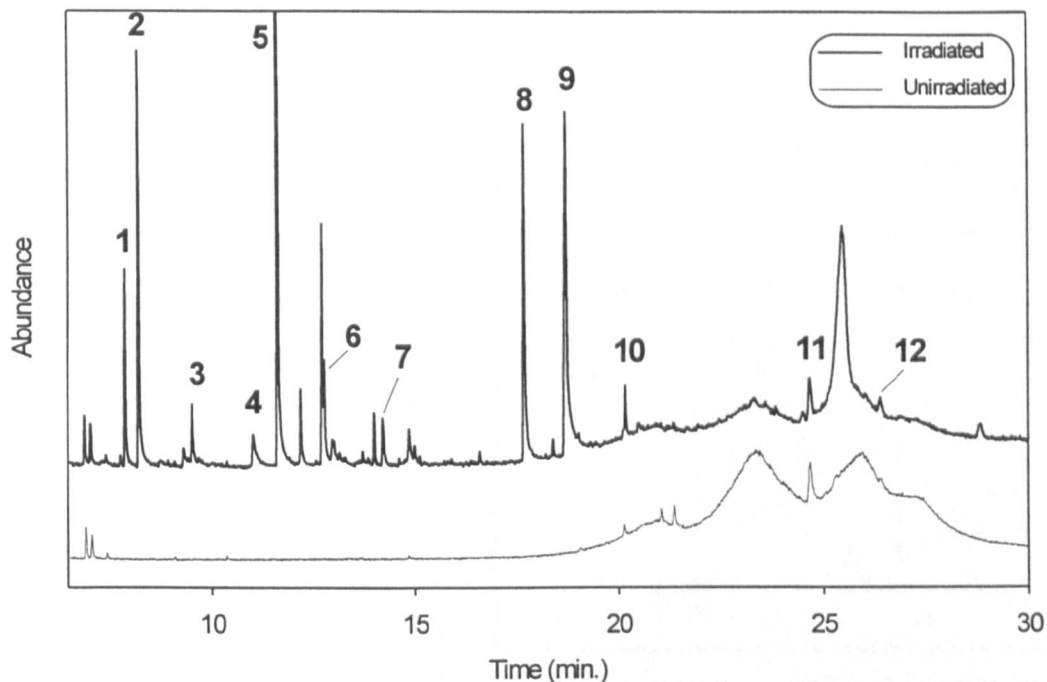
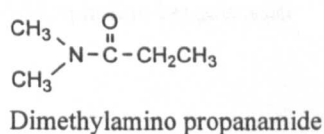


Figure 5.27 GC chromatograms of Irgacure 369 solution before and after irradiation in toluene

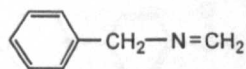
Peak 1



Retention time (min.)	m/z	I	Identity
7.89	101	100	M.+
	72	91	[M-Et] ⁺
	57	36	[M-N(CH ₃) ₂] ⁺
	44	67	N(CH ₃) ₂ ⁺

Peak 2

Benzaldehyde Retention time and mass spectrum as found for photolysis of benzoin



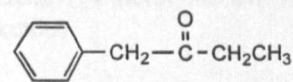
Peak 3

Formaldehyde benzyl imine

Retention time (min.)	m/z	I	Identity
9.511	119	49	M.+
	118	100	[M-H] ⁺
	91	19	PhCH ₂ ⁺
	77	19	Ph ⁺

Peak 4

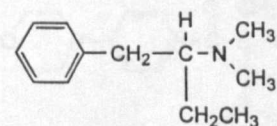
Benzoic acid Retention time and mass spectrum as found for photolysis of benzoin



Peak 5

1-Phenyl butan-1-one

Retention time (min.)	m/z	I	Identity
11.64	148	28	M.+
	91	88	PhCH ₂ ⁺
	57	100	CH ₃ CH ₂ C=O ⁺



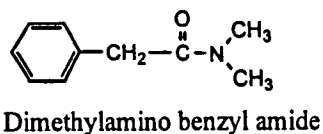
Peak 6

1-Phenyl 2-(N-dimethylamino) butane

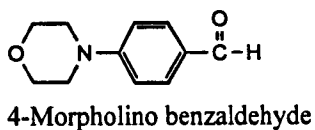
Retention time (min.)	m/z	I	Identity
12.77	178	60	M.+ (protonated)
	86	100	[M-PhCH ₂] ⁺

CI spectrum

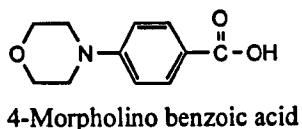
Figure 5.28 Photolysis products of Irgacure 369 by GC-MS in toluene

Peak 7

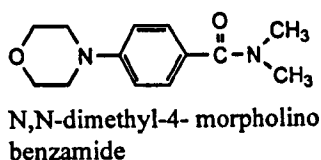
Retention time (min.)	m/z	I	Identity
14.21	163 91 72	30 15 100	M.+ PhCH ₂ + (CH ₃) ₂ NC=O+

Peak 8

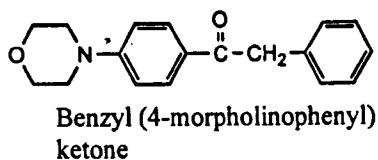
Retention time (min.)	m/z	I	Identity
17.69	191 133 132 105 77	94 100 82 5 19	M.+ [M-morpholine]+ Ph+

Peak 9

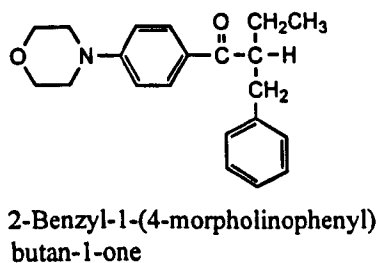
Retention time (min.)	m/z	I	Identity
18.70	207 190 149 132 121	68 4 100 13 5	M.+ [M-OH]+ [M-morpholine]+

Peak 10

Retention time (min.)	m/z	I	Identity
20.16	234 190	30 100	M.+ [M-N(CH ₃) ₂]+

Peak 11

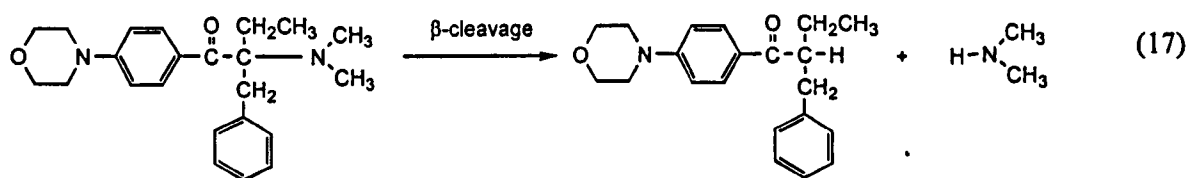
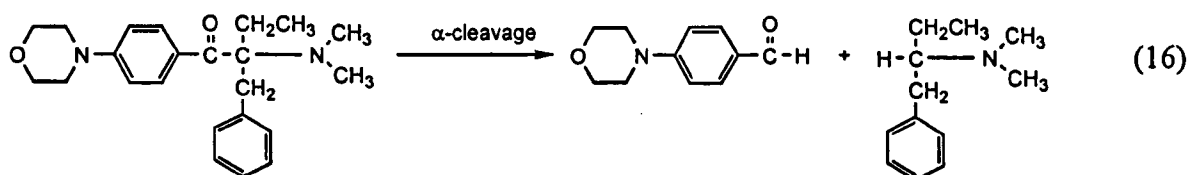
Retention time (min.)	m/z	I	Identity
24.66	281 190 132 91	19 100 7 11	M.+ [M-CH ₂ Ph]+ PhCH ₂ +

Peak 12

Retention time (min.)	m/z	I	Identity
25.64	324 282 190	100 76 28	M.+ (protonated) unknown

CI spectrum**Figure 5.28 (continued)***Photolysis products of Irgacure 369 by GC-MS*

Although the photoinitiator 2-benzyl-2-dimethylamino-1-(4-morpholinophenyl) butan-1-one (Irgacure 369) has not been widely studied, CIDNP, radical trapping and preparative photochemistry has been undertaken by Desobry et. al.⁴⁴, indicating that a cleavage reaction occurs in both the α and β -positions. In the results reported here α -cleavage was found to be the dominant mechanism, with cleavage followed by hydrogen abstraction giving rise to 4-morpholinobenzaldehyde and 1-phenyl 2-(N-dimethylamino)butane (16). Although β -cleavage could occur at one of three positions in the Irgacure 369 molecule, evidence was only found for cleavage at the C-N bond, since of the potential products following hydrogen abstraction, only 2-benzyl-1-(4-morpholinophenyl)butan-1-one was identified (17). Cleavage at the C-N bond would also be expected to give rise to dimethylamine (17), but this would have a retention time too short to be detected by this GC method.



The precipitate formed during irradiation was identified as 4-morpholinobenzoic acid since this peak was not present in the GC chromatogram unless the precipitate was redissolved by the addition of methanol.

As speculated by Desobry et. al.⁴⁴, the observation of 1-phenyl butan-2-one can be explained as a secondary reaction product of the α -cleavage reaction, where the two enamines formed from the primary radicals undergo hydrolysis, as shown in figure 5.29. The enamine intermediates were not detected in the experiments reported here. Dimethylamine is also reported to be produced by this reaction but as previously explained was not directly observed here⁴⁴.

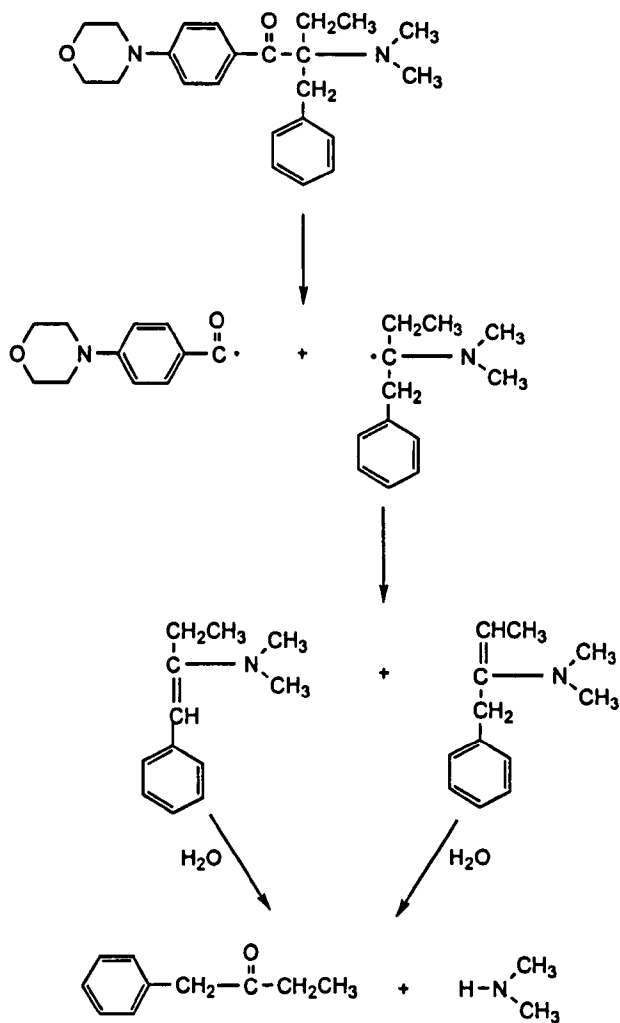
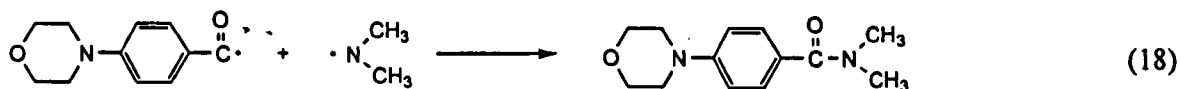


Figure 5.29 Formation of 1-phenyl butan-2-one from the Irgacure 369 primary aminoalkyl radical⁴⁴

N,N-dimethyl-(4-morpholino)benzamide was also observed here, as has previously been reported⁴⁴ and is speculated to be a termination reaction product of the primary α -cleavage substituted benzoyl radical and the primary β -cleavage nitrogen centered radical (18).



The N,N-dimethylamino propanamide is speculated to be the product of a secondary reaction similar to ones reported for the benzoyl radical¹⁴ and benzoin ethers^{20,53} involving a hydroperoxide intermediate of the primary aminoalkyl radical from the α -cleavage reaction. This is shown in figure 5.30.

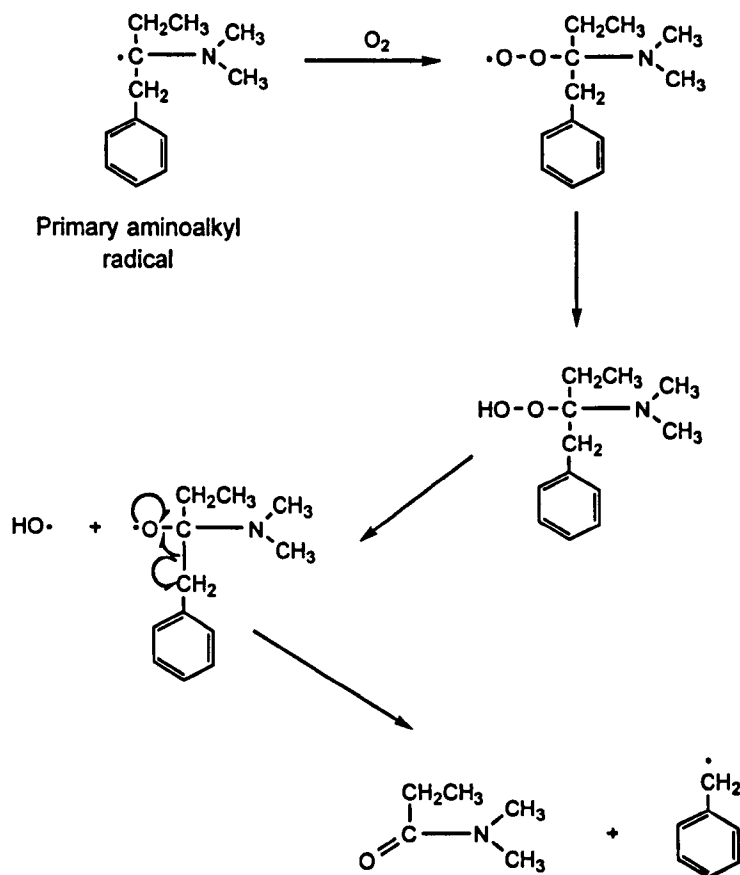


Figure 5.30 Formation of *N,N*-dimethylamino propanamide from the Irgacure 369 primary aminoalkyl radical

Additional weight is afforded to this hypothesis since the benzyl radical byproduct can be seen to be involved in another reaction, forming benzyl (4-morpholinophenyl) ketone in combination with the primary α -cleavage substituted benzoyl radical (19). Although the formation of this product could be speculated to involve the toluene solvent, this can be discounted because benzyl (4-morpholinophenyl) ketone is also observed in experiments using dichloromethane as the irradiating solvent. The benzyl radical could also be speculated to arise as a primary radical from the β -cleavage process, although as previously speculated, this is not thought to be likely.



The formation of the reaction products benzaldehyde, benzoic acid and formaldehyde benzyl imine cannot be reasonably explained, although all three compounds are also observed in experiments where the irradiating solvent is dichloromethane.

5.2.1.6 Thioxanthone type photoinitiators

The following photoinitiators were irradiated in dichloromethane, with the solutions before and after irradiation analysed by GC-MS:

Xanthone	
Thioxanthone	
Isopropyl thioxanthone	<i>(Quantacure ITX)</i>
2,4-Diethyl thioxanthone	<i>(Speedcure DETX)</i>
<i>t</i> .Butyl thioxanthone	
2-Chloro thioxanthone	<i>(Kayacure CTX)</i>
2-Propoxy thioxanthone	<i>(Quantacure PTX)</i>
1-Chloro-4-propoxy thioxanthone	<i>(Quantacure CPTX)</i>

Of the photoinitiators examined, only thioxanthone, isopropyl thioxanthone and 2,4-diethyl thioxanthone showed any change as a result of irradiation, the additional peaks detected being at trace level. These additional peaks could not be identified positively and are not thought to be significant in terms of the reaction mechanism of this type of photoinitiator.

5.2.1.7 Benzophenone type photoinitiators

The following photoinitiators were irradiated in dichloromethane, with the solutions before and after irradiation analysed by GC-MS:

Benzophenone	
4-Phenyl benzophenone	<i>(Trigonal 12)</i>
4-Methyl benzophenone	
4-Hydroxy benzophenone	
4-Methoxy benzophenone	
4-Chloro benzophenone	
2-Chloro benzophenone	
2,4,6-Trimethyl benzophenone	<i>(Esacure TZT)</i>
2-Benzoyl methyl benzoate	<i>(Daitocure OB)</i>
4-Benzoyl-4'-methyl diphenyl sulphide	<i>(Quantacure BMS)</i>
4,4'-Dimethoxy benzophenone	
4,4'-(Dimethylamino) benzophenone	<i>(Michler's ketone)</i>

Of the photoinitiators investigated only 4-phenyl benzophenone and 4,4'-(dimethylamino) benzophenone showed any change as a result of irradiation. In the case of 4-phenyl benzophenone a trace level of biphenyl was detected, but since none of the characteristic benzoyl radical byproducts were found, an α -cleavage reaction could not be confirmed.

In the absence of an amine synergist benzophenone type photoinitiators are generally regarded as unreactive, although 4-benzoyl-4'-methyl diphenyl sulphide has been reported to undergo cleavage at both carbon-sulfur bonds², as shown in figure 5.31. This cleavage reaction and its byproducts were not detected directly, but a slight odour is evident when formulations containing this photoinitiator are cured; suggesting that the cleavage reaction is very minor and the highly odorous byproducts are formed at a level lower than the detection limit of the GC-MS.

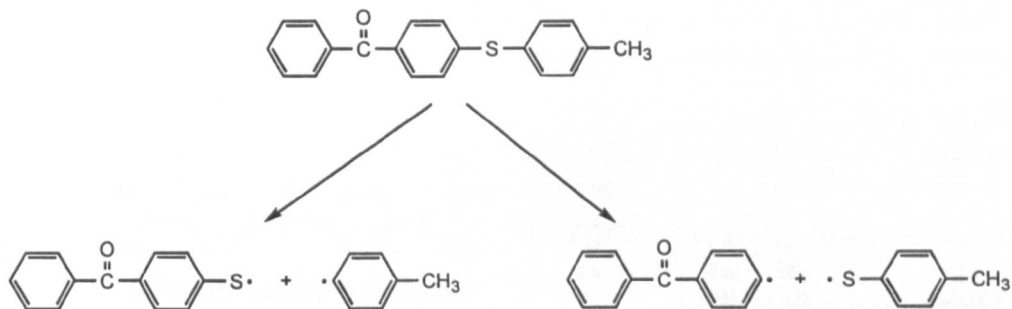


Figure 5.31 *Reported cleavage reactions of 4-benzoyl-4'-methyl diphenyl sulphide²*

4,4'-(Dimethylamino benzophenone (Michler's ketone)

The photoinitiator 4,4'-(dimethylamino)benzophenone contains both photoinitiator and synergist functionalities and therefore not surprisingly behaves differently to the other benzophenone derivatives. Figure 5.32 shows the GC chromatograms of an unirradiated and an irradiated solution of this photoinitiator in dichloromethane. The chromatogram peaks 1 and 2 have associated mass spectra. These have been interpreted and the results shown in figure 5.33.

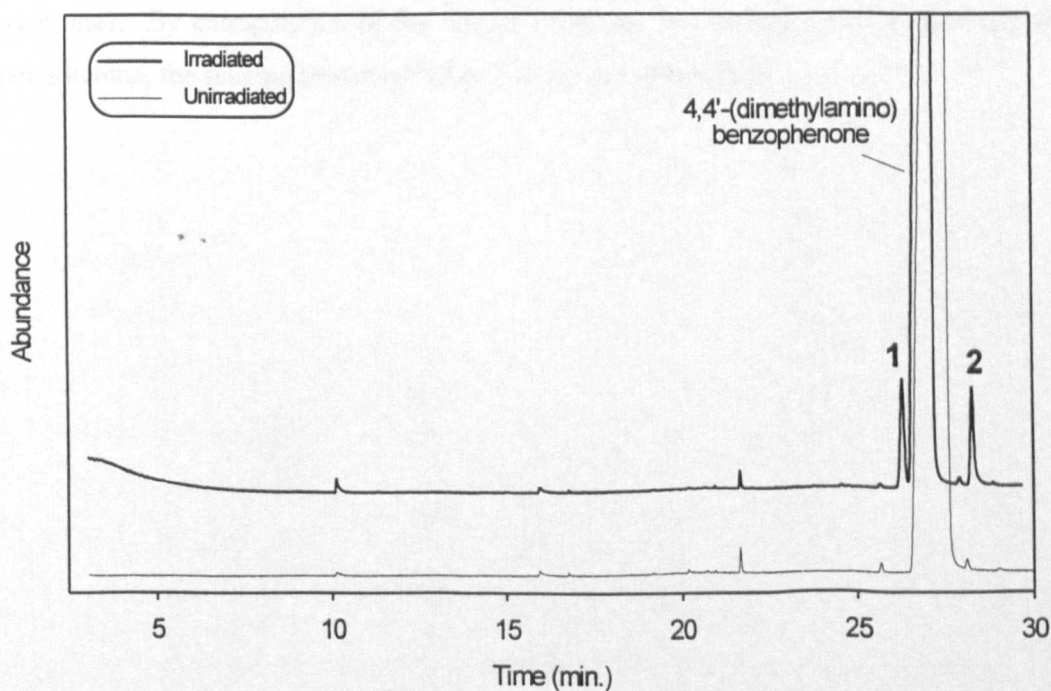
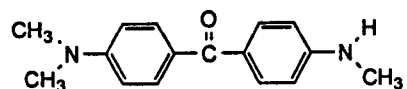
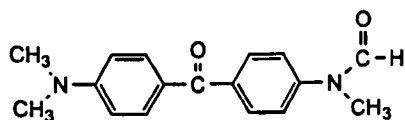


Figure 5.32 *GC chromatograms of 4,4'-(dimethylamino)benzophenone before and after irradiation in dichloromethane*

Peak 1

4-(dimethylamino)-4'-(methylamino) benzophenone

Retention time (min.)	m/z	I	Identity
26.29	254	100	M.+
	253	32	[M-H]+
	210	23	[M-N(CH ₃) ₂]+
	148	64	
	134	44	

Peak 2

4-(dimethylamino)-4'-(N-methyl formamide) benzophenone

Retention time (min.)	m/z	I	Identity
28.26	282	82	M.+
	281	12	[M-H]+
	238	2	[M-N(CH ₃) ₂]+
	224	7	[M-N(CHO)(CH ₃)]+
	162	2	
	148	100	

Figure 5.33 Photolysis products of Michler's ketone by GC-MS

Similar reaction products have been reported by Davidson et. al.⁶⁹ for the analogous N,N-dialkylanilines. By extrapolation of the reported reaction mechanism to the structurally similar Michler's ketone, the scheme shown in figure 5.34 can be speculated.

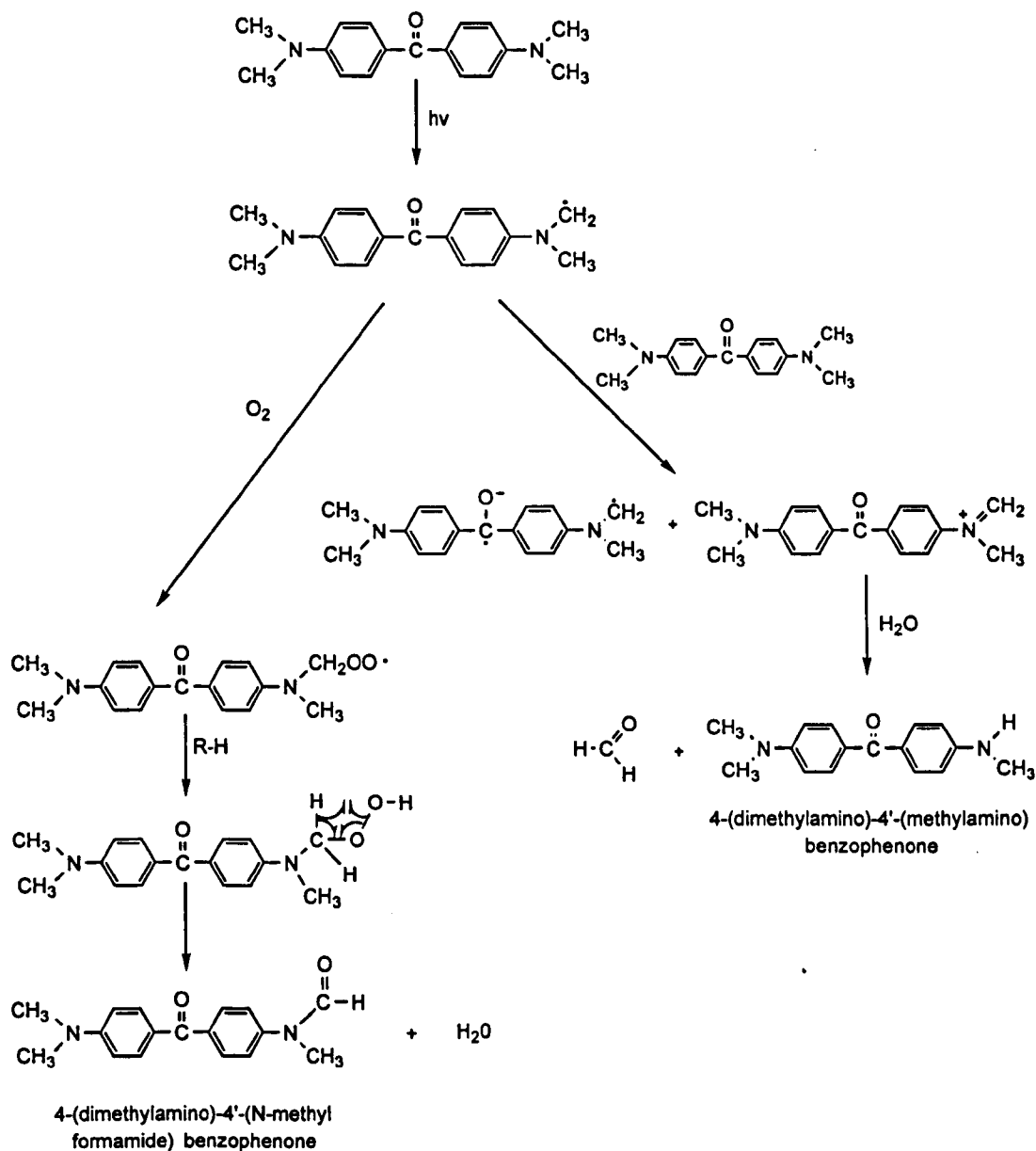


Figure 5.34 Further reactions of Michler's ketone following UV irradiation

5.2.1.8 Quinone type photoinitiators

The following photoinitiators were irradiated in dichloromethane, with the solutions before and after irradiation analysed by GC-MS:

2-Methyl anthraquinone

2-Ethyl anthraquinone

2-*t*.Butyl anthraquinone

Phenanthrene 9,10-quinone

(PI-ON)

The three anthraquinone derivatives gave conflicting results, with the *t*.butyl derivative showing no changes following irradiation but both the 2-methyl and 2-ethyl derivatives showing two types of changes:

1. The loss in each of a significant peak which, by virtue of the same molecular ion mass as the main peak, were assigned as positional isomers of the parent compound.
2. The formation of an additional peak with a molecular mass 14 amu higher than that of the parent compound.

The molecular weight of the additional peaks would be consistent with methyl substitution of the parent molecule. However, particularly in the case of the 2-ethyl anthraquinone, these results cannot be rationalised and further work is required to clarify them. In addition, irradiation of phenanthrene 9,10-quinone resulted in the formation of a significant byproduct which could not be positively identified.

5.2.1.9 Aromatic 1,2 diketone type photoinitiators

The following photoinitiators were irradiated in dichloromethane, with the solutions before and after irradiation analysed by GC-MS:

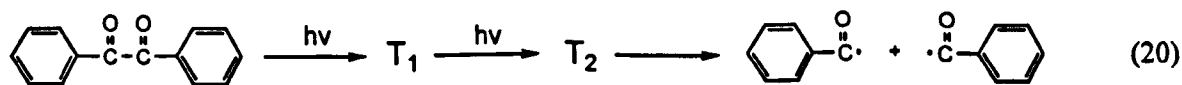
Benzil

4,4'-Dimethyl benzil

4,4'-Dimethoxy benzil

The irradiation of benzil was found to give rise to a small byproduct peak at 10.98 minutes, the retention time and mass spectrum consistent of which is consistent with benzoic acid. Similar results were found for the 4,4'-dimethyl benzil and 4,4'-dimethoxy benzil, forming 4-methyl benzoic acid and 4-methoxy benzoic acid respectively as byproducts.

The literature contains conflicting results regarding the stability of benzil when irradiated using UV light, with Ledwith et. al.³⁵ suggesting that benzil has good stability when irradiated in benzene such that no benzoyl radicals were detected by spin-trapping ESR experiments, and Bunbury et. al.⁷⁰ observing benzilpinacol, benzoin benzoate and benzoic acid following UV irradiation in isopropanol. 'Multiphotonic' cleavage has also been speculated by Scaiano and Johnston⁷¹, whereby α -cleavage occurs from the second excited triplet state following absorption of a second photon by the relatively long lived first excited triplet state (20).



Based on other work in this chapter, if benzil were to undergo an α -cleavage reaction to yield benzoyl radicals, the observation of benzoic acid would also be expected to be accompanied by the other characteristic byproducts; benzene, benzaldehyde and benzoin benzoate. Although the amount of benzoic acid detected in the work reported here is low, it is interesting to note that benzaldehyde was not detected, since this is usually the most abundant byproduct of the benzoyl radical. As a result of these observations a direct α -cleavage reaction can only be tentatively speculated, with further work required to define more fully the true situation.

5.2.1.10 Phenyl glyoxylates

Figure 5.35 shows the GC chromatograms of an unirradiated and irradiated solution of the photoinitiator phenyl glyoxylic acid methyl ester (Nuvopol PI 3000) in dichloromethane.

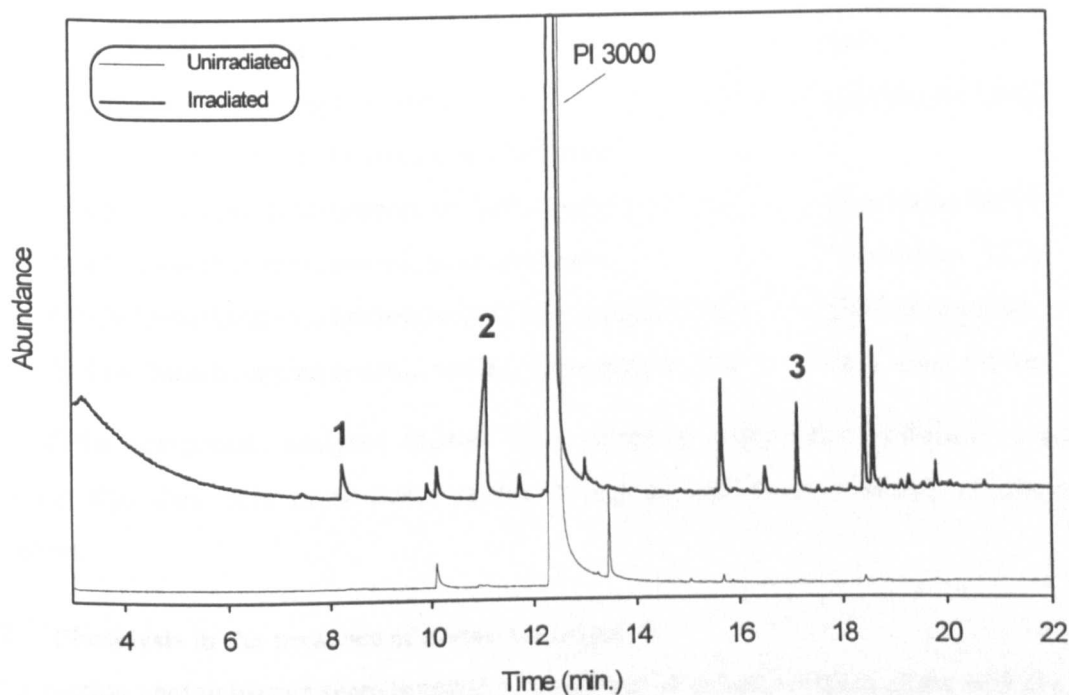
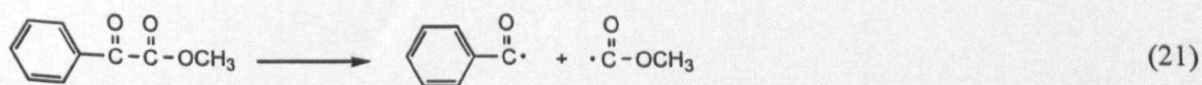


Figure 5.35 GC chromatograms of Nuvopol PI3000 solution before and after irradiation in dichloromethane

Although for phenyl glyoxylic acid methyl ester in inert solvents an intramolecular hydrogen abstraction from the ester group, followed by a fragmentation similar to a Norrish Type II reaction has been reported⁷³⁻⁷⁵, the exact reaction mechanism of this type of photoinitiator has not been firmly established. As such, in review articles the phenyl glyoxylates are sometimes classed as Type I photoinitiators^{72,76}, whereas in others¹ they are classed as Type II photoinitiators.

The data in figure 5.35 shows that Nuvopol PI3000 has undergone significant changes as a result of UV irradiation and has generated a number of byproducts. Further analysis showed that peaks 1 and 2 have retention times and mass spectra consistent with benzaldehyde and benzoic acid respectively, as has previously been interpreted for the photolysis of benzoin. Peak 3 was found to have a retention time and mass spectrum consistent with benzil, as has previously been interpreted for the photolysis of benzoin ethyl ether. These observed byproducts suggest that a α -cleavage reaction has taken place to give a benzoyl radical and an aliphatic carbonyl radical (21).



This hypothesis is contrary to the work of Hagemann¹, who concluded using TMPO radical trapping experiments that, since no trapped product was identified, the reaction mechanism of this photoinitiator was not via an α -cleavage mechanism.

5.2.1.11 Amine synergists

In order to discount any direct involvement in the radical generating process other than as a source of abstractable hydrogens, the following amine synergists were irradiated in dichloromethane, with the solutions before and after irradiation analysed by GC-MS:

N-Methyl diethanolamine	<i>MDEA</i>
(2-Dimethylamino)ethyl benzoate	<i>Quantacure DMB</i>
2-N,N-Dimethylamino benzoic acid ethyl ester	
4-N,N-Dimethylamino benzoic acid ethyl ester	<i>Quantacure EPD</i>
4-N,N-Dimethylamino benzoic acid amyl ester	<i>Quantacure MCA</i>
4-N,N-Dimethylamino benzoic acid (2-ethylhexyl) ester	<i>Quantacure EHA</i>
4-N,N-Dimethylamino benzoic acid (2-butoxyethyl) ester	<i>Speedcure BEDB</i>

None of the compounds analysed showed any change in composition following irradiation, indicating that their sole involvement in the curing process is as a source of abstractable hydrogens.

5.2.2 Photolysis in the presence of amine synergist

In this section photoinitiators representative of a number of structural types along with the amine synergist N-methyl diethanolamine (MDEA) were, depending on their solubility characteristics, dissolved in dichloromethane, methanol or toluene and irradiated in a shallow metal dish using a medium pressure mercury arc lamp. Any precipitate formed during irradiation was re-dissolved by the addition of a second solvent. Samples of the photoinitiator / amine solutions before and after irradiation were then analysed using GC-MS operating in an electron impact ionisation (EI) mode. Some samples were also analysed with the GC-MS operating in chemical ionisation (CI) mode using a methane reagent gas.

5.2.2.1 Type II photoinitiators

Type II photoinitiators were defined in chapter 1 as compounds which do not undergo cleavage reactions but which generate initiating radicals when irradiated in the presence of a hydrogen donor, typically a tertiary amine. Five basic structural types were defined. In this section one or more photoinitiators from each structural group have been investigated in combination with the amine synergist MDEA with respect to the formation of byproducts following UV irradiation.

i.e.

Structural type	Examples investigated
Benzophenones	Benzophenone 4-Benzoyl-4'-methyl diphenyl sulphide (<i>Quantacure BMS</i>)
Thioxanthenes	Isopropyl thioxanthone (<i>Quantacure ITX</i>) 1-Chloro-4-propoxy thioxanthone (<i>Quantacure CPTX</i>)
Anthraquinones	2-Ethyl anthraquinone
Aromatic 1,2 diketones	4,4'-Dimethyl benzil
Phenyl glyoxylates	Phenyl glyoxic acid methyl ester (<i>Nuvopol PI 3000</i>)

Benzophenone is both the most widely used photoinitiator for UV cured inks and coatings³⁰ and the one which has been most studied over the years; as such it is sensible to concentrate on this material initially.

It is well known that when exposed to UV light, a combination of benzophenone and a tertiary amine synergist in a typical UV curing formulation produces a benzophenone ketyl radical and an aminoalkyl radical, the latter of which is the principal initiating radical. The mechanism of this interaction has been outlined in chapter 1 and is also well covered in a number of texts^{1,69}.

Figure 5.36 shows the GC chromatograms of an unirradiated and irradiated solution of the photoinitiator benzophenone and the synergist MDEA in methanol.

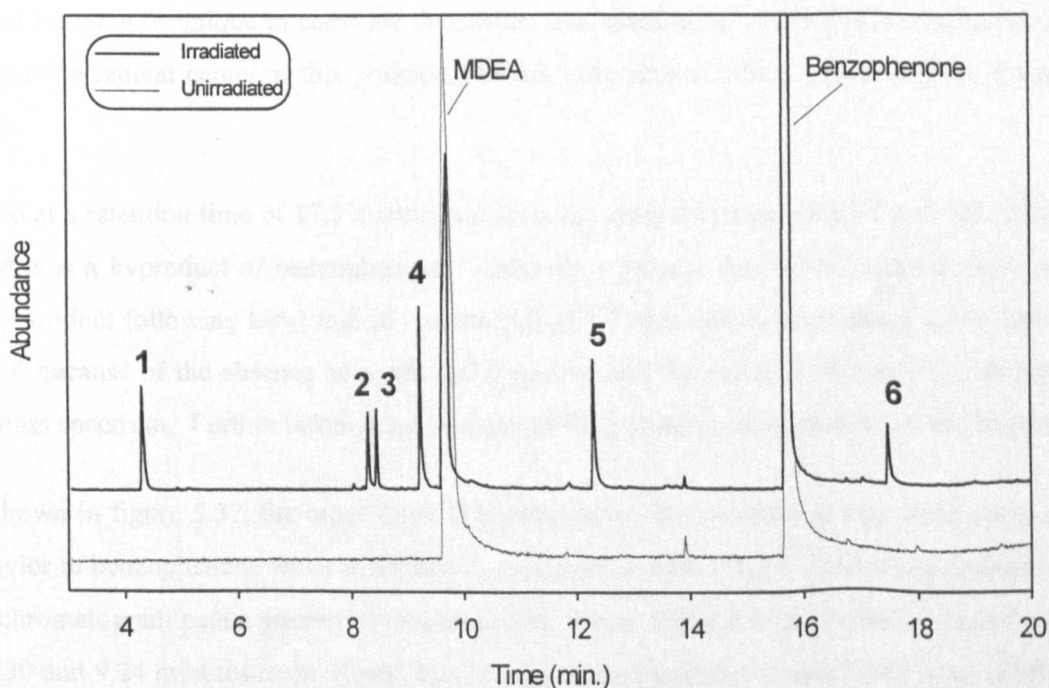
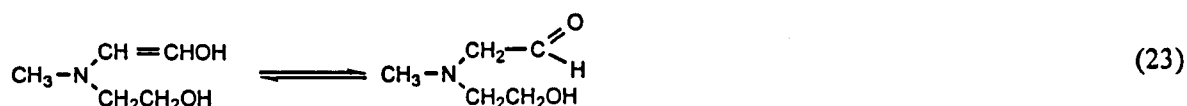
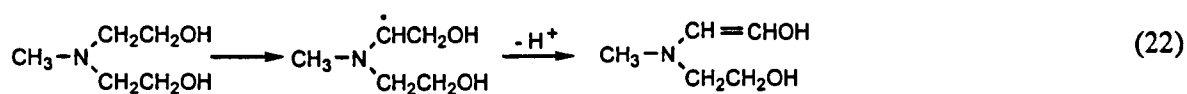


Figure 5.36 GC chromatograms of benzophenone / MDEA solution before and after irradiation in methanol

The data in figure 5.36 shows that, when irradiated with UV light, a combination of benzophenone and MDEA produces 6 byproducts at retention times of 4.30, 8.30, 8.49, 9.24, 12.32 and 17.50 minutes. Although insufficient information is available in the mass spectra of these peaks to positively identify any of them, for peaks 1-5, the fact that even mass fragments (typically m/z 42 and/or m/z 86) were found, with GC-CI-MS data indicating molecular weights of 87, 117 and 117 amu for peaks 1, 2 and 4 respectively, suggests that these compounds contain at least one nitrogen atom and are byproducts of MDEA. A molecular weight of 117 amu could also suggest an enamine type structure (22) containing a double bond adjacent to the nitrogen atom. The formation of this type of byproduct has been speculated by Davidson⁶⁹ for the structurally similar N-alkylamines. The product speculated in (22) would also be expected to undergo keto-enol tautomerisation (23), possibly accounting for the second byproduct with a 117 amu molecular weight.



If correctly assigned, these tautomers have an additional significance in that they show that hydrogen abstraction occurs at the α -position to the nitrogen from either of the two ethanol groups in MDEA. This is contradictory to the much referred to work of Göthe⁷⁷, who used an ESR radical trapping technique to conclude that whilst triethanolamine and N,N-dimethylethanolamine generated a radical center at this position, MDEA generated a radical center only on the methyl group.

Peak 6 at a retention time of 17.5 minutes contains the mass fragments m/z 77 and 105, indicating that this is a byproduct of benzophenone. Although a pinacol derivative has been reported as a likely product following ketyl radical recombination^{58,72}, this can be discounted as the identity of peak 6 because of the absence of a m/z 107 fragment and the presence of a m/z 105 fragment in the mass spectrum. Further information is required for a positive identification of this material.

As shown in figure 5.37, the other Type II photoinitiators investigated in this work show similar behavior to benzophenone when irradiated in combination with MDEA, generating a series of nine GC chromatogram peaks present at various levels. Peaks 1 and 4 in particular, at retention times of 4.30 and 9.24 minutes respectively, can be seen to be present at a significant level in all of the chromatograms and would appear to be a "fingerprint" for the Type II reaction mechanism. However, no comment can be made as to whether this is via a hydrogen abstraction or an electron / proton transfer mechanism.

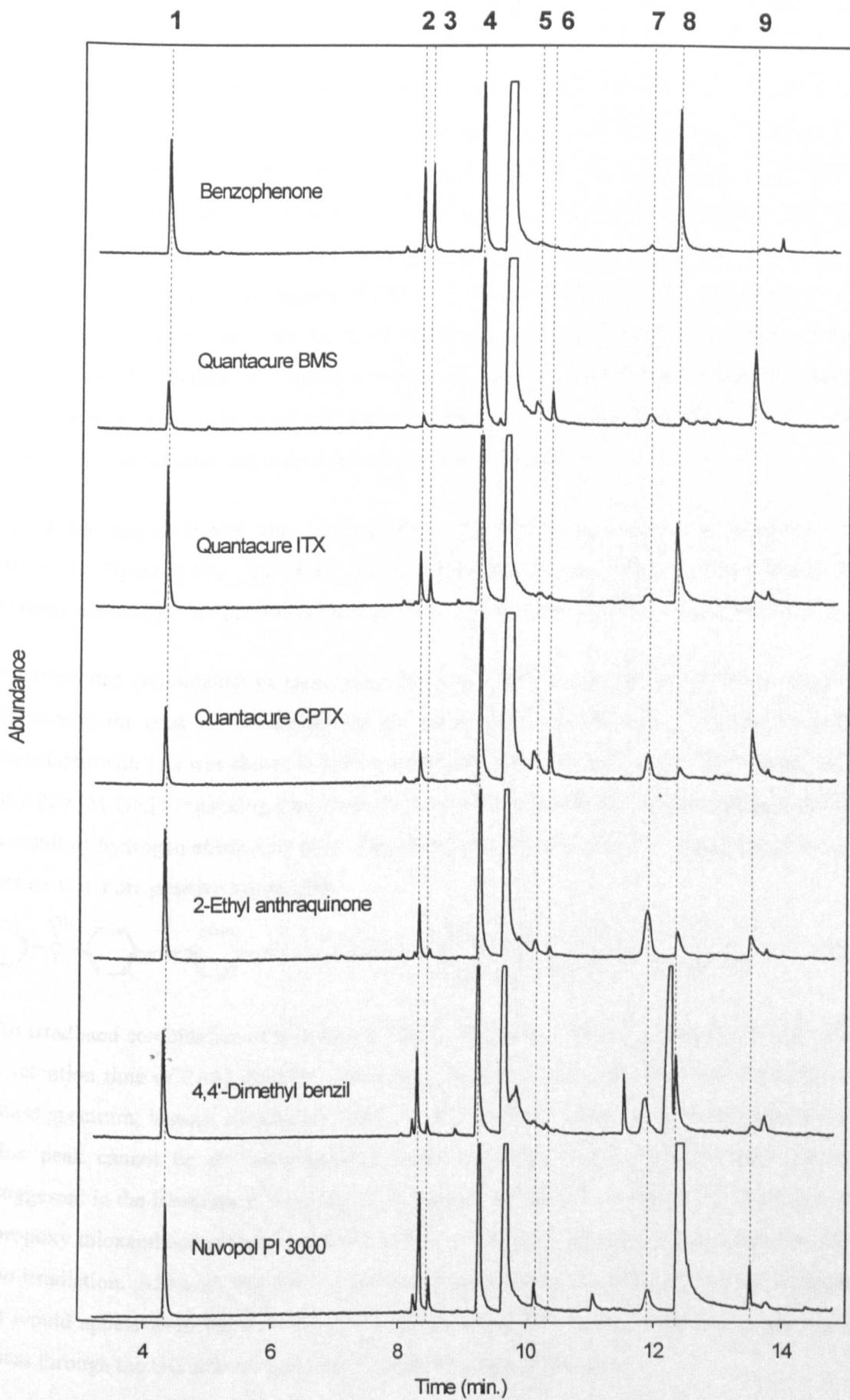
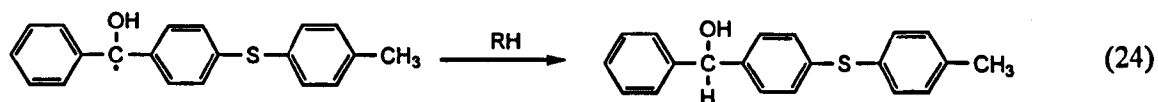


Figure 5.37 GC chromatograms of several Type II photoinitiators irradiated in solution with MDEA

The amine synergist MDEA appears in the chromatograms at a retention time of 9.68 minutes. With the exception of 4-methyl benzoic acid (12.27 minutes in the 4,4'-dimethyl benzil chromatogram) and unreacted Nuvopol PI 3000 (12.48 minutes retention time), all the peaks in the retention time range shown in figure 5.37 are thought to be MDEA byproducts. Other byproducts resulting from reactions with the solvent can be discounted at this stage because, for solubility reasons, Quantacure BMS, Quantacure CPTX and 2-ethyl anthraquinone were irradiated in dichloromethane whereas all the other samples were irradiated in methanol. As such, any byproducts with solvent would appear in only 3 or 4 of the samples, and in the case of those irradiated in dichloromethane, would be obvious from their mass spectra due to the chlorine atom's two significant isotopes. However, this is an area worthy of further study, with both the use of other techniques such as GC-IR to fully characterise the amine byproducts, and the use of other amine types to better understand the mechanism of reaction.

Some of the photoinitiators also showed other byproducts not in the chromatogram range displayed in figure 5.37. However, whilst important for individual photoinitiators, these byproducts are thought not to be important in terms of the overall Type II reaction mechanism;

1. An irradiated combination of Quantacure BMS and MDEA showed an additional significant chromatogram peak as a shoulder on the main photoinitiator peak. The mass spectrum associated with this was shown to have a molecular ion at m/z 306, with a small mass peak at m/z 289 $[M-OH]^+$ indicating that the product may be formed from the primary ketyl radical as a result of hydrogen abstraction (24). However, the presence of a large benzoyl m/z 105 peak prevents a more positive assignment.



2. An irradiated combination of Quantacure CPTX and MDEA showed a trace level byproduct at a retention time of 21.68 minutes. Although this could not be positively identified from the mass spectrum, isotope abundances show that the product contains a chlorine atom. As such, this peak cannot be the dehalogenated material 4-propoxy thioxanthone which has been suggested in the literature as the principal byproduct of CPTX⁷⁸. However, the formation of 4-propoxy thioxanthone cannot be ruled out since a significant precipitate was formed by CPTX on irradiation. Although this was redissolved by the addition of methanol prior to GC analysis, it would appear from the lack of any significant byproduct peak that the precipitate does not pass through the GC column under the experimental conditions used.
3. An irradiated combination of 4,4'-dimethyl benzil and MDEA showed two significant additional peaks in the GC chromatogram (16.83 and 18.85 minutes retention times) which could not be positively identified. The mass spectra of both peaks contained the 4-methyl

benzoyl fragment ion (m/z 119), with the 16.83 min. retention time peak showing an odd mass molecular ion (m/z 193) and an even mass fragment ion (m/z 162), suggesting the molecule contains a nitrogen atom. It is speculated that this chromatogram peak relates to a radical-radical termination byproduct involving the substituted benzoyl radical and an aminoalkyl radical. Insufficient spectral information is available for the 18.85 min. retention time peak to comment further on its identity.

4. Prior to irradiation, a mixture of Nuvopol PI 3000 and MDEA shows two very significant additional peaks in the GC chromatogram that would not be expected based on the individual materials. This suggests that a chemical reaction has taken place between the photoinitiator and the MDEA, although the identity of the products could not be determined from their mass spectra. This hypothesis is supported by the observation of a strong styrene-like odour from the solution, and the stipulation on the manufacturer's technical data sheet that this photoinitiator should not be used in conjunction with amine synergists, although no reason is given. Despite this, as shown in figure 5.37, Nuvopol PI 3000 still reacts via a Type II mechanism in the presence of MDEA.

A theory gaining acceptance within the field of radiation curing is that although the photoinitiator ketyl radical can undergo reactions such as chain termination and dimerisation⁵⁸, a significant proportion of these radicals are oxidized back to the original carbonyl functional photoinitiator molecule by atmospheric oxygen. This has been reported for benzophenones^{79,80}, thioxanthenes^{77,81} and anthraquinones⁸², and is shown in figure 5.38 using benzophenone as an example⁸⁰.

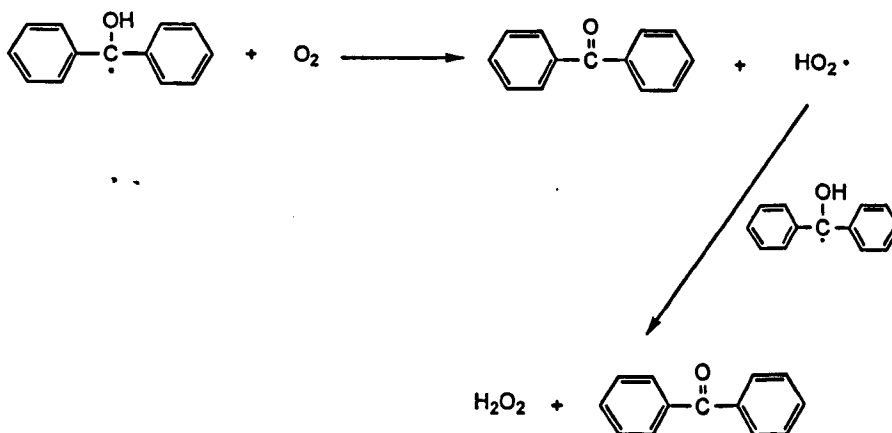
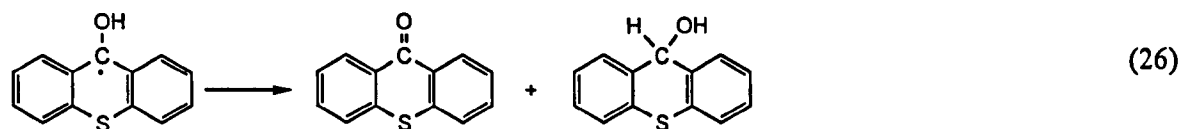
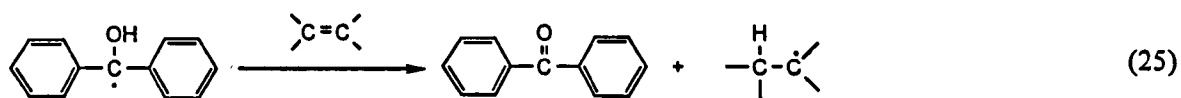


Figure 5.38 *The regeneration of benzophenone in the presence of atmospheric oxygen*⁸⁰

Regeneration of the parent photoinitiator molecule from a ketyl radical can also be achieved as a result of hydrogen transfer to a monomer double bond (26) or by disproportionation (27). The importance of the former cannot be determined without further work, but the latter can be discounted as relatively unimportant because no thioxanthenol type structures were observed as byproducts in this work.



5.2.2.2 Type I photoinitiators

In chapter 1, the most widely used cleavage photoinitiators were divided into seven basic structural types. In this section one or more photoinitiators from each structural group have been investigated in combination with the amine synergist MDEA with regard to byproducts following UV irradiation.

i.e.

Structural type	Examples investigated
benzoin ethers	benzoin methyl ether
acylphosphine oxides	2,4,6-trimethylbenzoyl diphenylphosphine oxide (<i>Lucerin TPO</i>)
benzil ketals	benzil dimethyl ketal (<i>Irgacure 651</i>)
hydroxyalkyl phenones	1-phenyl-2-hydroxy-2-methyl propan-1-one (<i>Darocure 1173</i>) 1-hydroxycyclohexy phenyl ketone (<i>Irgacure 184</i>)
α -aminoalkylphenones	2-benzyl-2-dimethylamino-1-(4-morpholinophenyl)butan-1-one (<i>Irgacure 369</i>) 2-methyl-1-[4-(methylthio)phenyl]-2-morpholinopropan-2-one (<i>Irgacure 907</i>) 3,6-bis (2-morpholinoisobutyryl) N-octyl carbazole (<i>Radstart N1414</i>)
dialkoxy acetophenones	diethoxy acetophenone (<i>DEAP</i>)
O-acyl- α -oximinoketones	1-phenyl-1,2-propanedione-2-(O-ethoxycarbonyl) oxime (<i>Quantacure PDO</i>)

Figure 5.39 shows the GC chromatograms of irradiated methanol solutions of the photoinitiators benzophenone, benzoin methyl ether, Irgacure 651, Darocure 1173 and Lucerin TPO in combination with MDEA.

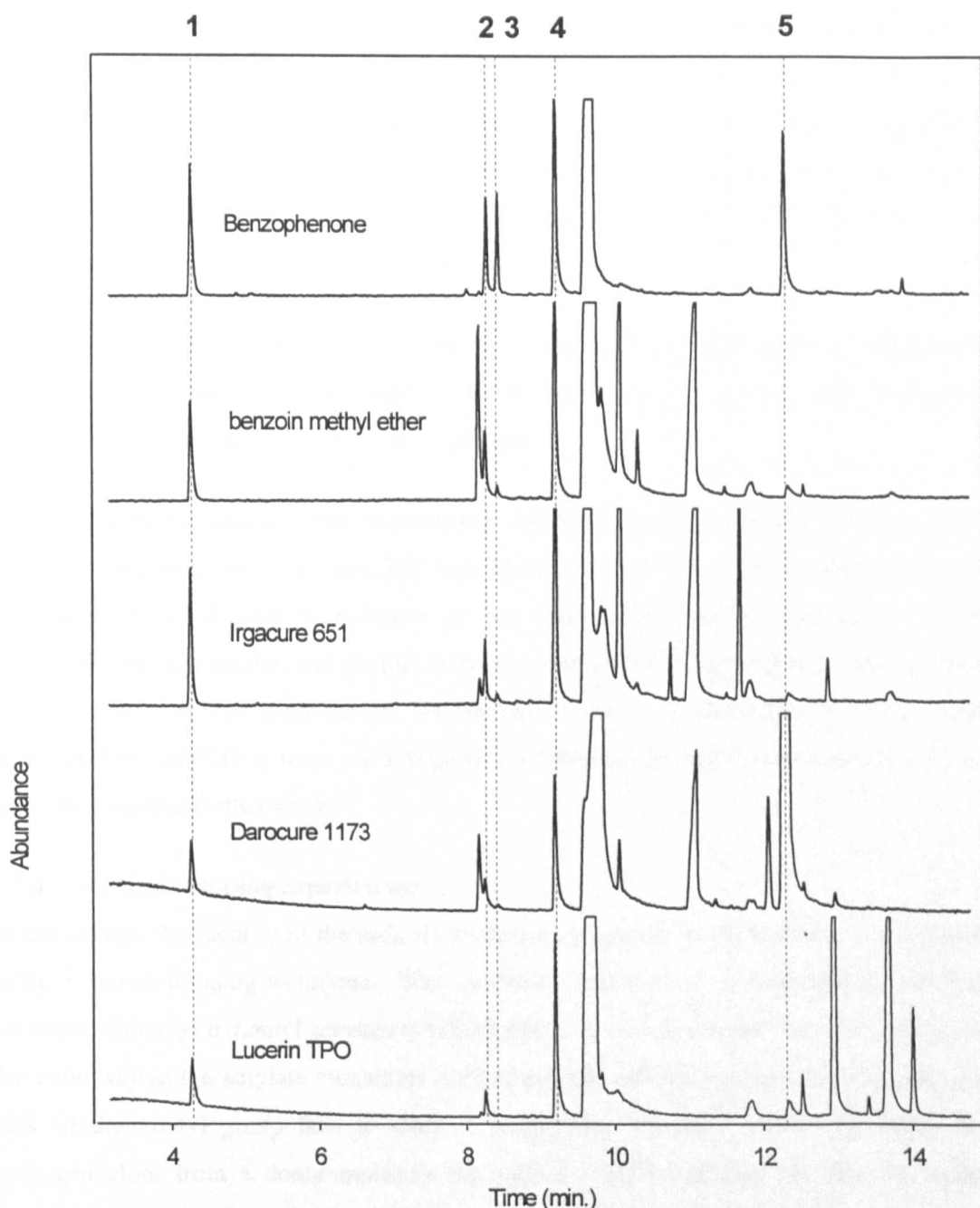


Figure 5.39 GC chromatograms of several Type I photoinitiators irradiated in methanol solution with MDEA. Benzophenone / MDEA included as a reference to show Type II behavior.

The data in figure 5.39 shows that, whilst Type I photoinitiators generate free radicals via a cleavage mechanism giving a number of byproducts (as previously defined), in the presence of the amine synergist MDEA they are also capable of generating radicals via a Type II mechanism. For the examples shown in figure 5.39 this is demonstrated by the presence of several Type II 'fingerprint' MDEA byproducts as have been previously defined for Type II character photoinitiators such as benzophenone. In particular, the chromatogram peaks at retention times of 4.30 and 9.24 minutes (peaks 1 and 4 respectively) are clearly present as MDEA byproducts for all the photoinitiators shown. These observations are significant in that they explain why Irgacure

651, Lucerin TPO and DEAP have been reported^{12,19} to show a considerable cure speed increase in the presence of amine synergist. This cure speed increase has previously been attributed only to a radical chain process reducing oxygen inhibition^{12,19}. The work reported here is supported by that of Johnson and Oldring³⁶ who have more recently speculated that the reactivity increase of the photoinitiator Darocure 1173 in the presence of amine synergist could not be attributed merely to a radical chain process reducing oxygen inhibition.

In addition to the photoinitiators shown in figure 5.39, another hydroxyalkylphenone type photoinitiator, Irgacure 184, was seen to demonstrate Type II behavior when irradiated in the presence of MDEA, as was diethoxy acetophenone.

Not all the photoinitiator types investigated showed Type II behavior; all the α -aminoalkyl phenones (Irgacure 907, Irgacure 369 and Radstart N1414) and the O-acyl- α -oximinoketone Quantacure PDO showed no evidence of the characteristic MDEA byproducts. These two structural types are similar, and distinct from the other photoinitiator types, in that they both have a nitrogen atom at the β -position to the carbonyl bond. It is speculated that this a significant factor in their inability to react via a Type II mechanism, although no mechanistic reason can be suggested without further work.

5.2.3 Radical trapping experiments

In this section the identity of the radicals produced by a range of photoinitiators was investigated using a radical trapping technique. This involved irradiation of a photoinitiator solution in the presence of methyl α -*t*.butyl acrylate (MTBA) which has been claimed⁴¹ to react with a radical in the same way as the acrylate monomers used in commercial coating formulations, but, due to the bulk of the *t*.butyl group fails to allow a propagation reaction. Following abstraction of a hydrogen atom from a donor molecule the radical / MTBA adduct can then be analysed by techniques such as GC-MS to determine the nature of the initiating radical.

A range of Type I and Type II photoinitiators were investigated by MTBA radical trapping, both in the presence and absence of the amine synergist MDEA. Samples were prepared depending on their solubility characteristics in either methanol or a methanol / dichloromethane mixture, with 2 %wt photoinitiator, 1 %wt MDEA (where applicable) and approximately 1 %wt of MTBA. A solution of MTBA in methanol was also irradiated in the absence of any photoinitiator or synergist and found not to show any GC chromatogram changes compared with the unirradiated sample.

Figure 5.40 shows GC chromatograms of a methanol solution of the photoinitiator benzil dimethyl ketal (Irgacure 651) exposed in the presence of MTBA. This is compared with data where the solvent is dichloromethane, but where no MTBA is present.

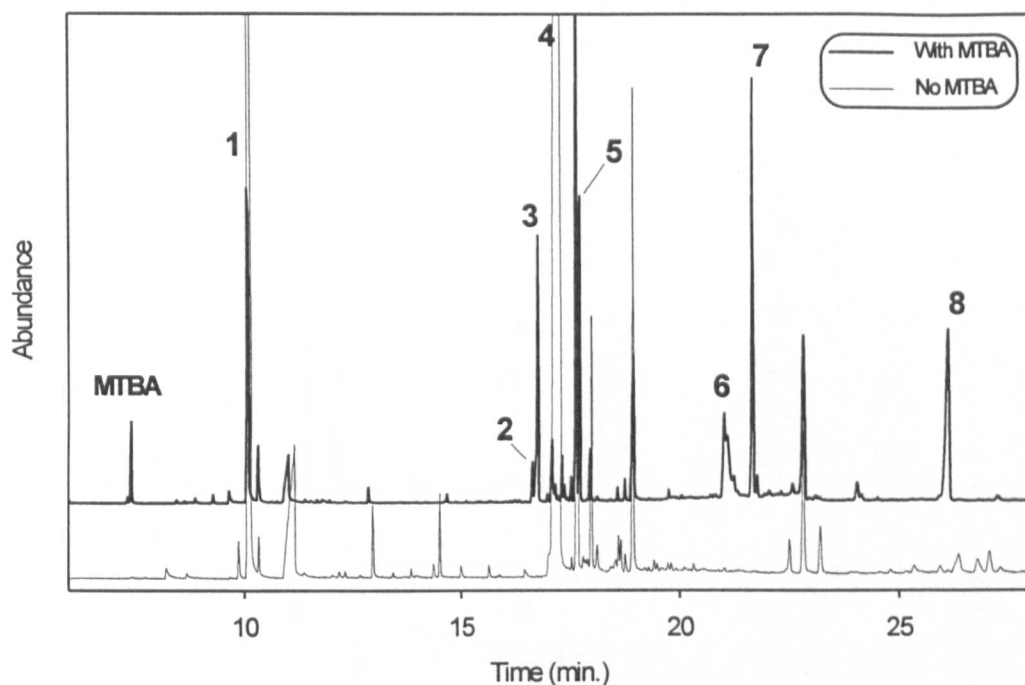


Figure 5.40 GC chromatograms of Irgacure 651 solution after irradiation in the presence and absence of the radical trap methyl α -*t*.butyl acrylate

The data in figure 5.40 shows that there are a number of significant changes in the GC chromatogram of Irgacure 651 when it is irradiated in the presence of MTBA compared with irradiation in its absence:

- The appearance of several additional peaks (peaks 2, 3, 5, 6, 7, 8)
- The absence of the byproduct benzil (peak 4)
- The formation of less methyl benzoate (peak 1)

The absence of benzil as a byproduct can be ascribed to the successful reaction of the benzoyl radical with the MTBA. As such, insufficient benzoyl radicals are present at any time to form benzil by a radical-radical termination reaction as previously described. Also, the formation of less methyl benzoate can be ascribed to the reaction of at least some of the dimethoxy benzyl radicals with MTBA prior to the well known secondary fragmentation reaction which gives methyl benzoate and a methyl radical^{13,14,16}. However, even assuming that radical / MTBA adducts are formed by the benzoyl, dimethoxy benzyl and methyl radicals, this does not explain the relatively large number of additional peaks in the GC chromatogram.

The data in figure 5.41 for the photoinitiator Irgacure 184 shows similar results to those for Irgacure 651. When irradiated in methanol solution in the presence of MTBA several additional peaks are observed (peaks 1-10) compared to irradiation in dichloromethane solution with no MTBA present. Also, cyclohexanone, one of the largest byproducts for this photoinitiator (see earlier) is absent, suggesting that the hydroxycyclohexyl radical is particularly reactive towards acrylate bonds.

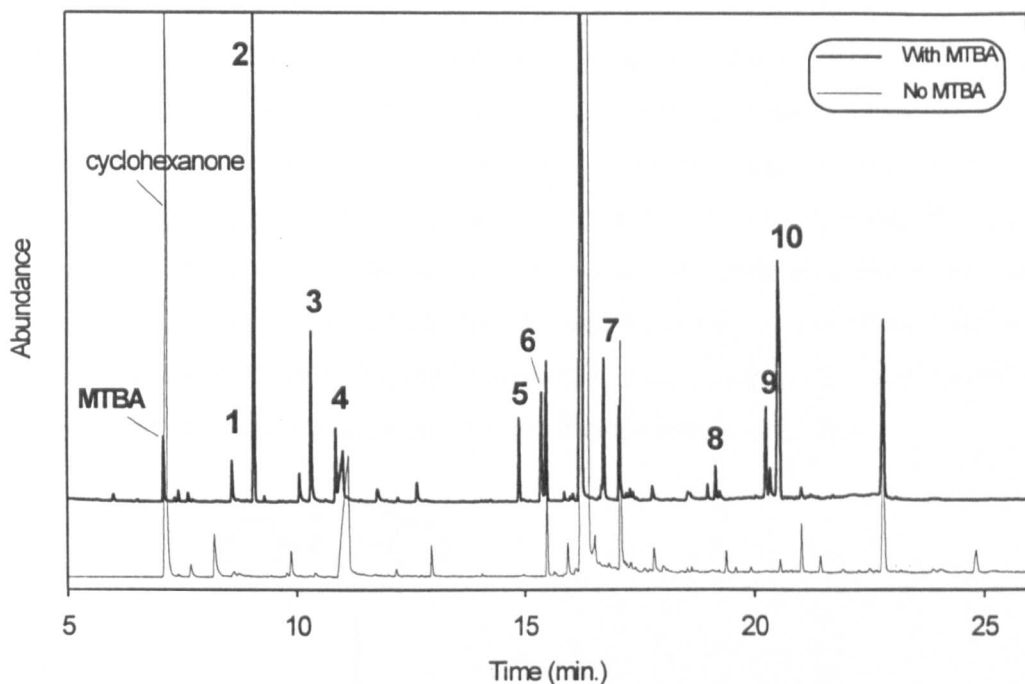
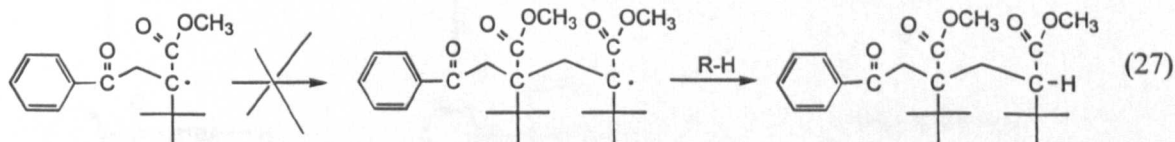
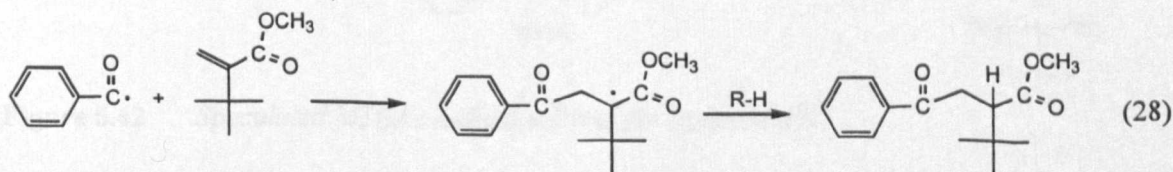


Figure 5.41 GC chromatograms of Irgacure 184 solution after irradiation in the presence and absence of the radical trap methyl α -*t*.butyl acrylate

When the results in figures 5.40 and 5.41 are compared, it is evident that with the exception of the peaks at 16.75 minutes, none of the additional peaks for irradiation in the presence of MTBA are similar for both photoinitiators. This is an important observation that discounts the possibility of some propagation occurring prior to hydrogen abstraction, since this would give rise to at least several peaks that are the same for both photoinitiators. i.e.



Additional weight is given to this argument since when irradiated in the presence of MTBA the chromatograms of benzoin methyl ether, diethoxy acetophenone and 1-phenyl-2-hydroxy-2-methyl propan-1-one (Darocure 1173) all show a significant peak at 16.75 minutes retention time as well as several unique peaks, although it is difficult to determine the exact number due to the complexity of the chromatograms. Because all five of these photoinitiators will cleave to give benzoyl radicals, the fact that the chromatogram peak at 16.75 minutes is common to all suggests that it is the product of the benzoyl radical reacting with MTBA, with the trapped radical subsequently abstracting a hydrogen atom from a donor molecule. i.e.



Although the mass spectra of GC-MS peaks assigned as MTBA / radical adducts are complex and difficult to assign a structure to, the fact that many of them contain m/z 105 fragments suggests that they contain benzoyl groups. This can only be possible if all the radicals generated in the initiation process are involved both in initiation and termination reactions with the MTBA, such that a number of benzoyl group containing MTBA / radical adducts are capable of being formed. This is supported by the observation that all five cleavage photoinitiators investigated produce a larger number of MTBA radical adducts than the number of primary initiating radicals formed. This is demonstrated in figure 5.42 using Irgacure 651 as an example and assuming that benzoyl, dimethoxy benzyl and methyl radicals are all formed in reasonable quantities.

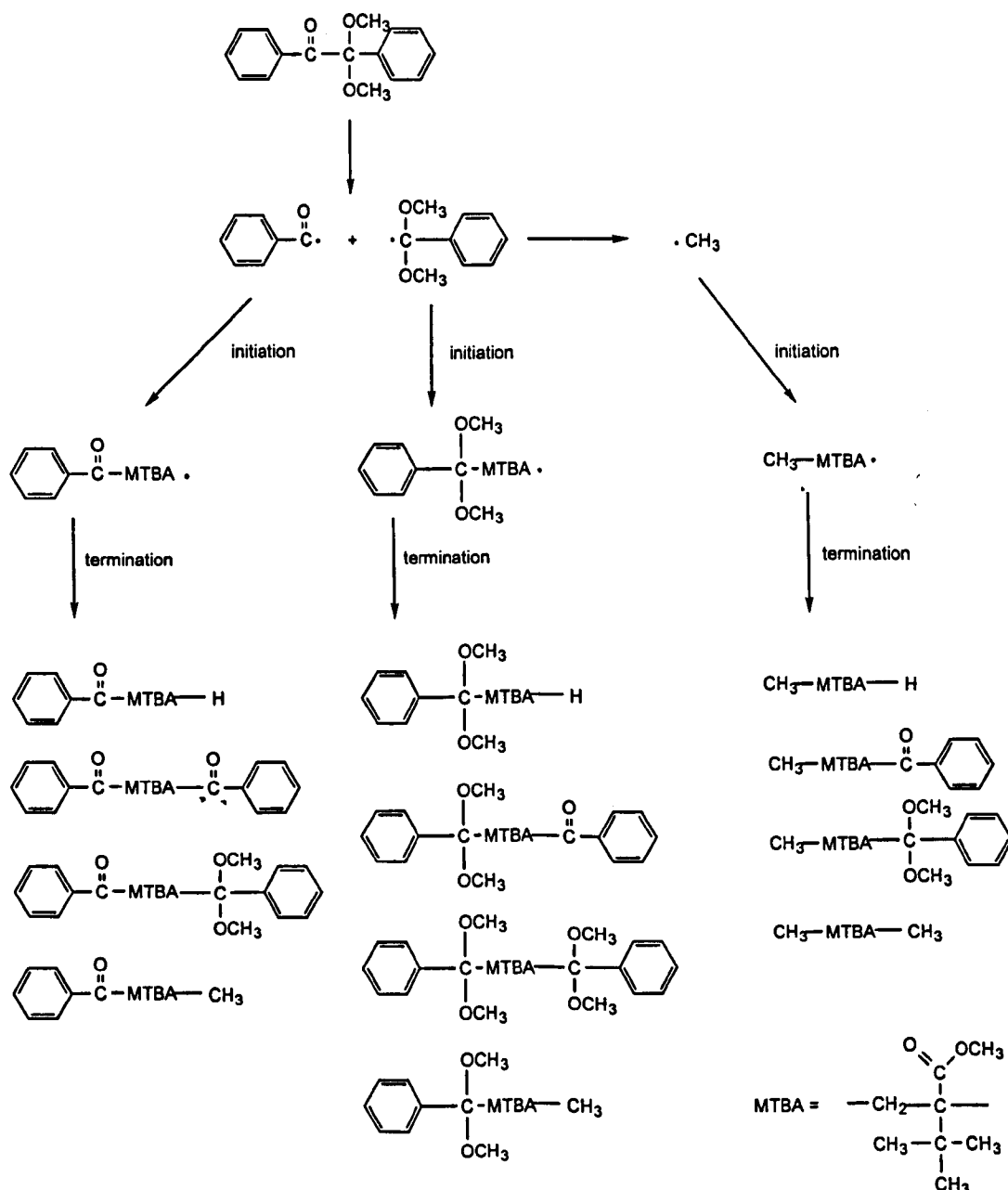


Figure 5.42 Speculated MTBA / radical adducts for Irgacure 651

Similar experiments using the Type II photoinitiator benzophenone and the amine synergist MDEA failed to show any significant additional GC peaks following irradiation, although byproduct peak intensities compared with Type I materials suggest a lower reaction efficiency.

The results of this radical trapping work, whilst inconclusive from the point of view of confirming the identity of the initiating radicals, are significant in that they raise doubts that particular radicals are involved in either initiation or termination reactions in acrylate free radical polymerisations. In particular they suggest that the substituted benzyl radical formed by most cleavage photoinitiators may provide significant initiation of the cure process, and not merely undergo termination reactions. Significantly more work in this area is required to prove the proposed theory, with better results likely to be obtained with a higher MTBA excess and using additional techniques such as GC-CI-MS and GC-IR (infrared detector) to identify the range of radical adducts formed.

5.3 CONCLUSIONS

A wide range of photoinitiators representing all the major structural types were, using GC-MS, investigated in a model system to determine their decomposition mechanism and byproduct formation upon UV irradiation. For all the photoinitiators investigated this was done in the presence and absence of the amine synergist N-methyl diethanolamine.

Those photoinitiators found to generate benzoyl radicals by a cleavage mechanism produced benzene, benzaldehyde, benzoic acid, benzil and benzoin benzoate as byproducts, with the latter thought to be a secondary reaction product of benzil and a benzoyl radical. Photoinitiators that generate a substituted benzoyl radical did not necessarily give rise to all the analogous substituted byproducts.

Whilst the results generally agreed with previously published literature, a large number of additional byproducts were identified, particularly for the relatively new α -aminoalkylphenone type photoinitiators. New reaction pathways were also speculated for some photoinitiators.

Contrary to a mechanism widely reported to be exclusively via α -cleavage, the hydroxyalkylphenone type photoinitiators 1-phenyl-2-hydroxy-2-methyl propan-1-one (Darocure 1173) and 1-hydroxycyclohexyl acetophenone (Irgacure 184) were found to undergo both α and β -cleavage reactions. However, their tendency to undergo β -cleavage appears to be dependent on the solvent used during irradiation, with further work required to clarify the extent of this effect.

The Type II reaction mechanism was found to be fingerprinted by the appearance of a number MDEA derived reaction byproducts in the GC chromatogram. With the exception of the α -aminoalkylphenone and O-acyl- α -oximino ketone type photoinitiators, which contain a nitrogen atom at the β -position to the carbonyl bond, these characteristic Type II byproducts were also seen for cleavage photoinitiators, indicating that they can react via a Type I or a Type II mechanism in the presence of an amine synergist.

Experiments for several cleavage photoinitiators using the radical trap methyl α -*t*.butyl acrylate (MTBA) failed to positively identify any radical / MTBA adducts. However, the number, retention time and mass spectra of the additional GC peaks detected following irradiation suggest that most or all of the primary radicals are involved in both initiation and termination reactions.

5.4 EXPERIMENTAL

5.4.1 Photolysis byproducts in the absence of amine synergist

With the exception of three materials, all photoinitiators and synergists were prepared at 2 %wt in HPLC grade dichloromethane. 2-Benzyl-2-dimethylamino-1-(4-morpholinophenyl) butan-1-one (Irgacure 369) was prepared in toluene, and both 2,4,6-trimethylbenzoyl diphenylphosphine oxide (Lucerin TPO) and bis (2,6-dimethoxybenzoyl)-2,4,4-trimethylpentyl phosphine oxide (BDTPO) were prepared in methanol. Samples were exposed to UV radiation for a period of 1 minute in a shallow metal dish with light from a Maccam Flexicure spot curing system (Maccam Photometrics, Livingstone, Scotland) fitted with a 400 Watt medium pressure mercury arc lamp. The light was directed through two flexible fluid filled light guides, the ends of which were a distance of approximately 5 cm from the sample.

Solutions of irradiated and unirradiated material were analysed by gas chromatography-mass spectroscopy (GC-MS) using a Hewlett-Packard 5890 GC fitted with a Hewlett-Packard 5971 mass selective detector operating in scan mode in the range 10-400 amu with electron impact (EI) ionisation. A 25m 0.22mm internal diameter non-polar capillary column was used with a 10 psi helium purge and a 280°C injection port temperature. Oven conditions were:

50°C isothermal for 3 minutes

50-300°C at 15°C / minute

300°C isothermal for 10 minutes

Additional experiments at a later date for some materials used the GC-MS operating in chemical ionisation mode (CI) with a methane reagent gas. New solutions of similar concentration were prepared for this work using HPLC grade methanol solvent with sufficient dichloromethane to dissolve any precipitate formed following irradiation. Irgacure 369 was prepared in HPLC grade toluene due to its instability in dichloromethane and low solubility in methanol.

5.4.2 Photolysis byproducts in the presence of amine synergist

With some exceptions, samples were prepared by dissolving 2 %wt photoinitiator and 1 %wt of the amine synergist N-methyl diethanolamine (MDEA) in HPLC grade methanol. Due to their low solubility in methanol, 4,4'-(dimethylamino)benzophenone (Michler's ketone), 1-chloro-4-propoxy thioxanthone (Quantacure CPTX), 4-benzoyl-4'-methyl diphenyl sulphide (Quantacure BMS) and 2-ethyl anthraquinone were prepared with 1 %wt MDEA in HPLC grade dichloromethane. Irgacure 369 / MDEA was prepared in HPLC grade toluene since the photoinitiator is unstable in dichloromethane solution and insufficiently soluble in methanol. Samples were exposed to UV radiation and analysed as described in 5.4.1.

5.4.3 Radical trapping experiments

Samples were prepared by dissolving 2 %wt photoinitiator and approximately 1-2 %wt methyl- α -*t*.butyl acrylate (kindly supplied by K. Dietliker of Ciba-Geigy, Basle, Switzerland) in HPLC grade methanol with the minimum amount of additional HPLC grade dichloromethane solvent required to dissolve the photoinitiator. Some samples were also prepared that contained an additional 1 %wt of MDEA. Samples were exposed to UV radiation and analysed as described in 5.4.1. Results were compared with earlier experiments where no MTBA was present, and where the irradiation solvent was dichloromethane.

5.5 REFERENCES

1. H J Hagemann in *Photopolymerization and Photoimaging Science and Technology*; N S Allen (Ed.), Elsevier Science Publishers Ltd., Barking, Essex, 1 (1989)
2. J P Fouassier, D J Lougnot; *Polym. Commun.*, **31**, 11 (1990)
3. A Costela, J Dabrio, J M Figuera, I Garcia-Moreno, H Gsponer, R Sastre; *Journal of Photochemistry and Photobiology A: Chemistry*, **92**, 213 (1995)
4. J P Fouassier; *Progress in Organic Coatings*, **18**, 229 (1990)
5. J C Scaiano, A F Becknell, R D Small; *Journal of Photochemistry and Photobiology A: Chemistry*, **44**, 99 (1988)
6. J Eichler, C P Herz, W Schnabel; *Die Angewandte Makromolekulare Chemie*, **91**, 1396, 39 (1980)
7. N S Allen, D Mallon, I Sideridou, A Green, A Timms, F Catalina; *European Polymer Journal*, **28**, 6, 647 (1992)
8. N S Allen, E Lam, E M Howells, P N Green, A Green, F Catalina, C Peinado; *European Polymer Journal*, **26**, 12, 1345 (1990)
9. N S Allen, D Mallon, I Sideridou, F Catalina, C Peinado, A Timms, A Green; *European Polymer Journal*, **29**, 11, 1473 (1993)
10. L Angiolini, D Caretti, C Carlini, E Corelli, J P Fouassier, F Morlet-Savary; *Polymer*, **36**, 21, 4055 (1995)
11. J C Netto-Ferreira, D Weir, J C Scaiano; *Journal of Photochemistry and Photobiology A: Chemistry*, **48**, 345 (1989)
12. J E Baxter, R S Davidson, H J Hagemann, G T M Harkvoort, T Overeem; *Polymer*, **29**, 1575 (1988)
13. H Fischer, R Baer, R Hany, I Verhoolen, M Walbiner; *J. Chem. Soc. Perkin Trans 2*, 787 (1990)
14. X T Phan; *J. Radiation Curing*, **13**, 1, 11 (1986)
15. S P Pappas; *Radiation Curing*, **8**, 3, 28 (1981)
16. M R Sandner, C L Osborne; *Tetrahedron Letters*, 415 (1974)
17. V D McGinniss in *Developments in Polymer Photochemistry - 3*; N S Allen (Ed), Applied Science Publishers Ltd, Barking, Essex (1982).
18. C L Osborne; *Radiation Curing*, **3**, 3, 2 (1976)
19. G Berner, R Kirchmayr, G Rist; *J. of Oil Col. Chem. Assoc.*, **61**, 105 (1978).
20. S P Pappas, V D McGinniss in *UV Curing Science & Technology*; S P Pappas (Ed.), Technology Marketing Corporation, Stamford, Connecticut, USA, 1 (1978)
21. C L Osborne, M R Sandner; *ACS Div. Org. Coat. Plast. Chem. Preprints*, **34**, 1, 660 (1974)
22. A Borer, R Kirchmayr, G Rist; *Helv. Chim. Acta.*, **61**, 305 (1978)
23. M Hamity, J C Scaiano; *J. Photochem.*, **4**, 229 (1975)

24. K E Russel, A V Toboloski; *J. Amer. Chem. Soc.*, **76**, 395 (1954)
25. C L Osborne, S L Watson; *Abstracts Of The 9th Central Regional Meeting Of The Amer. Chem. Soc.*, Charleston, West Virginia, USA, **poly 21**, 75 (1977)
26. EC Measurement and Testing Project: Directive 90/128/EEC and 92/39/EEC
27. C Renson, J M Loutz; *Proc. Conf. RADTECH-ASIA*, Tokyo, Japan, 356 (1988)
28. E Beck, M Lokai, E Keil, H Nissler; *Proc. Conf. RADTECH*, Nashville, USA, 160 (1996)
29. D. L. Easterby; *Proc. Conf. Aspects Of Analysis*, Egham, England, **Paper 8** (1994)
30. C. Armstrong, S.L. Herlihy; *Proc. Conf. Aspects Of Photoinitiation*, Egham, England, 1 (1993)
31. S M Johns, J W Gramshaw, L Castle, S M Jickells; *Deutsche Lebensmittel-Rundschau*, **91**, 3, 69 (1995)
32. S J Wilson in *Radiation Curing Of Polymers II*; D R Randell (Ed.), The Royal Society Of Chemistry, London, 125 (1991)
33. P K T Oldring in *Chemistry And Technology Of UV And EB Formulation For Coatings, Inks And Paints (Volume 3-Photoinitiators For Free Radical And Cationic Polymerisation)*; P K T Oldring (Ed.), SITA Technology Ltd., 1 (1991)
34. R Phillips; *Sources And Applications Of Ultraviolet Radiation*, Academic Press Inc., London, 56 (1983)
35. A Ledwith, P J Russel, L H Sutcliffe; *J. Chem. Soc. Perkin Trans 2*, **13**, 1925 (1972)
36. M A Johnson, P K T Oldring; *J. Oil Col. Chem. Assoc.*, **73**, 10, 415 (1990)
37. J E Baxter, R S Davidson, H J Hagemann, T Overeem; *Makromol. Chem., Rapid Commun.*, **8**, 311 (1987)
38. H J Hagemann, T Overeem; *Makromol. Chem., Rapid Commun.*, **2**, 719 (1981)
39. K Meir, M Rembold, W Rutsch, F Sitek in *Radiation Curing Of Polymers*; D R Randell (Ed.), The Royal Society Of Chemistry, London, 196 (1987)
40. I H Leaver, G C Ramsey; *Tetrahedron*, **25**, 5669 (1969)
41. W Rutsch, H Angerer, V Desobry, K Dietliker, R Husler in *Proc. 16th Int. Conf. Org. Coat. Sci. Tech.*, Athens, Greece, 423 (1990)
42. D Leopold, H Fischer; *J. Chem. Soc. Perkin Trans 2*, **4**, 513 (1992)
43. W Rutsch, G Berner, R Kirchmayr, R Hüsler, G Rist, N Buehler in *Organic Coatings-Science And Technology Volume 8*; G D Parfitt, A V Patsis (Eds.), Marcel Dekker Inc., New York, USA, 175 (1986)
44. V Desobry, K Dietliker, L Misev, M Rembold, G Rist, W Rutsch; *ACS Symposium Series No.417*, 92 (1990)
45. H Paul, H Fischer; *Helv. Chim. Acta.*, **56**, 1575 (1973)
46. F Jent, H Paul, H Fischer; *Chemical Physics Letters*, **146**, 3, 315 (1988)

47. H J Hagemann, P Oosterhoff, T Overeem, R J Polman, S Van der Werf; *Makromol. Chem.*, **186**, 2487 (1985)
48. W A Green, A W Timms; *Polymers Paint And Colour Journal*, **182**, 43 (1992)
49. F W McLafferty; *Interpretation Of Mass Spectra*, University Science Books, Mill Valley, California, USA, 91 (1980)
50. G Kornis, P de Mayo; *Can J. Chem.*, **42**, 2822 (1964)
51. J S Bradshaw, R D Knudsen, W R Parrish; *J. Chem. Soc., Chem. Commun.*, 1321 (1972)
52. R Kirchmayr, G Berner, R Husler, G Rist; *Farbe Und Lacke*, **88**, 910 (1982)
53. W Wang, G H Hu; *J. Appl. Polym. Sci.*, **47**, 1665 (1993)
54. F D Lewis R T Lauterbach, H G Heine, W Hartman, H Rudolph; *J. Amer. Chem. Soc.*, **97**, 1519 (1975)
55. S P Pappas, A K Chattopadhyay; *J. Polym. Sci., Polym. Letts. Edn.*, **13**, 483 (1975)
56. L H Carlblom, S P Pappas; *J. Appl. Polym. Sci.; Polym. Chem. Ed.*, **15**, 1381 (1977)
57. S Steenken, H P Schuchmann, C Von Sonntag; *J. Phys. Chem.*, **79**, 763 (1975)
58. A Gilbert, J Baggott, *Essentials Of Molecular Photochemistry*, Blackwell Science Publications, 287 (1991)
59. X T Phan; *J. Radiation Curing*, **13**, 1, 18 (1986)
60. J E Baxter, R S Davidson, H J Hagemann, K A McLauchlan, D G Stevens; *J. Chem. Soc.; Chem. Commun.*, **2**, 73 (1987)
61. T Sumiyoshi, W Schnabel, A Henne; *Polymer*, **26**, 141 (1985)
62. M Jacobi, A Henne, A Böttcher; *Polymer Paint and Colour Journal*; **175**, 636 (1985)
63. W Rutsch, K Dietliker, D Leppard, M Köhler, L Misev, U Kolczak, G Rist, *Proc. 20th Int. Conf. Org. Coat. Sci. Tech.*, Athens, Greece, 467 (1994)
64. W Rutsch, G Berner, R Kirchmayr R Hüsler, G Rist, N Bühler, *Proc. 10th Int. Conf. Org. Coat. Sci. Tech.*, Athens, Greece, 241 (1984)
65. K Dietliker, M W Rembold, G Rist, W Rutsch, F Sitek, *Proc. Conf. RADTECH, Florence, Italy*, 3-37 (1987)
66. K Meier, M Rembold, W Rutsch, F Sitek in *Radiation Curing Of Polymer*; D R Randell (Ed.), Royal Society Of Chemistry, 196 (1987)
67. S L Herlihy; *A Study Of The Volatile Materials Released By XV501 Printed Circuit Boards During The Post-Bake Stage Of Processing*, Coates Lorilleux Internal Report (1989)
68. N Arsu, R S Davidson, *J. Photochem. Photobiol. A: Chem.*, **84**, 291 (1994)
69. R S Davidson in *Radiation Curing In Polymer Science And Technology (Volume III- Polymerization Mechanisms)*; J P Fouassier and J F Rabek (Eds.), Elsevier Science Publishers Ltd., Barking, Essex, 153 (1993)
70. D L Bunbury, T M Chan, *Can. J. Chem.*, **50**, 2499 (1972)
71. J C Scaiano, L Johnston; *Pure Appl. Chem.*, **58**, 1273 (1986)

72. K K Dietliker in *Chemistry And Technology Of UV And EB Formulation For Coatings, Inks And Paints (Volume 3-Photoinitiators For Free Radical And Cationic Polymerisation)*; P K T Oldring (Ed.), SITA Technology Ltd., 59 (1991)
73. P A Leermakers, P C Warren, G F Vesley; *J. Am. Chem. Soc.*, **86**, 1768 (1964)
74. R S Davidson, D Goodwin; *J. Chem. Soc., Perkin Trans. II*, 993 (1982)
75. M V Encinas, E A Lissi, A Zanocco, L Stewart, J C Scaiano; *Can. J. Chem.*, **62**, 386 (1984)
76. H F Gruber; *Prog. Polym. Sci.*, **17**, 953 (1992)
77. S Göthe; *Proc. 17th FATIPEC Conf.*, **2**, 13 (1984)
78. N S Allen, D Mallon, A W Timms, W A Green, F Catalina, T Corrales, S Navaratnam, B J Parsons; *J. Chem. Soc. Faraday Trans.*, **90**, 1, 83 (1994)
79. A Dias; *Polymeric and Polymerisable Photoinitiators*, PhD thesis, University of Kent Canterbury (1994)
80. J N Pitts, R I Letsinger, R P Taylor, J M Patterson, G Rectenwald, J B Martin; *J. Amer. Chem. Soc.*, **81**, 1068 (1959)
81. D G Anderson, R S Davidson, J J Elvery; *Polymer*, **37**, 12, 2477 (1996)
82. G Li Bassi; *Double Liaison-Chimie des Peintures*, **32**, 361, 17 (1985)

CHAPTER 6

Factors affecting the polymerisation reaction

6.1 INTRODUCTION

Although a number of radiation curing technologies exist, for the purpose of this project the term UV curing has been defined in Chapter 1 as relating specifically to the UV initiated free radical polymerisation of acrylate double bonds. Within this context the presence of a photoinitiator in the formulation is to provide sufficient free radicals to effectively initiate the polymerisation chain reaction. Although the mechanism and course of this polymerisation reaction is not dependent on the photoinitiator used, the reaction rate R_p is, according to the equation¹:

$$R_p = K_p \cdot \left(\frac{R_i}{K_t} \right)^{\frac{1}{2}} \cdot [M] \quad (1)$$

K_p = propagation rate constant ($\text{dm}^3 \text{mol}^{-1} \text{s}^{-1}$), $[M]$ = concentration of acrylate double bonds (mol dm^{-3}), K_t = termination rate constant ($\text{dm}^3 \text{mol}^{-1} \text{s}^{-1}$) and R_i = rate of initiation.

However, the polymerisation kinetics of the entire radiation curing reaction are not as straightforward as this equation suggests. When curing takes place in an oxygen atmosphere, the reaction profile has a characteristic sigmoidal shape, as shown in Figure 6.1, where the profile can be divided into three distinct regions²:

- i) Induction period
- ii) Rapid polymerisation
- iii) Full cure

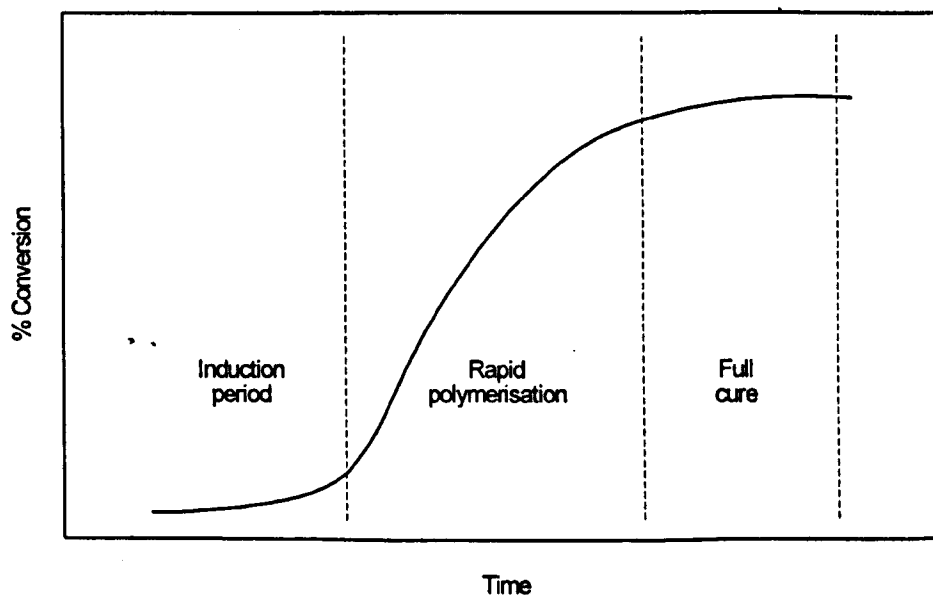


Figure 6.1 *Reaction profile of a typical UV curing reaction*

The induction period results from the effects of oxygen inhibition, such that once the dissolved oxygen has been consumed a rapid polymerisation reaction takes place, but quickly starts to slow again as the viscosity increases and a gel is formed. This is claimed to occur within only a few percent conversion³, with the rapidly increasing viscosity causing the growing radical chains to become trapped in the polymer network^{3,4}, preventing further reaction.

Although much of the polymerisation reaction occurs in the gel phase, it is claimed that the acrylate groups retain a relatively high mobility, since a temporary excess free volume results from the time lag between polymerisation and shrinkage⁵. Some additional mobility may also result from the movement of radical centres by hydrogen abstraction reactions. Despite this, 100% conversion was claimed to be almost impossible to achieve, with attainable conversion decreasing as acrylate functionality increases⁵.

Another suggested reason for the reduction in rate constant as the cure reaction proceeds is that the restricted mobility of free radicals following gelation reduces the photoinitiator quantum yield. This is a consequence of an inability of the newly formed radical pair to separate sufficiently and initiate new polymer chains before cage recombination occurs⁶.

Some work has also been done to quantify individual rate constants for propagation (K_p) and termination (K_t) reactions⁷⁻⁹, but their values were found to change continually during cure because of reduced diffusion. As a result, other factors such as formulation type, temperature and the presence of oxygen were also speculated to affect the values of K_p and K_t .

Despite the difficulties in fully defining the reaction kinetics of a UV curing reaction in its later stages, the polymerisation rate R_p can still be measured and used effectively in the early stages of cure where a steady state exists. This is possible since virtually no double bonds have reacted and the viscosity increase has not yet become a dominant factor in the kinetics.

6.1.1 Measuring curing efficiencies of photoinitiators and synergists

According to equation (1), the polymerisation rate R_p of a UV curing reaction is dependant on the rate of initiation R_i . Direct measurement of the rate can therefore be used to give quantum efficiencies of various photoinitiators, where values for the quantum yield of initiation Φ_i are obtained using equation (2).

$$R_i = \Phi_i \cdot I_0 \cdot (1 - 10^{-\epsilon c l}) \quad (2)$$

I_0 = incident light intensity, ϵ = molar extinction coefficient ($\text{mol dm}^{-3}\text{cm}^{-1}$),

c = concentration (mol dm^{-3}), l = path length (cm)

One of the principal requirements when producing data of this type is the use of a monochromatic light source, because of the variation of ϵ as a function of wavelength. This limits the direct commercial applicability of the results, where polychromatic medium pressure mercury lamps are used as standard. Measurement of polymerisation rate under commercial conditions (medium pressure mercury lamp, air environment and photoinitiators formulated on a weight percent basis) would more accurately be described as curing effectiveness, since it is the overall measure of the efficiency of light absorption, radical generation and the reactivity of derived radicals towards

acrylate double bonds. This approach represents the best way of defining the most reactive photoinitiators under their end use conditions.

As previously described, the use of empirical tests is often not sufficiently differentiating to provide an accurate measure of photoinitiator reactivity, so more quantitative instrumental techniques are commonly employed. The most widely used is infrared (IR) spectroscopy, which is used to measure the percentage of acrylate bonds reacted through changes in the acrylate C=C_{stretch} bands at 1620, 1640 cm⁻¹ or the acrylate C-H_{deformation} band at 810 cm⁻¹. This is often done by comparing the IR spectra before and after curing^{10,11}, but IR spectroscopy can also be used to follow the polymerisation reaction directly, either by recording the IR spectrum of a sample between successive UV exposures^{12,13}, or in a dynamic arrangement with continuous UV light exposure and monitoring of a particular IR absorption band^{14,15}. The latter was first described for studying UV curing reactions by Lee and Doorakian¹⁶ but has been developed and more extensively used for very fast reactions by Decker and Moussa^{2,6,17,18}, who termed the technique Real Time Infrared Spectroscopy (RTIR). RTIR offers a number of specific advantages over experiments involving alternate UV exposures and IR spectral acquisitions, the most important of which are; faster and more representative reaction times, less complex experiments and the elimination of post-cure effects between exposures.

Rapid advances in both equipment design and the computer power required for data handling during recent years have meant that RTIR can also be achieved using a rapid scanning Fourier Transform Infrared spectrometer (FTIR). This new technique, which would be more appropriately termed RT-FTIR, has the advantage over single wavelength measurements that the complete IR spectrum is obtained at every sampling interval, allowing a more in-depth study of the changes that occur during cure. RT-FTIR has been described in the literature¹⁹⁻²¹ but still suffers from slower reaction times than those possible using RTIR.

One of the aims of this work was to set up and validate an RT-FTIR instrument / method, as well as using it to provide a quantitative measure of the curing effectiveness for a range of photoinitiators. To the author's knowledge, this is something that has not been reported in the literature before, with published results normally reflecting a research or commercial interest in a particular class of photoinitiator. Where possible these literature references have been used to validate the results generated in this work.

Since Type II photoinitiators act via a bimolecular mechanism with an amine synergist, the chemical structure of the synergist will also have an influence on the efficiency of photoinitiation. This is particularly true because the active curing radical produced by this interaction is generally accepted to come from the amine molecule, either by a hydrogen abstraction or an electron and

proton transfer mechanism²². However, despite their obvious importance in Type II initiation processes, the structure / activity relationships of amine synergists attract less research interest than photoinitiators. Although some studies cover a relatively wide range of structure types²³, most refer to a more limited range such as simple aliphatic²⁴, aromatic²⁵ or photoinitiator functional amines²⁶⁻²⁸.

Only a few amine synergist types are generally used in the inks and coatings industry; the relative effectiveness of these and a number of other key materials are examined in this chapter.

6.1.2 Factors that affect the polymerisation reaction

One of the principal factors that affects the rate and extent of polymerisation in a UV curing reaction is the number of free radicals formed per unit volume by the photoinitiator. In the case of a Type I photoinitiator this is influenced by both the relative photoinitiator efficiency and the concentration of photoinitiator used. For Type II photoinitiators, the bimolecular nature of the reaction means that the type and concentration of the amine synergist will also have a significant effect on the number of initiating radicals formed. The effective curing of a coating to achieve the desired performance characteristics will however not be related simply to the radical density achieved. A number of other factors will also be important, such as the distribution of radicals through the film, the presence of amine to counter oxygen inhibition at the surface, and the functionality of the formulation.

The influence of photoinitiator concentration has been reported²⁹⁻³² but is complicated by a number of factors. Hencken²⁹ showed that there was an optimum photoinitiator concentration of 10 %wt for a thin printing ink formulation to give the fastest cure speed, but he also showed that this corresponded to the concentration at which the relative UV transmission dropped to 0 %, accounting for the rapid decline in cure speeds at higher photoinitiator levels.

The influence of photoinitiator concentration is also dependent on how the cure is measured, with minimum cure speed (thumb twist) or scratch resistance tests determining the film's physical properties and not the number of acrylate bonds reacted. At very high radical densities these parameters will be different, with a large percentage of acrylate bonds reacted, but the shorter kinetic chain length during the polymerisation changing considerably many of the resistance and physical properties. This effect was shown by Hanrahan³⁰, where the pendulum hardness of cured formulations containing increasing levels of photoinitiator resulted in a gradual lowering of the hardness values. It was suggested that a decline in observed properties above an optimum photoinitiator concentration could be due to the termination reaction becoming significant^{30,31}, but no evidence has been presented to support this theory.

The influence of temperature on the kinetics of a UV curing reaction has not been as well studied as might have been expected, with published results showing some marked inconsistencies. For experiments performed under nitrogen³³⁻³⁵, or with the exclusion of air³⁶, a general increase in polymerisation rate with increasing temperature was observed, but experiments in an air atmosphere³⁷ showed a decreasing polymerisation rate with increasing temperature. The latter was explained as a consequence of a chain transfer termination process whose activation energy is higher than that of the propagation reaction. Apparent negative activation energies were also observed by Moore³³ but no explanation was given. Further work is clearly required to unravel the true situation with regard to the effect of temperature, particularly in the presence of air.

6.2 RESULTS AND DISCUSSION

6.2.1 Developing an RT-FTIR system and procedure

In order to construct and effectively use a state of the art RT-FTIR system, consideration must be given to a number of factors that fall into three general categories; system configuration / data acquisition, sampling procedure and data handling. In this section a detailed description of the RT-FTIR system developed is presented in the context of these categories.

6.2.1.1 System configuration and data acquisition

A general schematic of the RT-FTIR system developed during this work is shown in figure 6.2. There are two key pieces of hardware involved; an FTIR bench which collects the IR spectral data, and a UV light source which simultaneously irradiates the sample.

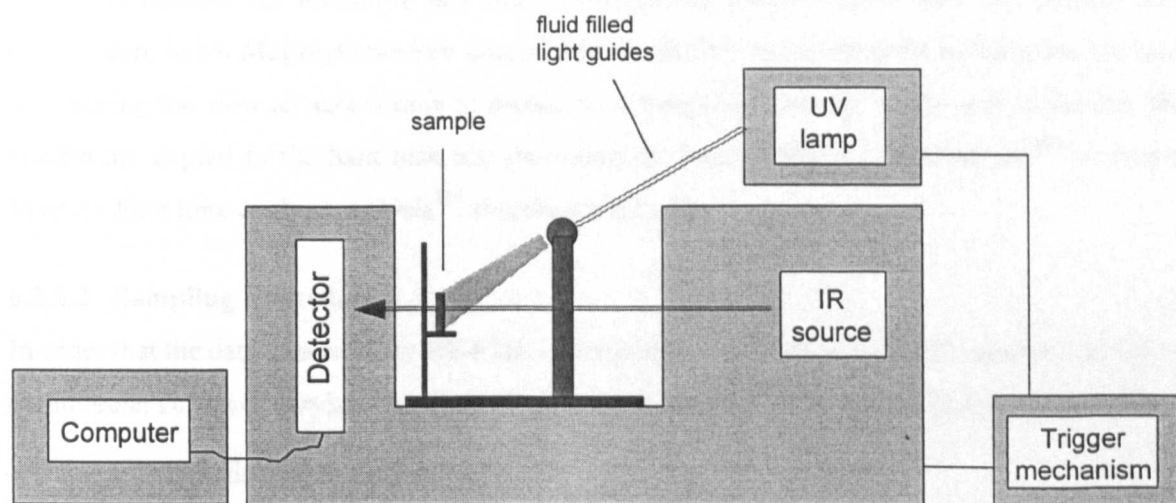


Figure 6.2 *General schematic of an RT-FTIR system*

The Unicam Research Series (RS) FTIR bench (Unicam, Cambridge, England) represents the core of the system and is optimised for rapid scanning and continuous data acquisition through the use of fast mirror speeds; a mercury cadmium telluride (MCT) detector and a bench resolution of 8 cm^{-1} . Although sampling rates of up to 30 scans per second are achievable by the bench, the configuration used has a sampling rate of 16 scans per second in order to optimise the data transfer rate, resolution and run duration.

The UV light source used is based around a Maccam Flexicure spot curing system (Maccam Photometrics, Livingstone, Scotland), consisting of a 400 Watt medium pressure mercury arc, or 400 Watt metal halide doped lamp inside a metal housing fitted with a timer, external trigger switch and high speed shutter. The light from the lamp is focused equally into two holes at the front of the housing, each of which contains one end of a flexible fluid filled light guide that directs the light to the sample area in the FTIR. The guides are held in a fixed position with respect to the sample by means of a specially constructed arch which is attached to the bench's standard

baseplate, and contains two holes through which the other ends of the two light guides fit. The holes are drilled at a converging angle such that the light from the two guides forms a single 1 cm radius circle on the sample. This arrangement has the advantage that the bench can be alternated between general FTIR work and RT-FTIR merely by installing or removing the light guides, or changing the baseplate if other sampling techniques such as diffuse reflectance are required.

All the events involved in the data acquisition including FTIR settings such as mirror velocities, resolution, iris size and number of spectra to be collected are controlled through the Mattson First MacrosTM software. Once the run has started, a switch box and trigger mechanism responds to a signal pulse from the FTIR at the end of the first scan, and sends a new signal to the Flexicure unit, activating the shutter mechanism and irradiating the sample with UV light for a predefined time. The FTIR collects 125 interferograms and simultaneously transfers them via a fast parallel data transfer card to a 4 Megabyte random access memory (RAM) virtual drive on a computer, the hard disk having too slow an access time to accept the information directly. At the end of the run, the spectra are copied to the hard disk and processed by another Mattson First MacroTM to give a Mattson First time evolved analysisTM absorbance data file.

6.2.1.2 Sampling procedure

In order that the data generated by RT-FTIR experiments is as valid as possible compared to the commercial curing of acrylate based coatings, there are several important sampling requirements;

1. Irradiation in the presence of air
2. Use of a representative film thickness
3. Use of an oligomer / monomer mixture

Most published results on RTIR involve the use of samples sandwiched between two KBr windows^{12,13,16,20}, typically using a spacer of known thickness. This arrangement excludes air and therefore limits the applicability of the results. Only the work of Decker^{2,6,17,18} was found to involve samples irradiated in the presence of air.

Although most work using RTIR involves spectral measurements in a transmission geometry, some work has been reported using specular reflectance¹⁹ and Attenuated Total Reflectance²⁰ (ATR) geometries. The latter measures curing only at the crystal interface which may cause problems in interpreting the results obtained if any cure gradient exists across the sample. A transmission geometry was favoured for this work because for its particular suitability for experiments in an air atmosphere.

For this work, a mixture of 80 parts oligomer to 20 parts monomer was used as a standard formulation to which photoinitiators and synergists were added. The oligomer was an aliphatic polyether urethane diacrylate, CN934 obtained from Cray Valley, and the monomer was trimethylolpropane triacrylate (TMPTA) from the Aldrich Chemical Co. Ltd. Both were used without further purification. The formulation was coated onto a single 2cm x 2cm KBr crystal using a glass rod, to give a film of approximately 10-12 μm thickness and of sufficiently high viscosity to prevent it flowing down the crystal when held vertically. At the end of the run the film was removed by immersion of the crystal in acetone, which partially destroys it and allows it to be wiped off the crystal surface with a tissue. The crystal could then be reused. This procedure was particularly effective for urethane oligomers and favoured their use over the more difficult to remove epoxy oligomers.

As detailed in chapter 4, the effects of UV light screening in a 10 μm thick film can be quite significant. For this reason the UV light absorption by components other than the photoinitiator were minimising by the use of an aliphatic oligomer, monomer and amine synergist.

6.2.1.3 Data handling

Once an RT-FTIR experiment has been processed and saved in the appropriate format, advanced IR software packages such as the Mattson First Time Evolved Analysis™ can be used to display the data. Whilst contour plots or 3-dimensional plots such as that shown in figure 6.3 can be constructed and very effectively show the changes that occur during cure, they are of little practical use in quantifying these changes.

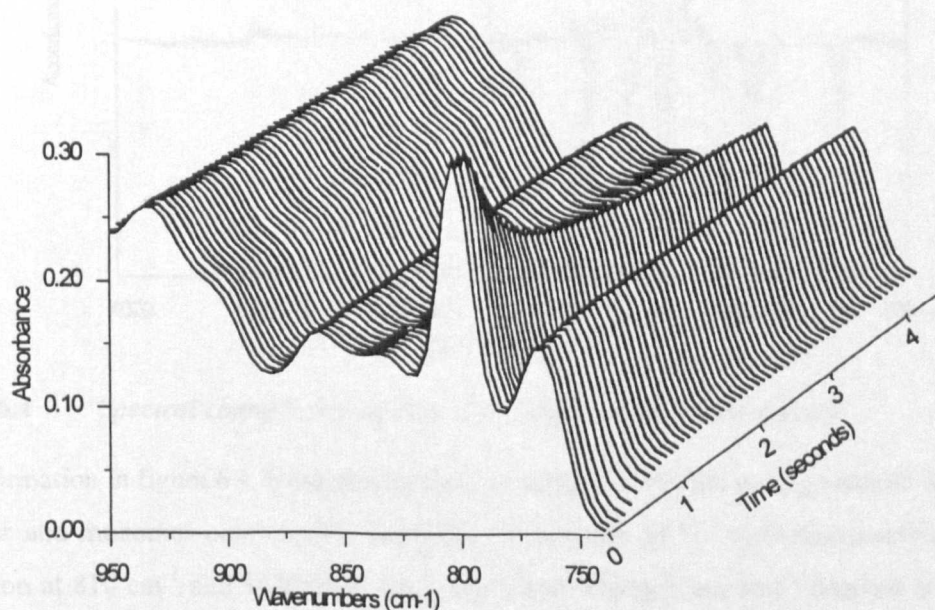


Figure 6.3 Changes in the IR spectrum ($900\text{-}750\text{ cm}^{-1}$) with time in an RT-FTIR experiment

Spectral changes occurring during cure can also be illustrated by overlapping a number of spectra at different stages in the cure process. This can be done using either an uncoated KBr window or the uncured material coated on the KBr window as the reference spectrum, as shown in figures 6.4a and 6.4b respectively. Figure 6.4a shows the spectral changes in relation to the uncured material, and is the clearest way of displaying the extent of these changes. The latter displays only the changes occurring in the spectrum, more clearly showing minor peak intensity changes, peak broadening and peak shifts.

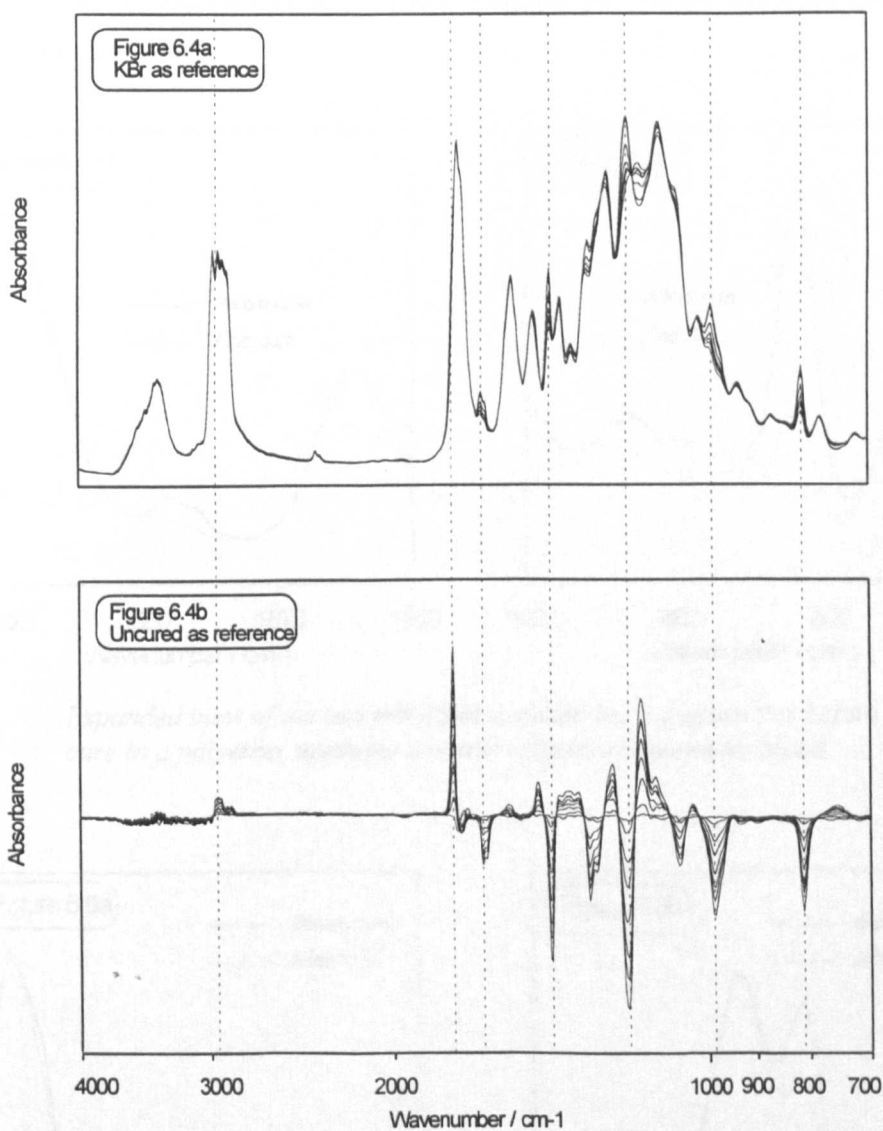


Figure 6.4 *Spectral changes during cure using different reference spectra*

The information in figure 6.4 demonstrates that, for a typical acrylate curing reaction involving the oligomer and monomer combination described, in addition to the well documented changes in absorption at 810 cm^{-1} and $1620/1640\text{ cm}^{-1}$, significant changes are also observed at 988 cm^{-1} , 1189 cm^{-1} , 1298 cm^{-1} and 1409 cm^{-1} in the fingerprint region. Minor spectral changes are also associated with the $\text{C-H}_{\text{stretch}}$ band at 2947 cm^{-1} . The apparently large change in the carbonyl $\text{C=O}_{\text{stretch}}$ band at 1700 cm^{-1} , shown in figure 6.4b, is associated with a peak narrowing at the high wavenumber side.

An expanded view of the 1620/1640 cm^{-1} and 810 cm^{-1} band regions, as displayed in figures 6.5a and 6.5b respectively, shows that, for a combination of the polyether urethane acrylate oligomer CN934 and the monomer TMPTA, both regions also have other non-acrylate bands which partially overlap those of interest. The extent of this problem varies according to the oligomer type used. Figures 6.6a and 6.6b show similar plots for formulations based on a typical epoxy oligomer / monomer blend using the same photoinitiator type and level. From figure 6.6 it is evident that there is less carbonyl band overlap with the 1620/1640 cm^{-1} doublet, but significantly more overlap of other bands adjacent to the 810 cm^{-1} acrylate band when using an epoxy oligomer compared to a urethane one.

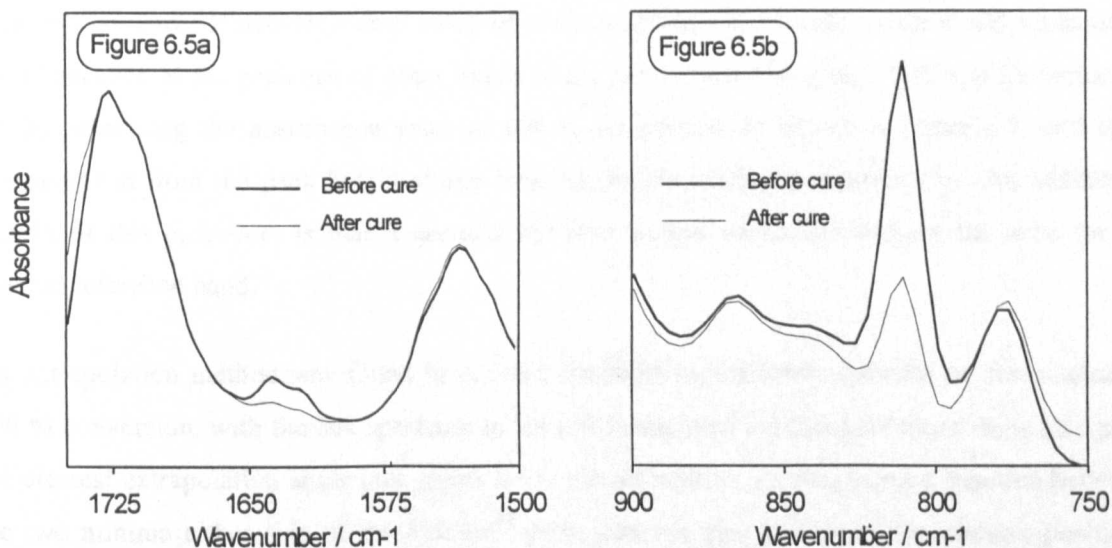


Figure 6.5 Expanded view of the two principal acrylate bond frequencies before and after cure in a polyether urethane acrylate oligomer / monomer blend

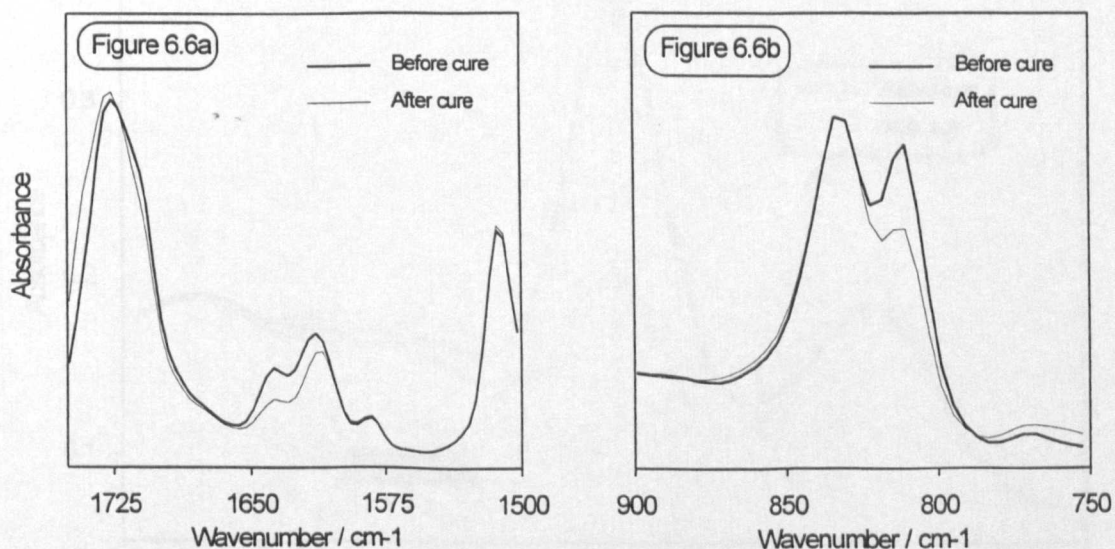


Figure 6.6 Expanded view of the two principal acrylate bond frequencies before and after cure in an epoxy acrylate oligomer / monomer blend

The most suitable way of quantifying the rate and extent of cure was considered to be through changes in the 810 cm^{-1} acrylate C-H_{deformation} band in formulations based on the aliphatic polyether urethane diacrylate oligomer CN934 and the monomer TMPTA.

It is known that the percentage of double bonds reacted can be calculated from peak area or peak height measurements at $1620/1640\text{ cm}^{-1}$ or 810 cm^{-1} using the general formula^{2,13};

$$\% \text{ Conversion} = \frac{(A_{810})_0 - (A_{810})_t}{(A_{810})_0} \times 100 \quad (3)$$

Peak area measurements are easily applicable to equation (3), since at 100 % conversion the peak area will be zero. However, a zero value of peak height at 100 % conversion is not necessarily found because of the presence of other bands in the same spectral region. This can be corrected for by estimating the absorbance value at 100 % conversion as shown in figure 6.7, and then subtracting it from the peak height at any time (t), before applying equation (3). An additional benefit of this procedure is that it corrects for film weight variations without the need for an internal reference band.

An extrapolation method was found to provide the most reproducible estimate of absorbance at 100 % conversion, with the last spectrum in the run being used for this procedure since this gave the clearest extrapolation angle (see figure 6.7). An alternative method using a baseline between the two minima either side of the 810 cm^{-1} peak was not practical since the minima positions shifted as a function of cure, making it necessary to integrate each of the 125 scans manually. This method also introduced errors due to the presence of adjacent absorbance bands.

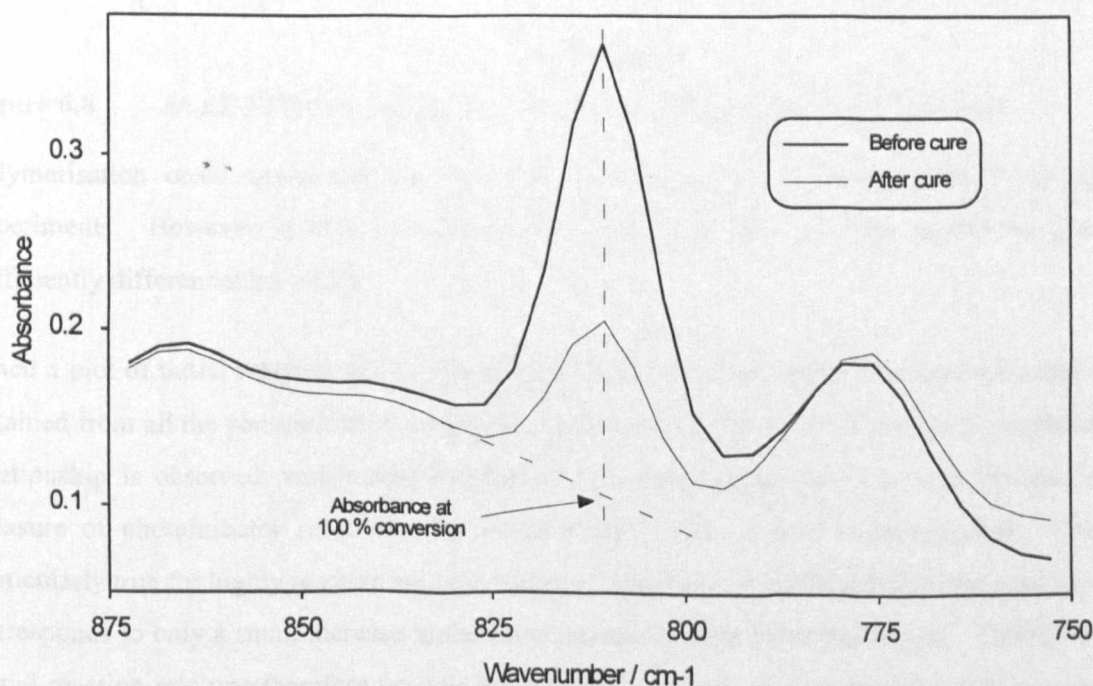


Figure 6.7 Estimation of the absorbance peak height value at 100% conversion

A Mattson First Macros™ program “Slice” was used to obtain an ASCII file of the peak height measurements at 810 cm^{-1} with time. This was then imported into a typical computer spreadsheet program and the absorbance value at 100% conversion subtracted from all the data points simultaneously, before applying equation (3) to generate a new ASCII file of percent conversion with time. Each sample would typically be run 3 or 4 times and an average data file of percent conversion with time generated in the spreadsheet.

The new average data file of percent acrylate bond conversion with time was plotted, as shown in figure 6.8, and two key pieces of information obtained:

1. The initial reaction rate ($\% \text{ s}^{-1}$) - calculated from the curve gradient at the steepest point
2. The final % conversion - the conversion value of the last data point in the run

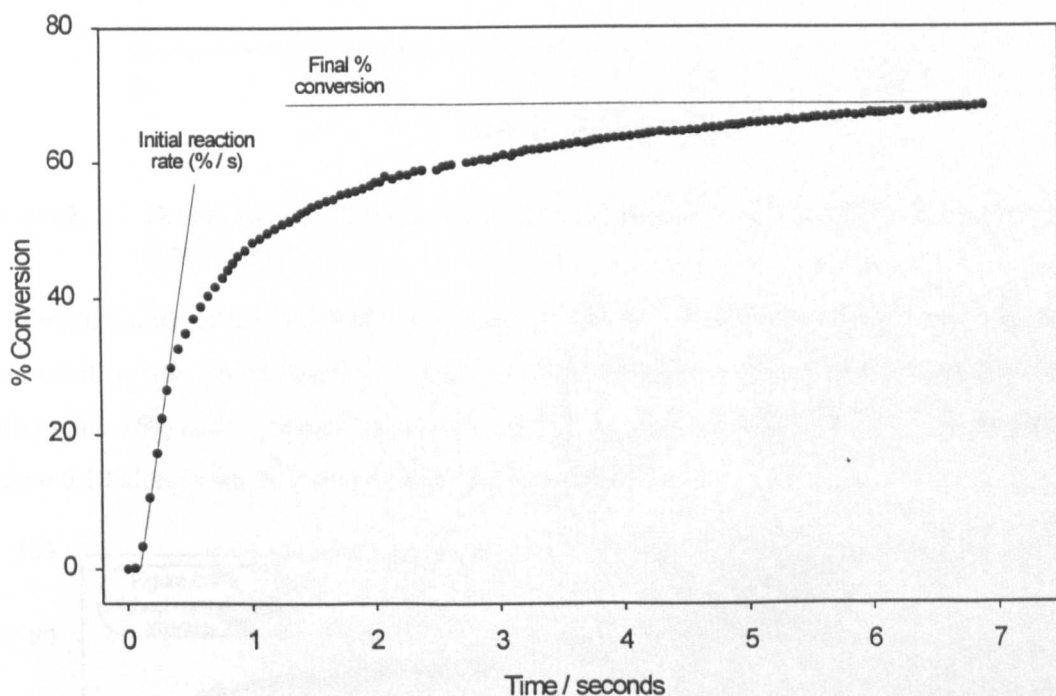


Figure 6.8 An RT-FTIR run displayed as % conversion of acrylate bonds with time

Polymerisation onset times can also be used as a measure of curing reactivity in RTIR experiments. However, in this case the data sampling rate was not high enough to provide sufficiently differentiating results.

When a plot of initial reaction rate vs. percent acrylate bond conversion is constructed using data obtained from all the photoinitiators evaluated in this work, as shown in figure 6.9, an exponential relationship is observed, which demonstrates that although either parameter can be used as a measure of photoinitiator reactivity, the initial reaction rate is more differentiating. This is particularly true for highly reactive systems where a large increase in measured initial reaction rate corresponds to only a small increase in the final percent acrylate bond conversion. The RT-FTIR initial reaction rate was therefore used as the principal measure of photoinitiator effectiveness in this work.

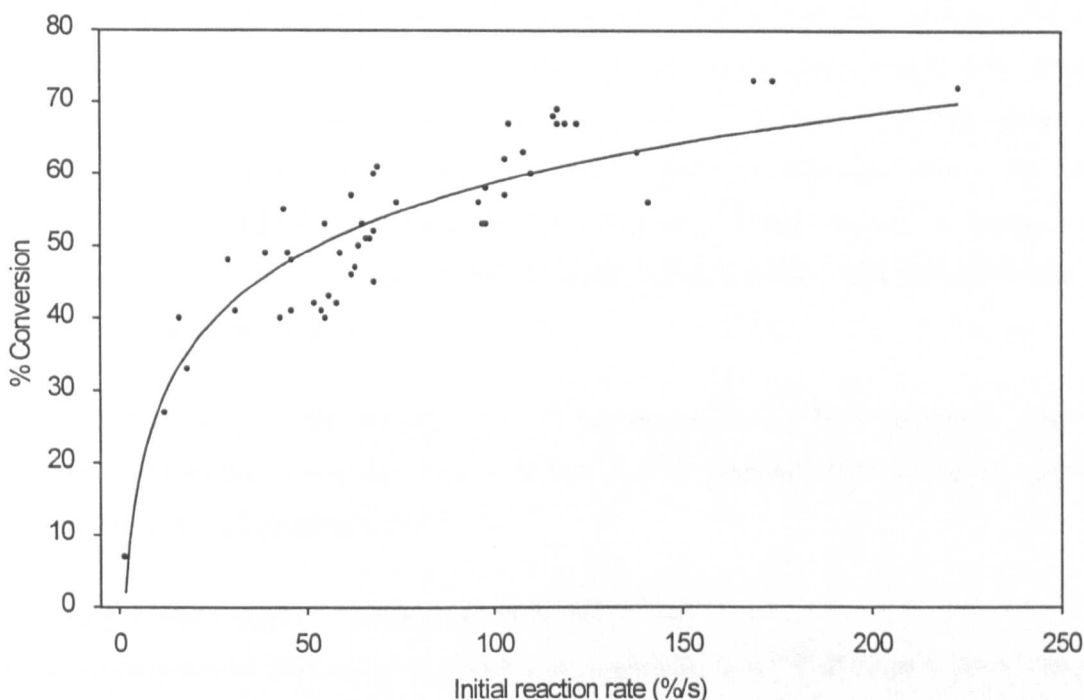


Figure 6.9 *The relationship between initial reaction rate and the final percent acrylate bond conversion*

The reproducibility of this RT-FTIR procedure was found to be good, with the two extremes of reproducibility; the photoinitiators 2-benzyl-2-dimethylamino-1-(4-morpholinophenyl) butan-1-one (Irgacure 369) and 1-phenyl-2-hydroxy-2-methyl propan-1-one (Darocure 1173), being shown in figure 6.10 along with their mean and variance statistics.

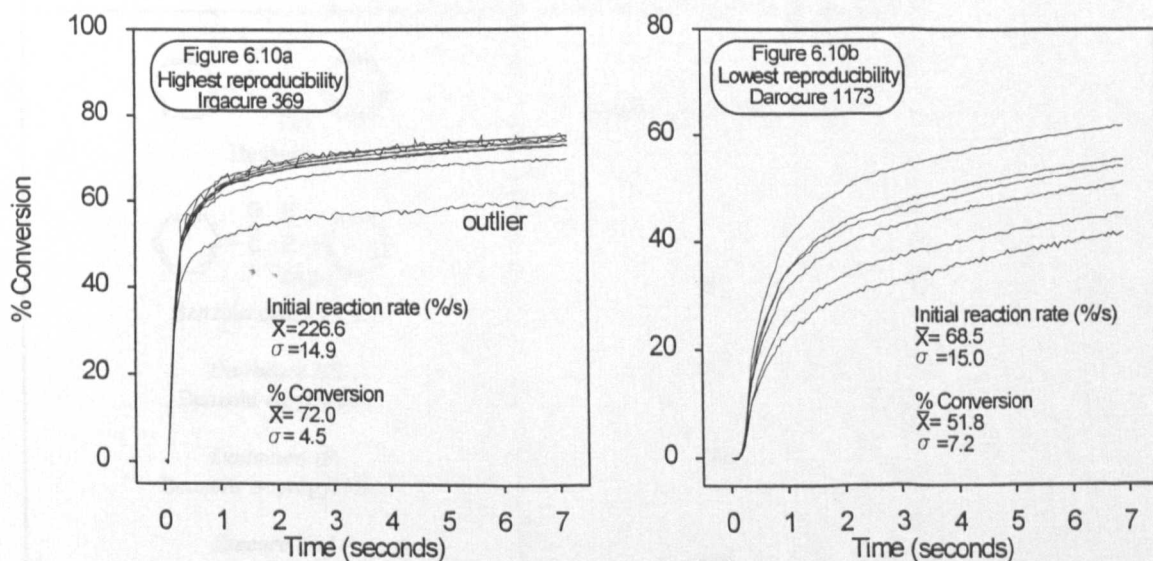


Figure 6.10 *Highest and lowest data reproducibility for RT-FTIR experiments*

In the case of photoinitiators such as Darocure 1173, shown in figure 6.10b, an average cure profile would be calculated on a computer spreadsheet from all the data, often with additional samples being run in order to improve the accuracy. However, in the case of photoinitiators such as Irgacure 369, shown in figure 6.10a, where the reproducibility of the technique is higher,

outliers can become obvious within a series of 4 or 5 runs. The cure profile of these outliers always showed a lower reactivity than the other runs in the series, and was ascribed to increased oxygen inhibition in low film thickness samples; with generally low absorption intensity of the IR spectra providing additional evidence for this. Where this situation arose the accuracy of the data was improved by running additional samples and eliminating any obvious outliers. An example of a curve that would be considered to be an outlier is shown in figure 6.10a, although in this case it still contributes to the statistics given.

In general it was found that strongly UV absorbing photoinitiators displayed greater reproducibility than weakly absorbing ones, and that Type II photoinitiators displayed greater reproducibility than Type I photoinitiators.

6.2.2 Curing effectiveness of photoinitiators by RT-FTIR

The curing effectiveness of different photoinitiators was assessed in an 80:20 ratio combination of the urethane diacrylate oligomer CN934 and the monomer TMPTA by RT-FTIR. The formulations also contained 2 %wt of the amine synergist N-methyl diethanolamine (MDEA). In order to maximise our understanding, the results presented here are discussed in terms of the chemical structures and UV absorption spectra; measured at 0.02 g dm^{-3} in methanol solution.

Benzoin ethers

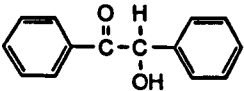
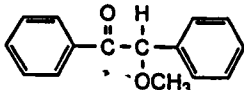
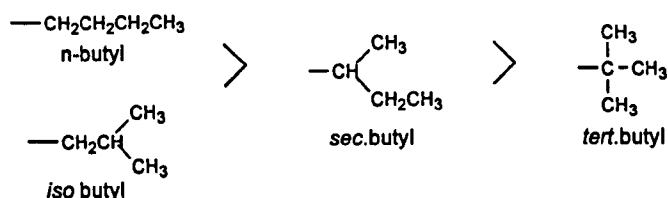
Photoinitiator	Initial reaction rate ($\% \text{ s}^{-1}$)
 Benzoin	Sample gels on preparation
 Benzoin methyl ether	63
<i>Daitocure EE</i> Benzoin ethyl ether	64
<i>Daitocure IP</i> Benzoin isopropyl ether	43
<i>Esacure EB3</i> Benzoin butyl / isobutyl ethers	67
<i>Esacure EB2</i> Benzoin isobutyl ether	46

Table 6.1 Rates of cure for benzoin ether photoinitiators in an oligomer / monomer blend by RT-FTIR

The results in table 6.1 show that the benzoin alkyl ethers tested have roughly similar reactivity, with only the isopropyl and isobutyl ethers showing slightly reduced reactivity relative to the others. The fact that the ether derivatives have virtually identical UV absorption spectra suggests that the reason for the difference is a chemical one. It is speculated that the benzoin isobutyl ether has a reduced reactivity due to its low chemical purity, since it was found by GC analysis to contain 7.6 % of the photochemically inactive benzoic acid isobutyl ester. It can also be speculated that the lower reactivity of the benzoin isopropyl ether is because it is based on a secondary alcohol whereas all the other derivatives are based on primary alcohols. Although further work with a range of pure benzoin ethers would be required to confirm this, the observations agree with those of Osborn and Sandner³⁸ who found that for a range of benzoin butyl ethers the order of reactivity was;



Hydroxyalkylphenones

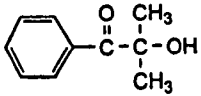
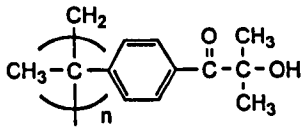
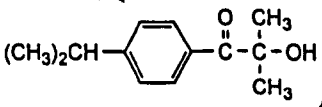
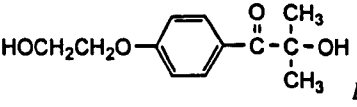
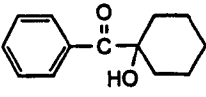
Photoinitiator	Initial reaction rate (% s ⁻¹)
 <p>Darocure 1173 1-Phenyl-2-hydroxy-2-methyl propan-1-one</p>	68
 <p>Esacure KIP Polymeric 1-phenyl-2-hydroxy-2-methyl propan-1-one</p>	55
 <p>Darocure 1116 4-Isopropyl-phenyl-2-hydroxy-2-methyl-2-propan-1-one</p>	74
 <p>Darocure 2959 4-(2-Hydroxyethoxy)-phenyl-2-hydroxy-2-methyl-2-propan-1-one</p>	119
 <p>Irgacure 184 1-Hydroxycyclohexyl phenyl ketone</p>	65

Table 6.2 Rates of cure for hydroxyalkylphenone photoinitiators in an oligomer / monomer blend by RT-FTIR

The results in table 6.2 show that fundamentally very similar molecules can give rise to distinctly different curing activity. The photoinitiators Darocure 1173 and Irgacure 184 represent the basic chemical structure within this group, with both showing the same reactivity and having very similar UV absorption spectra.

Substitution of an alkyl group at the 4-position in the aromatic ring leads to a red spectral shift in the case of Darocure 1116 and Esacure KIP, allowing them to utilise more of the output from the medium pressure mercury curing lamp, as shown in figure 6.11. This results in a slightly increased reactivity for Darocure 1116, as would be expected, but a slight decrease in reactivity for Esacure KIP. The lower reactivity is speculated to be a consequence both of the reduced mobility of the macroradical, and of the polymeric nature of the photoinitiator causing a viscosity increase in the formulation. This effect is discussed in greater detail in 6.2.5.

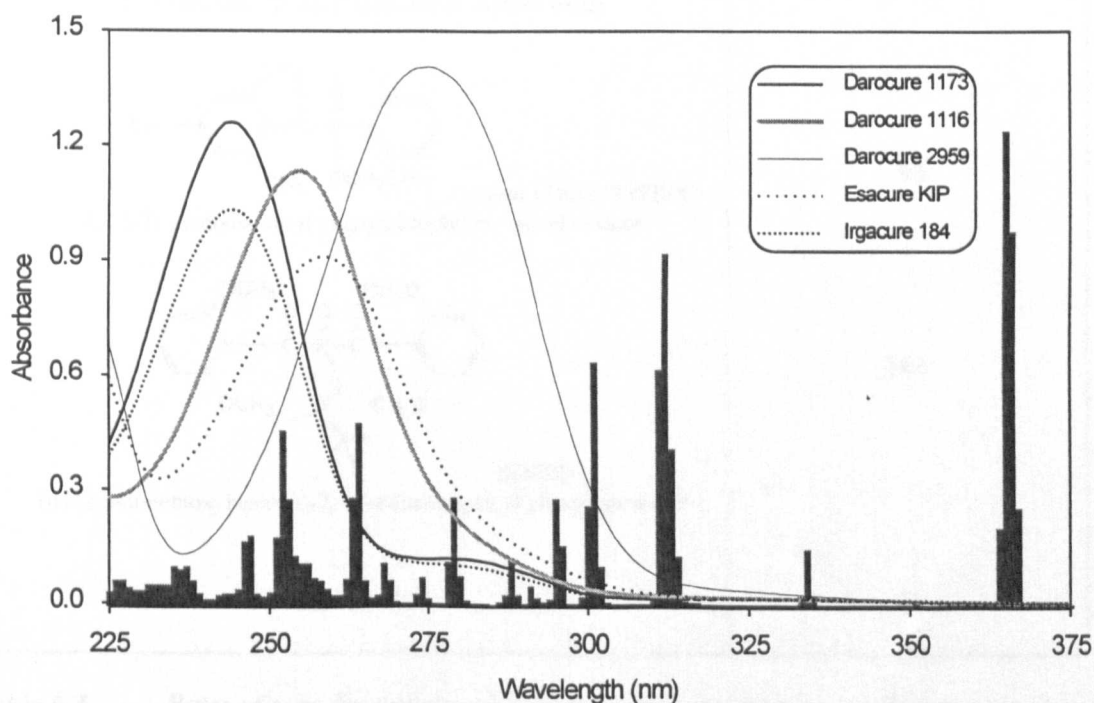


Figure 6.11 The UV absorption spectra of hydroxyalkylphenone photoinitiators and their relationship with a medium pressure mercury curing lamp emission spectrum

Substitution of a (2-hydroxyethoxy) group at the 4-position in the aromatic ring leads to a larger red absorbance shift and allows even greater light utilisation. For this reason, Darocure 2959 displays the highest curing activity within this class of photoinitiator.

These results differ somewhat from those reported by Ohngemach, Koehler and Wehner³⁹ who reported that the order of reactivity was:

$$\text{Darocure 1173} \geq \text{Darocure 1116} \gg \text{Darocure 2959}$$

Although a number of techniques were used to arrive at their conclusion, a detailed analysis of the experimental conditions reveals that all the tests involve thick films (50-200 μm) and high

photoinitiator concentrations (2-5 %wt). Due to their red shifted absorption bands, this will inevitably lead to a slight screening effect in the UVB region for Darocure 1116 and severe screening for Darocure 2959, causing both photoinitiators to appear, relative to Darocure 1173, less reactive than they actually are.

Acylphosphine oxides

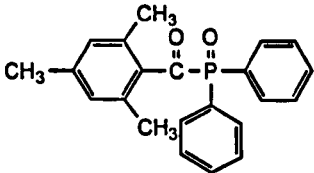
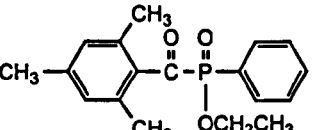
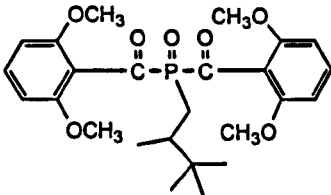
Photoinitiator	Initial reaction rate (% s ⁻¹)
 <p><i>Lucerin TPO</i> 2,4,6-Trimethylbenzoyl diphenyl phosphine oxide</p>	138
 <p><i>Lucerin LR8893X (TEPO)</i> 2,4,6-Trimethylbenzoyl phenylphosphinic acid ethyl ester</p>	98
 <p><i>BDTPO</i> Bis (2,6-dimethoxybenzoyl)-2,4,4-trimethylpentyl phosphine oxide</p>	141
Irgacure 1700	97

Table 6.3 Rates of cure for acylphosphine oxide photoinitiators in an oligomer / monomer blend by RT-FTIR

The results in table 6.3 show that the bis acylphosphine oxide, BDTPO, has the highest reactivity in this class, with Lucerin TPO, the most commonly used, being only marginally less effective. BDTPO is however only commercially available as a 1:3 blend with Darocure 1173 under the trade name Irgacure 1700. The reactivity of this blend is considerably lower than BDTPO alone because of the diluting effect of the less reactive Darocure 1173.

Although all three materials show similar UV absorption spectra, with weak (n-π*) bands extending into the near visible region, the spectrum for TEPO has a lower absorbance intensity and could account for its lower reactivity relative to the other two. It is also possible that TEPO's structural similarity to the acylphosphonate photoinitiators, known to be of lower reactivity⁴⁰, could be of importance.

Although the use of acylphosphine oxide photoinitiators is well known and well reviewed⁴¹⁻⁴⁵, the author could find no references comparing the relative curing efficiencies of these materials without the added influence of pigment or other photoinitiators.

α -Aminoalkylphenones

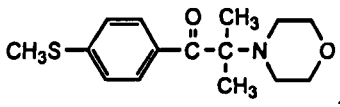
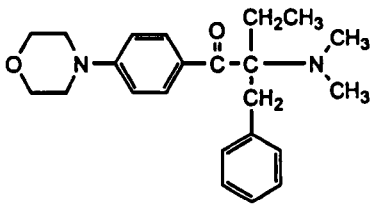
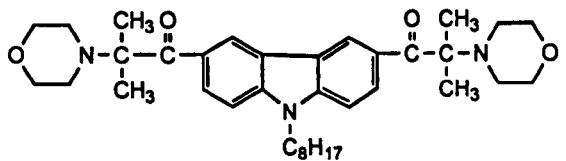
Photoinitiator	Initial reaction rate (% s ⁻¹)
 <p><i>Irgacure 907</i> 2-Methyl-1-[4-(methylthio)phenyl]-2-morpholino propan-2-one</p>	169
 <p><i>Irgacure 369</i> 2-Benzyl-2-dimethylamino-1-(4-morpholinophenyl) butan-1-one</p>	223
 <p><i>Radstart N1414</i> 3,6-Bis(2-morpholinoisobutyryl) N-octyl carbazole</p>	174

Table 6.4 Rates of cure for α -aminoalkylphenone photoinitiators in an oligomer / monomer blend by RT-FTIR

The results in table 6.4 show that the α -aminoalkylphenone photoinitiators investigated all have high reactivity. This is particularly true of Irgacure 369, which shows a significant performance advantage over every other commercially available photoinitiator.

The photoinitiators Irgacure 907 and Irgacure 369 have been extensively reported in the literature and their high reactivity widely accepted⁴⁶. The high reactivity of α -aminoalkylphenones has been principally associated with both their strong charge transfer character (π - π^*) absorption bands in the UVB region, and the importance of the α -amino substituent over other groups such as hydroxyls^{47,48}. The nature of the other substituents at the β -position has also been shown to be important, causing effects such as the (π - π^*) absorbance band trailing into the visible region for Irgacure 369, which has been linked to the high reactivity of this particular photoinitiator^{49,50}.

The use of α -aminoalkylphenones in conjunction with a thioxanthone photoinitiator has been reported to further increase their reactivity through a sensitization process. This has most often been observed with Irgacure 907, but has also been reported for Irgacure 369^{48,51-54}.

Miscellaneous Type I photoinitiators

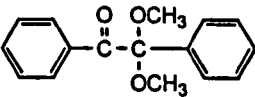
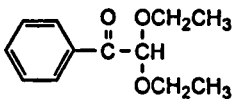
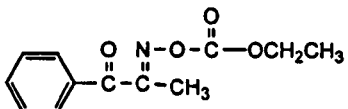
Photoinitiator	Initial reaction rate (% s ⁻¹)
 <p style="text-align: center;"><i>Irgacure 651</i> Benzil dimethyl ketal</p>	98
 <p style="text-align: center;"><i>DEAP</i> Diethoxy acetophenone</p>	46
 <p style="text-align: center;"><i>Quantacure PDO</i> 1-Phenyl-1,2-propanedione-2-(O-ethoxycarbonyl) oxime</p>	52

Table 6.5 *Rates of cure for miscellaneous Type I photoinitiators in an oligomer / monomer blend by RT-FTIR*

Although its use is declining in printing inks due to concerns over its odorous byproduct methyl benzoate, the photoinitiator Irgacure 651 has been widely used for a number of years in UV curing applications. On a practical level, Irgacure 651 is often interchangeable in formulations with the similarly UV absorbing α -cleavage photoinitiators Irgacure 184 and Darocure 1173. However, the results in tables 6.2 and 6.5 show that Irgacure 651 has a reactivity higher than either of these alternative materials. This observation is supported by the work of Decker⁴⁶, who found Irgacure 651 to be more reactive than Darocure 1173, and by Hoyle, Hensel and Grubb who found it more reactive than Irgacure 184, diethoxy acetophenone and benzoin isopropyl ether⁵⁵.

Diethoxy acetophenone (DEAP) is now rarely used within the printing ink industry, but is still an important photoinitiator mechanistically. The results in table 6.5 show that DEAP is of considerably lower reactivity than Irgacure 651, with which it is often compared. This finding is supported by the work of Berner, Kirchmayr and Rist³¹, and Hoyle, Hensel and Grubb⁵⁵, who also found Irgacure 651 to be more reactive than DEAP.

Quantacure PDO is also rarely used within the printing ink industry. The results table 6.5 show that Quantacure PDO is only slightly more reactive than DEAP and is less reactive than all the other commonly used α -cleavage photoinitiators.

Xanthenes and thioxanthenes

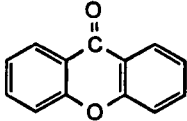
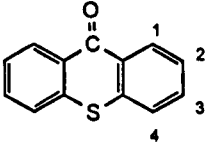
Photoinitiator	Initial reaction rate (% s ⁻¹)
 Xanthone	16
 Thioxanthone	not soluble
<i>Quantacure ITX</i> Isopropyl thioxanthone	116
<i>Speedcure DETX</i> 2,4-Diethyl thioxanthone	117
2- <i>t</i> .Butyl thioxanthone	104
<i>Kayacure CTX</i> 2-Chloro thioxanthone	110
<i>Quantacure PTX</i> 2-Propoxy thioxanthone	103
<i>Quantacure CPTX</i> 1-Chloro-4-propoxy thioxanthone	122

Table 6.6 Rates of cure for xanthone and thioxanthone photoinitiators in an oligomer / monomer blend by RT-FTIR

The thioxanthone class of photoinitiator represents one of the most widely used in the printing ink industry⁵⁶, with ITX being the established commercial standard. Although thioxanthone could not be evaluated due to its low solubility, the results in table 6.6 show that the thioxanthone derivatives all have a similarly high level of reactivity. The much higher reactivity of the thioxanthenes relative to xanthone is due to their strong (n-π*) absorbance bands in the wavelength region 350-400 nm, resulting from the electron donation effect of the sulfur atom, giving significantly increased UV light utilisation (see chapter 4).

There is some evidence to suggest that substitution in the 2-position gives compounds of lower reactivity than those substituted in the 4-position, since the 2-chloro, 2-*t*.butyl and 2-propoxy derivatives all show lower reactivities than the 2,4-diethyl and 1-chloro-4-propoxy derivatives. The Quantacure ITX is a physical mixture of the 2- and 4- substituted materials and therefore also shows high reactivity, although the ratio of isomers has not been determined or previously reported in the literature. The observation of higher reactivity from materials substituted in the 4-position compared to the 2- position has previously been reported in the literature^{32,57}.

Within the thioxanthone compound class, CPTX shows the highest reactivity, although its performance advantage over ITX in a non-pigmented system doesn't appear to be as high as has been previously claimed^{32,58}. There is also little evidence to confirm claims that DETX shows a performance advantage over ITX, both of which also have similar UV absorption spectra^{32,59}.

Benzophenones

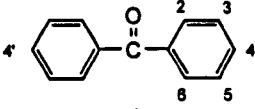
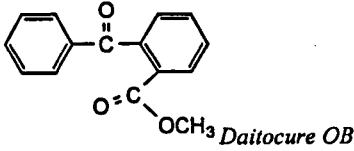
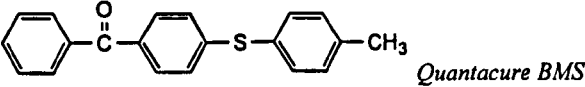
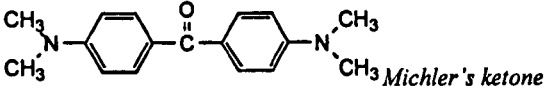
Photoinitiator	Initial reaction rate (% s ⁻¹)
 Benzophenone	29
<i>Trigonal 12</i> 4-Phenyl benzophenone	117
 2-Benzoyl methyl benzoate <i>Daitocure OB</i>	12
 4-Benzoyl-4'-methyl diphenyl sulfide <i>Quantacure BMS</i>	108
4-Chloro benzophenone	45
2-Chloro benzophenone	18
 4,4'-(Dimethylamino) benzophenone <i>Michler's ketone</i>	69
<i>Ethyl Michler's ketone</i> 4,4'-(Diethylamino) benzophenone	66
<i>Esacure T2T</i> 2,4,6-Trimethyl benzophenone	31
4-Methyl benzophenone	39
2-Methyl benzophenone	0
4-Methoxy benzophenone	62
4,4'-Dimethoxy benzophenone	44
4,4'-Diphenoxy benzophenone	68 (run hot)
4-Hydroxy benzophenone	39
2-Hydroxy benzophenone	0

Table 6.7 Rates of cure for benzophenone type photoinitiators in an oligomer / monomer blend by RT-FTIR

The results in table 6.7 show the effect of a range of substituent types and positions on the reactivity of benzophenone, with the considerable range of reactivities indicating the importance of a number of factors in the design of photoinitiator molecules;

Substitution of a methyl or chloro group into the 4-position of benzophenone results in a small shift of the ($\pi-\pi^*$) absorption band towards longer wavelengths and a slight reactivity increase, possibly due to the better light utilisation that the spectral shift provides. In contrast, substitution of chloro, methyl or benzoic acid methyl ester groups into the 2-position gives no spectral change and results in significantly reduced reactivity. It is speculated that substitution in the 2-position reduces reactivity by steric hinderance of the carbonyl bond, with the electron donating or withdrawing nature of the substituent group being of relatively little importance in this context.

The theory put forward doesn't readily explain why 2,4,6-trimethyl benzophenone, despite containing methyl groups in the 2- and 6- positions, has a reactivity similar to that of benzophenone. However, the reason for this anomaly can be seen using molecular modeling software such as Biosyms[™], where unlike benzophenone and 2-methyl benzophenone, 2,4,6-trimethyl benzophenone is shown to have a lowest energy conformation with the aromatic rings twisted out of plane, as shown in figure 6.12. This has previously been speculated by Dietliker for the structurally similar photoinitiator 2,4,6-trimethylbenzoyl diphenyl phosphine oxide⁴¹.

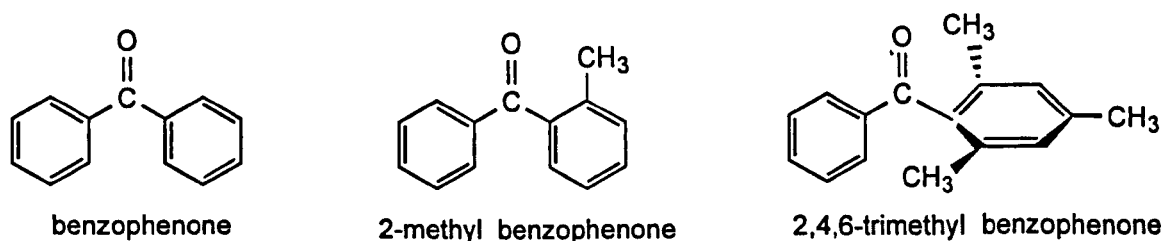


Figure 6.12 *Representations of the lowest energy conformations of benzophenone, 2-methyl benzophenone and 2,4,6-trimethyl benzophenone*

The deactivation of benzophenone by a hydroxy substituent in the 2-position is well known, and the basis of many commercial UV stabilisers⁶¹. The deactivation mechanism in this case is thought to be due to the intramolecular hydrogen bonding of the carbonyl oxygen with the phenolic hydrogen⁶¹.

Substitution of methoxy or phenoxy groups into the 4-position(s) of benzophenone, such as for the 4-methoxy, 4,4'-dimethoxy and 4,4'-diphenoxy benzophenones, results in a red shift of the ($\pi-\pi^*$) absorption band to around 285 nm and an increase in reactivity. The reactivity increase is speculated to be partially due to the better utilisation that the spectral shift provides, as shown in figure 6.13. However, even allowing for molecular weight differences, the similar UV absorption spectra for these materials and the observed reactivity differences between them suggests that the substituents also change the quantum efficiency of benzophenone. The higher reactivity and

quantum yield of 4,4'-diphenoxy benzophenone relative to benzophenone has been reported by Decker⁶². However, the extent of the increase in reactivity was not found to be as significant as was claimed.

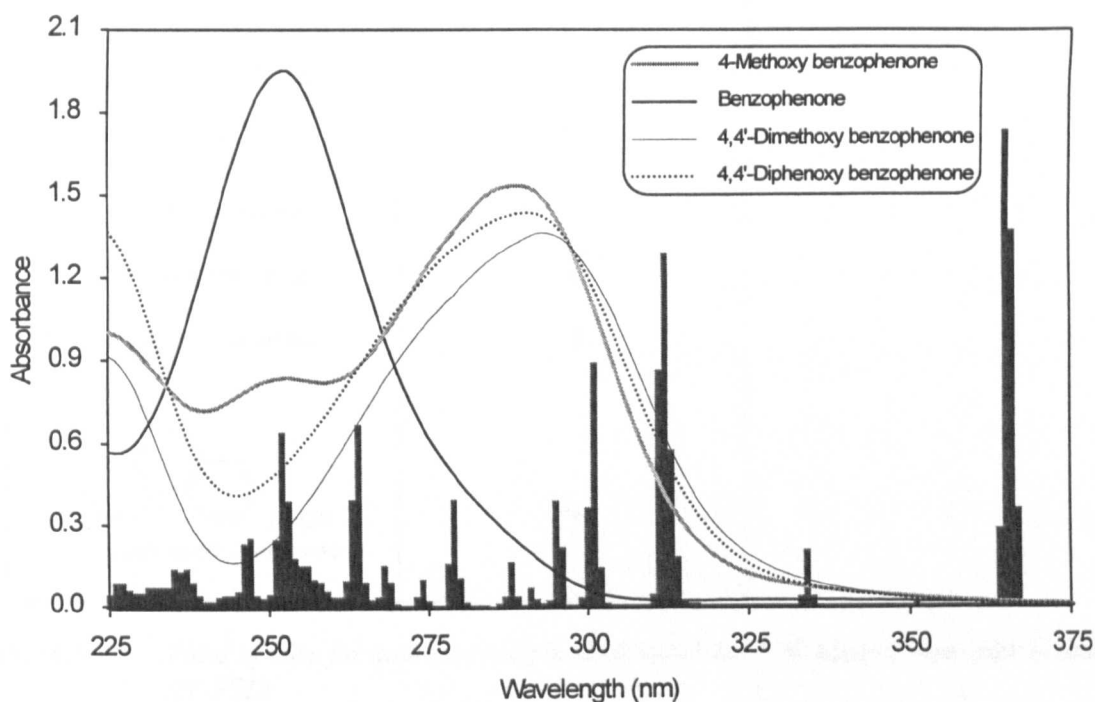


Figure 6.13 *The UV absorption spectra of substituted benzophenone photoinitiators and their relationship with a medium pressure mercury curing lamp emission spectrum*

4-Phenyl benzophenone was observed to show the highest reactivity of all the benzophenone type photoinitiators. Although it has a red shifted absorption band similar to the methoxy and phenoxy substituted benzophenones shown in figure 6.13, its high reactivity is likely to be associated mostly with the efficient intramolecular energy transfer reaction reported for this material⁶³.

The 4,4'-dialkylamino benzophenones, Michler's ketone and Ethyl Michler's ketone were shown to have reasonable, but not exceptional curing activity. However, it has been reported that these materials show considerably higher reactivity when used in combination with benzophenone. When used in this way, the two photoinitiators form a triplet exiplex that can be populated by excitation of either component, and results in the formation of the highly reactive alkylamino radical by electron transfer followed by proton transfer to the benzophenone carbonyl⁵³.

A mixture of N-methyl diethanolamine (MDEA) and 4-benzoyl-4'-diphenyl sulfide (Quantacure BMS) has been reported to show a rate of polymerization of methyl methacrylate in toluene slightly higher than that of a benzophenone / MDEA combination, but significantly lower than that of benzil dimethyl ketal⁶⁴. Results presented here suggest that under typical end use conditions, in conjunction with MDEA, the rate of polymerisation of BMS is in fact greater than for both other photoinitiators. The use of BMS is expected to be particularly effective in pigmented systems because of its strong charge transfer character absorption band centered at 315 nm.

Quinones

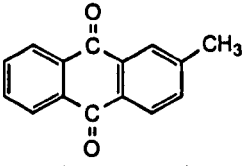
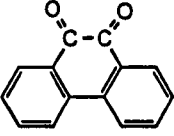
Photoinitiator	Initial reaction rate (% s ⁻¹)
 2-Methyl anthraquinone	55
2-Ethyl anthraquinone	58
2- <i>t</i> .Butyl anthraquinone	68
 Phenanthrene-9,10-quinone <i>PI-ON</i>	56

Table 6.8 *Rates of cure for quinone type photoinitiators in an oligomer / monomer blend by RT-FTIR*

The results in table 6.8 demonstrate that the quinone class of photoinitiator displays reasonable curing efficiency when compared to other classes such as the benzophenones. Despite this, quinone and anthraquinone type photoinitiators are no longer widely used. Their use has principally been associated in the past with electrographics applications where they have been reported to be highly reactive in combination with a coinitiator^{65,66}.

Reactivity for anthraquinone type photoinitiators can also be seen to increase with increasing alkyl substituent chain length. Since the UV absorption spectra for all these materials are very similar, this effect must be a consequence of photochemical efficiency differences.

Despite a relatively strong absorption band extending into the visible region, phenanthrene-9,10-quinone shows no performance advantage over the substituted anthraquinones.

Aromatic 1, 2-diketones

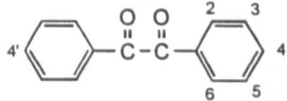
Photoinitiator	Initial reaction rate (% s ⁻¹)
 <p>Benzil</p>	54
4,4'-Dimethoxy benzil	103
4,4'-Dimethyl benzil	96

Table 6.9 Rates of cure for aromatic 1,2-diketone type photoinitiators in an oligomer / monomer blend by RT-FTIR

The results in table 6.9 demonstrate that although benzil is a reasonably effective photoinitiator, substitution in the 4-position of both aromatic rings by electron donating groups, such as methyl or methoxy, leads to a significant increase in cure performance. This performance increase is at least partially due to the substituents causing a red shifted absorbance, allowing better light utilisation in the 280-320 nm region, as shown in figure 6.14.

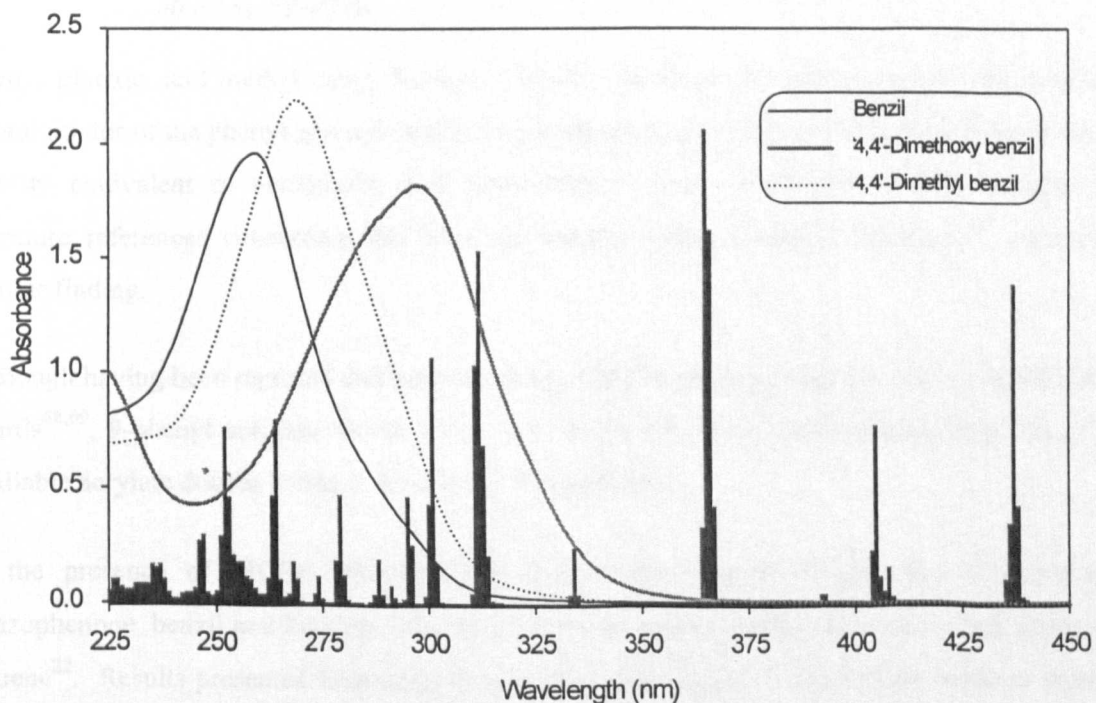


Figure 6.14 The UV absorption spectra of aromatic 1,2-diketone photoinitiators and their relationship with a medium pressure mercury curing lamp emission spectrum

The similar reactivity of the two substituted benzils, despite the much greater red shift in the case of the dimethoxy variant, indicates that the photochemical efficiency of 4,4'-dimethyl benzil is higher than that of the 4,4'-dimethoxy benzil.

Miscellaneous Type II photoinitiators

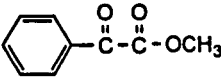
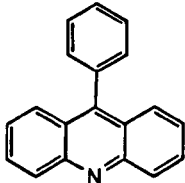
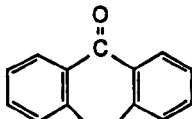
Photoinitiator	Initial reaction rate (% s ⁻¹)
 Phenyl glyoxylic acid methyl ester <i>Nuvopol PI3000</i>	62
 9-Phenyl acridine	1.3
 Dibenzosuberone	79.6

Table 6.10 *Rates of cure for miscellaneous type II photoinitiators in an oligomer / monomer blend by RT-FTIR*

Phenyl glyoxylic acid methyl ester, Nuvopol PI3000, represents the only commercially available photoinitiator of the phenyl glyoxylate type and is shown by the results in table 6.10 to have curing activity equivalent to commonly used photoinitiators such as Darocure 1173. Despite few literature references concerning this class of material being available, Hageman⁶⁷ reported a similar finding.

Although having been reported and patented as an effective photoinitiator for use in printed circuit boards^{68,69}, 9-phenyl acridine shows a very low curing efficiency, polymerising only 7% of the available acrylate double bonds in the RT-FTIR experiment.

In the presence of MDEA, dibenzosuberone has been reported to be less effective than benzophenone, benzil and 2-chloro thioxanthone for the polymerization of methyl methacrylate in toluene²². Results presented here suggest that dibenzosuberone has a reactivity between those of benzophenone and 2-chloro thioxanthone.

6.2.3 Curing effectiveness of amine synergists

Differential photocalorimetry (DPC) was considered to be a more appropriate technique for the evaluation of amine synergist reactivity than RT-FTIR; since many of the materials investigated are aromatic, with strong absorption bands in the UV region. As such, if the full spectral output of the medium pressure mercury lamp were used in a RT-FTIR experiment, the results would be

difficult to interpret because competitive light absorption would affect the observed reactivity. DPC can eliminate this problem by allowing irradiation of the sample with monochromatic light, which is absorbed by the photoinitiator but, with the exception of 4,4'-(dimethylamino benzophenone), not the amine synergist. The cure rate information obtained then relates specifically to the efficiency of alkylamino radical generation, and its subsequent reactivity towards acrylate double bonds.

The curing effectiveness of different amine synergists was assessed in an 80:20 ratio combination of the urethane diacrylate oligomer CN934 and the monomer TMPTA, with formulations containing 4 %wt of the photoinitiator isopropyl thioxanthone and 1 %wt of the amine synergist. Samples were irradiated at 50 °C in air using 420 nm monochromatic light. Care was also taken to ensure that the experimental conditions would not lead to self-screening by the photoinitiator. The DPC exotherm peak height ($W g^{-1}$) was used as a measure of reactivity, since this corresponds to the maximum reaction rate during the cure process.

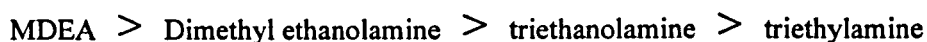
Aliphatic amines

Amine	Exotherm peak height ($W g^{-1}$)
None	0.37
Triethylamine	11.35
Triethanolamine	15.65
Tri-isopropanolamine	13.33
Dimethyl propanolamine	14.54
N-methyl diethanolamine	18.76 ± 0.6
N,N-dimethyl ethanolamine	17.75
N,N-diethyl ethanolamine	12.08
Ebecryl P115 $H_2C=CHC(=O)\left(OCH_2\underset{\substack{ \\ CH_3}}{CH}\right)_3C(=O)CH_2CH_2-N\begin{matrix} /CH_2CH_3 \\ \backslash CH_2CH_3 \end{matrix}$	12.34

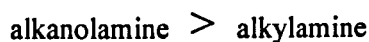
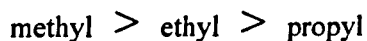
Table 6.11 Rate of cure for aliphatic amine synergists by DPC

The results in table 6.11 show that the addition of amine synergist makes a considerable difference to the reactivity of a formulation containing a Type II photoinitiator, but that the difference in

reactivity between amine types is quite limited. The results agree well with those published in the literature, with one widely reported reactivity trend^{24,70-72} being clearly evident;



Other reactivity trends are also evident, such as;



It has been suggested that these reactivity differences are a consequence of both the amine ionization potential and the number of α -hydrogens^{71,72}. Further work would be required to comment on the validity of this theory.

The reactivity of the aminoacrylate Ebecryl P115 has, to the author's knowledge not been published in a direct comparison with other commercially used amine synergists. These results show that its reactivity is quite low in comparison with commonly used aliphatic amines such as MDEA and triethanolamine, and explains the requirement by formulators to use much higher %wt concentrations.

Aromatic amines

The results in table 6.12 show that aromatic amines have a reactivity only slightly below those of the aliphatic amines, despite fewer α -hydrogens and much higher molecular weights.

Although the 4-N,N-dimethylamino benzoic acid esters all show a higher reactivity than N,N-dimethyl aniline, their reactivity is observed to decrease with increasing molecular weight, such that EHA is considerably less reactive than EPD. The 2-N,N-dimethylamino benzoic acid ethyl ester shows a lower reactivity than the 4-substituted materials, presumably due to the steric hinderance of the amine group by the bulky ester substituent.

The results obtained agree with those of Berner, Kirchmayr and Rist³¹ in that the esters of 4-N,N-dimethylamino benzoic acid show a greater curing effectiveness than N,N-dimethyl aniline. However, it has been reported by Christensen, Wooten & Whitman that Michler's ketone shows a significantly higher reactivity than either MDEA or Quantacure EHA⁷³. Although in the results presented here, the reactivity of Michler's ketone will be slightly suppressed due to self-screening at the irradiation wavelength, it is believed by the author that the high level of reactivity observed by Christensen et al.⁷³ is partially due to energy transfer sensitisation between the Michler's ketone and benzophenone combination used. In addition, since pendulum hardness was used as a measure of reactivity in their experiments, effects such as chain transfer and amine plasticisation may have had an influence in their results.

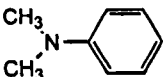
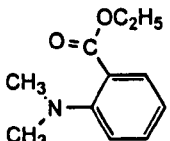
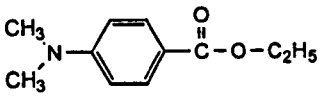
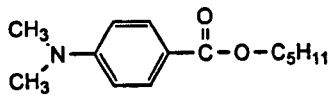
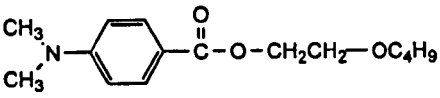
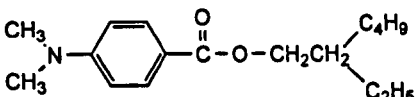
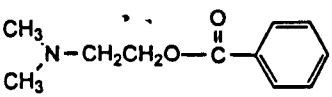
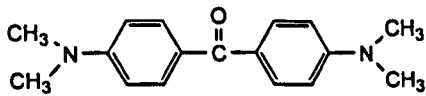
Amine	Exotherm peak height (W g ⁻¹)
No amine	0.37
 N,N-Dimethyl aniline	10.76
 2-N,N-Dimethylamino benzoic acid ethyl ester	14.75
 4-N,N-Dimethylamino benzoic acid ethyl ester <i>Quantacure EPD</i>	15.97
 4-N,N-Dimethylamino benzoic acid amyl ester <i>Quantacure MCA</i>	14.74
 4-N,N-Dimethylamino benzoic acid 2-butoxy ethyl ester <i>Speedcure BEDB</i>	14.86
 4-N,N-Dimethylamino benzoic acid 2-ethyl hexyl ester <i>Quantacure EHA</i>	12.54
 (2-Dimethylamino)ethyl benzoate <i>Quantacure DMB</i>	16.04
 4,4'-(Dimethylamino) benzophenone <i>Michler's ketone</i>	12.94

Table 6.12 Rate of cure for aromatic amine synergists by DPC

6.2.4 The effect of viscosity on oxygen inhibition in the polymerisation process

Oxygen inhibition is one of the most serious problems associated with acrylate based radiation curing technology. The two inhibitory mechanisms of oxygen; triplet quenching and radical scavenging, have been extensively documented^{1,67}, but not often studied directly in terms of other formulating variables. Oxygen inhibition has been shown to be responsible for the polymerisation induction period,^{2,3} and has also been associated with low overall cure rates^{74,75}.

The Differential Photo-Calorimetry (DPC) results in figures 6.15 and 6.16 show the effect of formulation changes on the exotherm peak area under air and nitrogen purge conditions. The formulations used were based on a trifunctional aliphatic urethane acrylate oligomer (Genomer T1200) with the reactive diluents tripropylene glycol diacrylate (TPGDA), shown in figure 6.15, and di-pentaerythritol pentaacrylate (Di-PETA), shown in figure 6.16. The reactive diluents were added at levels between 0 and 100 wt%. Samples also contained 2 %wt of the photoinitiator benzil dimethyl ketal (Irgacure 651) and were exposed using a 365 nm monochromatic light source.

In both formulation types, curing under nitrogen produces a more exothermic reaction than curing under air, as would be expected. However, the magnitude of the difference is constant for formulations based on Di-PETA but variable for formulations based on TPGDA, becoming larger with increasing monomer content such that the polymerisation activity in an air environment is very low for 100 %wt TPGDA but very high for 100 %wt Di-PETA. This was an unexpected finding since monomers such as those used are frequently termed “reactive diluents”, because of their ability to increase the cure speed of a coating.

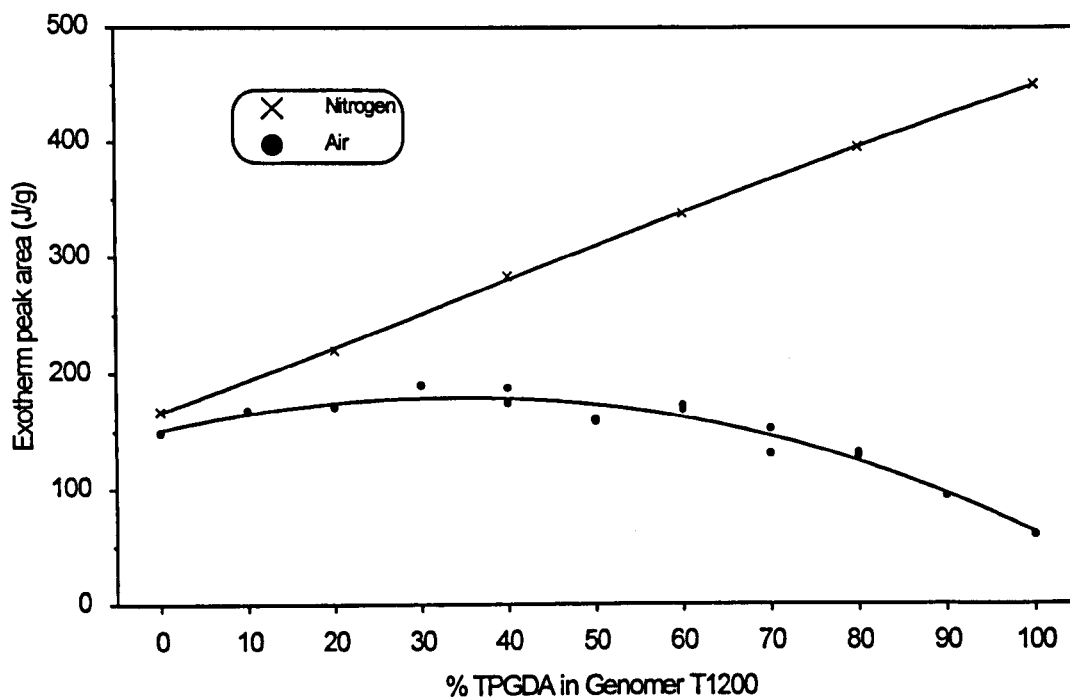


Figure 6.15 *The change in DPC exotherm peak area as a function of TPGDA content under air and nitrogen purges*

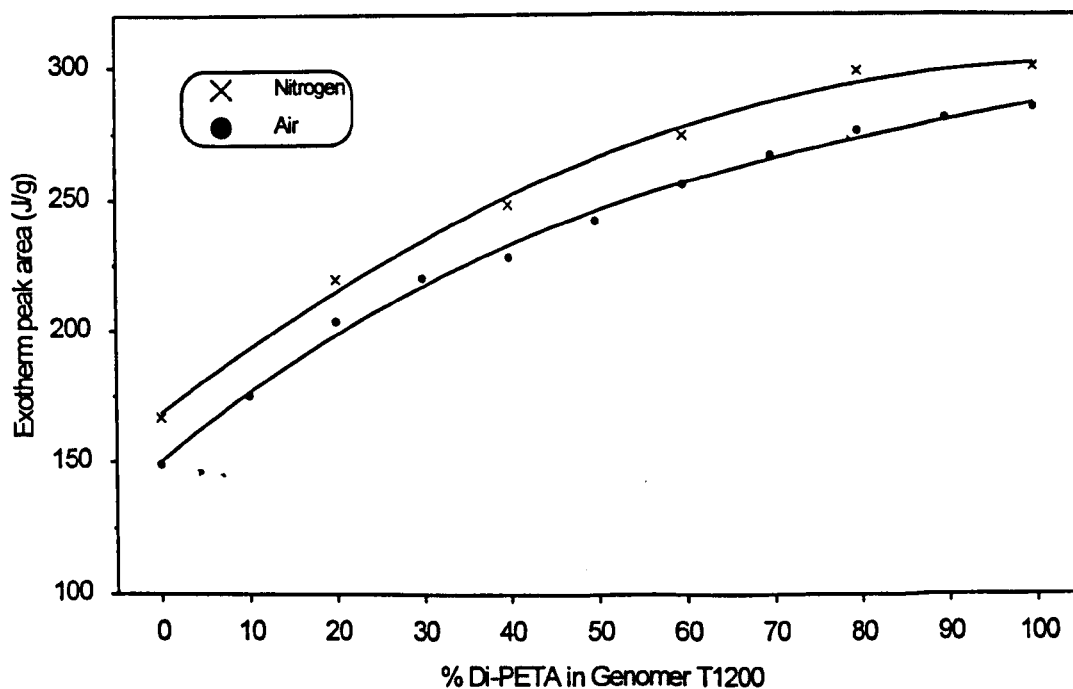


Figure 6.16 *The change in DPC exotherm peak area as a function of Di-PETA content under air and nitrogen purges*

The reason behind the observed curing differences for the two formulation types shown in figures 6.15 and 6.16 becomes apparent when the formulation viscosities are considered. From figure 6.17 it is evident that the high viscosity of Di-PETA produces little change in the formulation viscosity across the entire range of sample concentrations, whereas the low viscosity and strong viscosity cutting power of TPGDA produces a viscosity change of several orders of magnitude

across the concentration range. It can therefore be deduced that lower formulation viscosities allow much more rapid oxygen diffusion into the sample, with oxygen being replenished at an increasing rate relative to the almost constant initial rate of consumption by the polymerisation process. This causes a gradual lowering of reactivity, since more oxygen is present at any one time in the sample.

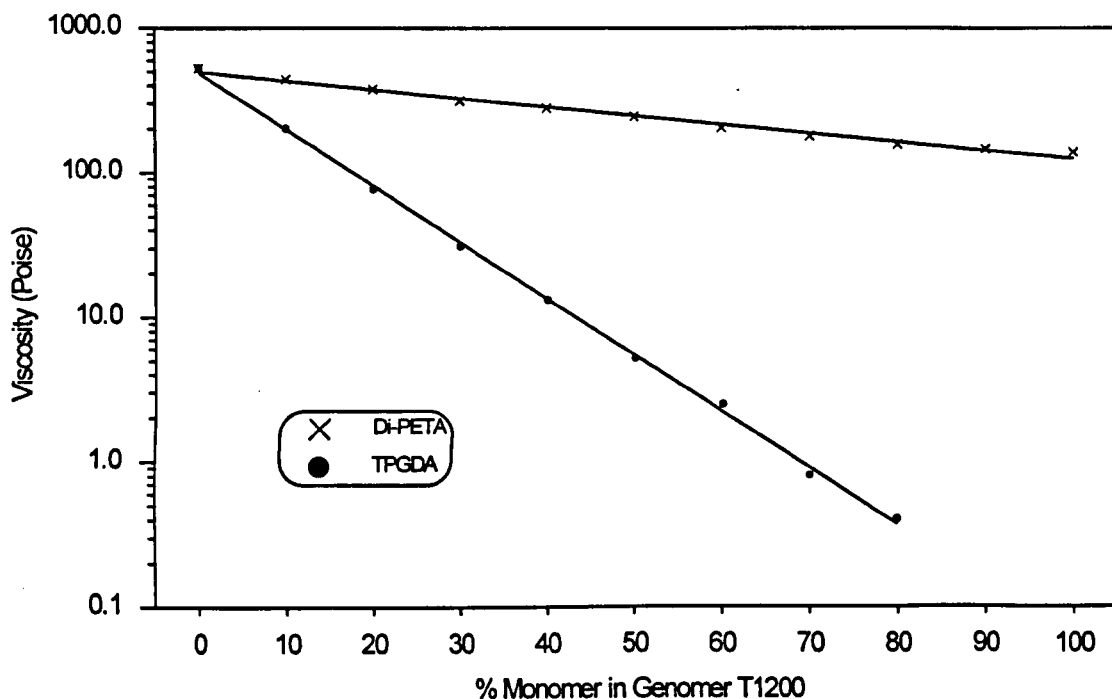


Figure 6.17 *Change in formulation viscosity as a function of monomer content*

Similar experiments to those shown in figures 6.15 and 6.16 were reported by Seng⁷⁶, where urethane acrylate formulations with increasing TPGDA concentrations were printed and cured by both EB and UV radiation. It was reported that for increasing monomer content, the samples cured by EB showed increasing hardness and decreasing extractable monomer, whereas the samples cured by UV showed decreasing hardness and increasing extractable monomer, results which were interpreted as differences in the curing mechanism for UV and EB processes. However, one crucial point was overlooked; the UV curing took place in an air environment and the EB curing took place in an inert nitrogen atmosphere. It is this essential difference that confirms the work reported here and also explains Seng's results.

The extent of the oxygen diffusion into formulations of different viscosities, and the subsequent effect on photopolymerisation activity, was investigated further using DPC. A series of formulations based on combinations of one of several monomers and the oligomer Genomer T1200, covering a viscosity range of 0.01 to 525 Poise were analysed. The ratio of exotherm peak height under air and nitrogen atmospheres was then plotted against the formulation viscosity, as shown in figure 6.18. The use of a reactivity ratio in this way has the effect of making these results independent of factors such as monomer functionality and degree of alkoxylation.

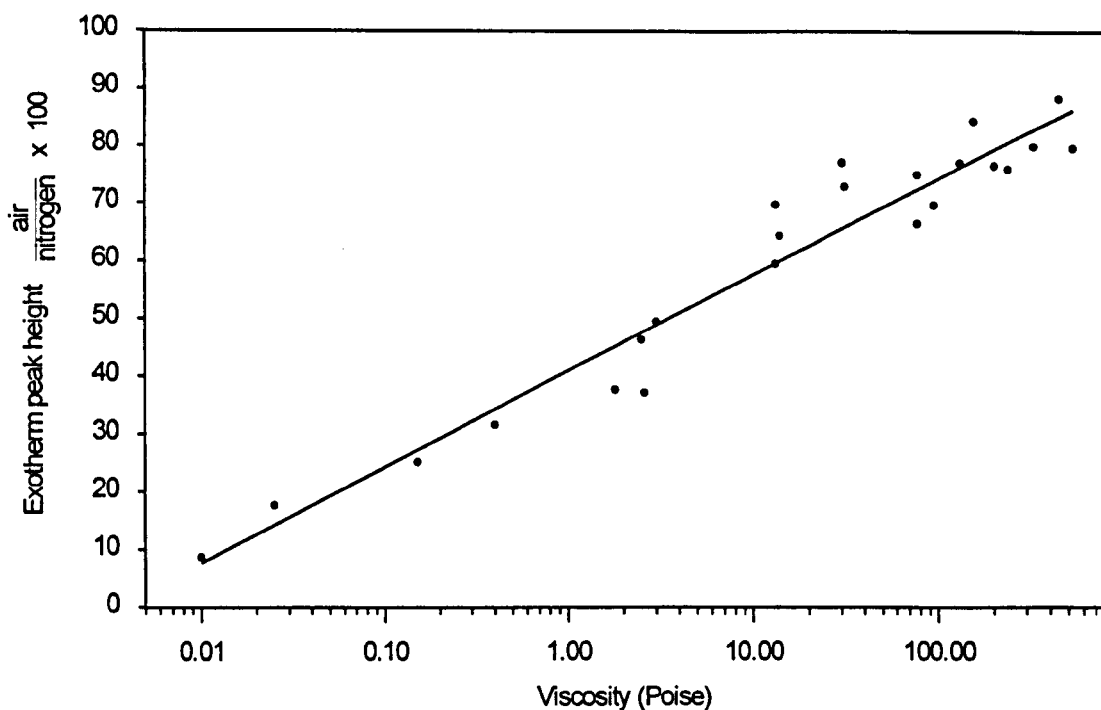


Figure 6.18 *The extent of oxygen diffusion as a function of formulation viscosity*

The results displayed in figure 6.18 demonstrates that there is a strong logarithmic correlation between formulation viscosity and the extent to which oxygen diffuses into a sample and inhibits the cure.

If the theory proposed is valid, it would be expected that a fixed formulation would show similar curing under air and nitrogen atmospheres at high viscosities (several hundred Poise), but show evidence of increased oxygen inhibition at lower viscosities. This situation can be achieved by the use of different curing temperatures to alter the viscosity.

Figure 6.19 shows how the curing activity, under both air and nitrogen, of a low viscosity formulation (50 %wt TPGDA in Genomer T1200) is affected by temperature. The variation of formulation viscosity with temperature is also shown. Figure 6.20 shows the results for a similar set of experiments using a high viscosity formulation (50 %wt Di-PETA in Genomer T1200).

The results in figures 6.19 and 6.20 demonstrate that a significant deviation between the reaction rate under air and nitrogen occurs at temperatures above 40 °C for 50 % Di-PETA in Genomer T1200, but at above -10 °C for 50 % TPGDA in Genomer T1200. Viscosity measurements were not possible down to temperatures of -10 °C, but a visual extrapolation for the TPGDA based formulation, and a direct measurement for the Di-PETA based formulation, confirms that both samples have viscosities of approximately 10-50 Poise at their respective deviation temperatures.

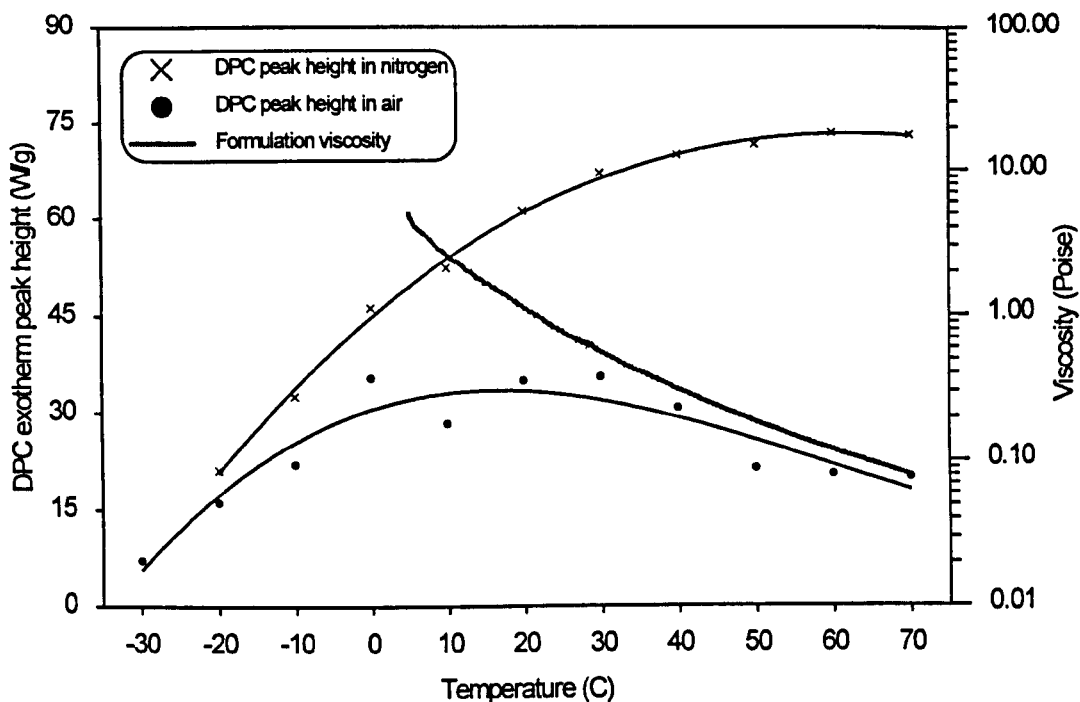


Figure 6.19 *Determination of the onset of oxygen inhibition for a formulation based on 50% TPGDA in the oligomer Genomer T1200*

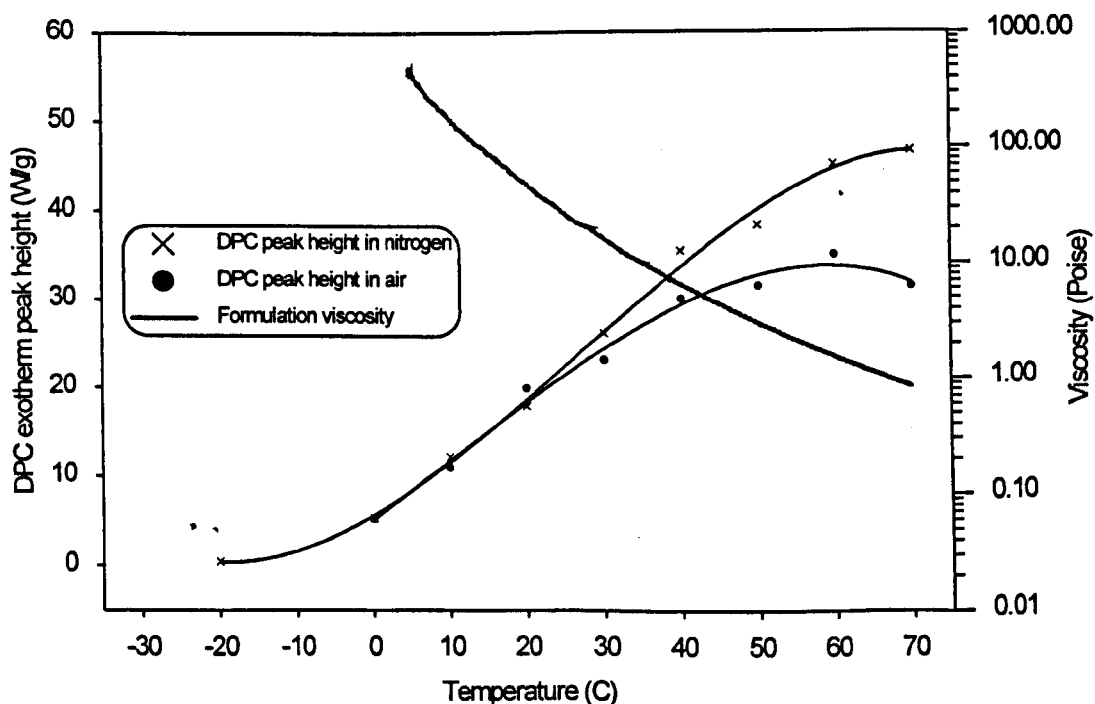


Figure 6.20 *Determination of the onset of oxygen inhibition for a formulation based on 50% Di-PETA in the oligomer Genomer T1200*

The results in this section clearly demonstrate that formulation viscosity is important in determining the extent of oxygen inhibition in UV curing reactions. However, extrapolation of these results down to typical printing ink and varnish film thicknesses of 2-5 μm is not straightforward, and requires further work concerning the distance molecular oxygen is able to migrate through different viscosity media.

6.2.5 The effect of photoinitiator concentration on cure efficiency

The rate and extent of cure for an oligomer / monomer blend containing increasing levels of photoinitiator were measured using Differential Photocalorimetry (DPC) and Real Time Infrared spectroscopy (RT-FTIR) respectively. Two photoinitiators were used; 1-phenyl-2-hydroxy-2-methyl propan-1-one (Darocure 1173) and its polymeric equivalent, Esacure KIP, where Esacure KIP is based on the same photoinitiator molecule, but as a pendant group on a hydrocarbon chain. These photoinitiators both generate free radicals via a cleavage mechanism (see Chapter 5) and have been shown earlier to have similar reaction efficiencies at a 2 %wt level.

An 80/20 blend of the oligomer CN934 and the monomer TMPTA, containing photoinitiator levels between 0.5 %wt and 15 %wt, were analysed by DPC at 40 °C in an air purge in the absence of amine synergist. A 334 nm monochromatic light source was used, since the very weak UV absorbance at this wavelength for both photoinitiators means that no screening of the incident light occurred in the experimental concentration range.

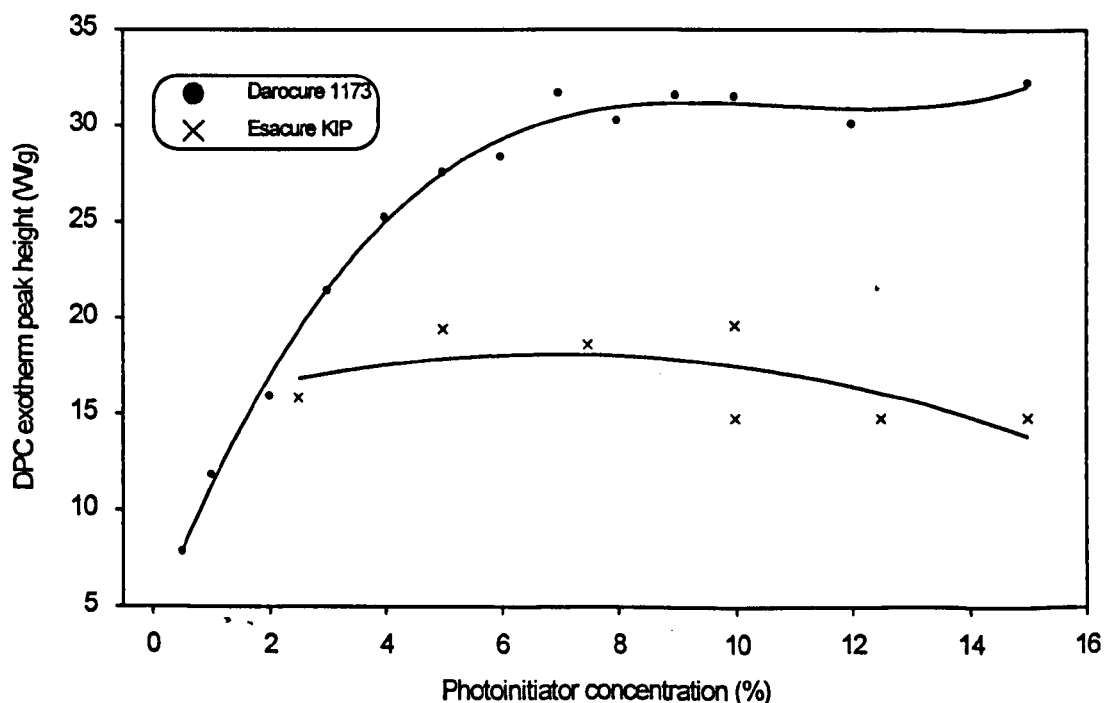


Figure 6.21 *Curing efficiency of two photoinitiators by DPC as a function of concentration*

The results in figure 6.21 show that the two photoinitiators behave quite differently as a function of concentration; Darocure 1173 shows an increasing cure response with concentration, up to a maximum of around 8 %wt photoinitiator, maintaining a constant reactivity at higher levels. In contrast, the Esacure KIP shows a generally lower reactivity, which decreases at concentrations above 6-8 %wt.

The different cure responses with increasing photoinitiator concentration for the two photoinitiators used is thought to be a consequence of their different effects on formulation viscosity; Darocure 1173 is a liquid photoinitiator which, like most photoinitiators, reduces the formulation viscosity³⁰. However, by virtue of its polymeric nature, Esacure KIP increases the formulation viscosity, the extent of this difference being shown in figure 6.22.

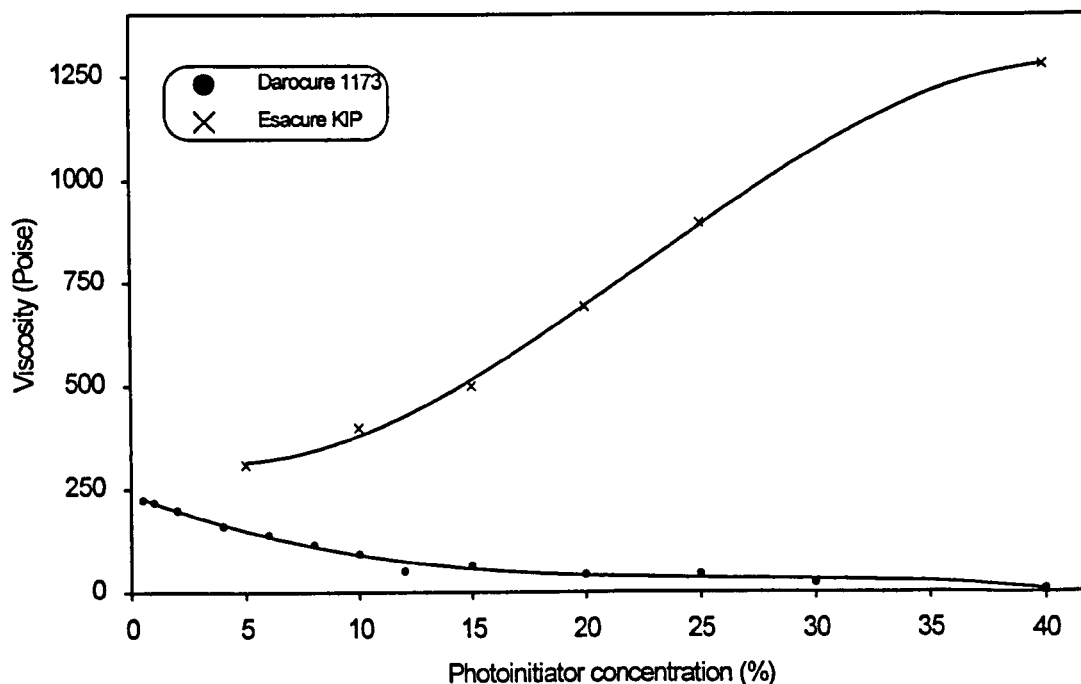


Figure 6.22 *Change in formulation viscosity as a function of photoinitiator concentration*

The information in figures 6.21 and 6.22 shows that, for formulations based on Esacure KIP and Darocure 1173, at low photoinitiator concentrations the differences in both reactivity and viscosity are quite small. However, at concentrations above 5 % wt this is not the case, with Darocure 1173 showing significantly higher reactivity than equivalent concentrations of Esacure KIP. It is speculated that, in addition to a low inherent mobility of the KIP derived macroradical, the higher viscosities of formulations containing this photoinitiator will also cause many radicals to become trapped in the growing polymer matrix, too far from any acrylate bonds to react with them. Significant cage recombination is also likely because of an inability of the primary radicals to separate quickly enough following cleavage. In contrast, increasing concentrations of Darocure 1173 result in both the production of many more free radicals because of their efficient escape from the solvent cage, and, because of the lower viscosity, allowing them to react with more of the acrylate bonds.

The apparently constant reaction rate by DPC for Darocure 1173 at concentrations above 8 %wt was investigated further using RT-FTIR, where the smaller sample thicknesses involved allow photoinitiator concentrations up to 40 %wt to be used before screening occurs in the region of the ($n-\pi^*$) transition at 320-370 nm.

The same formulations as previously used, containing increasing concentrations of Darocure 1173 and Esacure KIP were analysed using the RT-FTIR technique described in 6.2.1. The full spectral output of a 400W medium pressure mercury arc lamp was used in an air atmosphere at ambient temperature. The runs were processed to give the % acrylate bonds converted at the end of the UV exposure and are shown in figure 6.23.

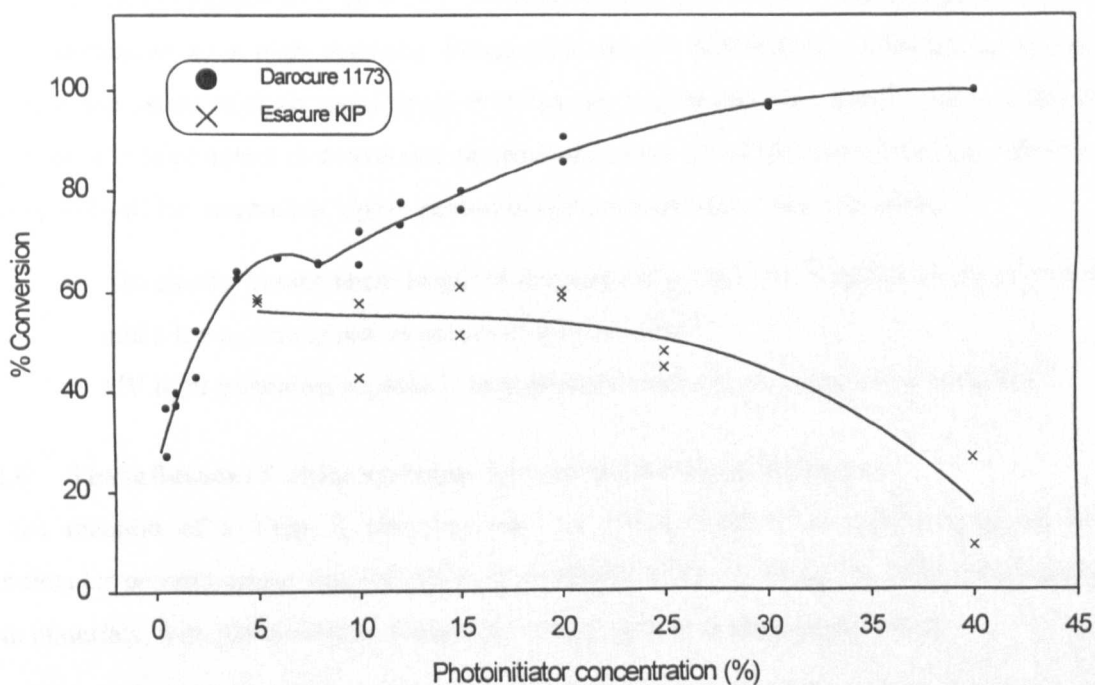


Figure 6.23 *Curing efficiency of two photoinitiators by RT-FTIR as a function of concentration*

The results in figure 6.23 show a similar trend to that observed for the DPC experiments, with the higher photoinitiator concentrations used showing the effect of the change in formulation viscosity even more clearly. Also evident is a local maximum in the curing efficiency at 6% of Darocure 1173. This may correspond to a radical density above which chain termination reactions are starting to become significant. However, at concentrations above 10 %wt, where the viscosity is starting to change significantly, rather than merely plateauing as indicated by the DPC results, RT-FTIR experiments show the reactivity to increase again, with 100% conversion of acrylate bonds being attained at photoinitiator concentrations of 30 or 40 %wt. Even assuming chain termination effects are significant at these very high photoinitiator concentrations, it is not hard to visualise the fact that there are much fewer acrylate bonds present in the formulation, and that in a low viscosity environment a free radical will be generated in very close proximity to, and has a high probability of reaction with these bonds. Although at high Darocure 1173 concentrations the fall in formulation viscosity is such that some increase in oxygen inhibition would be expected, it is speculated that this increase is rendered insignificant by the very high radical densities generated.

These experiments are of a limited practical significance since, in general, formulations contain a maximum of 5-7 %wt photoinitiator and are formulated to a constant viscosity. Also, the changes in viscosity associated with photoinitiator concentration means that it is difficult to design an experiment of this type to investigate the true effect of photoinitiator concentration. However, these experiments do go some way towards explaining why a relatively high photoinitiator concentration is required to cure a low viscosity varnish (<1 Poise) or flexographic ink (10-20 Poise) compared to a high viscosity lithographic ink (~ 400 Poise). Whether at a constant viscosity the extent of chain termination at increasing radical densities would lead to a decline in the reaction rate or extent of conversion remains unknown. It is however likely that a decrease in cure speed will be observed at higher photoinitiator concentrations due to either:

- The shorter kinetic chain length of the polymer giving rise to poorer physical properties and a lower cure speed; as proposed by Hanrahan³⁰.
- UV light screening, especially in pigmented coatings; as proposed by Hencken²⁹.

6.2.6 The influence of amine synergist concentration on cure efficiency

In the reaction of a Type II photoinitiator, the involvement of an amine synergist in the bimolecular process means that the observed reactivity will be a function of the concentration of both materials, with photoinitiator concentration having been investigated in 6.2.5.

It was reported in chapter 5 that there was some evidence to suggest most cleavage photoinitiators will, in the presence of an amine synergist, also react via a Type II mechanism. The exceptions to this observation were photoinitiators containing a nitrogen atom in the β -position, such as the α -aminoalkylphenones; found to react exclusively by a cleavage mechanism. The effect of amine synergist concentration can therefore be investigated for three classes of photoinitiator:

1. Type II character photoinitiators e.g. benzophenone
2. Type I character photoinitiators e.g. 2-methyl-1-[4-(methylthio)phenyl]-2-morpholino propan-1-one (Irgacure 907)
3. Photoinitiators with both Type I and Type II character e.g. benzil dimethyl ketal (Irgacure 651)

Type II character photoinitiators

The results of DPC experiments using formulations containing benzophenone and increasing weight percent concentrations of the amine synergist N-methyl diethanolamine (MDEA) are shown in figure 6.24. Samples were irradiated using 365 nm monochromatic light in both air and nitrogen atmospheres. Weight normalized exotherm peak area was used as a measure of curing reactivity.

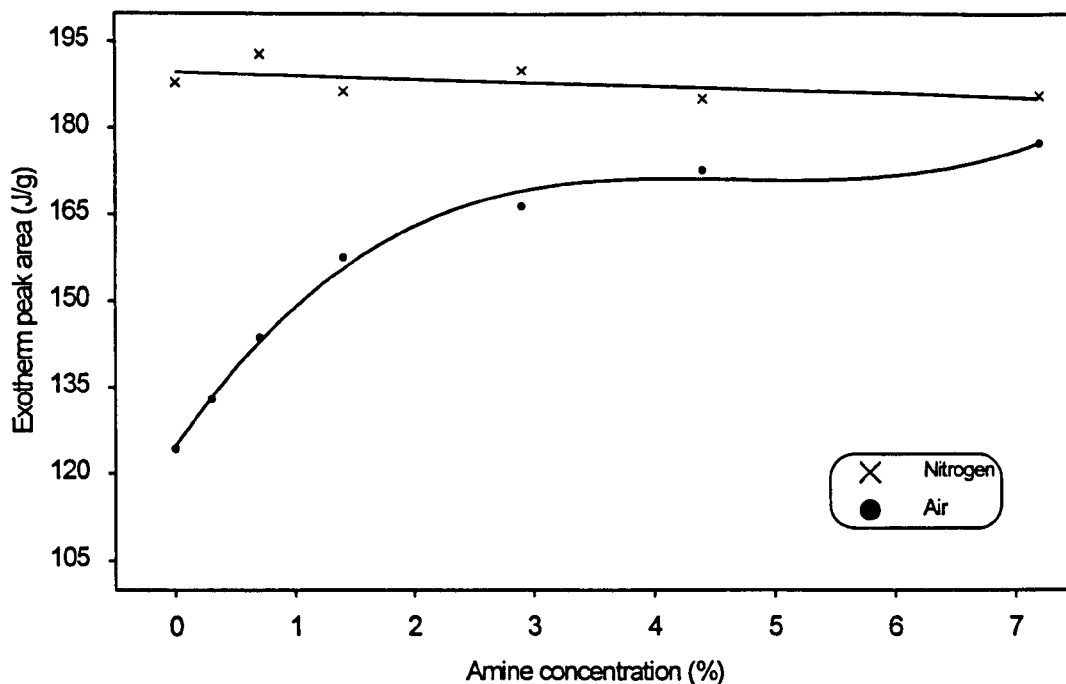


Figure 6.24 *Curing effectiveness of benzophenone as a function of amine synergist concentration*

The results in figure 6.24 show that in a nitrogen atmosphere benzophenone reactivity is unaffected by the concentration of amine synergist. However, in an air atmosphere the cure response increases significantly with amine concentration, particularly at low levels, and tends towards the reactivity observed under nitrogen.

It can be speculated that under these experimental conditions benzophenone operates to a significant extent by a direct hydrogen abstraction mechanism, possibly involving polyether groups in the oligomer. Two pieces of evidence support this theory; the independence of benzophenone reactivity on amine synergist concentration in a nitrogen atmosphere, and the relatively high reactivity of benzophenone in an air atmosphere with no amine synergist present. Direct hydrogen abstraction from monomers and oligomers by Type II photoinitiators has also been speculated by other workers⁷⁷.

The lower film thicknesses and formulation viscosities encountered in commercial curing applications will make oxygen quenching of the long lived benzophenone triplet state far more significant than it is under these experimental conditions. As such, initiation by direct hydrogen abstraction is unlikely to be as important as electron and proton transfer involving the amine synergist. The oxygen scavenging effect of the alkylamino radical produced by the electron and proton transfer mechanism will also then help to counter oxygen inhibition at the film surface.

Type I character photoinitiators

The results of DPC experiments using formulations based on 2-methyl-1-[4-(methylthio)phenyl]-2-morpholino propan-1-one (Irgacure 907), and containing increasing concentrations of the amine synergist MDEA, are shown in figure 6.25. Samples were irradiated using 365 nm monochromatic radiation in both air and nitrogen atmospheres, and the weight normalized exotherm peak area used as a measure of curing reactivity.

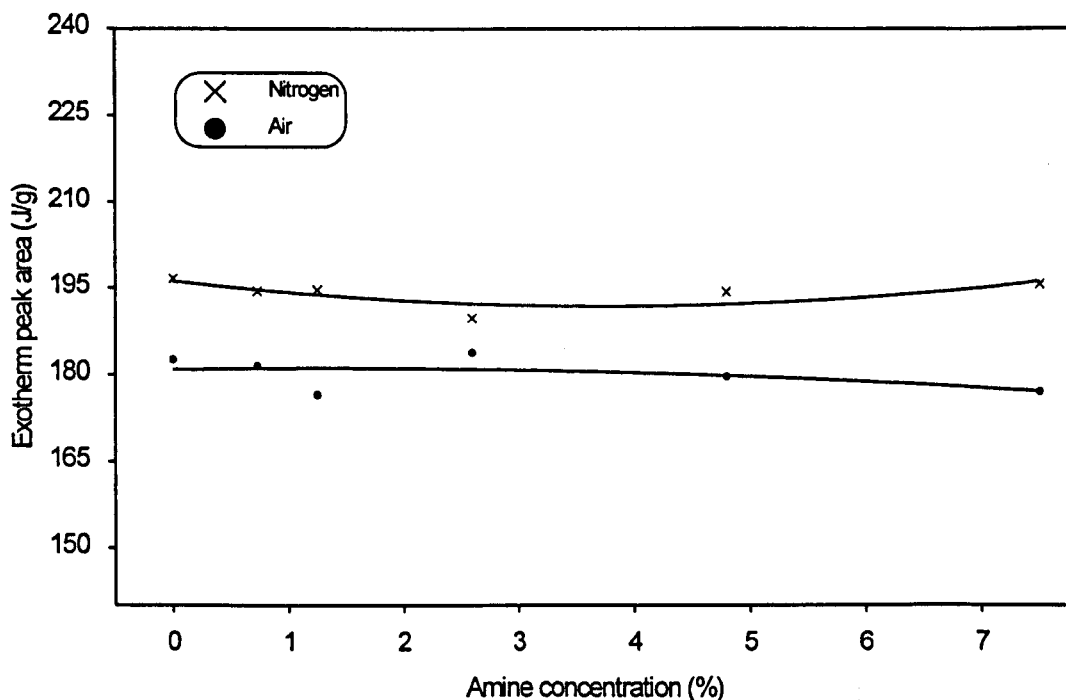


Figure 6.25 *Curing effectiveness of Irgacure 907 as a function of amine synergist concentration*

The results in figure 6.25 suggest that unlike for the Type II photoinitiator benzophenone, the reactivity of Irgacure 907 is independent of amine synergist concentration, with the lack of any observed reactivity decrease also indicating that no physical quenching by MDEA occurs. The relatively minor reactivity difference between results in air and nitrogen atmospheres also suggests that the triplet state is very short lived and not readily quenched by oxygen.

These results agree well with those presented in chapter 5, but contradict those of Davidson et. al., who found evidence of both hydrogen abstraction⁷⁸ and a performance increase in the presence of MDEA for this photoinitiator⁷⁹.

It is expected that the O-acyl- α -oximinoketone, Quantacure PDO, and the α -aminoalkylphenone photoinitiators Irgacure 369 and Radstart N1414, which both showed no Type II character in chapter 5 will behave similarly to Irgacure 907 in the presence of amine synergist.

Photoinitiators with both Type I and Type II character

The results of DPC experiments using formulations based on benzil dimethyl ketal (Irgacure 651), containing increasing concentrations of the amine synergist MDEA are shown in figure 6.26. Samples were irradiated using 385 nm monochromatic radiation in both air and nitrogen atmospheres, and the weight normalized exotherm peak area used as a measure of curing reactivity.

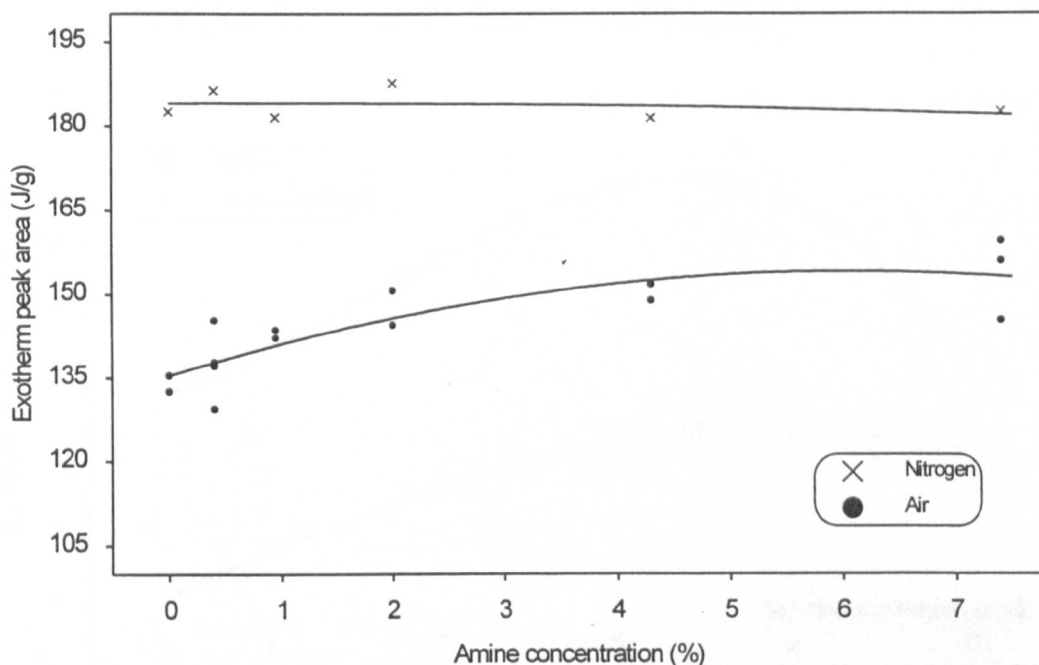


Figure 6.26 *Curing effectiveness of Irgacure 651 as a function of amine synergist concentration*

The results in figure 6.26 show that the reactivity of Irgacure 651 shows a limited amine dependence in an air atmosphere. This behaviour suggests that, in addition to the predominant Type I reaction, a Type II reaction is also occurring, where the interaction of the photoinitiator with MDEA generates alkylamino radicals that increase reactivity by scavenging oxygen. As with both other photoinitiator types investigated, in a nitrogen atmosphere the reactivity is independent of amine synergist concentration.

These results support those observed in chapter 5, since Irgacure 651 appears to show both Type I and Type II mechanisms in the presence of amine synergist. Similar behavior is expected for most other cleavage photoinitiators.

6.2.7 The influence of photoinitiator to amine synergist ratio on cure efficiency

The bimolecular nature of a Type II curing mechanism means that the cure efficiency is a function of both the photoinitiator and amine synergist concentrations. As such, the ratio of the two components at a fixed overall level will show a relationship, the basis of which is important, since within the printing ink industry photoinitiators and synergists are normally formulated to a fixed weight percent ratio and not a mol% ratio.

The differential photocalorimetry (DPC) results in figure 6.27 show how, for a mixture of the difunctional urethane acrylate CN934 and the monomer TMPTA, the changing %wt ratio of benzophenone and amine synergist affects the polymerisation rate. Samples contained a fixed level of 5 %wt benzophenone + amine synergist, with combinations ranging from 5 %wt benzophenone / 0 %wt amine, to 0.5 %wt benzophenone / 4.5 %wt amine. Irradiation was in an air purge at 50 °C using monochromatic light of either 365 nm or 380 nm, and the weight normalized exotherm peak height used as a measure of curing reactivity.

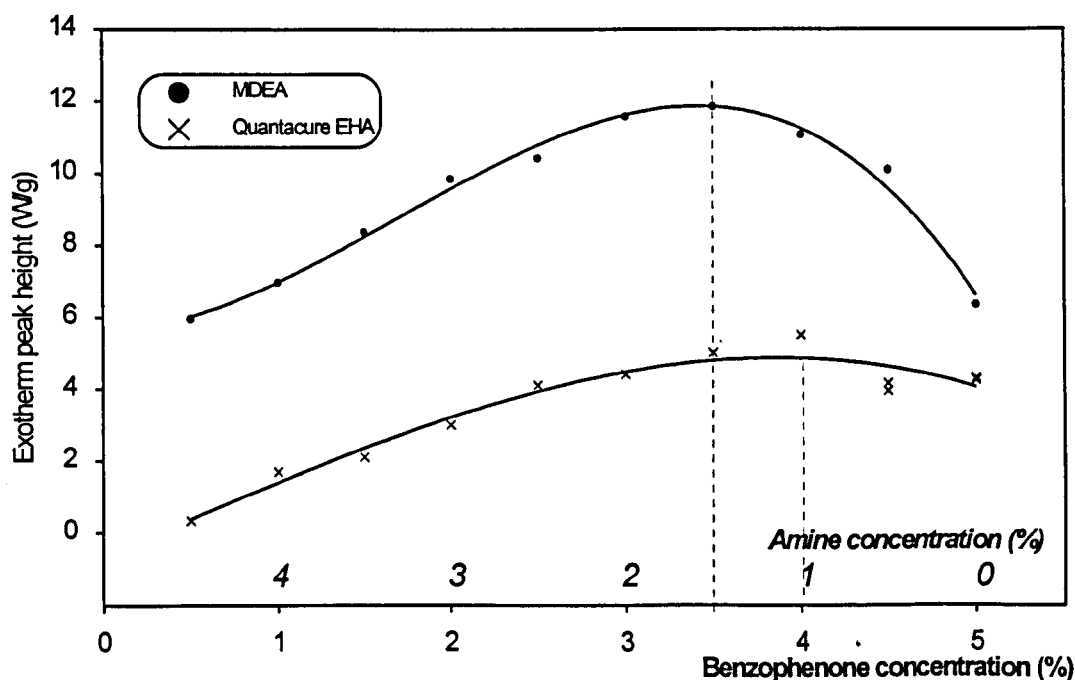


Figure 6.27 *The change in DPC exotherm peak height as a function of %wt ratio of benzophenone and amine synergist*

The results in figure 6.27 show that when MDEA is used as a synergist, a combination of 3.5 %wt benzophenone:1.5 %wt MDEA provides the highest reactivity, corresponding to a mol ratio of 1.5 benzophenone:1 MDEA. However, when using the synergist 4-N,N-dimethylamino benzoic acid (2-ethylhexyl) ester, Quantacure EHA, maximum reactivity is achieved at a level of 4 %wt benzophenone:1 %wt EHA, corresponding to a mol ratio of 6 benzophenone:1 EHA.

These results are somewhat surprising, particularly in view of the magnitude of the difference in peak mol ratio efficiency as a function of amine synergist type. However, despite being difficult to interpret in fundamental terms because of the use of weight based formulations, these results are useful in formulating terms because they indicate the optimum photoinitiator : synergist ratios for end use applications. A much greater understanding of the relationship would be achieved if similar experiments were done using different ratios of photoinitiator : synergists, but at a constant total molar concentration of the two species. Additional experiments examining the effect of other photoinitiator and synergist types would also be an area worthy of further study.

6.3 CONCLUSIONS

A real time infrared instrument based on a rapid scanning FTIR spectrometer has been set up, and a method validated for its use. Infrared (IR) data at 810 cm^{-1} is extracted and processed to provide a graph of percent conversion of acrylate bonds with time during UV irradiation. The initial rate of the curing reaction, obtained from the curve gradient at its steepest point, was found to be the best measure of sample reactivity.

The RT-FTIR was used to investigate the curing effectiveness of a wide range of photoinitiator molecules, including all those commercially available, and the results interpreted in terms of parameters such as molecular structure and UV absorption spectra. Results for particular materials agreed with those reported by other workers, but the wider picture generated by the examination of so many materials proved to be very informative. Acylphosphine oxides, thioxanthenes, and particularly α -aminoalkylphenones showed high curing activity. The results also agree well with those reported in chapter 4, where information about overall reactivity is inferred from the experiments used to investigate curing activity as a function of irradiation wavelength.

A strong logarithmic correlation was shown between the formulation viscosity and the extent of oxygen inhibition. For high viscosity formulations, little difference was observed between curing in air or nitrogen atmospheres, whereas at low viscosities curing in an air environment became severely retarded due to oxygen inhibition resulting from increased oxygen mobility into the film. This phenomenon was shown to be independent of the monomer type used.

The reactivity of a range of aromatic and aliphatic amine synergists was investigated using DPC. It was found that N-methyl diethanolamine (MDEA) showed the highest reactivity.

The percent conversion of acrylate double bonds was shown to have a complex relationship with the photoinitiator concentration. Some evidence suggested that chain termination was significant at photoinitiator concentrations above 6 %wt, but the photoinitiator's effect on formulation viscosity was also shown to be important. Use of photoinitiator concentrations as high as 30 or 40 %wt allowed 100 % acrylate bond conversion to be achieved.

Data was presented that supports the theory presented in chapter 5, that the α -aminoalkylphenone photoinitiators have no significant interaction with amine synergists, but that most other α -cleavage photoinitiators will react to some extent by a Type II mechanism in the presence of amine. It was also shown that in a nitrogen atmosphere, the reactivity of benzophenone is independent of amine synergist concentration, allowing speculation that a hydrogen abstraction mechanism involving polyether groups in the oligomer is favourable under the experimental conditions used.

6.4 EXPERIMENTAL

6.4.1 Curing effectiveness of photoinitiators by RT-FTIR

Formulations were prepared by dissolving 2 %wt of photoinitiator and N-methyl diethanolamine (MDEA) in an 80/20 blend of an aliphatic polyether urethane diacrylate oligomer (CN934) and the monomer trimethylolpropane triacrylate (TMPTA). The RT-FTIR experimental procedure and data manipulation were as described in 6.2.1. The initial reaction rate (% of total acrylate bonds converted per second) was used as the measure of photoinitiator reactivity

6.4.2 Molecular modeling of benzophenone derivatives

The molecular conformation of several benzophenone derivatives were determined using Biosym polymer, Discover 2.9 energy minimisation and Insight II (version 2.3.7) visualisation softwares, running on a Silicon Graphics Indigo 2 computer with 'extreme' graphics engine.

6.4.3 Curing effectiveness of amine synergists by DPC

A Perkin Elmer (Beaconsfield, Bucks.) Differential Scanning Calorimeter (DSC7), fitted with a Differential Photocalorimetry Accessory (DPA7) was used. Formulations were prepared by dissolving 4 %wt of isopropyl thioxanthone and 1 %wt of the amine synergist in an 80/20 blend of the oligomer CN934 and the monomer TMPTA. Samples of approximately 0.8 mg were irradiated with monochromatic light of wavelength 420 nm using an Osram XBO 400W xenon lamp in an air atmosphere at a temperature of 50 °C. These conditions ensured that no competitive light absorption by the amines occurred, and that sufficient oxygen inhibition existed to allow the amines to display differentiating initiating and radical scavenging ability. Sample weight normalized exotherm peak height measurements (Wg^{-1}) were used as a measure of the amine reactivity.

6.4.4 The effect of oxygen inhibition

DPC data

A Perkin Elmer (Beaconsfield, Bucks.) Differential Scanning Calorimeter (DSC7), fitted with a Differential Photocalorimetry Accessory (DPA7) was used. Formulations were prepared containing 0, 10, 20, 30, 40, 50, 60, 70, 80, 90 and 100 %wt of the monomers tripropylene glycol diacrylate (TPGDA) and di-pentaerythritol pentaacrylate (Di-PETA) in a trifunctional polyether urethane oligomer (Genomer T1200). Samples also contained 2 %wt of the photoinitiator benzil dimethyl ketal. Monochromatic UV light of wavelength 365 nm from an Osram HBO 100W/2 medium pressure mercury short arc lamp was used to irradiated the samples under both air and nitrogen purge conditions at a temperature of 40 °C. Sample weights of approximately 0.8 mg were used, with the sample weight normalized exotherm peak area (Jg^{-1}) being used as a measure of curing reactivity.

Additional formulations were prepared based on combinations of Genomer T1200 with the monomers di-trimethylol propane tetraacrylate (Di-TMPTA), neopentyl glycol propoxylate diacrylate (NPGPDA), glycerol propoxylate triacrylate (GPTA), pentaerythritol tetraacrylate (PETA), and trimethylol propane ethoxylate triacrylate (TMPTOEA). Particular formulations were chosen that covered the viscosity range 0.01-525 poise. Experimental conditions were as described above, but the sample weight normalized exotherm peak height (Wg^{-1}) was used as a measure of curing reactivity. Curing temperatures of either 25 °C or 32 °C were used in order to provide the desired viscosity range.

Formulations containing 50 %wt of TPGDA and Di-PETA in the oligomer Genomer T1200, and containing 2 %wt of benzil dimethyl ketal were analysed by DPC under similar conditions to those described above, but using exposure temperatures between -30, and 70 °C. The sample weight normalized exotherm peak height (Wg^{-1}) was used as a measure of curing reactivity.

Viscosity data

Static viscosity measurements were made using an ICI cone and plate viscometer at either 25 °C or 32 °C, corresponding to the experimental temperatures used in the DPC experiments. Viscosity vs. temperature profiles were measured using a Bohlin CS-50 controlled stress rheometer (Bohlin Instruments, Cirencester) between 5 and 70 °C using parallel plates, a fixed stress of 5 Pascals and a temperature ramp rate of 2 °C per minute.

6.4.5 The effect of photoinitiator concentration on cure efficiency

DPC data

A Perkin Elmer (Beaconsfield, Bucks.) Differential Scanning Calorimeter (DSC7), fitted with a Differential Photocalorimetry Accessory (DPA7) was used. Formulations were prepared based on an 80/20 blend of the oligomer CN934 and the monomer TMPTA, containing levels of the photoinitiators 1-phenyl-2-hydroxy-2-methyl propan-1-one (Darocure 1173), or its polymeric equivalent (Esacure KIP), between 0.5 and 15 %wt. Monochromatic UV light of wavelength 334 nm source from an Osram HBO 100W/2 medium pressure mercury short arc lamp was used to polymerise the samples at 40 °C in an air purge. The sample weight normalized exotherm peak area (Wg^{-1}) was used as a measure of reactivity.

Viscosity data

Viscosity measurements were made using an ICI cone and plate viscometer at 25 °C.

RT-FTIR data

The same formulations as described for DPC experiments were used for RT-FTIR experiments. Additional samples containing photoinitiator concentrations of 20, 25, 35 and 40 %wt were also prepared and analysed. The RT-FTIR experimental procedure and data manipulation were as described in 6.2.1. The final % acrylate bonds converted was used as a measure of curing reactivity.

6.4.6 The influence of amine synergist concentration on cure efficiency

A Perkin Elmer (Beaconsfield, Bucks.) Differential Scanning Calorimeter (DSC7), fitted with a Differential Photocalorimetry Accessory (DPA7) was used. Formulations were prepared based on an 80/20 combination of CN934 and TMPTA, containing 4 %wt of the photoinitiators benzophenone, 2-methyl-1-[4-(methylthio)phenyl]-2-morpholino propan-1-one (Irgacure 907) or benzil dimethyl ketal (Irgacure 651), each containing increasing levels of the amine synergist MDEA between 0 and 7.5 %wt. Approximately 0.8 mg of benzophenone or Irgacure 907 containing samples were irradiated using 365 nm monochromatic UV light from an Osram HBO 100W/2 medium pressure mercury short arc lamp at a temperature of 40 °C. Irgacure 651 containing samples were also irradiated at a temperature of 40 °C, but in order to reduce its curing activity sufficiently to be within the differentiating capabilities of the instrument, 385 nm monochromatic radiation from an Osram XBO 400W xenon lamp was used. The sample weight normalized exotherm peak area (Jg^{-1}) was used as a measure of reactivity.

6.4.7 The influence of photoinitiator to amine synergist ratio on cure efficiency

A Perkin Elmer (Beaconsfield, Bucks.) Differential Scanning Calorimeter (DSC7), fitted with a Differential Photocalorimetry Accessory (DPA7) was used. Formulations were prepared based on an 80/20 combination of CN934 and TMPTA, containing a mixture of 5 %wt of a benzophenone and either MDEA or 4-N,N-dimethylamino benzoic acid (2-ethylhexyl) ester, (Quantacure EHA). The ratio of benzophenone and amine varied between 0.5 %wt benzophenone and 4.5 %wt amine to 5 %wt benzophenone with no amine, in 0.5 %wt increments. For benzophenone / MDEA formulations, samples of approximately 0.8 mg were irradiated using 365 nm monochromatic light from an Osram HBO 100W/2 medium pressure mercury short arc lamp at 50 °C in an air purge. For benzophenone / Quantacure EHA formulations, irradiation was under similar conditions but using 380 nm monochromatic radiation from an Osram XBO 400W xenon lamp. This longer wavelength ensured that no competitive light absorption by the EHA occurred. The sample weight normalized exotherm peak height (Wg^{-1}) was used as a measure of reactivity.

6.5 REFERENCES

1. E Selli, I R Bellobono in *Radiation Curing in Polymer Science and Technology (Volume 3-Polymerization Mechanisms)*; J P Fouassier, J F Rabek (Eds), Elsevier Science Publishers Ltd., Barking, Essex, 1 (1993)
2. C Decker, K Moussa; *Makromol. Chem.*, **189**, 2381 (1988)
3. J G Kloosterboer; *Advances In Polymer Science*, **84**, 1 (1988)
4. M J Hanrahan; *Journal Of Radiation Curing* **19**,14 (1991)
5. J G Kloosterboer ,G M M Van de Hei, R G Gossink, G C Dortant; *Polymer Communications*, **25**, 322 (1984)
6. C Decker; *Macromolecules*, **23**, 5217 (1990)
7. C Decker, K Moussa; *Euro. Polym. J.*, **26**, 393 (1990)
8. G R Tryson, A R Schultz; *J. Polym. Sci. :Polym. Phys. Edn.*, **17**, 2059 (1979)
9. K S Anseth, C M Wang, C N Bowman; *Polymer*, **35** (15), 3243 (1994)
10. S Paul; *Surface Coatings International*; **8**, 336 (1994)
11. G Plews, R Phillips; *Journal Of Coatings Technology*; **51** (648), 69 (1979)
12. G L Collins, D A Young, J R Costanza; *Journal Of Coatings Technology*, **48** (618), 48 (1976)
13. J M Julian, A M Millon; *Journal Of Coatings Technology*; **60** (765), 89 (1988)
14. B de Ruiter, J de Vlleger, J Bowman; *Proc. Conf. RADTECH*, Edinburgh, Scotland, 596 (1991)
15. L Misev, M Kunz, R Strobel; *Proc. Conf. RADTECH*, Maastricht, Holland, 93 (1995)
16. G A Lee, G A Doorakian; *Journal Of Radiation Curing*, **4**, 2 (1977)
17. C Decker, K Moussa; *Makromol. Chem.*, **191**, 963 (1990)
18. C Decker, K Moussa in *ACS Symposium Series No.417*, 439 (1990)
19. D B Yang; *Journal Of Applied Polymer Science: Part A: Polymer Chemistry*, **31**, 199, (1993)
20. A Udagawa, F Sakurai, T Takahashi; *Journal Of Applied Polymer Science*, **42**, 1861 (1991)
21. J E Dietz, B J Elliot, N A Peppas; *Macromolecules*, **28** (15), 5163 (1995)
22. J P Fouassier in *Radiation Curing in Polymer science and Technology (Volume 1-Fundamentals and Methods)*; J P Fouassier, J F Rabek (Eds.), Elsevier Science Publishers Ltd., Barking, Essex, 49 (1993)
23. R.S Davidson, J W Goodin; *Euro. Polym. J.* ,**18**, 597 (1982)
24. S Göthe; *Proc. 17th conf. FATIPEC*, **2**,13,(1984)
25. J L Mateo, P Bosch, A E Lozano; *Macromolecules*, **27**, 7794 (1994)
26. N S Allen, E Lam, E M Howells, P N Green, W A Green, F Catalina, C Peinado; *Euro. Polym. J.*, **26** (12), 1345 (1990)
27. N S Allen, D Mallon, I Sideridou, W A Green, A Timms, F Catalina; *Euro. Polym. J.*, **28** (6), 647 (1992)

28. J L Mateo, P Bosch, F Catalina, R Sastre; *Journal of Polymer Science Part A: Polymer Chemistry*, **29**, 1955 (1991)
29. G Henken; *American Ink Maker*, **56** (3), 57 (1978)
30. M J Hanrahan; *Proc. Conf. RADTECH*, Chicago, Illinois, USA., 249 (1990)
31. G Berner, R Kirchmayr, G Rist; *J. Oil Col. Chem. Assoc.*, **61**, 105 (1978)
32. A Green, A Timms, P Green; *Polymers Paint And Colour Journal*, **182** (4299), 40 (1992)
33. J E Moore, S H Schroeter, A R Schultz, L D Stang; *Journal Of Radiation Curing*, **25**, 90 (1976)
34. A J Doornkamp, Y Y Tan; *Polymer Communications*, **31**, 362 (1990)
35. M G Tilley, M Trapp, K Webb; *Proc. Conf. RADTECH*, Boston, USA, 48 (1992)
36. A J Evans, C Armstrong, R J Tolman; *J. Oil Col. Chem. Assoc.*, **61**, 251 (1978)
37. R Levin, A Hale, A L Harris, N J Levinos, F C Schilling; *Proc. Conf. ACS Polym. Mat. Sci. & Eng.*, **72**, 524 (1995)
38. C L Osborn, M R Sandner; *ACS Div. Org. Coat. Plast. Chem. Preprints*, **34**, 1, 660 (1974)
39. J Ohngemach, M Koehler, G Wehner; *Proc. Conf. RADTECH Florence, Italy*, 639 (1989)
40. M Jacobi, A Henne; *Polymers Paint And Colour Journal*, **175**, 4150, 636 (1985)
41. K Dietliker in *Radiation Curing In Polymer Science And Technology (Volume II- Photoinitiating Systems)*, J P Fouassier, J F Rabek (Eds), Elsevier Science Publishers Ltd., Barking, Essex, 155 (1993)
42. A F Cunningham, V Desobry, K Dietliker, R Hüsler, D G Leppard; *Chimia*, **48**, 9, 423 (1994)
43. W Rutsch, K Dietliker, D Leppard, M Köhler, L Misev, U Kolczak, G Rist; *Proc. 20th Int. Conf. Org. Coat. Sci. Tech.*, Athens, Greece, 467 (1994)
44. E Beck, E Keil, M Lokai, J Schröder; *Radcure Letter*, **5**, 67 (1994)
45. H F Gruber; *Prog. Polym. Sci.*; **17**, 953 (1992)
46. C Decker, K Moussa; *Journal Of Coatings Technology*, **65**, 819, 49 (1993)
47. W Rutsch, G Berner, R Kirchmayr, R Hüsler, G Rist, N Bühler; *Proc. 10th Int. Conf. Org. Coat. Sci. Tech.*, Athens, Greece, 241 (1984)
48. K Dietliker, M Rembold, G Rist, W Rutsch, F Sitek; *Proc. Conf. RADTECH*, Florence, Italy, 3-37 (1987)
49. M Köhler, L Misev, V Desobry, K Dietliker, B M Bussian, H Karfunkel in *Radiation Curing Of Polymers II*; D R Randell (Ed.), Royal Society Of Chemistry, London, 163 (1991)
50. W Rutsch, G Berner, R Kirchmayr, R Hüsler, G Rist, N Buehler in *Organic Coatings: Science And Technology* G D Parfitt, A V Patsis (Eds.), New York (1986)
51. J P Fouassier, D Ruhlmann; *Proc. Conf. RADTECH*, Edinburgh, Scotland, 499 (1991)
52. V Desobry, K Dietliker, R Hüsler, L Misev, M Rembold, G Rist, R Rutsch in *ACS Symposium Series No.417*, 92 (1990)

53. K Dietliker in *Chemistry and Technology of UV and EB Formulation for Coatings Inks and Paints (Volume 3-Photoinitiators for Free Radical and Cationic Polymerization)* P K T Oldring (Ed), SITA Technology Ltd., London, 59 (1991)
54. G Berner, K Meier, K Dietliker, R Hüsler; *European Patent 138754-A* (1983)
55. C E Hoyle, R D Hensel, M B Grubb; *Journal Of Radiation Curing*, **October**, 22 (1984)
56. C Armstrong, S L Herlihy; *Proc. Conf. Aspects Of Photoinitiation*, Egham, Surrey, 1 (1993)
57. N S Allen, F Catalina, J.Luc-Gardette, P N Green, W A Green, O Fatinkun; *J. Oil Col. Chem. Assoc.*, **70**, 11, 332 (1987)
58. W A Green, A W Timms; *Proc. Conf. RADTECH*, Boston, USA, 33 (1992)
59. D G Anderson, J Elvery, R S Davidson; *Proc. Conf. RADTECH*, Maastricht, Holland 565 (1995)
60. A Valet; *Polymers Paint & Colour Journal*, **May**, 31 (1985)
61. J R Merrill; *J. Phys. Chem.*, **65**, 2023 (1961)
62. C Decker, K Moussa; *J. Polym. Sci.:Part C: Polymer Letts.*, **27**, 347 (1989)
63. V L Ermolaev, A N Terenin; *J. Chim. Phys.*, **55**, 698 (1958)
64. J P Fouassier, D J Lougnot; *Polymer Communications*, **31**, 11, 418 (1990)
65. J Hutchinson, A Ledwith; *Advances In Polymer Science*, 14-49 (1974)
66. A Ledwith, G Ndaalio, A R Taylor; *Macromolecules*, **8**, 1 (1975)
67. H J Hageman in *Photopolymerization And Photoimaging Science And Technology*; N S Allen (Ed.), Elsevier Science Publishers Ltd., Barking, Essex, 1 (1989)
68. D Braun, R Gehrisch; *Polymer Photochemistry*, **6**, 415 (1985)
69. Hitachi Chemical Co. Ltd.; *European Patent EP0503076A1* (1991)
70. C L Osborn; *Journal Of Radiation Curing*, **3** (3), 2 (1976)
71. V D McGinniss in *Developments In Polymer Photochemistry-3*; N S Allen (Ed.), Applied Science Publishers Ltd., Barking, Essex, 1 (1982)
72. N S Allen, F Catalina, J L Mateo, R Sastre, W Chen, P N Green, W A Green in *ACS Symposium Series No. 417*, 72 (1990)
73. J E Christensen, W L Wooten, P J Whitman, *Journal Of Radiation Curing*, **July**, 35 (1987)
74. C Decker, T Bendaikha; *Euro. Polym. J.*, **20**, 753 (1984)
75. C Decker, K Moussa; *Journal Of Coatings Technology*, **62**, 55 (1990)
76. H P Seng; *Proc. Conf. RADTECH*, Florence, Italy, 163 (1989)
77. N Arsu, R S Davidson, R J Holman; *J.Photochem. Photobiol. A: Chem.*, **87**, 169 (1995)
78. R S Davidson in *Molecular Associations I*, R Foster (Ed), Academic Press, London (1975)
79. R S Davidson, N Arsu; *J.Photochem. Photobiol. A: Chem.*, **84**, 291 (1994)

CHAPTER 7

General conclusion

This project has concentrated on the UV curing of acrylate based free radical systems for inks and coatings. By considering the processes which occur both before and during cure, the factors which most influence photoinitiation efficiency and the suitability for use of particular photoinitiators and synergists were determined to be:

1. Photoinitiator physical properties
2. UV light utilisation
3. Reaction mechanism and photodecomposition products
4. Photoinitiator reactivity

These subjects were investigated in detail using a wide range of photoinitiators and synergists, with the principal aim being to provide the necessary information to enable a formulator to quickly choose the most appropriate combination of materials to suit any application. A number of analytical techniques have been used to aid this investigation, with results largely in agreement with existing literature knowledge. However, the comprehensive nature of this project and the large number of materials investigated has been the key to highlighting trends, mechanisms and theories not previously reported.

Photoinitiator physical properties

The importance of the volatility / thermal stability of photoinitiators and synergists was discussed in terms of specific applications such as inks for printed circuit boards and microwavable food packaging. A range of materials were analysed by thermogravimetric analysis (TGA) and thermogravimetric analysis-mass spectroscopy (TGA-MS) to define the processes which occur on heating. Although most photoinitiators were found to volatilise on heating, some thermal decomposition was also observed, with a number of other materials showing clear multistage thermal decomposition. Several photoinitiators were also observed to show desublimation behaviour following volatilisation, allowing speculation that this is the source of potential problems with both the printing process and contamination of the end product.

The relative solubilities of a range of photoinitiators are presented and the importance of this property discussed in terms of materials which have been commercialized or claimed to show significant advantages over existing photoinitiators, but which have failed to gain any significant market share because of their poor solubility characteristics.

UV light utilisation

Largely expanding on the ideas and thought processes of a number of authors, two questions relating to the curing of printing ink and coating formulations were addressed:

- How much light does the photoinitiator receive?
- How effective is the photoinitiator in converting light of particular wavelengths into free radicals?

It was found that, for UV absorbance spectra acquired under a standard set of conditions, by introducing scaling factors into the Beer-Lambert law, these spectra could be manipulated to provide the UV absorbance and transmission spectra of individual materials and combinations of materials at specified concentrations and film thicknesses. This procedure proved to be accurate at any reasonable concentration and film thickness encountered in the printing ink industry. Results using pigments were found to be more variable because of inconsistencies in the extent of dispersion in the solvent, although solutions to this problem were suggested. The use of transmission spectra in predicting photoinitiator screening was also introduced.

For a series of differently pigmented coatings, by measuring the light transmitted to various depths within the coating it was possible to determine which wavelengths were responsible for surface cure and which were responsible for through cure. General approaches to achieving greater through cure were also discussed.

Using the technique of differential photocalorimetry (DPC), formulations containing different photoinitiators were cured with each of the peak emission wavelengths from a medium pressure mercury lamp to determine which wavelengths were the most important in terms of providing cure. It was found that, with the exception of thioxanthone type photoinitiators which utilise principally the 365 nm emission wavelength, commonly used photoinitiators gain most of their curing reactivity from the short UV wavelengths around 300 nm. Although the experimental procedure did not allow investigations in the 250-300 nm region, these wavelengths were shown not to be capable of being involved in providing significant through cure since they do not penetrate far enough into the film. The effect that different pigments have on the balance of the cure response with irradiation wavelength was also shown, as well as indicating which photoinitiators should provide the best cure response in combination with different pigment types.

Energy transfer and electron / proton transfer sensitization were also investigated using DPC, where it was found that all the α -aminoalkylphenone type photoinitiators investigated appear to be sensitized by thioxanthenes, although the relative cure response was found to be related to the structure of both molecules. Low levels of Michler's ketone and ethyl Michler's ketone were identified as providing a significant performance increase in combination with benzophenone through a sensitization mechanism. These experiments demonstrated that specific combinations of materials could be chosen to overcome both photochemical efficiency limitations with individual photoinitiators and the lack of available incident light in specific wavelength regions.

Reaction mechanisms and photodecomposition products

The printing ink industry is under increasing commercial and legislative pressure regarding extractable and migratable material in UV cured products, particularly in food packaging applications. As such, the reaction mechanism of a range of photoinitiators was studied in a model system and the reaction byproducts identified in order to allow a more appropriate choice of materials. Although largely in agreement with existing literature knowledge, a number of additional byproducts and mechanisms were identified because of the large number of materials investigated. In particular, the ability of most cleavage photoinitiators to generate alkylamino radicals in combination with an amine synergist through a Type II reaction, and the involvement of both primary radicals in initiation and termination reactions was identified.

Photoinitiator reactivity

A new instrument based on a rapid scanning infrared spectrometer was set up to measure the changes in the IR spectrum of a material with time during UV exposure. Described as real time Fourier transform infrared spectroscopy (RT-FTIR), this instrument and method showed some distinct advantages over other similar instruments reported in the literature. It was subsequently used to measure the rate of polymerisation for a wide range of photoinitiators by monitoring the depletion of the acrylate double bonds during cure. These results were then compared to available literature knowledge and interpreted in terms of factors such as chemical structure and UV light utilisation. Acylphosphine oxide, thioxanthone and particularly α -aminoalkylphenone type photoinitiators were shown to be highly reactive. The effectiveness of amine synergists was also investigated using DPC, where N-methyl diethanolamine was found to be the most reactive.

APPENDIX 1 — General Experimental

Photoinitiators and synergists

Aldrich Chemical Co. Ltd.

The following photoinitiators and synergists were obtained from the Aldrich Chemical Co. Ltd. and used without further purification; benzoin, benzoin methyl ether, benzoin isobutyl ether, diethoxy acetophenone, benzophenone, 4-phenyl benzophenone, 4-chloro benzophenone, 2-chloro benzophenone, 4,4'-(dimethylamino) benzophenone, 4,4'-(diethylamino) benzophenone, 4-methyl benzophenone, 2-methyl benzophenone, 4-methoxy benzophenone, 4,4'-dimethoxy benzophenone, 4-hydroxy benzophenone, 2-hydroxy benzophenone, xanthone, thioxanthone, benzil, 4,4'-dimethyl benzil, 4,4'-dimethoxy benzil, 9-phenyl acridine, 2-methyl anthraquinone, 2-ethyl anthraquinone, 2-t.butyl anthraquinone, phenanthrene-9,10-quinone, N,N-dimethyl aniline, triethylamine, triethanolamine, tri-isopropanolamine, N,N'-dimethyl propanolamine, N-methyl diethanolamine, N,N-dimethyl ethanolamine and 2-N,N-dimethylamino benzoic acid ethyl ester.

Ciba-Geigy Ltd.

The following photoinitiators were obtained from Ciba-Geigy and used without further purification (trade names given in brackets); 1-phenyl-2-hydroxy-2-methyl propan-1-one (*Darocure 1173*), 4-isopropyl-phenyl-2-hydroxy-2-methyl-2-propan-1-one (*Darocure 1116*), 4-(2-hydroxyethoxy)-phenyl-2-hydroxy-2-methyl-2-propan-1-one (*Darocure 2959*), 1-hydroxy-cyclohexyl phenyl ketone (*Irgacure 184*), 2-methyl-1-[4-(methylthio)phenyl]-2-morpholino propan-2-one (*Irgacure 907*), 2-benzyl-2-dimethylamino-1-(4-morpholinophenyl) butan-1-one (*Irgacure 369*) and benzil dimethyl ketal (*Irgacure 651*).

A 1:3 blend of photoinitiators 1-phenyl-2-hydroxy-2-methyl propan-1-one (*Darocure 1173*) and bis (2,6-dimethoxybenzoyl)-2,4,4-trimethylpentyl phosphine oxide (*BDTPO*) was also obtained under the trade name *Irgacure 1700*. This was used as received, but also used to obtain a pure sample of *BDTPO* by washing with n-hexane to remove the *Darocure 1173*, followed by recrystallisation of *BDTPO* from a diethyl ether / n-hexane mixture.

Great Lakes Chemical Corp.

The following photoinitiators and synergists were obtain from the Great Lakes Chemical Corp. and used without further purification (trade names given in brackets); isopropyl thioxanthone (*Quantacure ITX*), 2-t.butyl thioxanthone, 2-propoxy thioxanthone (*Quantacure PTX*), 1-chloro-4-propoxy thioxanthone (*Quantacure CPTX*), 1-phenyl-1,2-propanedione-2-(O-ethoxycarbonyl) oxime (*Quantacure PDO*), 4-benzoyl-4'-methyl diphenyl sulfide (*Quantacure BMS*), phenyl glyoxic acid methyl ester (*Nuvopol PI3000*), dibenzosuberone, 4-N,N-dimethylamino benzoic acid ethyl ester (*Quantacure EPD*), 4-N,N-dimethylamino benzoic acid amyl ester (*Quantacure MCA*),

4-N,N-dimethylamino benzoic acid 2-ethylhexyl ester (*Quantacure EHA*) and (2-dimethylamino)ethyl benzoate (*Quantacure DMB*).

Lambson speciality chemicals

The following photoinitiators and synergists were obtained from Lambson speciality chemicals and used without further purification (trade names given in brackets); 2,4-diethyl thioxanthone (*Speedcure DETX*) and 4-N,N-Dimethylamino benzoic acid 2-butoxyethyl ester (*Speedcure BEDB*).

Siber Hegner

The following photoinitiators were obtained from Siber Hegner and used without further purification (trade names given in brackets); benzoin ethyl ether (*Daitocure EE*), benzoin isopropyl ether (*Daitocure IP*), 2-benzoyl methyl benzoate (*Daitocure OB*) and 2-chloro thioxanthone (*Kayacure CTX*).

Croxton and Garry

The following photoinitiators were obtained from Croxton and Garry and used without further purification (trade names given in brackets); polymeric 1-phenyl-2-hydroxy-2-methyl propan-1-one (*Esacure KIP*), 2,4,6-trimethyl benzophenone (*Esacure TZT*) and a blend of benzoin n-butyl and benzoin isobutyl ethers (*Esacure EB3*).

BASE

The following photoinitiators were obtained from BASF and used without further purification; 2,4,6-trimethylbenzoyl diphenylphosphine oxide (*Lucerin TPO*) and 2,4,6-trimethylbenzoyl phenylphosphinic acid ethyl ester (*Lucerin LR8893X*).

Kromachem

The photoinitiator 3, 6-bis (2-morpholinoisobutyryl) N-octyl carbazole was obtained from Kromachem under the trade name *Radstart NI1414* and used without further purification.

Lancaster

The photoinitiator 4,4'-diphenoxy benzophenone was obtained from Lancaster and used without further purification.

UCB

The amine synergist based on a Michael addition reaction product of diethylamine and tripropylene glycol diacrylate was obtained from UCB under the trade name *Ebecryl P115* and used without further purification.

Radiation curable oligomers and monomers

The following radiation curable oligomers and monomers were obtained from Cray-Valley and used without further purification (trade names given in brackets); a polyether urethane diacrylate oligomer (*CN934*), tripropylene glycol diacrylate (SR306), di-pentaerythritol pentaacrylate (SR399), di-trimethylol propane tetraacrylate (SR355), neopentyl glycol propoxylate diacrylate (SR9003), glycerol propoxylate triacrylate (SR9020), pentaerythritol tetraacrylate (SR295), and trimethylol propane ethoxylate triacrylate (SR454).

The radiation curable monomer trimethylolpropane triacrylate was obtained from the Aldrich Chemical Co. Ltd. and used without further purification.

A trifunctional polyether urethane acrylate oligomer was obtained from Great Lakes Chemical Corp. under the trade name Genomer T1200 and used without further purification.

Pigments

All pigments used as part of the work reported here were obtained from the Coates Lorilleux raw material stores and used without further purification. Individual suppliers could not be identified for these materials because of the purchasing and coding systems used.